Modelling Steroidal Hormone Transport and Evaluating Best Management Practices in New Zealand Dairy Farming Systems

A thesis

submitted in fulfilment

of the requirements for the degree of

Doctor of Philosophy in Engineering

at

The University of Waikato

by

Muhammad Adnan Majeed

2026

Acknowledgement

In the name of Allah, the Most Gracious, the Most Merciful. All praise is due to Allah, the Lord of the worlds (Al Quran, Surah Al-Fātiḥah 1-2).

I owe my deepest gratitude to my chief supervisor, Dr Mark Lay, whose calm encouragement and steadfast support guided every stage of this thesis. From refining the research concept through to final editing, his expert advice and genuine concern for my well-being made this work possible. Our bike rides, hikes, and dog walks provided both restorative breaks and invaluable opportunities to discuss ideas in a relaxed environment. Dr Mark's kindness, patience, and willingness to help whenever asked were a constant source of motivation and made this thesis possible.

I am also grateful to my co-supervisors: Dr Danielle Bertram for her assistance with MATLAB coding and facilitating my role as a sessional assistant; Dr Graeme Glasgow and Dr Megan Bostan for their early guidance during the project's initial phase.

I am grateful to Environmental Engineering Technical Officer Steven Wu for his invaluable assistance with laboratory testing, always ensuring I had the necessary equipment, glassware, and technical support to conduct soil and estrogen analyses. I also thank the Soil Science Laboratory at the School of Science for granting me full access to their facilities and for the ready assistance of all technical staff, whose expertise and resources were essential to completing my laboratory work.

Thanks are due to my lab colleagues: Sureka, for training me in estrogen determination using LC-MS; Illisa Ishan, for meticulous editing support; Marianne Hull for connecting me with dairy farmers and securing access to dairy farms, as well as her invaluable assistance in conducting interviews with dairy owners, which greatly enriched my research, and Zain Ali, for his prompt help with MATLAB programming whenever I needed it.

I am profoundly thankful to Dr. Jessica, a kind-hearted dairy owner, who warmly welcomed me to her farm and generously provided access to her dairy operations as a research site. She eagerly shared valuable information about her cows, farm management practices, soil data, and

nutrient testing reports from the regional council. Her unwavering support and kindness left a lasting impact on my research. Tragically, Dr. Jessica passed away last year due to a brain tumor, and I dedicate this acknowledgment to her memory with heartfelt gratitude.

I would like to express my sincere gratitude to the Higher Education Commission (HEC) of Pakistan for their financial support through the PhD scholarship.

I appreciate my land lady Dr Sayyad Bano and her brother Irshad in New Zealand for their warm welcome and practical support that helped me settle here.

My heartfelt thanks go to my family, especially my elder brothers, Muhammad Tayyab Majeed, Adil Majeed and my sisters, for their unwavering financial and emotional support throughout my doctoral journey.

I dedicate this thesis to my loving mother and father (late), whose sacrifices and steadfast belief in my education made this achievement possible despite hardship.

Finally, I extend my deepest gratitude to my wife, Memona, whose patience and encouragement over the past three and a half years sustained me through moments of stress and distance. Although we lived together for only nineteen days after our wedding, Memona has remained in Pakistan, patiently awaiting my return. Her unwavering support, understanding, and encouragement across the distance have been my greatest motivation throughout this PhD.

Abstract

This doctoral research developed and applied two modelling approaches to simulate and assess estrogen (estrone E1, and 17β-estradiol E2) transport from an intensive dairy farm system located in the Waikato region, New Zealand. The first approach was a numerical unsaturated zone model implemented in MATLAB, coupling Richards' equation with a Green-Ampt infiltration framework and advection, dispersion, and sorption processes to track estrogen movement through soil. The second approach employed a GIS-based ArcSWAT catchment model to simulate surface runoff, sediment yield, and estrogen transport at the farm watershed scale, including the evaluation of best management practices (BMPs). The novelty of this research lies in the dual-scale modelling of estrogen transport through both soil and surface runoff pathways and the spatially explicit, quantitative assessment of existing best management practices specifically for estrogen mitigation rather than nutrient reduction alone.

Soil Model results indicate that estrogens are largely retained and attenuated in the upper soil layers, reducing the risk of leaching to groundwater. The model showed that both E1 and E2 undergo strong sorption near the surface and substantial microbial degradation, with >90% of the applied mass removed within the top ~1 m over a 90-day simulation. Estradiol was more mobile than estrone, with its concentration front advancing deeper (~0.5–0.6 m). Concentrations declined steeply with depth, and values below ~1.5 m were negligible under steady infiltration.

Infiltration-driven pulses produced by surface boundary input led to episodic colloid mobilization, which enhanced estrogen transport to mid-depths. Free and attached colloid time series showed synchronous peaks, indicating that mobile colloids can act as vectors for hormone movement. These findings suggest that under normal conditions, leaching risk is low, but during rapid infiltration following effluent application, colloid-facilitated transport may temporarily extend hormone movement deeper into the profile. Overall, the results align with experimental column studies, confirming that estrogen is primarily confined to shallow soil and largely degraded in situ, while emphasizing the importance of managing infiltration timing and flow dynamics.

For the dairy farm studied, the ArcSWAT model provided a spatially explicit assessment of estrogen transport via runoff and erosion. Critical source areas (hotspots) for estrogen and sediment loss were identified at the subbasin level. Under baseline (pre-BMP) conditions, eight

subbasins were predicted to generate the highest estrogen concentrations in runoff (often >15 ng/L) and severe sediment yields. One subbasin emerged as the most critical, with annual runoff volumes exceeding ~1500 mm and sediment losses on the order of ~3.9 t/ha, concomitant with elevated estrogen loads. Several other subbasins showed overlapping high runoff and erosion, indicating that both dissolved and sediment-bound estrogen transport mechanisms are at play in these areas. The model indicated that surface water contamination is a primary concern, as these high-runoff zones efficiently deliver estrogens to streams (e.g. the Maungatea Stream on the farm's boundary). To mitigate these exports, the effectiveness of BMP scenarios was evaluated in ArcSWAT, including constructed wetlands, riparian buffer strips, grazing management, and effluent application timing management. All BMPs reduced estrogen and sediment delivery to some degree, but their performance varied.

Constructed wetlands placed at critical drainage points showed the greatest overall impact, trapping 50-90% of sediment from upstream areas and removing an estimated 30-70% of estrogen loads via sedimentation, sorption, and microbial degradation in wetland ponds. Riparian buffers were similarly effective: vegetated buffer strips along stream channels filtered runoff, resulting in sediment transport reductions of about 16-80% (average ~42%) in high-erosion subbasins and estrogen concentration reductions on the order of 30-85% in runoff, through enhanced infiltration and filtering of hormone-laden sediment. Improved grazing management (e.g. rotational grazing and reduced stocking rates in wet periods) yielded moderate benefits, with an average ~17.5% decrease in sediment loss (due to better soil cover and less compaction) and commensurate declines in runoff (~12%) and estrogen exports. Effluent management (avoiding manure irrigation during wet weather and optimizing application rates) provided 5-25% lower sediment losses and up to 10-30% reductions in runoff, thereby modestly cutting estrogen runoff concentrations (5-50%). Notably, after implementing an effective riparian buffer scenario, peak estrogen levels in runoff from the worst areas fell from ~19.1 ng/L (baseline) to below 7 ng/L, and peak sediment yields dropped from ~3900 kg/ha to under 1000 kg/ha.

These quantitative improvements underscore that targeted BMP adoption can substantially reduce estrogen loading to surface waters. The catchment modelling highlighted where and which interventions yield the greatest water-quality benefits: for instance, combining wetlands and buffers in the most critical subbasins would address both high runoff and erosion, greatly reducing the transport of both dissolved and particle-bound estrogens to streams.

Table of Contents

List of Figures

List of Tables

Chapter 1
Introduction

This chapter presents the background, research objectives, scope, and justification of the study focused on modelling estrogen transport in New Zealand dairy farming systems. It outlines the motivation for modelling estrogen (estrone (E1) and 17β-estradiol (E2)) using MATLAB, along with a watershed-scale modelling approach employing Arc SWAT for Best Management Practices. Together, these approaches aim to provide a comprehensive understanding of estrogen dynamics from paddock to catchment scale.

1.1 Background

Dairy farming in New Zealand has undergone significant intensification over the past few decades. Herd sizes and milk production have increased rapidly, driven by economic incentives, and this has entailed greater use of inputs such as fertilizer, imported feed, and irrigation water (Hawke & Summers, 2006a). The national dairy herd had grown by roughly 100,000 cows per year in recent years, and most farms were more densely stocked (DairyNZ, 2016). According to the latest data from the 2023-2024 (DairyNZ, 2024), the national dairy herd has experienced a decline over the past decade, with a 5% decrease in the number of milking cows. This reduction contrasts with the earlier trend of annual increases. However, despite the decrease in cow numbers, milk production has remained relatively stable. In the 2023-2024 season, dairy companies processed 20.5 billion liters of milk containing 1.88 billion kilograms of milk solids, representing a 0.5% increase in milk solids compared to the previous season (DairyNZ, 2024). The Waikato region exemplifies this trend: it hosts about 23% of New Zealand's dairy cows on pasture-based farms (DairyNZ, 2016) and 22.9% from the latest data (DairyNZ, 2024). Figure 1.1 illustrates the distribution of dairy cows in New Zealand. While this expansion underpins a multi-billion-dollar industry, it also raises environmental concerns. Intensive dairy land use contributes to elevated nutrient runoff, sediment loss, and microbial contamination of water bodies (Burkitt et al., 2017).

Recent attention has turned to less visible contaminants, such as steroid hormones, that are excreted by cattle and may enter soils and waterways through farm effluent disposal. Indeed, dairy farm effluent has been identified as a source of endocrine-disrupting contaminants in the environment (Goeury et al., 2022). As stocking rates and effluent loads increase, the potential

for these micro-pollutants to affect surrounding soil and water resources increases (Betteridge et al., 1999; Proffitt et al., 1995).

Steroid hormones like estrone (E1) and 17β-estradiol (E2) are natural endocrine-disrupting chemicals (EDCs) of particular concern in dairy farming systems (Fenner-Crisp et al., 2000; Pagsuyoin et al., 2012). These estrogens are produced by livestock and can be released into the environment via manure and urine (J. B. Gadd, Tremblay, et al., 2010). Once applied to land (e.g. when dairy effluent is irrigated onto pastures), a portion of E1 and E2 may be mobilized by rainfall runoff or percolate into the soil (Arnon et al., 2008). Although they occur at trace concentrations, natural estrogens are potent endocrine disrupting chemicals (EDCs) capable of interfering with the reproductive biology of wildlife (Colborn et al., 1994).

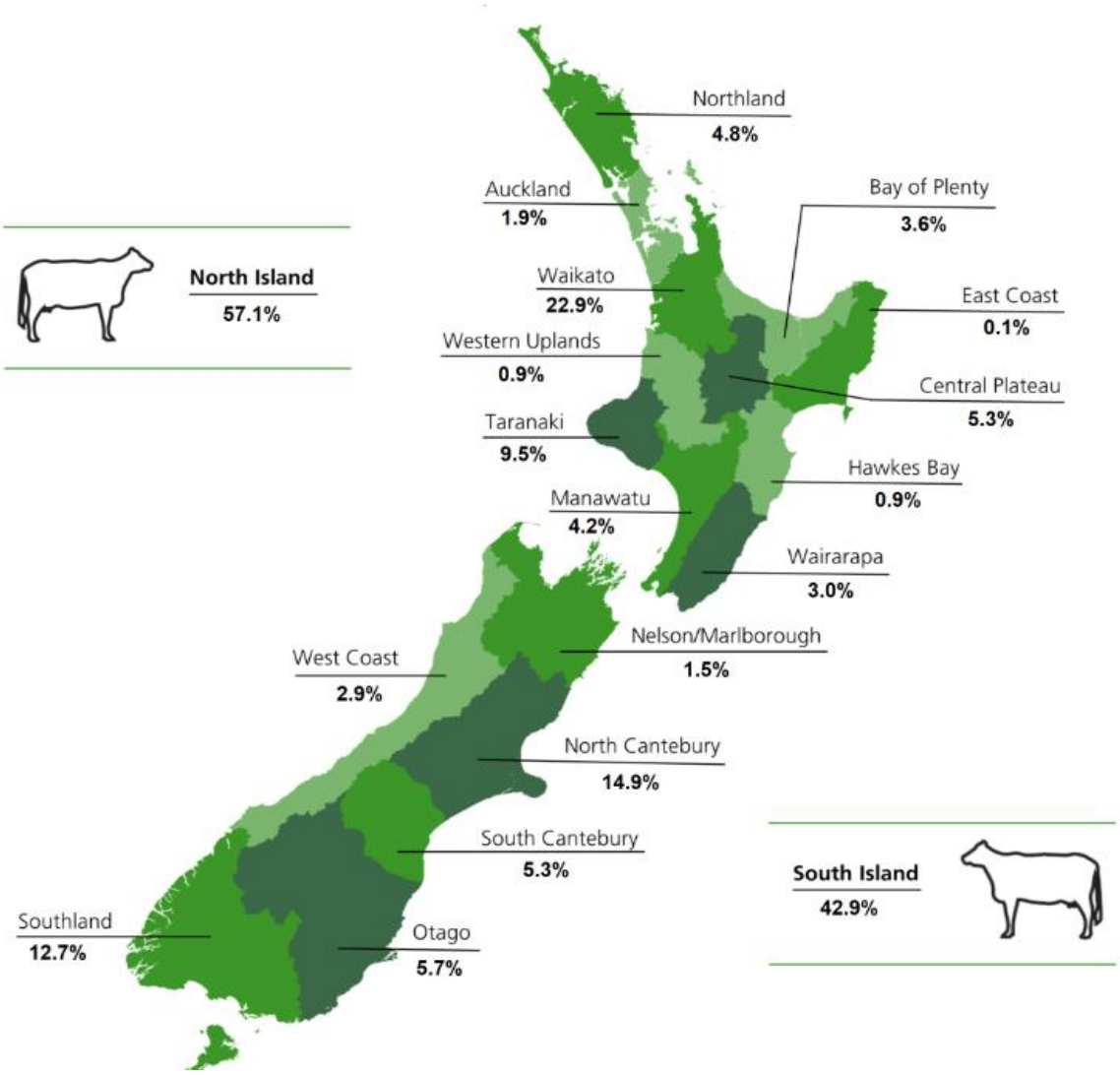

Figure 1-1 Regional distribution of dairy cows 2023-2024 (DairyNZ, 2024)

Studies have shown that even nanogram-per-litre levels of E1 or E2 in water can cause endocrine effects such as the feminization of fish and reproductive impairments in aquatic organisms (Baldigo et al., 2015; Thorpe et al., 2003). Livestock-derived estrogens have been detected in soils, drainage waters, and streams near agricultural sites around the world, confirming that land-applied manures can introduce these hormones into the environment (Goeury et al., 2022; Hanselman et al., 2003; Jenkins et al., 2008; Ying et al., 2002). Once released, their persistence and transport are governed by a range of factors. In soil, estrogens tend to sorb strongly to organic matter and fine particles, which can retain them near the surface (Yamamoto et al., 2003). Over time they can degrade biologically, but degradation rates vary and are influenced by temperature, moisture, and microbial activity (Bai et al., 2015; Stumpe & Marschner, 2010a).

Field studies report estrogen half-lives on the order of days to weeks under typical conditions, indicating that these compounds may persist long enough to be transported during rainfall events (Bradley et al., 2009; Jenkins et al., 2008). Strong sorption causes a fraction of E1/E2 to become attached to soil and sediment, which can later be carried into waterways via erosion and runoff. Sediment loss from pastures not only degrades water quality but also serves as a carrier for sorbed estrogens, facilitating their movement into streams (Burkitt et al., 2017; Lambert et al., 1985; L. Lee et al., 2003). During storm events, surface runoff can rapidly mobilize both dissolved and particle-bound hormones into drainage networks (Biswas et al., 2017; Jenkins et al., 2006). Conversely, a portion of the hormones can infiltrate downward with percolating water, potentially leaching to shallow groundwater if not degraded in the soil profile (Arnon et al., 2008; Mahjoub et al., 2011). Given these dynamics, there is a clear need to understand the fate and transport pathways of E1 and E2 in agricultural landscapes that experience high loads of manure in the form of direct grazing cows or effluent application. Accurately predicting how much estrogen will remain in soils versus export to water is critical for assessing ecological risks.

Additionally, if estrogenic compounds enter drinking water sources, they could also pose human health risks over long-term exposure (Colborn et al., 1994; Fenner-Crisp et al., 2000), although ecological impacts are the primary worry. In New Zealand, the pasture-based dairy farming context presents a unique combination of high hormone loading and vulnerable receiving environments (Foote et al., 2015). The humid, temperate climate of regions like Waikato leads to regular rainfall-driven runoff, which can transport farm contaminants into

nearby streams. Meanwhile, the free-draining soil profiles on many dairy farms create pathways for leaching under certain conditions.

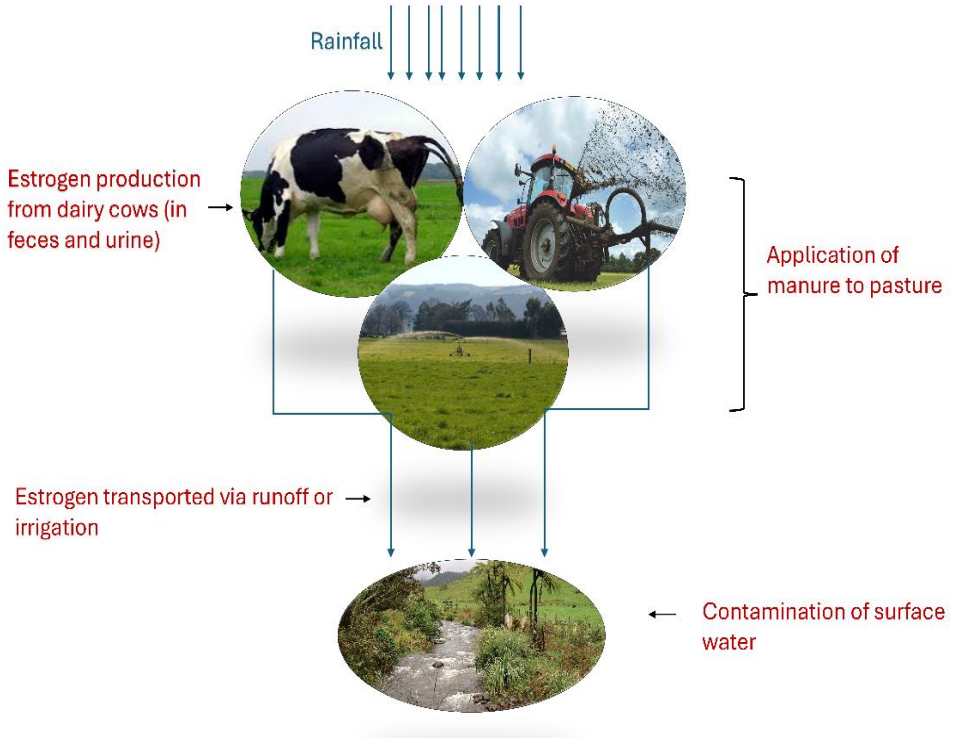

Figure 1-2 Pathways of estrogen transport from dairy farms to surface waters through manure application, rainfall, runoff, and irrigation

This combination of surface runoff and infiltration processes means that steroid hormones may travel via multiple routes. Figure 1.2 illustrates estrogen transport pathways from dairy farming systems. Estrogens excreted by dairy cows via feces and urine are applied to pastures through manure irrigation. Rainfall and irrigation mobilize estrogens, resulting in surface runoff and potential contamination of nearby water bodies. Understanding these transport mechanisms is required for developing strategies to mitigate estrogen pollution. Modelling offers a valuable approach for this purpose, allowing simulating of estrogen behaviour under varying conditions of soil, hydrology, and management. In fact, given the complexity of measuring trace contaminants across a landscape, simulation tools are increasingly seen as critical for predicting contamination risks and informing mitigation strategies (Donovan & Monaghan, 2021; Hildebrand et al., 2006; Jenkins et al., 2008; Mitasova et al., 1996; J. Prater, 2012a). The following sections outline the objectives and scope of this thesis, which is centered on modelling the fate and transport of E1 and E2 in a New Zealand dairy farming environment.

1.2 Research Questions and Objectives

The primary objective of this research is to develop and apply two independent modelling approaches to simulate and assess estrogen transport from dairy farms. The first approach involves developing a detailed numerical model for estrogen transport in unsaturated soils using Richards' and Green-Ampt's equations and advection-dispersion processes, implemented in MATLAB. The second approach applies the ArcSWAT model via ArcMap to simulate surface runoff, sediment yield, and estrogen transport across the entire dairy farm. This parallel modelling approach ensures a comprehensive understanding of estrogen transport at both soil profile and watershed scales.

This thesis addresses the following questions related to estrogen transport in dairy farming environments and provides insights into the role of environmental factors, management practices, and landscape characteristics.

- What is the fate and transport of estrogen (E1 and E2) under typical dairy farm conditions?
- Should we be concerned about estrogens for groundwater pollution or surface water pollution?
- Where are the critical source areas (hotspots) for estrogen and sediment runoff on the farm?
- How effective are best management practices (BMPs) in reducing estrogen and sediment transport to waterways?

To answer these questions, the study pursues four objectives:

- To develop a numerical model to simulate estrogen transport within agricultural soils based on the Green-Ampt model for infiltration and Richards' equation for soil water dynamics and advection-dispersion mechanisms for estrogen transport. The model outputs are cross-checked with laboratory column studies for validation and accuracy.
- To independently apply the Arc SWAT (Soil and Water Assessment Tool) model using ArcMap for spatial data analysis and hydrological simulation of estrogen transport at

the watershed scale. Laboratory-derived data are used as model inputs, while field validation remains a task for future research.

- To identify critical source areas (hotspots) of estrogen contamination across the dairy farm using Arc SWAT outputs, enabling targeted mitigation strategies.
- To evaluate the effectiveness of selected best management practices (BMPs), such as constructed wetlands, effluent management, grazing management and riparian buffers, in reducing estrogen contamination at the catchment scale.

Through these objectives, the thesis presented detailed numerical modelling and catchment-scale analysis to comprehensively assess steroid hormone transport in an intensive grazing system. The outcomes are expected to improve our ability to predict estrogen contamination and to design effective control strategies.

1.3 Research Scope and Justification

1.3.1 Scope of Research

In this research, we developed a customized numerical model specifically designed to simulate the transport of estrone (E1) and estradiol (E2) in soil. A key innovation of this model is the incorporation of the Green-Ampt equation to represent surface infiltration processes, effectively capturing the dynamics of wetting front movement influenced by macropores and preferential flow pathways.

This approach addresses the limitations of previous modelling studies that often relied on generic, built-in models lacking customization for specific contaminants like estrogens. By focusing on the unique transport characteristics of E1 and E2, this model provides a better understanding of their behavior in soil, offering valuable insights for environmental management and policy development.

Most existing environmental models and past studies have focused on either leaching in the soil or runoff at the watershed scale, but not both simultaneously for steroid hormones. Common farm-scale models in New Zealand (e.g. Overseer, SPASMO) (F. X. M. Casey et al., 2003a; Michael Dunbier et al., 2013; Sarmah et al., 2005) and widely used watershed models (e.g. SWAT, GLEAMS, HYDRUS) (A. Leonard et al., 1987; Neitsch et al., 2011; Simunek & van Genuchten, 1999) were originally developed to track nutrients and sediments, and they do not explicitly account for estrogen's unique behaviours such as sorption and degradation.

While various best management practices have been recommended to curb nutrient and sediment loss from farms, their efficacy for removing or reducing steroid hormones is not well documented. In particular, constructed wetlands and similar treatment systems are known to attenuate pollutants and are suggested as a mitigation option for farm effluents, but there is little quantitative analysis of how effective they are at filtering out estrogens under field conditions. No widely used catchment-scale model currently includes estrogen removal processes in BMP features. This represents a gap in our ability to evaluate management interventions for estrogen pollution. By modifying the Arc SWAT model to simulate scenarios with and without BMPs (such as wetlands or buffer zones), this thesis provides spatial modelling assessments of estrogen mitigation strategies at the farm scale. The results will help determine how much improvement in water quality can be expected from such practices, specifically regarding E1 and E2 loads.

1.3.2 Justification of the Study

The Waikato region of New Zealand, characterized by its high density of dairy farming, provides both the motivation and an appropriate setting for this study. With nearly a quarter of the nation's cows located in Waikato (DairyNZ, 2016, 2024), the region's soils and waters receive a substantial and continuous input of livestock-derived contaminants, including E1 and E2. The combination of intensive farming and the region's rainfall patterns makes surface runoff an important pathway for contaminant movement. At the same time, Waikato's free-draining allophonic and pumice soils present a risk of leaching into groundwater (McLeod et al., 2019; Sarmah et al., 2008a). This environmental vulnerability means that any hormone pollution from farms could readily spread into natural water systems, highlighting an urgent need for mitigation in this area. Focusing the study on a representative Waikato dairy farm ensures that the findings will be directly applicable to local conditions where the risk is high, and can inform regional environmental management and policy.

Moreover, improving predictive modelling tools for estrogen transport has practical significance for both regulators and farmers. Currently, water quality regulations and farm effluent management plans mostly target nutrients (nitrogen, phosphorus) and sediment, largely because models for these are well-developed and their impacts are well known. Incorporating hormones into environmental models will enable stakeholders to also consider EDCs in their decision-making. If we can reliably simulate where and when estrogen losses occur on a farm, we can design better intervention strategies and guide resource allocation

(such as placing a wetland in a location that intercepts the majority of estrogen-laden runoff). In the long term, such modelling supports proactive mitigation planning, helping to evaluate the benefits of improved effluent treatment, grazing management changes, or landscape engineering (like wetland construction) before they are implemented on the ground. Given that experimental trials for hormone mitigation can be logistically challenging and time-consuming, a model provides a cost-effective means to test scenarios and support evidence-based policy.

1.4 Thesis Structure

This thesis is organized into eight chapters. Following this general introduction, the other seven subsequent chapters are:

Chapter 2 presents a detailed literature review on estrogen fate and transport in the environment and on existing modelling approaches. It reviews known processes influencing estrogen mobility in soils and water (sorption, degradation, runoff, etc.) and evaluates prior models and studies, thereby establishing the context and parameters for the modelling work undertaken.

Chapter 3 describes the study site - a dairy farm in Whitikahu, Waikato, including its physical characteristics and management practices. Key details about the farm's soil types, topography, climate, effluent management system, and land use are provided to ground the modelling in a real-world scenario.

Chapter 4 the thesis develops a soil infiltration and unsaturated transport model for E1 and E2. This chapter outlines the numerical model built (in MATLAB) to solve the Green-Ampt infiltration and Richards' equations for water movement, coupled with convection-dispersion equations for estrogen transport with sorption and decay. Simulation results are presented to illustrate how estrogens leach through the soil under rainfall events and how soil properties affect their retention or movement.

Chapter 5 then focuses on the data preprocessing and ArcSWAT setup for watershed-scale modelling. It details how spatial data (DEM, land use, soil maps) and farm management data were processed, how the ArcSWAT model was configured for the catchment, and how estrogen fate parameters were integrated into SWAT's framework.

Chapter 6 presents the results of the hydrological and estrogen transport simulation at the catchment scale. This includes analysis of surface runoff patterns, sediment yields, and the modelled concentrations/loads of E1 and E2 in different sub-basins of the farm. The chapter identifies hotspots of estrogen and sediment loss, examines seasonal variations, and discusses the implications for contaminant pathways on the landscape.

Chapter 7 evaluates best management practices (BMPs) using the ArcSWAT model under various scenarios. It investigates how interventions such as constructed wetlands, riparian buffers, or changes in effluent application influence runoff volume, sediment export, and estrogen loads. By comparing scenario outcomes, this chapter assesses the potential effectiveness of BMPs in reducing estrogen contamination.

Chapter 8 presents conclusions and recommendations, serves as the final chapter of this thesis, consolidating the findings from both the numerical modelling of steroidal hormone transport through soil profiles and the GIS-based modelling of estrogen transport via surface runoff and sediment yield and provides recommendations.

Together, these chapters build a comprehensive understanding of steroid hormone transport from paddock to catchment and offer insights into mitigating their environmental impact in New Zealand's dairy farming systems.

Chapter 2

Literature Review: Estrogen Fate, Transport, and Modelling Approaches

2.1 Introduction

This chapter reviews existing modelling approaches for estrogen fate and transport in surface water and groundwater systems. It discusses the key processes influencing the estrogen movement, evaluates different modelling frameworks, and identifies critical gaps in current research. Numerical modelling provides a structured approach to simulate these processes, integrating key parameters that influence estrogen behaviour in soil environments. However, the accuracy of such models depends heavily on the quality and relevance of input data. This chapter also reviews literature-derived parameters used in the estrogen transport model developed in this study. These parameters include sorption coefficients, degradation rates, advection-dispersion properties, and soil hydraulic characteristics, among others. A range of modelling approaches has been used to study contaminant transport in agricultural systems (see Section 2.14), primarily focusing on nutrients, sediments, and pesticides at either soil-profile or catchment scales. However, these models rarely represent the specific behaviour of steroidal hormones, and Best Management Practices (BMPs) are often evaluated indirectly using nutrient or sediment proxies. Within this context, the present study adopts a dual-scale modelling approach, as outlined in Chapter 1, to explicitly examine estrogen transport and BMP performance.

Estrogens, particularly estrone (E1) and 17β-estradiol (E2), are among the most studied endocrine-disrupting chemicals (EDCs) due to their potential ecological and human health risks. These compounds, primarily excreted by livestock, poultry, and humans, enter aquatic systems through manure application, wastewater discharge, surface runoff, and leaching into groundwater (Hanselman et al., 2003; Ying et al., 2002). Even at nanogram-per-liter (ng/L) concentrations, estrogens have been shown to cause feminization of fish, reproductive impairments, and population-level effects in aquatic organisms (Vajda et al., 2011). Their persistence in the environment is influenced by sorption, degradation, and transport processes, which vary based on soil properties, microbial activity, and hydrological conditions (Arnon et al., 2008; Stumpe & Marschner, 2010a). Given their potential to accumulate in sediments and enter drinking water supplies, accurate modelling of estrogen fate and transport is critical for predicting contamination risks and informing mitigation strategies (Barel-Cohen et al., 2006; Shore & Shemesh, 2003).

Over the last two decades, there has been a major increase in intensity in dairy farming in New Zealand. The increase in dairy farm intensity has required an increase use of some external inputs, in fertilizer, feed and water, which experience significant environmental impacts (Foote et al., 2015). In the year ending March 2023, the dairy sector contributed $11.3 billion to New Zealand's GDP, accounting for 3.2% of the total. Of this, dairy farming contributed $8 billion (2.2% of GDP), while dairy processing added the remainder (Maciver, 2023). Over the past 15 years, the national herd size has grown at a rate of approximately 102,000 cows per annum, and the total (effective) dairy farmed area has increased by approximately 28,000 ha per annum (Laurenson et al., 2017). According to the most recent New Zealand Dairy Statistics 2023-24 report, the Waikato region continues to host the largest proportion of dairy cows, accounting for approximately 22.9% of the national herd. Following Waikato, North Canterbury contributes about 14.9% of the national cow population. Southland, known for its cooler climate and favorable soil conditions, supports approximately 12.7% of New Zealand's dairy cows. Taranaki, another historically important dairy farming area, accounts for approximately 9.5% of the national herd (DairyNZ, 2024).

2.2 Endocrine-Disrupting Chemicals (EDCs)

According to the United States Environmental Protection Agency (USEPA) (Fenner-Crisp et al., 2000), endocrine disruptors, such as steroid hormones, are chemicals that can interfere with the synthesis, secretion, transport, binding, action, or removal of natural hormones in the body that are responsible for maintenance, reproduction, development, and/or behaviour. Endocrine disruptors (EDs) or also known as endocrine disrupting chemicals (EDCs), can also bind to hormone receptors in aquatic organisms and can activate or interfere with hormone synthesis and metabolism (Bhandari et al., 2015; Zhao et al., 2019). From EDCs produced from dairy farm effluent, steroid hormones (estrogens) are considered the most researched chemical in past (Bilal and Iqbal, 2019; Colucci et al., 2001; Combalbert et al., 2012; Johnson et al., 2006; Liu et al., 2012; Nghiem et al., 2004; Qi and Zhang, 2016; Yamamoto et al., 2003; Zhang et al., 2016).

Estrogenic hormones are mainly discharged by humans and animals into the soil and water environment either directly or after undergoing some wastewater treatment processes, which are not commonly designed or capable of removing such contaminants. Manure-borne estrogenic hormones can pose a high potential risk to aquatic life (Bai et al., 2015). There is a major concern over the fate and transport of these waste-borne steroidal estrogens, as manure

spray on agricultural land, these compounds lead to endocrine disruption in aquatic species, even at very low concentrations (Lee et al., 2018; Tyler et al., 1998).

EDCs include a range of substances that have been shown to exhibit endocrine disrupter activity. These include both natural and man-made chemicals, including alkyl phenols (APs), phthalates, bisphenol-A (BPA), pesticides, steroidal hormones and inorganic substances such as cadmium and mercury (Spengler et al., 2001). This research will focus mainly on the steroid hormones' transport and fate in the natural environment.

2.3 Impact of Steroid Estrogens on Human Health and the Environment

2.3.1 Human Health Risks of Steroid Estrogens

Estrogens are an essential part of normal human body functions, but have potentially serious adverse effects if they are accumulated in the environment and enter the human and animal food supply. High consumption of estrogens above the threshold level can increase the heart disease and high risk of cancer in humans (Adeel et al., 2017). Excessive estrogen exposure in humans has been linked to a range of adverse health effects, as reported by other studies (Diamanti-Kandarakis et al., 2009; Guillette & Gunderson, 2001; Heindel et al., 2015; Schug et al., 2013; Shore & Shemesh, 2003; Vandenberg et al., 2012) such as,

- Increased risk of breast cancer in women due to estrogen receptor activation (Diamanti-Kandarakis et al., 2009)
- Disruptions in metabolic functions leading to obesity, insulin resistance, and diabetes (Heindel et al., 2015)
- Bone disorders caused by altered calcium homeostasis and osteoporosis(Vandenberg et al., 2012).
- Reproductive health impacts, including hormonal imbalances, menstrual irregularities, and infertility(Schug et al., 2013; Shore & Shemesh, 2003)
- Testicular abnormalities and inflammation, with observed decreases in sperm quality and function and increased risks of prostate cancer and developmental disorders (Adeel et al., 2017).

Human exposure to steroid estrogens occurs through multiple pathways, including ingestion of contaminated water and food, and inhalation of airborne particles. Long-term exposure to even trace amounts of estrogens can lead to hormonal disruptions, particularly in pregnant women, infants, and individuals with endocrine-related diseases (Guillette & Gunderson, 2001).

2.3.2 Environmental Fate and Transport of Steroid Estrogens

Sarmah & Northcott (2008) described Endocrine-disrupting chemicals (EDCs) are a class of pollutants that have raised concerns due to their potential to interfere with the hormonal systems of wildlife and humans. EDCs encompass a wide range of substances, including natural and synthetic hormones, industrial chemicals, pesticides, and pharmaceuticals. These compounds can enter the environment through various pathways, such as wastewater treatment plant effluents, agricultural runoff, and industrial discharges (Kopperi et al., 2016). Understanding the fate and behaviour of EDCs in the environment is crucial for assessing their potential risks and developing effective mitigation strategies (Aris et al., 2014; Khanal et al., 2006; Shrestha et al., 2012; Ying et al., 2002). The persistence of EDCs in environmental compartments like water and soil is a critical factor influencing their potential for long-term exposure and ecological impact (Guillette & Gunderson, 2001).

The complexity of estrogen sorption mechanisms, noting that various soil properties influence the sorption behaviour of steroid estrogens (Bonin & Simpson, 2007). The transport of steroid hormones through soil is also influenced by hydrological factors, such as rainfall and irrigation practices. The transport of manure-borne testosterone under varying rainfall conditions was investigated by You & Zhang (2016), revealing that the intensity of rainfall significantly affects the leaching and runoff of these hormones to waterbodies. Similarly, Arnon et al (2008) discussed how interactions between hormones and manure, along with preferential flow paths in the soil, can enhance the transport rates of these contaminants to groundwater. This shows the importance of considering hydrological dynamics when modelling the fate of steroid hormones in agricultural systems.

Moreover, the environmental impact of steroid hormones extends beyond their transport and degradation. The presence of these hormones in soil can lead to bioaccumulation in plants and aquatic organisms, posing risks to food safety and ecosystem health. For example, studies have shown that the application of biosolids and wastewater effluents to agricultural land can result in higher levels of steroid hormones in crops, raising concerns about potential endocrine disruption in consumers (Shargil et al., 2015). Also, biological processes dominate the degradation of steroids under various environmental conditions, suggesting that the risks associated with these hormones may be overestimated if solely based on their chemical persistence (Gineys et al., 2012). The occurrence of steroid hormones in different environmental matrices, such as sediments and runoff, further complicates the assessment of

their ecological risks. The challenges in detecting low levels of estrogens in urban estuaries emphasise the need for sensitive analytical techniques to monitor these contaminants (Reddy & Brownawell, 2005). Similarly, S. Liu et al. (2012) reported the presence of various steroids in swine and dairy cattle farms, indicating that farming practices significantly contribute to the environmental loading of these hormones. This points to the necessity for comprehensive monitoring and management strategies to mitigate the impact of steroid hormones in agricultural landscapes.

2.4 Physiochemical Properties of Steroid Hormones

The fate and transport of endocrine-disrupting chemicals (EDCs), including steroid estrogens, are primarily governed by their physicochemical properties (Figure 2.1). A detailed understanding of these properties is essential for predicting their partitioning behavior, mobility, and transformation in the soil-water environment. Due to their hydrophobic characteristics, most EDCs, including estrogens, exhibit a strong tendency to adsorb onto solid surfaces rather than remain in the aqueous phase (Tong et al., 2019). The key physicochemical parameters influencing estrogen transport include the octanol-water partition coefficient (K_{ow}), aqueous solubility, and Henry's Law constant (H_c). These properties determine sorption potential, volatilization tendency, and dissolution behaviour. Hc is their volatilisation potential and is also an indicator of the likelihood of evaporation during the treatment process. Whereas K_{ow}, this coefficient represents the equilibrium concentration ratio of a compound in n-octanol and water, providing an estimate of hydrophobicity. Higher K_{ow} values indicate greater affinity for organic matter and sediment adsorption, leading to reduced mobility in aqueous systems (Baronti et al., 2000). Estrogens with high K_{ow} values tend to persist longer in the environment by accumulating in sediments rather than remaining in dissolved form. The stability of estrogens largely depends on their physicochemical behaviour. The water solubility and water-octanol coefficient (K_{ow}) physicochemical properties are found to play an important role in controlling the stability of estrogens in the environment. A high Kow value shows that estrogens have highly hydrophobic properties and tend to adsorb onto sediment and accumulate in the environment for a long time (Aris et al., 2014). It is considered that free estrogens are less soluble than conjugated estrogen. However, pH can affect the solubility of estrogens, such as at pH 4 and pH 7 water solubility of estrogens was the same and in order of E1 to E2, and least one was 17 α -ethynylestradiol EE2, but at pH 10 relative solubility of estrogens is considered higher (Adeel et al., 2017). Table 2.1 presents some key physiochemical properties of steroid hormones.

Table 2-1 Physicochemical properties of steroid hormones (Adeel et al., 2017; Aris et al., 2014; Sarmah et al., 2006).

Compound	**Formula**	**Molecular weight**	**Water solubility (mg/l at 20 °C)**	**Vapor Pressure (mm Hg)**	**Log K_{ow}**
Estrone (E1)	$C_{16}H_{22}O_2$	270.4	13	$2.3 *10^{-10}$	3.43
17β-estradiol (E2)	$C_{18}H_{24}O_2$	272.4	13	$2.3 *10^{-10}$	3.94
Estriol (E3)	$C_{18}H_{224}O_3$	288.4	13	$6.7 *10^{-15}$	2.81
17α-ethynylestradiol (EE2)	$C_{20}H_{24}O_2$	296.4	4.8	$4.5 *10^{-11}$	4.14

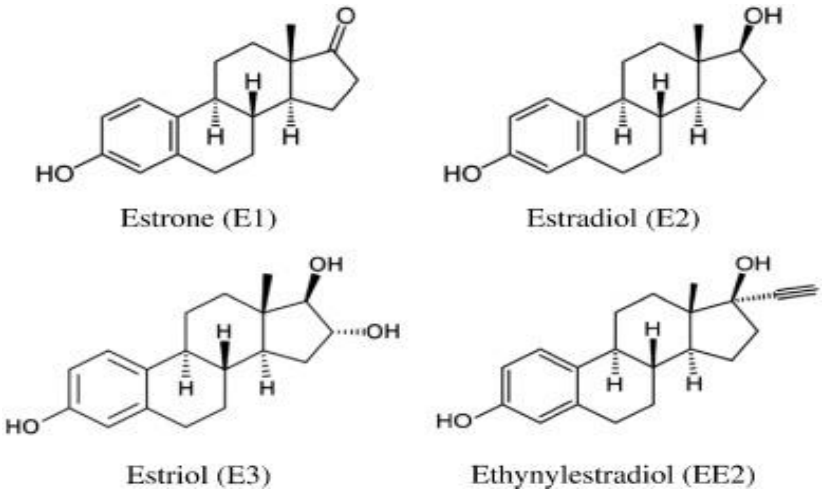

Figure 2-1 Physicochemical properties and structure of natural and synthetic estrogen hormones (Aris et al., 2014)

The partitioning behaviour of estrogens between aqueous and solid phases is a key factor influencing their environmental fate. Strong sorption to organic matter, sediments, and sludge reduces the volatilization and photodegradation, prolonging their persistence in the environment (Baronti et al., 2000). Additionally, environmental factors such as soil organic carbon content, pH, and microbial activity further modulate the mobility and degradation rates of estrogens in natural systems.

Sorption dynamics play a crucial role in controlling the mobility and bioavailability of estrogens in soil systems. Scherr et al. (2009) investigated the sorption behaviour of estrone (E1) and estrone-3-sulfate (E1-3S), reporting that sorption isotherms were nonlinear, with E1-3S exhibiting a sorption potential one order of magnitude lower than E1. The effective distribution coefficient (K_{deff}) for E1 ranged from 34.2 to 71.7 L/kg, whereas for E1-3S, it was

lower (4.0-4.9 L/kg). These results indicate that conjugated estrogens, such as sulphated forms, have much higher mobility than their free counterparts and may contribute more significantly to groundwater contamination.

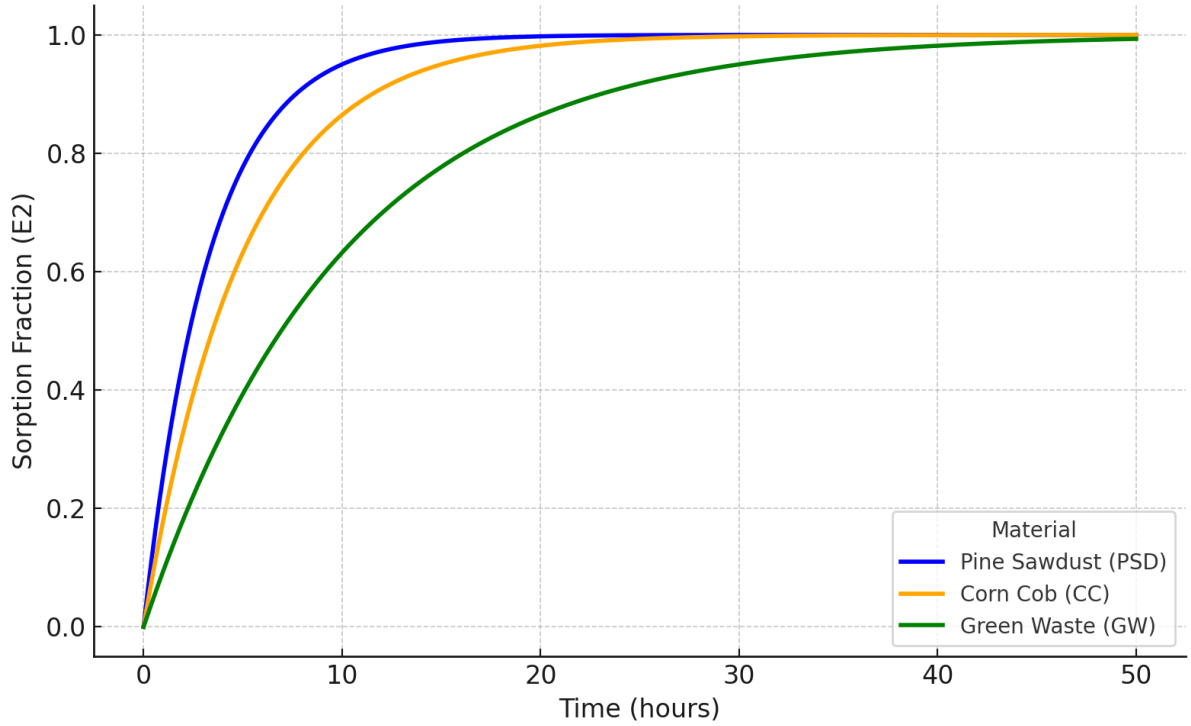

Figure 2-2: Estrogen (E2) Sorption rates over time for different materials (PSD, CC, GW) (based on data from Sarmah et al., 2010)

Further studies by Sarmah et al., (2010) examined the effect of biochar amendments on estrogen sorption in soil. The study found that adding biochar significantly increased the sorption affinity for both E2 and E1, with K_{deff} values for E2 rising from 35 to 311 L/kg depending on biochar type. The addition of 1% pine sawdust biochar led to a 1400% increase in E2 sorption, suggesting that biochar amendments could be a promising strategy for reducing estrogen leaching in agricultural soils, as shown in Figure 2.2.

A high K_{ow} value, coupled with low aqueous solubility, suggests that estrogens exhibit significant hydrophobicity, favouring sediment adsorption and long-term environmental accumulation (Aris et al., 2014). These physicochemical characteristics highlight the importance of sorption-desorption dynamics in controlling estrogen mobility and their potential impacts on aquatic and terrestrial ecosystems.

2.5 Dairy Farm and Steroid Hormones

In countries such as Australia and New Zealand, open grazing is a normal practice, and huge amounts of excreta are directly deposited onto pastureland. Several dairy farms dispose of their dairy farm effluent (both liquid and solid) directly on fields without any treatment, which actually comes from the dairy shed sump (Houlbrooke et al., 2004). The latest data from (DairyNZ, 2024) shows cows numbers increased by 0.6% to 4.7 million, still 2% below the five-year average of 4.8 million. Average herd size had increased to 448 cows per herd, with 10,485 herds nationally.

The application of dairy farm effluent (DFE) to pastureland is a double-edged sword. On one hand, it is a rich source of nutrients that enhance soil fertility and crop productivity, such as phosphorus and nitrogen (Jamal Abu-Ashour et al., 1994; Zanon et al., 2020). On the other hand, it is a potential source of contaminants, and pathogens including the faecal bacteria *Escherichia coli (E.coli), Salmonella, Campylobacter, Brucella abortus,* etc. (Aislabie et al., 2011) and steroid hormones (Hanselman et al., 2003; Yost et al., 2014; You & Zhang, 2016). The application of dairy farm effluent on agricultural land is reported to result in high crop productivity and soil fertility over a longer time as compared to inorganic fertiliser (Fan et al., 2017; Zanon et al., 2020).

2.5.1 Types and Concentration of Steroid Hormones in Dairy Farm Effluent

The natural steroid hormones17β-estradiol (E2), estrone (E1), 17α-estradiol (17α) also written as (E2α), estriol (E3) and synthetic17α-ethinylestradiol (EE2) are the most dominant estrogens found in the natural environment and naturally produced by humans and animals and are frequently detected in dairy farm effluent and the surrounding environment (Combalbert et al., 2012; Tyler et al., 1998; Gineys et al., 2012; Sarmah et al., 2006)). Estrone (E1) is the most abundant and could be detected in most of the water and soil samples (Lee et al., 2018; Lei et al., 2009; Sarmah et al., 2010). Although all estrogens have adverse effects on aquatic organisms, estrogens have the greatest endocrine-disrupting potencies, there are inconsistencies within the literature (Zhao et al., 2019). Nghiem et al. (2004) reported that natural estrogenic hormones such as estrone (E1) and 17β-estradiol (E2) have much endocrine-disrupting potency and can be many thousand times higher than that of other synthetic chemicals. However, Thorpe et al. (2003) findings imply that EE2 is approximately 11 to 27 times more potent than E2, while E2 is 2.3 to 3.2 times more potent than E1. Synthetic pharmaceutical estrogens are considered more potent than natural estrogens (Tyler et al., 1998).

E2 is the primary metabolite with the highest potency, whereas 17α and E1 are considered secondary metabolites with low potency. E3 is known to be the final metabolite with the least potency (Khanal et al., 2006). Dairy cows commonly excrete 17α, E2, E1, and E3 (Gadd et al., 2010), while other animal species mainly excrete E2, E1, and E3 (Khanal et al., 2006; Shore and Shemesh, 2003).

Sarmah et al. (2006) and Sarmah et al., (2008) range the of steroid estrogens from 1 to 48 ng L^{-1} for E2, 1 to 76 ng L^{-1} for E1, and < 1 to 7 ng L^{-1} for EE2 in dairy effluent samples collected from several dairy farms across the Waikato region of New Zealand. It is observed that human females excrete about 5 μg/day each of estrone and estradiol and males about 10 mg/day of androgens, however, the amount of excreted estrogens of pregnant women can be 1000 times higher, depending on the stage of pregnancy (Shore and Shemesh, 2003). A non-pregnant dairy cow can excrete approximately 0.8-1.2 mg/day of 17α, and a non-pregnant cow excrete approximately 0.6-1.4 mg/day of E1; whereas a pregnant dairy cow could excrete up to 11.4 mg/day of 17α, and a pregnant sow excretes up to 10.8 mg/day of E1 (Khanal et al., 2006). Daily faecal estrogen excretions of a cow are reported 1820 - 4080ug/d in China (Liu et al., 2012). The excretion rates and types of estrogens differ in different species, such as dairy farm effluent containing a large amount of 17α over E2, however, 17α is rarely found in swine and poultry manures (Khanal et al., 2006).

Table 2-2:Estrogen hormones in the excretion of livestock (Excretion amount in ug/day per 100 kg live animal weight) (Khanal et al., 2006).

Steroidal Hormone origin		**Estrone (E1)**	**17 β -estradiol (E2)**
Cattle	Bulls (slurry)	<2	<2
	Milk cows (slurry)	255-640	170-1230
	Milk cows (10 days before parturition)	840-1000	42.2-700
Swine	Swine (slurry)	<2-84	<2-64
	Sow (faeces, late gestation)	15-28	N/A
Poultry	Immature broilers (male and female)	Total 65-133	
	Hens(laying)	254	533
	Roosters	670	93

Dairy farm effluent is mainly composed of urine and faecal matter. Free estrogens are dominant in faeces and conjugated estrogens are primarily excreted in urine. Most of the estrogen (E2 and E1) excreted in cow faeces is in free form, and the contribution of urine, where estrogen is present in the form of conjugates, to the total estrogen excreted is commonly less than 20%

(Gadd et al., 2010; Shore and Shemesh, 2003). The conjugate forms normally include sulphate and glucuronides, such as estrone-3-sulphate, 17-estradiol-3-sulphate, 17β-estradiol-3-glucuronide and 17-estradiol-3,17-disulfate (Ma and Yates, 2017). 17α-estradiol is found at the highest concentration (730 ng/L) in dairy farm effluent followed by estrone (E1) (100 ng/l), 17β-estradiol (E2) (24 ng/L) and conjugated estrogens (estrone-3-sulphate, 17α-estradiol-3-sulphate and 17β-estradiol-3,17-disulfate) were in the range of 12-320 ng/L which is 22% of total estrogens (Gadd et al., 2010). These conjugated estrogens can get into free estrogen in the presence of bacteria *E.coli*. *E coli* produces Beta-glucuronides an enzyme that has the ability to de-conjugate estrogens into free estrogens (Andaluri et al., 2012).

2.6 Sources and Occurrence of Steroidal Estrogens in the Environment

Steroid hormones, once excreted, enter the soil and water systems through various pathways, including direct deposition, effluent irrigation, and runoff from pasture. Their mobility and persistence are largely influenced by sorption to soil particles, biodegradation, hydraulic conductivity, and preferential flow pathways (Colucci et al., 2001; Yamamoto et al., 2003). Livestock excrete estrogens as part of natural metabolic processes, releasing them into the environment via faeces and urine. It has been estimated that sheep, poultry, and dairy cows collectively produce approximately four times more estrogens than the entire human population in the UK, with dairy cows contributing the largest proportion (Johnson et al., 2006).

The primary source of steroidal estrogens in the environment is livestock excretion, including cattle, pigs, and sheep, which account for a significant proportion of environmental endocrine-disrupting chemicals (EDCs) (Bilal & Iqbal, 2019). Agricultural activities further contribute to the introduction of estrogens into the environment through pesticide application, land spreading of sewage biosolids and dairy farm effluent irrigation. These activities introduce substantial amounts of 17β-estradiol (E2) and estrone (E1) into soil and water systems (Baronti et al., 2000; Fan et al., 2008a; Khanal et al., 2006). In the United States alone, dairy cattle contribute nearly 90% of the total estrogen load (Zheng et al., 2012). The concentration of free and conjugated estrogens in dairy farm effluent varies, typically ranging between 40 to 200 ng/L, with notable contributions from urine, faeces, and wash-down water from milking parlours (Tremblay et al., 2018).

Field studies have confirmed the presence of steroidal estrogens in surface runoff, raising concerns about their persistence in aquatic environments. A study conducted in New Zealand

found estrogen concentrations exceeding detection limits in 67% of surface runoff samples, with estrone (E1) being the most frequently detected estrogen, present in 63% of samples at concentrations ranging from 0.63 to 400 ng/L. Other estrogens, such as 17α-estradiol (17α-E2), were detected in 24% of surface water samples, with concentrations ranging from 0.65 to 2400 ng/L, while 17β-estradiol (E2) was found in 9% of samples, with levels ranging from 1.3 to 2400 ng/L. Estriol (E3) was present in 4% of samples, with concentrations between 3.2 and 470 ng/L (Mina et al., 2016). These findings indicate that estrogens persist in surface runoff, posing potential risks to aquatic ecosystems.

Steroidal estrogens have also been detected in natural water bodies, including rivers, lakes, ponds, and groundwater, across different geographic regions (Dutta et al., 2010; Steiner et al., 2010a). However, their concentrations in stream water are generally low, often below 1 ng/L (Shore & Shemesh, 2003). The contamination of groundwater occurs primarily through leaching from surface applications of dairy farm effluent, improperly managed manure storage systems, and septic system failures. A study in Japan reported E2 concentrations of 32.9 ng/L in river water, highlighting the potential for surface water contamination from land-based sources (Matsuoka et al., 2005). The extent of estrogen leaching into groundwater depends on soil composition, rainfall intensity, and preferential flow pathways, which can accelerate its transport through the soil matrix (Aislabie et al., 2011).

The binding behaviour of estrogens in the soil varies significantly, influencing their retention or transport to groundwater. Research from Bonin & Simpson (2007) suggests that estradiol (E2) and testosterone tend to bind to the soil matrix at shallow depths (approximately 5 cm). However, while testosterone has been detected in groundwater, E2 remains largely bound to the upper soil crust (Shore & Shemesh, 2003). A contrasting study found that 88% of testosterone was retained in the soil, with no evidence of testosterone leaching beyond 20 cm (Qi & Zhang, 2016). Laboratory-based investigations further support these findings, with studies indicating that E2 concentrations in surface water ranged from 150 to 2300 ng/L in pasture runoff containing dairy farm effluent (Casey et al., 2003). Similarly, a New Zealand study found estrogenic activity in 83% of surface water samples and 75% of groundwater samples, suggesting widespread contamination across dairy-intensive regions (Tremblay et al., 2018). In dairy farming watersheds, Tremblay et al. (2018) found that estrone was the predominant estrogen detected in waterways, with concentrations ranging from non-detectable to 4.2 ng/L, while 17α-estradiol and 17β-estradiol were detected at lower concentrations. The

measured estrogenic activity, represented as 17β-estradiol equivalents (EEq), ranged from 0.02 to 1.44 ng/L in stream water samples. Gadd and Tremblay et al. (2010) measured the concentrations of 17α-estradiol, estrone (E1), and 17β-estradiol (E2) in dairy shed effluent, reporting ranges of 110-11,000 ng/L, 10-580 ng/L, and 1-310 ng/L, respectively. Additionally, conjugated estrogens, mainly estrone-3-sulfate, were detected in most effluent samples at concentrations ranging from 12 to 180 ng/L. Similar findings were reported by Sarmah et al. (2006), who found that dairy farm effluent contained 17β-estradiol at concentrations of 19-1360 ng/L and estrone at 41-3123 ng/L, significantly higher than those in piggery or goat farm effluents. The total estrogen load in dairy effluent varied between 60 and 4000 ng/L.

The direct excretion of steroid hormones by livestock into water bodies is considered a major contributor to estrogen contamination, often outweighing the impact of agricultural pathways such as manure application and runoff. Unlike human-derived estrogens, which primarily enter water bodies via wastewater treatment plant effluents, livestock-derived estrogens are directly deposited into the environment through grazing and farmyard runoff. This unregulated deposition creates more complex and variable pathways of estrogen transport, heavily influenced by hydrological conditions, soil type, grazing intensity, and farm management practices (Johnson et al., 2006).

Given the widespread occurrence of steroidal estrogens in surface and groundwater systems, it is evident that dairy farm effluent and direct livestock excretion serve as major contributors to environmental estrogen loads. The variability in soil retention, surface runoff dynamics, and preferential flow pathways further complicate the prediction of estrogen transport and accumulation in the environment. These factors highlight the need for improved effluent management practices and comprehensive monitoring programs to better understand and mitigate the risks associated with steroid hormone contamination in agricultural landscapes.

2.7 Quantities of Dairy Farm Effluent Produced in New Zealand

The annual livestock estrogen discharge in the United States and European Union is estimated at 83,000 kg/yr, which is about twice the rate of human estrogen discharge (Adeel et al., 2017). In New Zealand, Australia and Europe, open grazing is a common practice which results large amount of excreta being deposited on pasture land directly. However, on dairy farms, such as milking sheds and collecting yards, 6 to 10% excreta is deposited. Dairy farm yards and milking areas are regularly cleaned daily, producing effluent of approximately 50 L per cow per day

(Bolan et al., 2009). The contribution of water to effluent also comes from rainfall-runoff over the milking shed yard roof. In New Zealand, it is estimated that about 70 million m^3 of effluent is generated from dairy sheds, 50 million m^3 from meat processing plants and 4 million m^3 from pig farms annually (Saggar et al., 2004). Some key NZ studies summarised in Table 2.3.

Table 2-3: Summary of some of New Zealand's estrogen studies and their key findings

(J. B.Gadd, Tremblay, et al., 2010)	Concentrations of 17α-estradiol (110-11,000 ng/L), estrone (10-580 ng/L), and 17β-estradiol (1-310 ng/L) in dairy shed effluents. Conjugated estrogens, primarily estrone-3-sulfate (12-180 ng/L), contribute significantly to total estrogen load. 17α-estradiol contributes significantly to overall estrogenic activity despite lower potency than 17β-estradiol.
(Sarmah & Northcott, 2008)	DT50 values for 17β-estradiol (0.24-1.5 d), 17α-ethynylestradiol (0.29-1.1 d), in river water-sediment slurries. DT90 values for the same compounds range from 0.9 to 2.8 days under both aerobic and anaerobic conditions, 5.1 to 4.69 days.
(Tremblay et al., 2018a)	Estrone is the predominant steroid estrogen in dairy farm watersheds (ND-4.2 ng/L). 17α-estradiol and 17β-estradiol are detected at lower concentrations. Estrogenic activity (EEq) ranges from 0.02 to 1.44 ng/L in stream water.- Direct discharge, cattle access to streams, and runoff contribute to estrogen contamination
(Sarmah et al., 2006a)	Dairy effluent has higher levels of 17β-estradiol (19-1360 ng/L) and estrone (41-3123 ng/L) than piggery or goat effluent.- Total estrogen load varies from 60 to ~4000 ng/L in dairy effluent.
(Steiner et al., 2010a)	E1 and E2 are transported through soil via preferential/macropore flow and colloidal-enhanced transport. - Mass recoveries of E1 (0.3-13%) and E2 (0.06-0.7%) in leachate from 70 cm soil depth- Developed a state-space mixing-cell model for E1 and E2 transport. used a range of retardation factor (*R*) values from the literature to model estrogen transport. The *R* factor values ranged from 42 to 249 for E2 and 14 to 137 for E1.
(Scherr et al., 2009)	Sorption isotherms of estrone (E1) and estrone-3-sulfate (E1-3S) are nonlinear.- E1-3S has lower sorption potential than E1. - Kd_eff values for E1 (34.2-71.7 L/kg) and E1-3S (4.0-4.9 L/kg) in soils. Mediator solution (CaCl2 vs. artificial urine) significantly influences sorption.
(Sarmah et al., 2010)	Biochar amendment increases soil sorption affinity for E2 and E1. Kd_eff values for E2 range from 35 to 311 L/kg in biochar-amended soils. - Pine sawdust biochar shows the highest sorption capacity.
(J. B.Gadd, Northcott, et al., 2010)	The effectiveness of two passive secondary biological treatment systems, the two-pond system (2PS) and the advanced pond system (APS)in reducing steroid estrogen concentrations and estrogenic activity in dairy shed effluent (DSE) in New Zealand, E1 and 17α-Estradiol were the dominant estrogens detected, with reductions of up to 100% in some cases

2.8 New Zealand Dairy Farm Effluent System

New Zealand has 448 cows per herd, with 10,485 herds and most of the time, cows are kept on pasture (DairyNZ, 2024). The cows are milked twice a day during the 9-month dairy season. Cows spend 2.5 to 3 hours in the milking parlour per day. During this time, urine and faecal waste accumulate in the parlour, which is then washed away using high-pressure hoses, requiring large volumes of water for cleaning (Sukias et al., 2003). The application of farm dairy effluent (FDE) to land instead of direct discharge to the water body is a common mechanism for disposal in New Zealand. The dairy farm in the Waikato region, FDE application to pasture land has risen from 35% in 1997 (Longhurst et al., 2000) to 100% in 2004 (Hawke and Summers, 2006). Land application of FDE liquid as irrigation and solid as solid fertilizer can provide valuable organic matter and nutrients to the soil, however, mismanagement and improper application timing can lead to groundwater and surface water contamination (Hawke and Summers, 2006).

Dairy farm effluent can be dealt with as liquids, slurry or solids. Liquid effluent, which contains solid material less than 10% and can be conveyed through gravity flow, pumps or using piping system and is treated in oxidation ponds or by land application as irrigation water. The second type of dairy farm effluent is slurry, which contains 10 to 20% solids and requires a vehicle spreader for land application. Effluent with more than 20% solids is known as sludge, which requires mechanical spreading equipment commonly with scrapers, buckets and front-end loaders (DairyNZ, 2011, 2015)

Effluent treatment in New Zealand is primarily carried out through land application or oxidation ponds, which facilitate sedimentation, biological treatment, and nutrient recycling. These systems are designed to reduce environmental contamination, though their effectiveness depends on farm-scale management, climate conditions, and soil properties. Further details about the oxidation ponds and effluent treatment systems are described in Chapter 3.

2.9 Mechanisms for Estrogenic Hormone Removal

The removal of steroidal estrogens from wastewater and dairy effluent occurs through physical removal, biological degradation, and chemical advanced oxidation (CAO) (Koh et al., 2008; Z. Liu et al., 2009). However, biodegradation contributes less than 10% to estrogen removal, necessitating additional treatment methods (Koh et al., 2008).

2.9.1 Physical Removal

Physical methods include adsorption onto activated carbon and membrane filtration. Activated carbon adsorption is effective due to its high surface area, but high costs and difficult regeneration limit its large-scale use (Choi et al., 2005; Huang et al., 2019; Sophia A & Lima, 2018). Membrane filtration, especially nanofiltration (NF) and reverse osmosis (RO), removes over 95% of steroid estrogens and other contaminants (Kim et al., 2007; Nghiem et al., 2004; Ternes et al., 2002; Urase et al., 2005). Carbon nanotubes (CNTs) also show high efficiency in removing estrogens like EE2 and BPA (Babaei et al., 2016; Joseph et al., 2011).

2.9.2 Biological Degradation

Biological treatment, mainly activated sludge, trickling filters, and bioreactors, plays a key role in reducing estrogenicity in wastewater. Activated sludge systems can remove up to 88% of EDCs, with efficiencies of 83% for E1, 99.9% for E2, and 78% for EE2 (Johnson et al., 2000; Ternes et al., 2002). However, conjugated estrogens may deconjugate, leading to secondary contamination (Andersen et al., 2003; Svenson et al., 2003).

In dairy effluent treatment, (J. B. Gadd, Northcott, et al., 2010) evaluated two passive treatment systems: a two-pond system and an advanced pond system, both designed to remove estrogens from dairy effluent. They found that anaerobic treatment increased free estrogen concentrations due to deconjugation, but subsequent aerobic treatment significantly reduced total estrogen levels. Winter months showed lower efficiency, highlighting the need for enhanced seasonal treatment strategies.

2.9.3 Chemical Advanced Oxidation (CAO)

CAO involves strong oxidants to degrade estrogens via oxidation-reduction reactions (Deng & Zhao, 2015; Z. Liu et al., 2009). Ozone oxidation effectively removes residual estrogens after aerobic treatment (Ermawati et al., 2007). The pyrolysis of biosolids removes >95% of estrogens, producing biochar with reduced hormonal activity for soil amendment (Hoffman et al., 2016). Modified biochar, enhanced through steam activation and chemical treatment, improves adsorption capacity (Ahmed et al., 2016; Klinar, 2016; Sarmah et al., 2010).

A coagulation-based method has also been developed to flocculate and settle colloidal particles in dairy effluent, reducing E. coli concentrations by 90% and lowering health risks to farm workers (Cameron & Di, 2019; Huang et al., 2019) and could, in principle, reduce estrogens.

Effective estrogen removal requires integrated treatment strategies. Physical methods like activated carbon and membranes provide high efficiency but are costly. Biological processes, such as activated sludge, offer moderate removal but struggle with seasonal variations and deconjugation effects. Hybrid treatment approaches that combine physical, biological, and chemical processes are increasingly recognised as a promising means of improving overall estrogen removal by leveraging the strengths of individual methods. CAO, pyrolysis, and biochar present promising long-term solutions, although further optimization is needed for widespread application in dairy effluent management, and care would be needed to make it economically and practically feasible at the farm scale.

2.10 Half-Lives of Estrogens

The half-life of estrogens depends primarily on their degradation rate and reflects the time required for their concentration to decrease by half. First-order decay kinetics is commonly used to determine estrogen half-lives, while degradation rates can be estimated from decay curves (Adeel et al., 2017). The persistence of estrogens varies across different environmental conditions, with higher degradation rates in summer than in winter. For instance, estrone (E1) and 17β-estradiol (E2) degrade within five days in summer but take around seven days in winter (Matsuoka et al., 2005). However, 17α-ethinylestradiol (EE2) exhibits significantly lower degradation rates compared to E1 and E2, making it more persistent.

Due to their hydrophobic properties, estrogens generally have short half-lives in water and sediment, ranging from 2 to 6 days (Adeel et al., 2017). Estrogens typically degrade in both soil and water, ultimately mineralizing into carbon dioxide and other byproducts (Colucci et al., 2001). The half-lives of E1 and E2 vary across soil types. For instance, in loamy soil, E1 and E2 degrade within 0.92 and 0.29 days, while in sandy loam, E1 degrades in 1.7 days and estriol (E3) in 0.22 days. In silt loam, degradation times for E1 and E2 are 0.61 and 0.48 days, respectively by Colucci et al. (2001). The half-lives of estrogens in surface water are generally shorter than in soil or sediments. Cao et al. (2010) estimated the half-lives of E1, E2, and EE2 in water as 4.1, 3.33, and 83.3 days, respectively. In contrast, estrogens persist longer in soil, with half-lives of 8.3 days for both E1 and E2 and 330 days for EE2. Sediments show even greater persistence, with E1 degrading in 42 days, E2 in 4.2 days, and EE2 persisting up to

1700 days (Cao et al., 2010). Fan et al. (2007) results indicated that 6% of E2 and 63 % of testosterone could be mineralised to CO_2 and other polar compounds through abiotic chemical processes under both aerobic and anaerobic conditions. The half-life of steroid estrogens is estimated to be approximately 2 to 6 days in surface waters and sediments. However, E2 is found most readily biodegradable and can even degrade under various anaerobic conditions. EE2 is considered relatively more resistant to biodegradation (Yu et al., 2004). In surface water, E1 is found more persistent than E2 and in greater quantities, it is because of the conversion of other estrogens to E1 (Casey et al., 2003; Fan et al., 2007).

2.11 Interconversion Cycle of Estrogens

Estrogens such as estrone (E1), 17β-estradiol (E2), and estriol (E3) undergo reversible metabolic transformations, forming a dynamic interconversion cycle influenced by microbial activity (Casey et al., 2003; Fan et al., 2007; Goeppert et al., 2014). Certain microorganisms, including *Escherichia coli (E. coli)*, can deconjugate estrogens, facilitating their conversion between different forms (Figure 2.3). Several studies confirm that E1 is the primary degradation product of E2, indicating a dominant conversion pathway in soil and wastewater environments (Casey et al., 2003; Fan et al., 2007).

Microbial activity plays a crucial role in estrogen transformation within soil and runoff. Mansell et al. (2011) reported a 25% decrease in 17α-estradiol, accompanied by an equivalent increase in E1 and E2, suggesting microbial-mediated interconversion. Similarly, Prater et al., (2015) observed the oxidation of E2 to E1, followed by the reconversion of E1 to E2 within 24 hours in swine manure, highlighting the rapid cycling of estrogens in manure-rich environments.

However, not all estrogens exhibit efficient biodegradation under anaerobic conditions. Cajthaml et al., (2009) found that EE2 (5 mg/L) remained undecomposed in anaerobic environments, concluding that EE2 degradation is significantly slower compared to natural estrogens. This persistence suggests that EE2 may accumulate in anaerobic sediments, posing a long-term environmental risk.

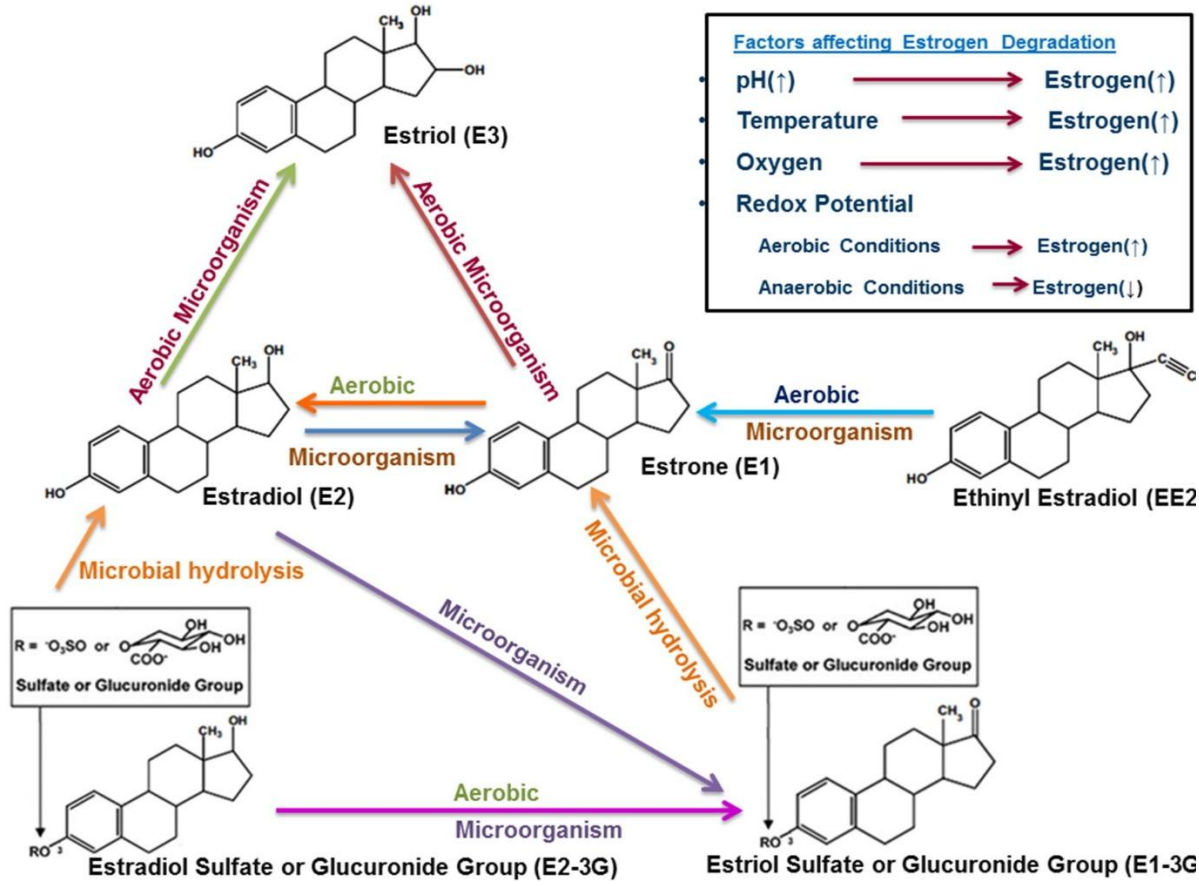

Figure 2-3: Natural and synthetic estrogens interconversion pathways (Adeel et al., 2017)

2.12 Transformation Processes of Estrogens

Estrogens undergo multiple transformation pathways in the environment, including sorption to soil and sediments, biotransformation, photo transformation, and plant uptake (S. Bircher et al., 2015; Caupos et al., 2011; Colucci et al., 2001; Hildebrand et al., 2006; Peterson et al., 2005; Shrestha et al., 2012; Y. Zhang et al., 2016). These processes determine estrogen attenuation, influencing their mobility, persistence, and bioavailability.

2.12.1 Sorption to Sediments and Soils

Sorption is a process that controls the fate and transport of estrogens in soil. Due to their hydrophobic nature, estrogens tend to sorb to sediments, exhibiting low water solubility and high octanol-water partitioning coefficients (K_{ow}) (Andaluri et al., 2011; S. Bircher et al., 2015; Hildebrand et al., 2006). However, during high-intensity rainfall events, sorbed estrogens can

be mobilized, increasing their potential for groundwater contamination (Qi & Zhang, 2016; Tong et al., 2019).

Sorption behaviour is influenced by soil characteristics, including pH, organic matter content, texture, and moisture (Yamamoto et al., 2003). Colucci et al., (2001) found that estrogen sorption increases with soil moisture content and temperature. Fine sediment particles enhance hormone retention, affecting their persistence in aquatic systems (Y. Zhang et al., 2016).

Sorption processes are often modelled using adsorption isotherms, including Freundlich, Langmuir, and Temkin models, which help predict the partitioning of estrogens between solid and liquid phases. Freundlich sorption isotherms are widely used for estrogen transport predictions in soils and sediments (Fan et al., 2007, 2008; Tong et al., 2019; Z. Yu et al., 2004) .

2.12.2 Biotransformation

Microbial degradation plays a key role in estrogen transformation, occurring under both aerobic and anaerobic conditions (S. Bircher et al., 2015; Robinson et al., 2017). Aerobic biotransformation is faster, with up to 99% removal efficiency (Ermawati et al., 2007). Anaerobic conditions, however, lead to slower degradation rates, prolonging estrogen persistence (Zheng et al., 2012).

Factors influencing biotransformation include temperature, moisture content, and initial estrogen concentrations (Zheng et al., 2012). Xuan et al., (2008) observed that estrogen degradation increased with soil moisture (10 - 20%) and temperature (15 - 25°C), with peak degradation at 35°C. Additionally, conjugated estrogens can undergo hydrolysis, converting them into free estrogens, and further influencing their fate (Bai et al., 2015).

2.12.3 Photo transformation

Photodegradation is a major removal pathway for estrogens in surface waters, occurring via direct and indirect photo transformation. Indirect photodegradation, which involves dissolved organic matter (DOM) and humic acids, enhances degradation rates more effectively than direct photo transformation (Caupos et al., 2011). Chowdhury et al., (2010) found that humic acid can increase estrogen degradation, while higher initial estrogen concentrations reduced photo transformation efficiency.

Studies show that photodegradation can remove up to 67% of E1 (Caupos et al., 2011; Chowdhury et al., 2010). These findings suggest that light-mediated transformation can significantly reduce estrogen concentrations in surface waters under favourable conditions.

2.12.4 Plant Uptake

Plants can absorb estrogens from soil and water, particularly in riparian buffer zones, where they help reduce estrogen loads from agricultural runoff (S. Bircher et al., 2015). Although limited research exists, Card et al. (2012) detected estrogens in maize root tissues at concentrations up to 0.19 μmol/g, while Bircher et al., (2015) observed E2, EE2, and zearalenone uptake in poplar trees, demonstrating their potential for estrogen removal.

Plant uptake efficiency depends on root uptake mechanisms, transpiration stream tension, and chemical properties like the octanol-water partitioning coefficient ($LogK_{ow}$) (S. Bircher, 2011). Optimal estrogen uptake occurs at $LogK_{ow}$ values of 1.0 -3.5, while higher values (>4) indicate strong sorption to roots rather than translocation. Wetland plants such as *Scirpus validus* and *Populus deltoides nigra* have shown the ability to remove E1, E2, E3, and EE2 from contaminated water (S. Bircher, 2011). Imai et al. (2007) showed the *Portulaca oleracea* (a garden plant) in Japan, has a great ability to remove EDCs such as E2 from water and this plant is not very effective at estrogen concentrations up to 250 μM (micro-molar) and temperature from 15 to 30 and pH from 4 to 7.

2.13 Effect of Dairy Farm Effluent Application on Soil

The increasing intensity of dairy farming has led to greater use of fertilizers and effluent applications to maintain soil fertility and crop productivity. In New Zealand, commonly used inorganic fertilizers include phosphate fertilizers (e.g., superphosphate), nitrogenous fertilizers (e.g., urea, ammonium sulphate), and compound fertilizers (e.g., di-ammonium phosphate, DAP) (Foote et al., 2015). However, dairy farm effluent (DFE) application is an alternative, cost-effective method for returning essential nutrients to the soil. It is estimated that 60-85% of the total nitrogen in DFE is available for plant uptake (Barkle et al., 2000). While 80-90% of applied nutrients are retained in soil treatment systems, a portion reaches freshwater bodies, posing environmental risks (Houlbrooke et al., 2004). To prevent nutrient leaching and runoff, effluent should be applied when soil moisture deficits allow storage in the soil profile (R. Monaghan et al., 2008; R. M. Monaghan & Smith, 2004).

2.13.1 Soil Types and Hydraulic Properties in the Waikato Region

The Waikato region contains 400 different soil structures, dominated by Pumice (21.7%) and Allophanic (22.2%) soils, which are well-drained with rapid infiltration rates (DJ Houlbrooke et al., 2010; Hewitt, 1993). Most Waikato dairy farms are located on rolling volcanic landscapes (>7° slope), where DFE application can influence soil properties. Effluent irrigation has been linked to gradual changes in hydraulic conductivity, although these changes are difficult to measure (Hawke & Summers, 2006b).

2.13.2 Impact of Dairy Effluent on Soil Physical Properties

Studies indicate that the land application of organic wastes such as compost and poultry manure improves soil porosity, macro-porosity, saturated hydraulic conductivity, and water retention (Mbagwu, 1989). Similarly, DFE application increases phosphorus, nitrogen, and potassium levels (Ahaneku, 2014). Research on Horotiu and Te Kowhai soils in Waikato found that effluent irrigation decreased bulk density in Horotiu soils, while macro-porosity remained unchanged in both soils and soil pH increased (Sparling et al., 2001). Additionally, high organic matter in DFE improves long-term soil fertility, but effluent application can also clog pores and reduce soil hydraulic conductivity (Cook et al., 1994; Hawke & Summers, 2003).

The transport of bacteria (e.g., *E. coli*) from dairy effluent occurs primarily through rapid water fluxes, particularly via preferential flow paths (Unc & Goss, 2004). Soil water movement occurs through matrix flow (uniform infiltration), preferential flow (via cracks and macropores), and surface runoff. Preferential flow results in 1.5 to 2.5 times faster solute transport than expected (Jamal Abu-Ashour et al., 1994). The water-holding capacity of soil varies, ranging from 45-55 mm/m for sandy soils to 175-190 mm/m for clay soils (DairyNZ, 2015).

2.13.3 Microbial and Chemical Changes in Soil Due to Effluent Irrigation

A lysimeter study on four Waikato soil types found that free-draining soils (Waihou and Atiamuri) transported fewer microbes due to matrix flow, while poorly drained soils (Te Kowhai and Netherton) exhibited higher microbial transport due to macropore flow (Aislabie et al., 2011). Regular DFE irrigation increases soil organic carbon, pH, and nitrogen levels, influencing estrogen sorption and mobility (Barkle et al., 2000; Tong et al., 2019).

Effluent irrigation raises pH and electrical conductivity (EC) in topsoil layers but shows minimal impact beyond 40 cm depth (Hawke & Summers, 2003). Higher pH and temperature decrease the adsorption of estrogens like E2, enhancing their mobility (Tong et al., 2019). While inorganic nitrogen (NH_4^+ and NO_3^-) from effluent can be rapidly leached or absorbed by plants, organic nitrogen accumulates in soil crusts, affecting long-term nutrient cycling (Hawke & Summers, 2003; Hewitt, 1993).

2.14 Available Computer Models for Estimating Nutrient loss and Estrogens in New Zealand's Waterways

The prediction of nutrient and contaminant losses from agricultural land is increasingly important for both economic and environmental management. Intensified fertilizer use and increased dairy stocking rates have led to elevated nutrient levels and contaminants, including estrogens, in soil and waterways. However, direct measurement of nutrient losses is complex, making simulation models a crucial tool for assessing potential losses and evaluating the impact of land-use practices (Cichota and Snow, 2009). Several computer simulation models are commonly used in New Zealand to estimate nutrient runoff and transport at field and watershed scales. These models incorporate various land-use practices, soil properties, and hydrological processes to predict pollutant movement in agricultural landscapes. Some widely used models include:

- SWAT (Soil and Water Assessment Tool) – A widely used model for watershed-scale hydrology, nutrient transport, and sediment dynamics (Neitsch et al., 2011).
- GLEAMS (Groundwater Loading Effects of Agricultural Management Systems) – A model designed to simulate pesticide, nutrient, and sediment transport from agricultural lands (A. Leonard et al., 1987).
- ANSWERS (Areal Nonpoint Source Watershed Environment Response Simulation) – A field-scale model for runoff and erosion prediction (Faycal Bouraoui & Theo A. Dillaha, 1996)
- SPARROW (Spatially Referenced Regressions on Watershed Attributes) – A large-scale model for nutrient transport predictions in river networks (Elliot et al., 2005).
- OVERSEER – A New Zealand-specific model for predicting nutrient losses at the farm scale, widely used for farm management and policy assessments (Ledgard S F et al., 1999; Wheeler et al., 2009).

- MitAgator – Developed to identify critical source areas of nutrient and contaminant losses, integrating mitigation strategies at the farm level (Risk et al., 2015; W McDowell et al., 2014) (McDowell et al., 2014; Risk et al., 2015).
- NZ-FARM and ROTAN – Regional-scale models for nutrient loss estimation and economic assessments in New Zealand's river catchments (Cichota & Snow, 2009).
- SPASMO (Soil-Plant-Atmosphere System Model) and HYDRUS-1D – Models used to simulate water flow, solute transport, and nutrient leaching in soil (F. X. M. Casey et al., 2003b; Šimůnek et al., 2016, 2024) .

2.15 Limitations in Estrogen Transport Modelling and Development of an Estrogen Transport Model

While existing models effectively predict nutrient and sediment transport, they are not designed to simulate estrogen transport from dairy farm effluent applications to surface runoff and waterways. Most widely used models in New Zealand and internationally focus primarily on nitrogen, phosphorus, and sediment dynamics, but lack the capability to account for estrogen sorption, degradation, colloidal transport, and preferential flow pathways. This limitation hinders accurate predictions of steroid hormone contamination risks, particularly in pasture-based dairy farming systems where land-applied effluent serves as a key estrogen source.

To address this gap, a custom numerical model was developed in MATLAB to simulate estrogen transport in soil, incorporating key processes such as sorption, degradation, and colloidal transport. Additionally, the ArcSWAT model was modified to simulate surface runoff-driven estrogen transport, integrating field-specific hydrological and soil data for New Zealand dairy pasture systems.

This integrated modelling approach ensures:

- Realistic representation of estrogen transport, incorporating hydrological interactions, soil infiltration, and surface runoff dynamics.
- GIS-based spatial analysis of estrogen contamination risks across different landscapes and farm management practices.
- More accurate risk assessments, addressing the limitations of existing nutrient-focused models that do not account for estrogens.

The MATLAB-based numerical model and modified ArcSWAT framework provide a solution for predicting estrogen fate and transport in pastoral farming systems, allowing for better-informed environmental management strategies.

Subsequent chapters will present the model's development and application in New Zealand's dairy landscapes to assess estrogen transport through soil and surface water pathways.

Chapter 3

Dairy Farm Characterization: Soil, Hydrology, and Effluent Management

3.1 Introduction

This chapter describes the dairy farm selected for this research, focusing on characteristics that directly influence estrogen fate and transport. Accurate characterization of the farm, including its soil, climate, hydrology, and management practices, is essential for developing a reliable numerical model for estrogen transport through soil profiles and surface runoff. Specifically, the chapter details the farm's geographic and topographic setting, soil properties, dairy management practices, hydrological characteristics, vegetation coverage, and sources of estrogen inputs. Understanding these aspects provides a solid foundation for the modelling approaches presented in subsequent chapters, facilitating precise simulations and effective environmental risk assessments.

3.2 Description of the Study Area

The dairy farm selected for this study is located in Whitikahu, Waikato region, New Zealand (coordinates: 37°38'21"S, 175°20'56"E), approximately 20 km northeast of Hamilton city. The farm covers a total area of approximately 110 hectares, primarily utilized for pasture-based dairy farming.

The herd consists of 280 cows, with 120 actively milked. Milking operations follow a seasonal schedule, commencing in July and concluding in May, aligning with regional practices to optimize milk production during peak pasture growth periods. Cows are typically dried off during June and early July, allowing for rest before the subsequent calving season.

The farm employs a rotational grazing system, with cows primarily feeding on ryegrass-based pastures. To maintain optimal nutritional intake, especially during periods of reduced pasture growth, the diet is supplemented with silage. On average, pasture constitutes approximately 75% to 85% of the cows' diet, with supplements like maize silage comprising up to one-third of the total feed intake during summer months.

Farm infrastructure includes a herringbone milking shed, a feed pad facility, and an effluent storage system consisting of a single earthen pond designed to store dairy effluent prior to land application.

Topographically, the farm landscape is gently rolling, with slopes varying from approximately 3.4% to 14%, as determined by drone-derived digital elevation models (DEMs) 1m- Lidar. The average elevation range across the farm is from approximately 40 meters above sea level. This gently sloping terrain significantly influences surface runoff dynamics and infiltration patterns, essential considerations in modelling estrogen transport pathways.

The region experiences a temperate climate, characterized by mild summers and cool winters. Average annual rainfall is approximately 837 mm on the farm, distributed unevenly throughout the year, influencing seasonal soil moisture conditions and runoff generation. Temperature and evapotranspiration vary seasonally, further impacting farm hydrology and subsequent contaminant transport processes.

Detailed maps derived from GIS analysis and drone imagery illustrating farm boundaries, topography, slope direction, and major infrastructural features are provided to clearly visualize spatial characteristics influencing estrogen transport.

3.3 Seasonal Milking and Calving Management

Dairy farming in the Waikato region follows a seasonal cycle that aligns milking with peak pasture growth periods. Pasture growth is highest in spring, corresponding to peak milk production. Typically, cows are mated or artificially inseminated around early October, ensuring calves are born from mid-to-late July, thereby optimizing lactation during spring (MPI, 2024; Te Ara Encyclopedia of New Zealand,). Milk production gradually declines from autumn, with cows generally dried off between May and July. During the dry-off period, cows are relocated to feed pads or different areas of the farm to allow pasture recovery or renovation.

The calving period is strategically managed. Calves are usually separated from their mothers shortly after birth, once they have consumed colostrum-rich milk. Initially kept in warm, dry conditions, calves are fed milk through artificial systems, then gradually transitioned to cereal-based feeds and eventually to grass as their digestive system (rumen) develops. Female calves (heifers) are retained for future herd replacement, mated around 15 months to calve at approximately two years of age. Male calves (bull calves) are generally sold for beef production or slaughtered for veal. While traditional practice involves milking cows twice daily, a growing number of farms adopt once-a-day milking systems to reduce labour and operational costs,

accepting a slight reduction in milk yield for the operational advantages gained (Ministry for Primary Industries, 2024). In our dairy site milking once a day is adopted.

To provide a visual representation of the study site, Figures 3.1 to 3.8 present key farm infrastructure and operational features relevant to this research. These images illustrate essential components such as the milking shed, machinery storage, feed pad, silage storage, and effluent pond, which directly influence farm management practices, nutrient cycling, and estrogen transport processes. The effluent storage pond and feed pad are particularly important in understanding potential estrogen sources and their pathways in soil and water systems. By integrating these features into the numerical and GIS-based modelling framework, this study aims to assess how farm management practices influence estrogen fate and transport in surface and subsurface environments.

Figure 3-1: Aerial view of the dairy farm study site located in Whitikahu, Waikato region, New Zealand, highlighting important farm features relevant to estrogen transport modelling. Key features include: (1) milking shed; (2) farm machinery storage/garage; (3) residential building; (4) feed pad area; (5) silage storage area; (6) effluent storage pond; (7) pasture with visible slope influencing surface runoff; (8) nearby surface water stream adjacent to the effluent pond; and (9) farm tracks facilitating cow movement and paddock access

Figure 3-2: Aerial images showing key infrastructure of the dairy farm: (Top-left) milking shed; (Top-right) farm machinery storage and garage.

Figure 3-3: Feed pad and silage storage area at the dairy farm. The silage bunkers store both grass and maize silage, which are used to supplement pasture feed during periods of low grass availability.

3.4 Farm Management Practices

This section describes the farm management practices at the dairy farm.

3.4.1 Feeding and Nutrition Management

The farm follows a rotational grazing system, where cows are moved between paddocks to maximize pasture utilization and recovery. On average, pasture constitutes 75% to 85% of the cows' diet, while supplementary feed accounts for the remaining portion, ensuring consistent milk production and cow health.

To supplement pasture, silage made from grasses and maize is stored in dedicated silage bunkers on-site as shown in Figure 3.4. The farm utilizes both locally produced and imported silage to maintain a stable feed supply and is categorised as “System Four” (Ministry for Primary Industries, 2024). In 2021, the farm imported approximately 50 tonnes of grass silage and 80 tonnes of maize silage, while on-site production yielded 40 tonnes of grass silage and 120 tonnes of maize silage. This combination of local and external feed sources helps balance the cows' diet and mitigate seasonal fluctuations in pasture availability. During milking periods, cows also receive grain-based concentrates as part of their ration to improve energy intake. These feeds play a critical role in sustaining milk yield and reproductive efficiency, particularly when pasture protein content is insufficient.

Figure 3-4: The silage storage (left) and feed pad area (right), where supplementary feed is stored and distributed to cows when pasture growth is insufficient

3.4.2 Dairy Effluent Management

Effluent management is a key component of farm operations, ensuring nutrients are recycled efficiently while minimizing environmental impacts. The milking shed and feed pad areas generate large amounts of effluent, primarily from cow excreta, wash-down water, and feed waste (Figure 3.5). Standard wash-down water usage per cow is 50-70 litres per milking and a lactating cow produces approximately 50-60 kg of dung and urine per day (DairyNZ, 2020b)**.** On average, the study site produces approximately 21.66 m^3 of effluent per day, amounting to ~6,500 m^3 annually. The effluent is collected in a single earthen storage pond before being applied to pasture as fertilizer, enhancing soil fertility (Figure 3.6).

The effluent application follows a controlled land-spreading schedule to prevent overloading the soil with nutrients and minimize runoff risks. Application rates are determined based on soil moisture levels, pasture nutrient demand, and environmental regulations.

Figure 3-5: Milking shed facilities at the dairy farm. (Left) Inside view of the milking shed, where cows are milked using an automated milking system. (Right) Holding and entry area where cows line up before milking. A huge amount of effluent is generated in this area due to post-milking washdown, which contributes to the overall effluent load managed on the farm.

Figure 3-6: The effluent storage pond (images at different angles), where dairy effluent is collected before being applied to pasture as fertilizer.

3.4.3 Cow Movement and Paddock Access

The farm infrastructure includes well-maintained raceways connecting different paddocks (Figure 3.7), allowing for efficient cow movement between grazing areas and the milking shed. These raceways reduce soil compaction and erosion, contributing to better pasture health and improved water infiltration.

By integrating grazing strategies, supplementary feeding, and effluent management, the farm maintains efficient resource use while minimizing environmental impacts. These management practices directly influence nutrient cycling and contaminant transport, providing critical inputs for the estrogen fate and transport modelling discussed in later chapters.

Figure 3-7: Farm infrastructure for cow movement and water supply. (Left) A drinking water system is installed in the paddocks, ensuring cows have access to fresh water while grazing. (Right) Farm raceways connecting different paddocks, which facilitate cow movement between grazing areas and the milking shed

3.5 Farm Layout and Spatial Organization

A detailed farm map, Figure (3.8), is presented for understanding the spatial arrangement of key infrastructure, paddocks, and natural features, which influence farm operations, effluent management, and water movement. This Figure provides an overview of the study site, illustrating:

- Effluent management areas, including the effluent pond, feed pad, and bunker storage, which are important in determining nutrient and estrogen runoff risks.
- Raceways and paddock divisions are designed to optimize cow movement and rotational grazing while minimizing soil compaction and pasture damage.
- Natural features, such as waterways, bush reserves, and proposed wetland areas, which play a role in water quality regulation and biodiversity conservation.
- Hydrological elements, including water bores and surface drainage pathways, impact runoff, infiltration, and groundwater recharge.

This map provides a spatial reference for subsequent discussions on topography, hydrology, and land characteristics, which are further examined in Section 3.4. Understanding farm layout is crucial for assessing potential estrogen transport pathways, as the proximity of effluent zones to waterways can influence contaminant movement and environmental impact.

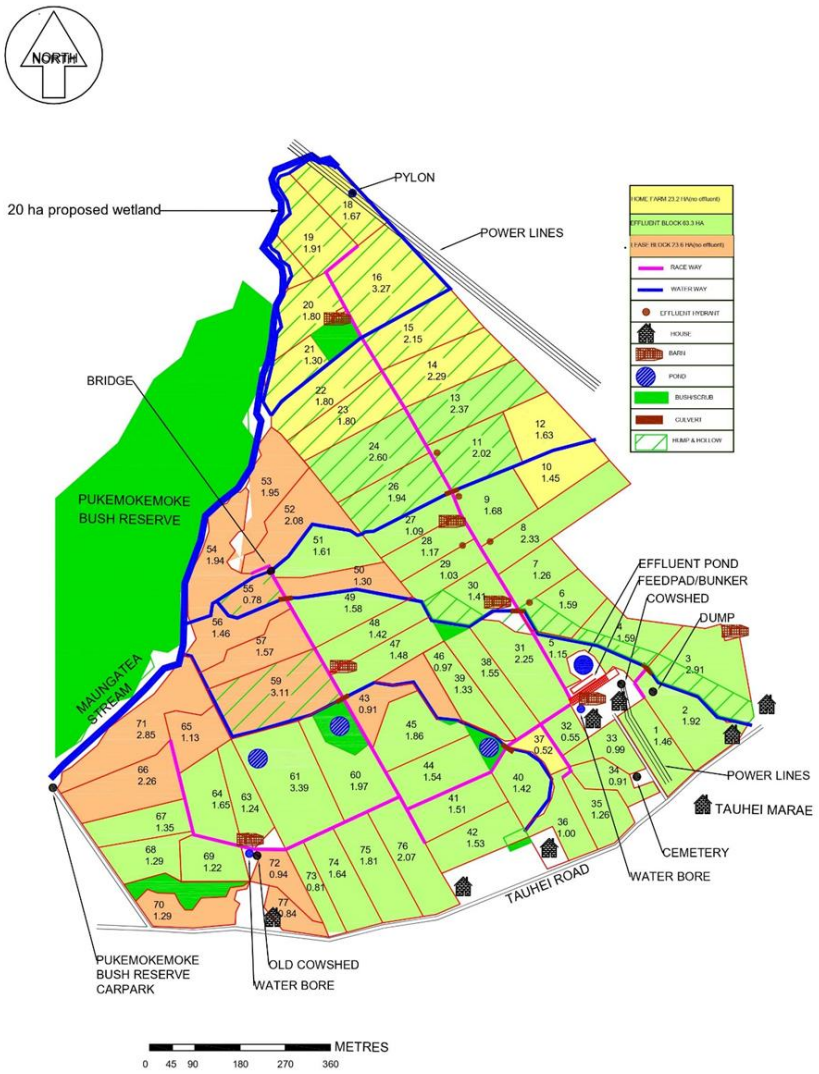

Figure 3-8: Spatial layout of the dairy farm, highlighting key features such as paddocks, raceways, effluent storage areas, waterways, and surrounding natural reserves.

3.6 Dairy Effluent Treatment Systems in New Zealand

Effluent management is a critical component of dairy farming in New Zealand, ensuring compliance with environmental regulations while maintaining soil and water quality. Various effluent treatment systems have been implemented across the country, ranging from passive treatment methods to advanced engineered solutions (Bolan et al., 2009). This section provides an overview of common effluent treatment systems in New Zealand and their relevance to the study site.

3.6.1 Passive Two-Pond System

The two-pond system has been widely used in New Zealand since the 1970s for treating dairy farm effluent. This system consists of an anaerobic pond (4-5 m deep), followed by an aerobic pond (1-1.5 m deep). The anaerobic pond facilitates the breakdown of organic material through microbial activity, releasing methane and carbon dioxide as byproducts. The aerobic pond, relying on natural aeration and algal photosynthesis, further degrades organic matter and removes suspended solids before discharge into a receiving water body (Craggs et al., 2004; Hawke & Summers, 2006a).

Despite its simplicity, the two-pond system has limitations. Effluent discharge from oxidation ponds still contains organic matter, nutrients, and suspended solids that can impact water quality. Elevated nutrient levels, particularly nitrogen and phosphorus, contribute to eutrophication and depletion of dissolved oxygen in water bodies (Hickey et al., 1989).

3.6.2 Traditional Pond System (One-Pond System)

A one-pond system is a simplified version of the two-pond system, where effluent flows directly from the milking shed and feed pad into a single storage pond. The effluent is then irrigated onto paddocks using traveller irrigators. A stone trap is installed at the inlet to remove coarse solids, such as sand, gravel, and organic debris, which could otherwise clog irrigation systems. This system is installed at the study site, where the effluent pond serves as a holding reservoir before land application.

3.6.3 3.6.3 Mechanically Aerated Pond

Mechanically aerated ponds incorporate mechanical aerators to enhance oxygen transfer, reducing reliance on algal photosynthesis. These systems promote nitrification, converting ammonia into nitrate, which is more readily absorbed by pasture crops (J. P. S. Sukias et al., 2003; W. Hamilton et al., 2006). While effective, aerated ponds require energy input and maintenance, making them more costly than passive systems.

3.6.4 Passive Solid Effluent Separators

Effluent from milking parlors and feed pads often contains high levels of suspended solids, which can clog irrigation equipment and reduce system efficiency. Passive solid separators,

such as weeping walls and stationary screens, allow liquids to seep through perforated barriers while retaining solid materials(Van Horn et al., 1994). Weeping walls are commonly used in New Zealand dairy farms, relying on gravity-driven separation. Studies show that stationary screens can remove 20–30% of organic matter from dairy effluent, improving handling and application efficiency (DairyNZ, 2012; Van Horn et al., 1994).

3.6.5 Advanced Pond Systems (APS)

An Advanced Pond System (APS) (Craggs et al., 2004) is a more efficient alternative to traditional two-pond treatment. It consists of:

- An anaerobic pond (similar to the conventional two-pond system).
- A high-rate pond, which promotes algal growth to enhance nutrient removal.
- Algal settling ponds, where algae settle, reducing nutrient concentrations.
- A maturation pond, providing final treatment before reuse or discharge.

APS systems occupy the same footprint as conventional two-pond systems but offer improved pathogen removal, reduced odor, and higher nutrient recovery.

Figure 3-9: Various dairy effluent treatment systems in New Zealand. (Top-left) traditional two-pond system with anaerobic and aerobic ponds; (Top-right) effluent pond at the study site; (Bottom-left) mechanically aerated pond; (Bottom-right) schematic representation of an advanced pond system from (Craggs et al., 2004), including fermentation, high-rate, algal settling, and maturation ponds.

Table 3-1: Comparison of different dairy farm effluent treatment systems in New Zealand, highlighting their components, functions, advantages, disadvantages, and applicability to the study site

Treatment System	Components	Function	Advantages	Disadvantages	Usage at Study Site
Two-Pond System	Anaerobic pond (4-5 m), Aerobic pond (1-1.5 m)	Breakdown of organic matter, nutrient removal	Simple, low maintenance, widely used	Incomplete removal of nutrients and pathogens	No
One-Pond System	Single pond with stone trap	Effluent storage and land application	Easy to implement, low cost	High risk of nutrient runoff, limited treatment	Yes
Mechanically Aerated Ponds	Mechanically aerated pond with oxygen supply	Faster organic matter degradation, nitrification	Improved efficiency, better ammonia removal	High energy costs, requires maintenance	No
Passive Solid Separators	Weeping walls, stationary screens	Separation of solids from liquid effluent	Reduces clogging, improves handling	Limited nutrient removal, requires frequent cleaning	No
Advanced Pond System (APS)	Anaerobic pond, high-rate pond, algal settling ponds, maturation pond	Improved nutrient removal, pathogen reduction, odor control	Higher efficiency, better environmental performance	Higher initial cost requires proper management	No

3.7 Effluent Management at the Study Site

The study site utilizes a traditional one-pond system, where effluent from the milking shed and feed pad is directed into an effluent pond via a stone trap as shown in Figure 3.10. The stored effluent is then applied to paddocks using a travelling irrigator. While effective, this system relies on land application to manage effluent, necessitating careful scheduling to prevent nutrient leaching and runoff.

Given the potential estrogen contamination concerns, alternative treatment options, such as solid-liquid separation and enhanced pond aeration, could be explored to improve effluent quality before land application.

Figure 3-10: Effluent management at the study site. (Left) Effluent pond designed for temporary storage and treatment of dairy farm wastewater; (Right) Stone trapping system at the dairy farm, which helps separate solid materials such as gravel, sand, and organic debris from the effluent before it enters the main storage

3.8 Farm Hydrology and Water Management

Effective hydrology and water management are important components of any sustainable dairy farming, directly influencing pasture productivity, animal health, and environmental stewardship. In New Zealand, dairy farms utilise various water sources, implement comprehensive effluent management systems, and monitor surface water movement to mitigate potential contamination pathways.

3.8.1 Water Sources on the Farm

The dairy farm relies on multiple water sources to support milking operations, irrigation, and livestock hydration. The primary water sources include:

- Bore Water: The farm has water bores that provide a reliable groundwater supply for livestock drinking, washdown, and irrigation.
- Rainfall Contribution: The region experiences seasonal rainfall, which contributes to soil moisture balance but can also increase surface runoff during high-intensity events.
- Surface Water Streams (Not Used): A nearby Maungatea water stream flows along the farm boundary, acting as a natural drainage channel for surface runoff. While this stream plays a role in local hydrology, it is not used as a direct water source for farm operations to prevent potential contamination and regulatory concerns.

3.8.2 Effluent Water Cycle

Effluent from the milking shed washdown, feed pad, and holding yards is collected and stored in the effluent pond. Liquid effluent is applied to pasture as a fertilizer, returning nutrients and organic matter to the soil. Effluent infiltrates into the soil, enhancing moisture retention but also posing risks of nutrient leaching into groundwater. During high rainfall events, excess effluent can contribute to surface runoff, increasing the risk of estrogen transport to waterways (Ahaneku, 2014).

Figure 3-11: Effluent solid spreader used on dairy farm for applying solid dairy effluent onto pasture

3.8.3 Surface Water Movement and Contamination Pathways

The movement of water across the farm landscape determines how nutrients, sediments, and estrogens travel through the system. Key hydrological pathways include: Excess rainfall or over-applied effluent can generate surface runoff, transporting estrogens and nutrients toward nearby streams. Sloped pasture areas increase runoff risks, especially if soil infiltration capacity is exceeded (Silburn et al., 2011). Estrogens and nutrients can percolate through the soil profile, reaching shallow groundwater (Arnon et al., 2008). Water can bypass the soil matrix through macropores and cracks, allowing rapid transport of dissolved contaminants (R. M. Monaghan & Smith, 2004).

3.8.4 Implications for Water Quality and Environmental Risk

The hydrology of the farm directly influences the fate of estrogens in the environment. Poorly managed effluent irrigation, runoff, and infiltration can contribute to: Estrogen contamination in surface water (via runoff to streams) (Dutta et al., 2012), Groundwater contamination (through leaching and preferential flow) and Excess nutrient loading, affecting soil health and water quality (Arnon et al., 2008).

3.9 Climate and Weather Conditions

The hydrological processes on the dairy farm are primarily influenced by climatic variables, including air temperature, rainfall, solar radiation, evapotranspiration, relative humidity, sunshine hours, and wind speed. These climatic factors directly affect pasture growth, soil moisture balance, and effluent management, influencing nutrient and estrogen transport dynamics across the farm landscape.

3.9.1 Hamilton Climate Overview

Hamilton, New Zealand, experiences a temperate maritime climate, characterized by moderate temperatures, consistent rainfall, and variable wind conditions.

3.9.1.1 Temperature

The average annual temperature in Hamilton ranges between 11°C and 17°C, with January being the warmest month (~20°C) and July the coldest (~10°C) (Tait et al., 2006). These temperature variations are influenced by geographical features and prevailing weather systems that affect New Zealand's climate (Drost et al., 2006).

3.9.1.2 Rainfall

Hamilton receives an annual average rainfall of ~1,200 mm, with the majority occurring during winter (June–August) (Tait et al., 2006; Tait & Turner, 2005). Orographic effects from surrounding hills and northwesterly winds from the Tasman Sea influence rainfall distribution (Sansom & Renwick, 2007; Tait et al., 2006). Rainfall is not evenly distributed, with peak precipitation in winter due to frequent frontal weather systems (Prince et al., 2021).

3.9.1.3 Wind Speed and Direction

Hamilton experiences an average wind speed of ~12 km/h, (3.3 m/s) with stronger winds typically occurring in spring and summer due to dominant high-pressure systems (Tait et al., 2006). The northwest wind is the predominant wind direction, influencing both temperature and moisture transport across the region (Drost et al., 2006).

3.9.1.4 Climate Variability and Change

Hamilton, like the rest of New Zealand, is experiencing climate variability and shifts due to climate change. Studies indicate changes in temperature trends, seasonal precipitation, and the frequency of extreme weather events, which could impact agriculture and water resource management (Wilson et al., 2011). These climatic shifts necessitate continuous monitoring and adaptation to mitigate potential adverse effects on pasture growth, effluent management, and soil moisture balance (Wratt et al., 2006).

Figure 3.12 represents the average trend of climatic variables in Hamilton, Waikato.

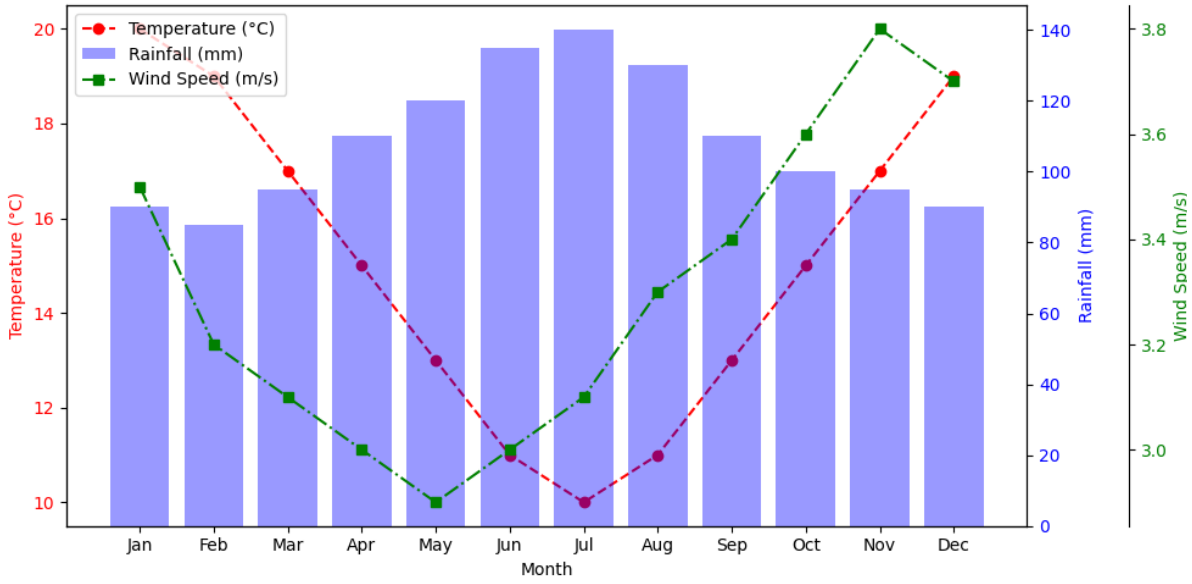

Figure 3-12: Monthly climate trends in Hamilton, New Zealand, based on historical data from 1972 to 2019. The plot shows the seasonal variation in average temperature (°C), total rainfall (mm), and average wind speed (m/s), highlighting the influence of seasonal changes on climatic variables (Drost et al., 2007; Prince et al., 2021; Sansom & Renwick, 2007; Tait et al., 2006; Tait & Turner, 2005).

3.10 Data Collection and Climate Characteristics of Dairy Farm Site

Climatic data for the study site were obtained from NIWA's Virtual Climate Station Network (VCSN) at the farm's location (latitude: -37.77389, longitude: 175.30517, elevation: 45m). The dataset includes daily climatic records from June 2020 to May 2021, covering key meteorological parameters such as daily precipitation (mm/day), relative humidity (%), minimum and maximum air temperature (°C), sunshine duration (hrs/day), solar radiation (MJ/m²), evapotranspiration (mm/day), calculated using the Penman-Monteith equation, wind speed (m/s). It is important to note that VCSN data is not freely available to the public. Access requires a formal request to NIWA and is typically provided for academic and research purposes.

3.10.1 Rainfall and Evapotranspiration

Rainfall and evapotranspiration show distinct seasonal patterns (Figure 3.13). Rainfall is highest during the winter months (June-August), peaking at approximately 138 mm in July, while the driest period occurs during summer (December-February), with minimum precipitation recorded in December. In contrast, evapotranspiration follows an inverse trend, with higher values in summer due to increased solar radiation and temperature, reaching its peak in January and February.

3.10.2 Temperature Trends

Seasonal temperature fluctuations follow a predictable trend (Figure 3.14). Maximum temperatures range from approximately 15°C in winter (July) to 27°C in summer (January–February), while minimum temperatures drop as low as 6°C in July. These patterns align with historical climate data for the Hamilton region.

3.10.3 Atmospheric Conditions

Relative humidity, wind speed, and solar radiation collectively impact water balance and transport processes at the study site (Figure 3.15). Humidity remains high during winter (~88%) and decreases in summer (~78%). Wind speeds are relatively low, averaging between 1.9 m/s and 2.7 m/s, consistent with the region's sheltered inland location. Solar radiation increases significantly in summer, peaking at ~22 MJ/m², enhancing evapotranspiration and influencing soil drying rates.

These factors are essential for understanding estrogen mobility, as they regulate moisture levels, microbial activity, and degradation pathways. Which directly influence surface runoff and estrogen transport dynamics The climatic trends observed at the study site are consistent with historical data for the Waikato region, confirming the reliability of the dataset used in this study. The seasonal interplay of precipitation, temperature, and solar radiation highlights potential pathways for estrogen transport, particularly through surface runoff in wet months and increased volatilization and degradation during dry periods. These climatic conditions will be further integrated into the modelling framework to assess estrogen fate and transport dynamics in dairy farming environments.

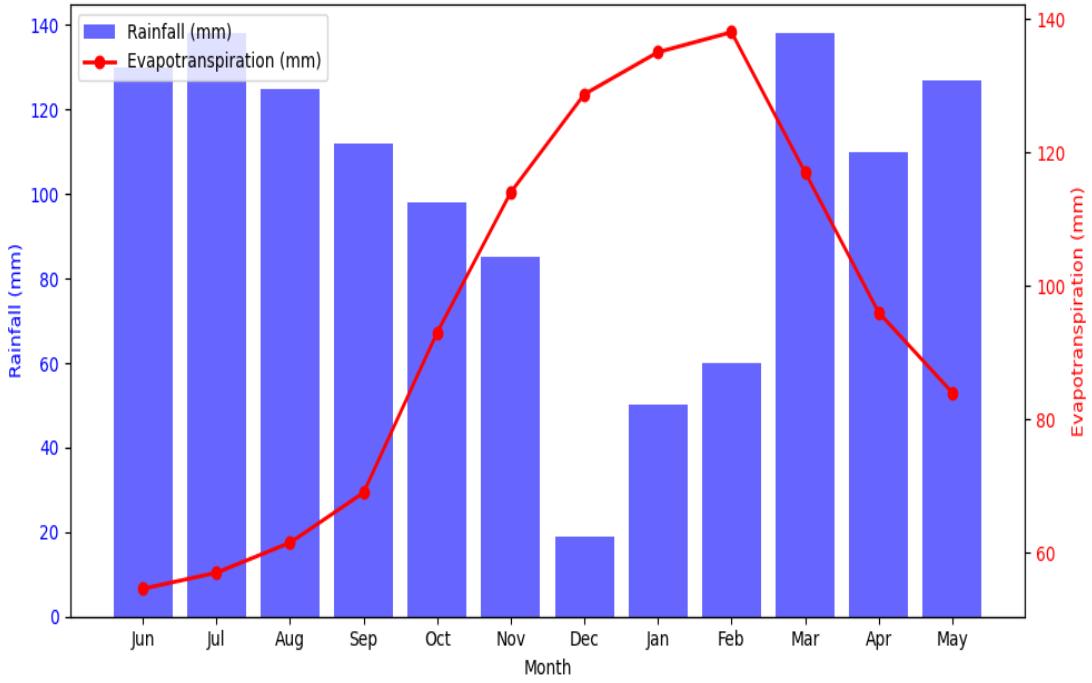

Figure 3-13: Monthly rainfall (mm) and ET(mm) at the study site.

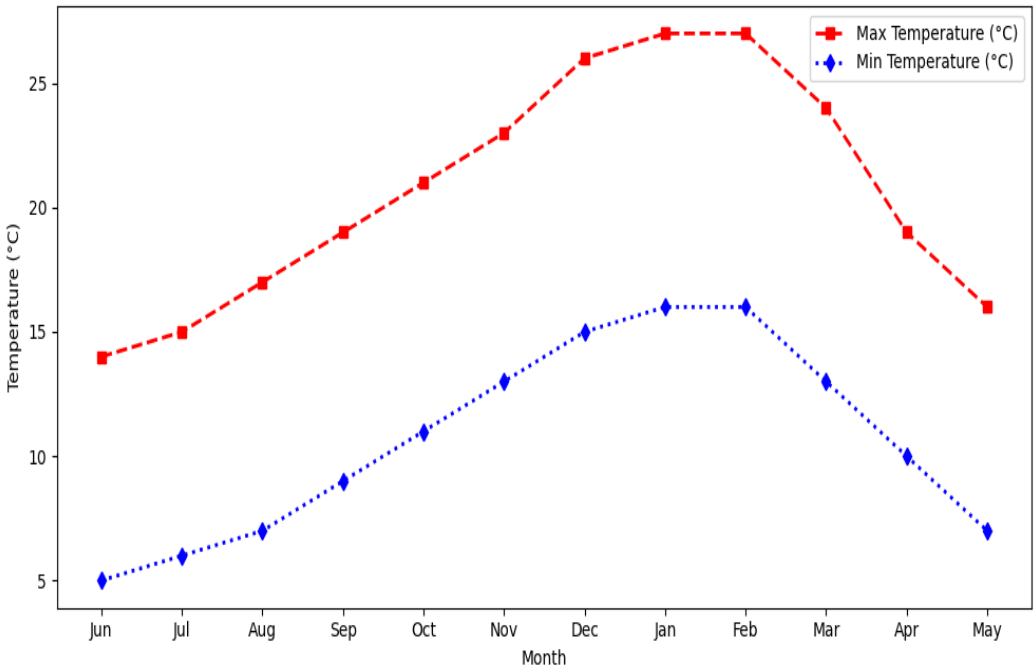

Figure 3-14: Monthly maximum and minimum temperature (oC) at the study site.

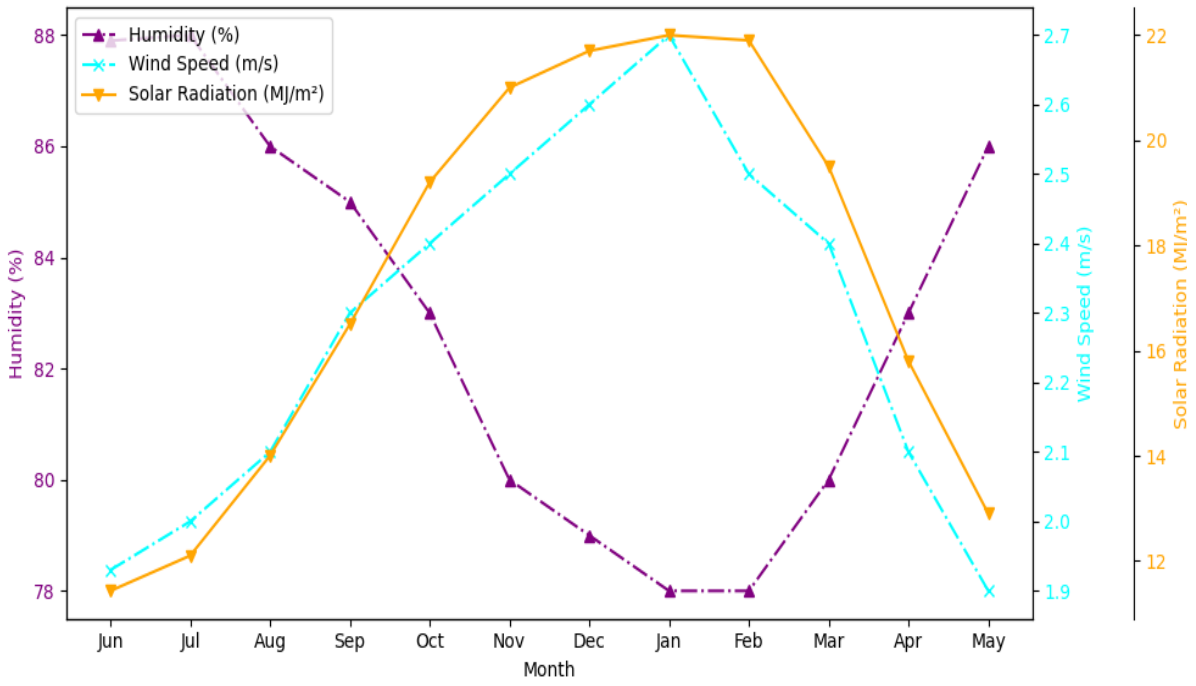

Figure 3-15: Monthly variations in relative humidity (%), wind speed (m/s), and solar radiation (MJ/m²)

3.11 Soil Characteristics of the Study Site

The soil properties at the study site were obtained from S-map, New Zealand's digital soil database developed by Manaaki Whenua – Landcare Research (*S-Map Online | Manaaki Whenua - Landcare Research*, 2025). The study site is classified under the Granular Soil Order in the New Zealand soil classification system. These soils are clayey in nature, formed from strongly weathered volcanic rocks or ash, and are known for their moderate drainage capacity and high soil water-holding ability. The topsoil predominantly has a clay texture with no significant presence of stones, while the subsoil consists mainly of loam textures with a notable presence of rock fragments within 100 cm of the mineral soil depth.

3.11.1 Soil Physical Properties

- Texture Profile: The topsoil is primarily clay, transitioning into a loam subsoil.
- Depth Class: The soil is classified as deep (>1m), allowing extensive plant rooting depth.
- Drainage: The soil is moderately well-drained with low vulnerability to waterlogging under non-irrigated conditions.
- Permeability: The soil permeability varies from rapid in the upper layers to moderately slow in deeper horizons (72 - 4 mm/hr).

- Bulk Density:
    - Topsoil: 1.09 g/cm³
    - Subsoil: 1.26 g/cm³
- Aeration: High aeration in the root zone ensures good oxygen availability for plant growth.
- Water Holding Capacity: The profile available water (PAW) is high (151 mm in the top 60 cm), contributing to its suitability for pasture growth.

3.11.2 Soil Chemical Properties

- Cation Exchange Capacity (CEC): The soil exhibits a CEC range of 12-24.9 cmol/kg, indicating a moderate ability to retain essential nutrients.
- Soil pH: The site's soil is typically moderately acidic, which can influence nutrient availability and microbial activity.
- P-Retention: The topsoil phosphorus retention is medium (46%), affecting fertilizer management strategies.

3.11.3 3.11.3 Soil Management Factors

- Nutrient Leaching: The nitrogen (N) leaching vulnerability is low, reducing the risk of groundwater contamination.
- Structural Stability: The soil has a low structural vulnerability, making it resilient to compaction and degradation.
- Bypass Flow: The presence of preferential flow pathways is high, which may influence the transport of contaminants, including estrogens.

These soil characteristics are required to understand nutrient cycling, water retention, and contaminant transport within the study area, particularly for assessing the movement of estrogens in surface runoff and infiltration pathways. The combination of high water-holding capacity, moderate permeability, and clay-loam texture makes this soil suitable for dairy farming but also highlights the need for careful effluent and nutrient management to prevent leaching into surrounding water bodies.

3.12 Soil Sampling and Laboratory Analysis

While S-map provides valuable spatial soil data, including texture, cation exchange capacity (CEC), and drainage characteristics, site-specific laboratory analysis was conducted to validate key parameters such as soil texture, bulk density, particle density soil moisture, PH, hydraulic conductivity and organic matter ensuring that the dataset used in SWAT modelling and estrogen transport simulations was accurate and representative. By integrating S-map data with site-specific laboratory measurements, we ensured that the modelling inputs reflect real field conditions, improving the accuracy and reliability of the study's predictions.

The sampling strategy was designed to capture variations in soil properties that influence hydrological processes, infiltration, preferential flow, and estrogen transport. Laboratory analyses were conducted at the University of Waikato, following standardized protocols to ensure accuracy and relevance for numerical modelling.

3.12.1 Soil Sampling Procedure

Soil samples were collected systematically across different locations within the dairy farm study site to ensure representativeness. The sampling covered paddock areas, drainage pathways, and effluent-applied zones.

- Sampling Depths: Samples were taken at 0-10 cm, 10-30 cm, and 30-50 cm depths to assess variations in soil properties affecting surface runoff and deeper infiltration.
- Sampling Equipment: Soil cores were extracted using a hand auger and stainless steel soil coring tubes to minimize contamination.
- Sample Preservation: Collected samples were stored in sealed polyethylene bags and transported under controlled conditions. For chemical analysis, samples were air-dried and sieved to <2 mm before testing.

Figure 3-16: Field sampling at the study site: (Left) Soil core extraction using a hand auger for laboratory analysis of physical and chemical properties; (Right) Drainage pathway where water samples were collected to assess suspended sediment load, nutrient content and potential estrogen transport in surface runoff.

A series of laboratory tests were conducted to characterize the physical properties of the soil, which are critical for hydrological modelling and estrogen transport simulations.

3.12.2 Particle Size Distribution

The particle size distribution (PSD) of soil samples was determined using the Malvern Mastersizer 3000 at the University of Waikato's Earth Sciences Department (Mastersizer | Laser Diffraction Particle Size Analyzers | Malvern Panalytical.). This method employs laser diffraction to classify soil particles into sand, silt, and clay fractions. The analysis was conducted following standardized laboratory procedures to ensure accuracy in estimating soil texture.

3.12.2.1 Soil Sample Preparation

To ensure accurate PSD measurement, soil samples were subjected to a standardized preparation procedure. The samples were first air-dried and sieved to <2 mm to remove larger particles and plant debris. To eliminate organic matter that could interfere with particle dispersion, 10% hydrogen peroxide (H_2O_2) was added and left overnight, followed by gentle heating to accelerate decomposition. Sodium hexametaphosphate (10% Calgon solution) was then introduced as a dispersant to prevent clay particles from forming aggregates. Additionally, the samples underwent ultrasonic dispersion for 5 minutes to further disaggregate fine particles before analysis.

3.12.2.2 Measurement and Analysis

The prepared samples were analyzed using the Malvern Mastersizer 3000, which employs laser diffraction to measure particle sizes ranging from 0.01 μm to 2000 μm. The system provided a detailed classification of the soil texture, helping to determine permeability, infiltration capacity, and preferential flow potential. The procedure followed the Standard Operating Procedures (SOPs) of the University of Waikato's Earth Sciences Laboratory and was cross-referenced with S-map soil data to validate the result.

The below figure 3.17 shows the particle size distribution. The soil samples show Dv10 (1.50 μm) which means 10% of the particles are smaller than 1.50 μm (very fine particles, indicative of clay or fine silt), Dv50 (18.9 μm): 50% of the particles are smaller than 18.9 μm (suggests silt-dominated composition), and Dv90 (127 μm): 90% of the particles are smaller than 127 μm (indicative of fine sand and silt fractions).

New Zealand soil classification system (Hewitt, 1993) helps in understanding the soil's texture and its implications for water retention, infiltration, and estrogen transport.

- Clay Fraction (< 2 μm): The presence of fine clay particles is indicated by Dv10, which is approximately 1.5 μm. While some clay is present, it does not dominate the soil composition.
- Silt Fraction (2-50 μm): The majority of the soil falls within this range, as Dv50 is recorded at 18.9 μm. This suggests that the soil is predominantly silty, contributing to moderate water retention and slow permeability.
- Sand Fraction (50-2000 μm): A small proportion of the soil is classified as sand, with Dv90 recorded at 127 μm. This indicates that only a minor portion consists of fine sand particles, with very little coarser material present.

The results suggest that the soil is silt loam or silty clay loam, which aligns with previous S-map data indicating the Hamilton soil series (typically silt loam/caly laom).

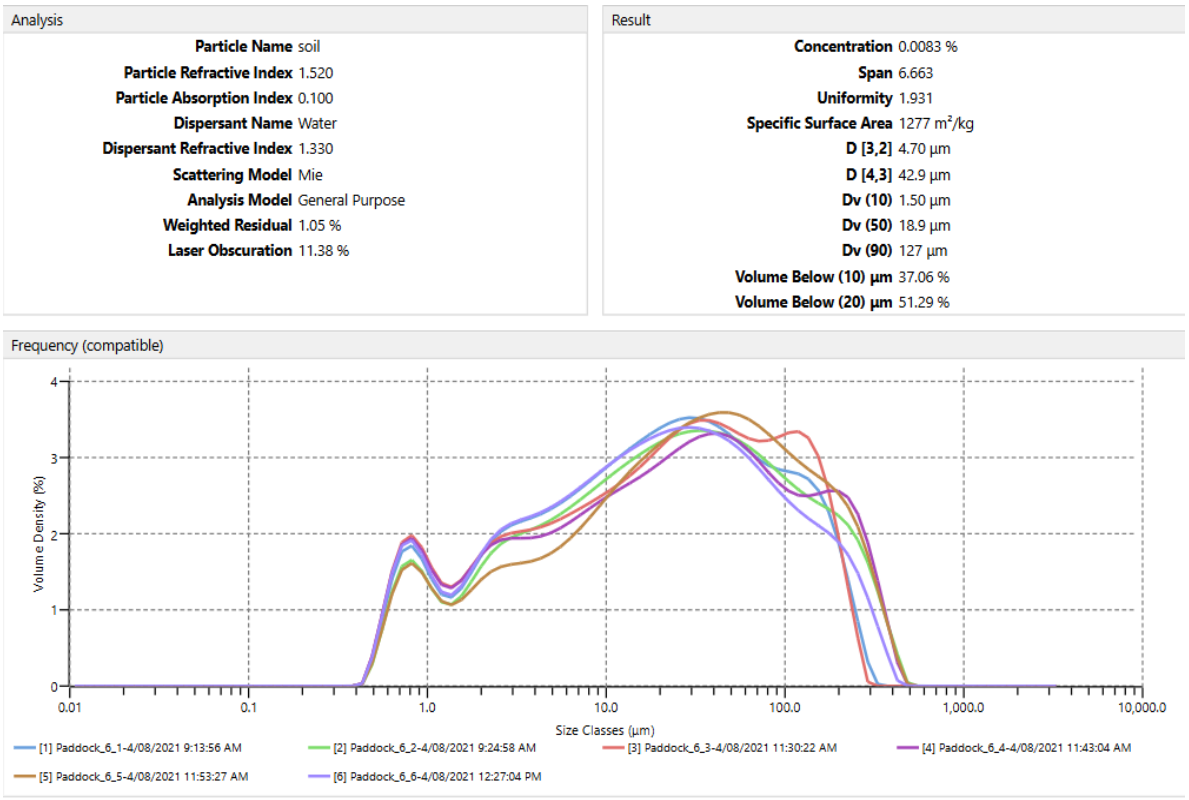

Figure 3-17: Particle size distribution of soil samples from the study site, analyzed using the Malvern Mastersizer 3000

3.12.3 Bulk Density & Porosity

Bulk density values were measured by collecting undisturbed soil cores and and oven-dried at 105°C for 24 hours to remove moisture and calculating the ratio of dry soil mass to total core volume. Higher bulk density values indicate more compacted soil, reducing water infiltration and increasing surface runoff potential.

Table 3-2: Bulk density, soil moisture and porosity for soil samples collected

Soil Depth (cm)	Bulk Density (g/cm³)	Porosity (%)	Soil moisture content (%)
0-10	1.18	55.5	34.2
10-30	1.28	51.7	28.5
30-50	1.35	49.1	23.8

Soil porosity (given in Table 3.2) was derived from bulk density values, assuming a particle density of 2.65 g/cm³ (Hewitt, 1993). Porosity determines the soil's ability to retain and transmit water, influencing preferential flow pathways and estrogen transport mechanisms.

3.12.4 Soil Moisture Content

Soil moisture content (Table 3.2) was analyzed using the gravimetric method, where samples were weighed before and after oven drying at 105°C for 24 hours. Additionally, NIWA's virtual climatic station data was used to cross-validate laboratory results. Soil moisture is a key factor in estrogen mobility, affecting dissolved phase transport and sorption dynamics.

3.12.5 Soil pH

The pH of the soil samples was measured using a 1:2.5 soil-to-water suspension method. Air-dried soil samples were sieved to <2 mm to remove coarse particles. 10 g of sieved soil was placed into a clean 50 mL beaker. 25 mL of deionized water was added to the soil sample to create a 1:2.5 soil-to-water ratio (Figure 3.18). The suspension was stirred thoroughly and allowed to equilibrate for 30 minutes to ensure proper interaction between soil particles and water. A calibrated pH meter (Hanna Instruments) was used to measure the pH of the supernatant. The probe was rinsed with deionized water before and after each reading to avoid contamination. Readings were taken twice for each sample, and the average value was recorded. The measured pH values ranged from 5.8 to 6.5, indicating slightly acidic soil conditions. These values are consistent with typical silt loam soils found in the region and align with S-map database values. The slightly acidic nature of the soil suggests moderate estrogen sorption potential and microbial activity, influencing estrogen degradation rates.

Figure 3-18: Soil pH measurement setup. (Left) Prepared soil suspensions (1:2.5 soil-to-water ratio) equilibrating before measurement. (Right) pH probe immersed in a soil solution for reading using a calibrated pH meter

3.12.6 Hydraulic Conductivity

Since silt loam soils have lower permeability, we used the Falling Head Permeameter method, which is more appropriate for lower-permeability soils. The methodology follows Darcy's Law, which describes fluid flow through porous media and is widely used in hydraulic conductivity measurements for fine-grained soils like silt loam, which characterizes our study site. A reservoir or standpipe containing water is connected to the bottom of the soil sample. Water slowly percolates upward, pushing out any trapped air. This process continues until water emerges at the top of the sample, confirming full saturation. The initial head height (h_1) was recorded. Water was allowed to flow through the soil, and the head height (h_2) was recorded at fixed time intervals. The test continued until the rate of decline in the water head stabilized.

By using the following equation;

$$k = \frac{2.3 \cdot a \cdot L}{A \cdot \Delta t} \log\left(\frac{h_1}{h_2}\right)$$

Where, k is hydraulic conductivity (mm/, a is the cross-sectional area of the standpipe, A is the cross-sectional area of the soil sample, L is the length of the soil sample (cm), h_1,h_2 are initial and final head levels in the standpipe (cm) and Δt is the time interval for water level drop (s).

Table 3-3: Observed Readings for Hydraulic Conductivity Measurement

Depth (cm)	Initial Head (h_1) cm	Final Head (h_2) cm	Time (s)	Sample Area (A) cm²	Standpipe Area (a) cm²	Column Length (L) cm	Hydraulic Conductivity (mm/hr)
0–10	30	18	180	28.27	0.785	5	58.3
10–30	30	20.5	240	28.27	0.785	5	42.5
30–50	30	23.2	300	28.27	0.785	5	34.8

Hydraulic conductivity values calculated from the analysis are given in Table 3.3 and fall within the expected range of 72-4 mm/hr from S-map soil.

3.13 Drone-Based High-Resolution DEM Data Collection

To accurately characterize the topography of the study site, an initial drone-based Digital Elevation Model (DEM) survey was conducted for one paddock using a DJI drone (property of the University of Waikato) equipped with a high-resolution RGB camera. However, due to

flying license restrictions, further drone flights were not permitted over the entire dairy farm site. As a result, while the Pix4D software was used to process and generate a high-resolution DEM for the surveyed paddock, a more comprehensive LiDAR-based 1m DEM published by Waikato Regional Council was later utilized for GIS-based modelling in the subsequent chapter.

The survey was conducted using a pre-programmed flight path to ensure systematic coverage of the entire study site. Flight altitude was optimized to balance resolution and coverage, at 100 meters. Ground control points (GCPs) were placed and surveyed using a differential GPS to improve georeferencing accuracy. Images collected from the drone were processed using photogrammetry software (e.g., Pix4D,) to generate a high-resolution DEM. The final output provided a detailed elevation model with a resolution of 10 cm, useful for localized surface analysis.

Figure 3-19: Drone-based survey for high-resolution DEM generation at the dairy farm site. The DJI drone was deployed (top left) and launched from a designated landing pad (top right) to capture aerial imagery of the site. The ground control setup (bottom left) was established for accurate georeferencing, and a GNSS receiver(bottom right) was used for additional spatial calibration.

3.14 Conclusion

Chapter 3 provided a comprehensive characterization of the dairy farm site, covering key aspects such as hydrology, soil properties, climate, and topography, essential for subsequent numerical modelling. The key findings from this chapter include:

- Effluent and Water Management: The farm primarily relies on bore water and rainwater for its operations, with effluent collected in a single earthen pond before being applied as fertilizer. Surface water bodies, such as the Maungatea Stream, serve as natural drainage pathways but are not utilized for farm water supply.
- Soil Properties and Laboratory Validation: Soil characterization was performed using a combination of S-map data and laboratory experiments at the University of Waikato. Physical properties such as bulk density, porosity, hydraulic conductivity, pH and particle size distribution were measured to validate and refine soil input parameters for hydrological and contaminant transport modelling.
- Hydrological and Climatic Conditions: The study site experiences a temperate maritime climate with seasonal variations in rainfall, temperature, evapotranspiration, and wind speed. These climatic variables were obtained from NIWA's Virtual Climate Station Network (VCSN.
- A high-resolution 1m LiDAR DEM from the Waikato Regional Council was used for large-scale GIS-based modelling.

These foundational datasets will be integrated into the following chapters, focusing on numerical modelling of estrogen fate and transport in soil and surface water systems, ensuring realistic representation and improved prediction accuracy.

Chapter 4
Modelling Steroid Hormone Transport in New Zealand Dairy Pasture: A Numerical Approach

4.1 Introduction

This chapter explores the transport of steroid hormones, specifically Estrone (E1) and 17β-Estradiol (E2), in soil environments typical of New Zealand dairy farms. This chapter aims to provide a detailed numerical model simulating the complex transport processes of estrogens. The numerical and mathematical modelling of steroid hormones, particularly estrogens, in the soil is a critical area of research due to the environmental implications of these compounds, especially in agriculture. Numerical models are necessary for simulating the complex interactions between estrogens and soil components, to predict how these hormones behave under various agricultural practices (Shrestha et al., 2012).

Estrogens, such as 17β-estradiol and estrone, are often infiltrated into soils through the application of animal manure such as from dairy farms, where recycling treatments are common for reproductive management (Tremblay et al., 2018). The presence of steroid hormones in agricultural soils raises concerns about their potential to leach into groundwater, affecting aquatic ecosystems and human health (J. Gadd et al., 2010). Various factors, including soil composition, organic matter content, and the presence of biosolids, influence the fate of estrogens in soil (Stumpe & Marschner, 2010a, 2010b). For instance, studies have shown that the interaction between estrogens and soil organic matter affects their sorption and degradation rates (Stumpe & Marschner, 2010a). The sorption potential of estrogens can vary widely, with estimates suggesting that the no-effect concentration (PNEC) for estrogens in soil ranges from 1 to 700 $\mu g\ kg^{-1}$ (Kopperi et al., 2016). Furthermore, the dynamics of estrogen degradation in soils can be complex; some studies report half-lives for these compounds ranging from 5 to 25 days, indicating that while they may degrade relatively quickly, environmental conditions can influence their persistence (Schoenborn et al., 2015). Estimating estrogen behaviour in soils is essential for predicting their environmental impact. The application of mathematical models can help simulate the transport and transformation of estrogens in soil-water systems quickly, providing insights into how these compounds might work under various agricultural practices (Shrestha et al., 2012). Additionally, the use of advanced analytical techniques, such as gas chromatography-tandem mass spectrometry (GC-

MS/MS), has enhanced the ability to detect and quantify these hormones in complex matrices like soil and manure (Hansen et al., 2011). This capability is crucial for developing effective management strategies to mitigate the risks associated with estrogen contamination in agricultural environments.

4.2 Numerical Modelling of Estrogens

Estrogens, including 17β-estradiol and estrone, are prevalent in animal waste and can affect soil and water quality, leading to potential ecological and health risks (Andaluri et al., 2011; Hanselman et al., 2003). Using numerical models is useful for exploring how estrogens interact with soil components. These models help forecast the behaviour of these hormones across various agricultural practices (Shrestha et al., 2012). The importance of numerical models lies in their ability to simulate the transport mechanism, degradation, and sorption of these compounds in soil systems, thereby providing insights into their environmental fate and guiding management practices to mitigate their impact. The modelling of estrogen transport and degradation can help to understand the mechanisms by which these compounds interact with soil matrices, which provides an understanding of their potential to leach into groundwater or runoff into near-surface water bodies (Khanal et al., 2006; Yost et al., 2014).

One of the critical aspects of numerical models is their ability to account for various soil properties that influence estrogen behaviour. For example, the adsorption capacity of different soil types can vary widely, with some soils exhibiting higher sorption capabilities due to their organic matter content (Maeng, 2023). Research has shown that estrogens can be strongly sorbed to soils, with studies indicating that over 85% of certain estrogens can rapidly sorb to sandy soils (Hildebrand et al., 2006). Moreover, the degradation kinetics of estrogens in soil have been shown to follow complex patterns, often better described by biexponential models rather than simple first-order kinetics (Xuan et al., 2008). This complexity arises from various factors, including microbial activity and soil moisture content, and soil temperature, which can affect the rate at which estrogens degrade. Numerical models that incorporate these dynamics can provide more accurate predictions of estrogen persistence and transformation in agricultural soils, which is vital for assessing the environmental risks associated with their application (Colucci et al., 2001; Shrestha et al., 2012).

In addition to understanding the fate of estrogens in soil, numerical models can also provide information about management practices aimed at reducing estrogen contamination. Some studies have demonstrated that the transport of estrogens in agricultural systems can be

influenced by factors such as preferential flow and colloidal transport mechanisms, increasing the risk of groundwater contamination (Steiner et al., 2010a). By simulating these processes, models can help identify best management practices that minimise the risk of estrogen leaching into groundwater or surface water, thereby protecting aquatic ecosystems and human health.

Furthermore, the integration of numerical models with field data can enhance their predictive capabilities. For example, research has utilized field lysimeters to study the transport of estrogens under real-world conditions, allowing for the calibration and validation of numerical models (Steiner et al., 2010). Such approaches can lead to a better understanding of the environmental behaviour of estrogens and inform regulatory frameworks aimed at managing their use in agricultural practices.

Various numerical approaches have been developed to model estrogen transport. Numerical models, such as the HYDRUS-1D and HYDRUS-2D models (Šimůnek et al., 2016, 2024), have been extensively utilised to simulate the transport of estrogens and other contaminants under different soil conditions, incorporating advection-dispersion equations with sorption and degradation processes. Fan et al.. (2008) developed a model that incorporates degradation, sorption, and transport processes for 17β-estradiol in undisturbed soils. This model highlights the importance of biological and chemical interactions in determining the fate of estrogens, demonstrating that both processes significantly influence their transport dynamics. Moreover, Dutta et al., (2010) focused on steroid hormone surface runoff from poultry litter-amended soils, highlighting the need for models that can account for different environmental conditions and their effects on estrogen transport. The two-site sorption model has also been employed to describe estrogen breakthrough curves in soil columns by (Dutta et al., 2010, 2012). These models account for equilibrium and kinetic sorption, better capturing the time-dependent interactions between estrogens and soil particles (Casey et al., 2005).

Physical models, such as those employed by Steiner et al. (2010), have provided insights into the transport mechanisms of estrogens through soil. Their research indicated that estrogens are primarily transported via preferential and macropore flow, with colloidal-enhanced transport contributing to deep estrogen transport. Their study highlighted that standard convection-dispersion models underestimate estrogen migration when preferential flow is not incorporated. Additionally, the influence of environmental factors, such as temperature and microbial activity, on estrogen degradation rates is often inadequately represented in existing

models. Similarly, Gall et al. (2011) highlighted the role of subsurface tile drains in altering the natural hydrology of soil and expediting the transport of hormones, yet the modelling of these systems remains underdeveloped. Furthermore, the lack of comprehensive studies examining the fate and transport of estrogens at environmentally relevant concentrations, including metabolite formation and sorption dynamics, presents another critical gap (Goeppert et al., 2016). These findings underscore the necessity of refining numerical models to incorporate multi-domain transport processes, integrating matrix flow, preferential pathways, and colloidal interactions.

The current study develops a numerical model for estrogen transport in New Zealand dairy soils, specifically tailored to silt loam soils under intensive pasture management. The model integrates Richards' equation for water flow, the convection-dispersion equation for solute transport, and non-linear sorption isotherms to simulate estrogen-soil interactions. Furthermore, it incorporates preferential flow and colloidal transport mechanisms, addressing limitations in conventional models. By coupling Green-Amp infiltration dynamics with solute transport equations, the model ensures an accurate representation of water and estrogen fluxes, improving predictive capabilities. The inclusion of real-world soil and hydrological data from New Zealand ensures that the model outputs are relevant for local agricultural conditions.

4.3 Mechanisms of Estrogen Transport

The transport of estrogens in soil is controlled by a combination of physical, chemical, and biological processes, which influence their mobility, retention, and degradation. These mechanisms include advection, dispersion, sorption, degradation, preferential flow, and colloidal transport. The extent to which estrogens move through the soil profile depends on factors such as soil type, organic matter content, microbial activity, and hydrological conditions. Understanding these processes is crucial for predicting estrogen behavior in agricultural environments and developing numerical models to assess potential risks to groundwater and surface water.

4.3.1 Advection and Dispersion

Advection refers to the transport of estrogens with moving water. In agricultural soils, estrogens infiltrate the soil along with rainfall or irrigation water, with their movement largely determined by the hydraulic conductivity and water content of the soil (Steiner et al., 2010). Studies have shown that silt loam soils in New Zealand dairy pastures have moderate

permeability, meaning advection-driven estrogen transport occurs at a moderate rate, depending on rainfall intensity and soil saturation levels (Sarmah et al., 2010).

Dispersion, on the other hand, results from variations in water flow paths and velocity, causing estrogens to spread out in the soil matrix. The degree of dispersion depends on soil structure and pore connectivity. Soils with high heterogeneity or well-defined preferential pathways exhibit greater dispersion, leading to wider distribution of estrogen concentrations in the subsurface (Dutta et al., 2012). Experimental studies using soil column tests have demonstrated that dispersion is stronger in structured soils with high organic matter content, where water movement varies between micro and macropores (Goeppert et al., 2016). However, in homogeneous sandy soils, dispersion effects are lower, and estrogen movement is more controlled by advection (Hildebrand et al., 2006).

4.3.2 Sorption and Retention Dynamics

Sorption plays a crucial role in determining the mobility and persistence of estrogens in soil. It occurs when estrogens bind to soil particles, limiting their transport. The extent of sorption depends on:

- Soil organic matter (OM) content: Higher OM leads to stronger sorption due to hydrophobic interactions (Stumpe & Marschner, 2010b).
- Soil texture: Clay-rich soils have higher sorption potential due to increased surface area and cation exchange capacity (Lee et al., 2003)
- Estrogen properties: Estradiol (E2) tends to sorb more strongly than estrone (E1), leading to differences in their environmental fate (Sarmah et al., 2006a).

Previous studies have applied the Freundlich and Langmuir isotherms to describe estrogen sorption in different soils (Casey et al., 2005). In general, high organic carbon soils exhibit strong non-linear sorption, making estrogens less mobile (Dutta et al., 2010). However, under changing environmental conditions (e.g., varying pH, temperature, or microbial activity), desorption can occur, leading to delayed transport (Prater et al., 2016). Chun et al. (2005) reported that 17β-estradiol has log K_{oc} values ranging from 2.6 to 4.0, indicating strong sorption potential, particularly in soils with high organic content. Similar log K_{oc} values are reported in the range of 2.3 to 4.2 for E2 and 2.5 to 4.1 for E1 (Lee et al., 2003; Prater et al., 2016; Sarmah et al., 2006a). Additionally, Yost et al. (2014) found that hormones and

phytoestrogens persisted longer than expected in soil prior to slurry application, suggesting that interactions with soil matrices significantly influence their environmental fate. Sorption and degradation are intertwined processes that dictate the fate of steroid hormones once they enter the soil (Zheng et al., 2012).

4.3.3 Degradation and Transformation

The persistence of estrogens in soil is regulated by microbial and abiotic degradation.

1. Microbial degradation: Bacteria present in soil break down estrogens into less active metabolites. The transformation of 17β-estradiol (E2) to estrone (E1) is a key step in estrogen degradation (Colucci et al., 2001). Studies have shown that degradation rates increase under aerobic conditions but slow down under anaerobic conditions (Sarmah & Northcott, 2008).
2. Abiotic degradation: Chemical oxidation and hydrolysis contribute to estrogen breakdown, but these processes are slower than microbial degradation (Bartelt-Hunt et al., 2012; C.-P. Yu et al., 2013).

Degradation rates vary widely depending on temperature, microbial community diversity, and soil moisture levels. Laboratory experiments have reported faster degradation in well-aerated soils, with half-lives of 0.24 to 1.5 days under aerobic conditions, whereas in anaerobic soils, estrogens persist for 4.69 to 5.1 days (Sarmah & Northcott, 2008). Column experiments by Das et al., (2004) provided additional degradation rate coefficients, demonstrating how estrogen breakdown varies with soil depth and moisture availability.

4.3.4 Preferential Flow and Macropore Transport

One of the most significant factors influencing estrogen leaching is preferential flow, where water and dissolved estrogens bypass the soil matrix and move rapidly through (D'Alessio et al., 2014; Monaghan & Smith, 2004; Steiner et al., 2010):

- Macropores (cracks, wormholes, root channels).
- Fractures in structured soils.
- Bypass flow, which occurs when infiltration exceeds the soil's water-holding capacity.

Arnon et al. (2008) found that estrogens were detected in sediments at depths of up to 32m, suggesting that standard transport models underestimate deep leaching due to preferential flow pathways. Similarly, Mahjoub et al. (2011) demonstrated that highly permeable sandy soils enhance estrogen leaching, contrasting with structured soils where macropore flow dominates. Field and lysimeter studies in New Zealand dairy pastures confirm that preferential flow significantly contributes to rapid estrogen movement following rainfall events (Gall et al., 2011; Steiner et al., 2010).

4.3.5 Colloidal Transport and Facilitated Mobility

Colloidal transport is another important pathway for estrogen movement. Colloids (small organic or mineral particles) can adsorb estrogens and enhance their mobility in soil (Chambers et al., 2014; Huang et al., 2019; Prater, 2012; Prater et al., 2015, 2016). This mechanism is particularly important when:

- Colloid concentrations are high (e.g., after manure application).
- Colloids remain suspended in water, preventing estrogen sorption onto stationary soil particles.
- Hydraulic conditions promote colloid movement, such as during intense rainfall events.

Figure 4.1 illustrates the hydrological and physicochemical processes governing estrogen transport in soil. Rainfall and surface deposition introduce estrogens into the system, where they undergo sorption, desorption, degradation, and transport. Matrix flow (porous media flow) represents slow estrogen movement through soil micropores, whereas preferential flow (macropores and fractures) allows rapid bypassing of sorption zones, increasing leaching potential. Colloid-facilitated transport further enhances estrogen mobility, carrying sorbed estrogens beyond expected retention depths. Estrogen movement is influenced by sorption kinetics (Freundlich isotherm), microbial degradation, and soil hydraulic properties, determining the extent of groundwater contamination risks.

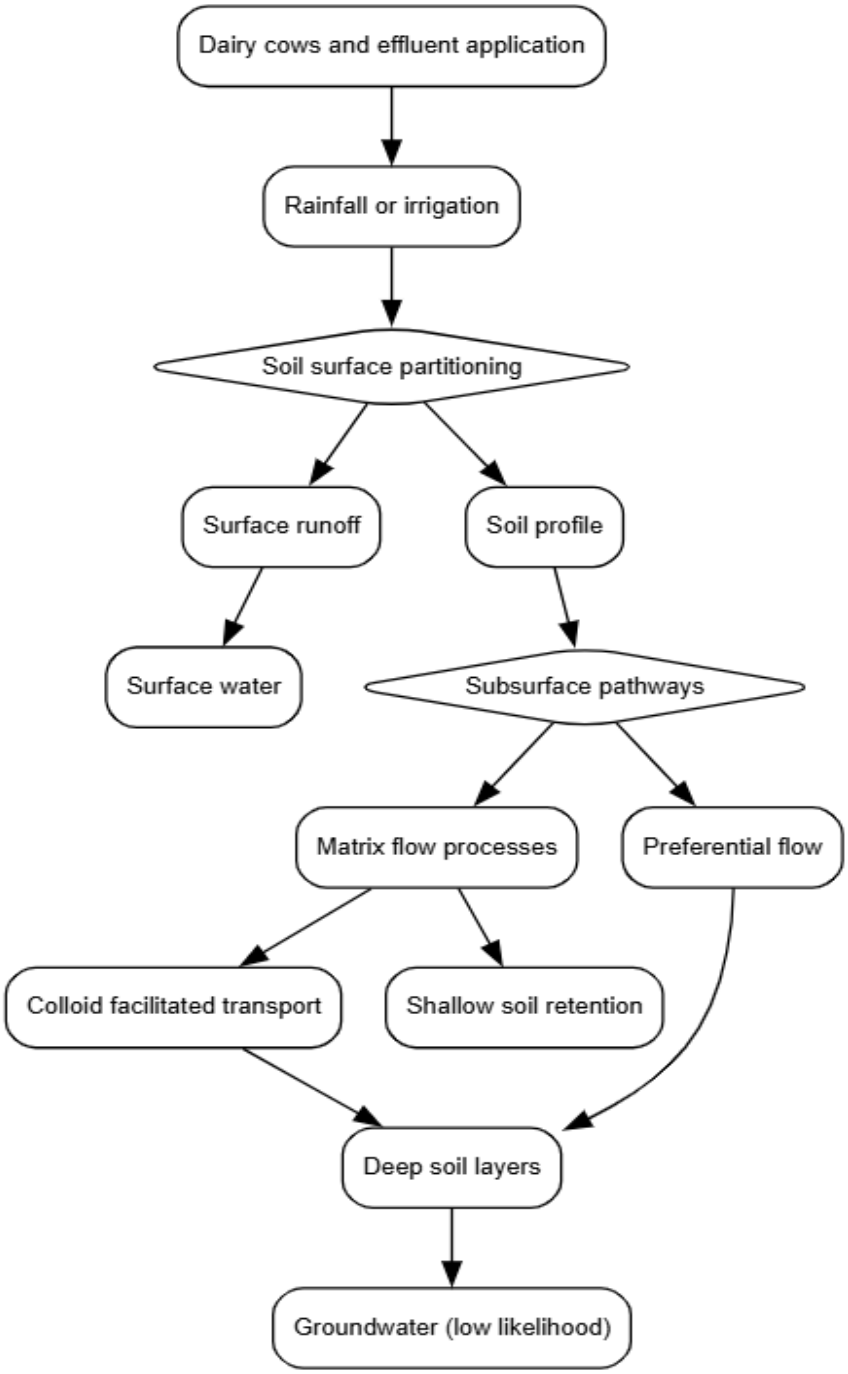

Figure 4-1: Flowchart of Estrogen (E1 and E2) Transport Mechanisms in Soil Systems

4.4 Column Studies and Transport Dynamics

Column studies provide controlled conditions to examine estrogen mobility, sorption, and degradation under realistic soil conditions. These experiments help to validate numerical models by simulating vertical transport, preferential flow, and interactions with soil

components. Key factors influencing estrogen transport include soil texture, organic matter content, and hydraulic conditions.

4.4.1 Insights from Column Experiments

Several studies have used soil columns to investigate estrogen movement, degradation, and retention in different soil types. Casey et al. (2005), conducted long-term column studies on estrogen mobility in natural soils. Their findings indicated that while E2 and E1 strongly sorb to soil, under certain conditions, non-equilibrium transport mechanisms like preferential flow can enhance their mobility. Goeppert et al. (2016) examined the transport behavior of free and conjugated estrogens (E1, E2, and estrone sulfate (E1-3S)) in sandy clay loam soil). The results demonstrated that E1-3S moved almost conservatively, while E2 and E1 were retained and degraded. Yu et al. (2020), investigated the stereoselective transport of 17α-E2 and 17β-E2 in soil columns. They found that sorption and transformation rates varied with depth, with E2 converting into estrone (E1) at different depths. Das et al. (2004), found that column length affects estrogen mobility. Shorter columns (7-10 cm) exhibited higher E2 transport, while longer columns (15-30 cm) retained and degraded estrogens more efficiently. Casey et al. (2005) used small soil columns (7 cm length), while Das et al. (2004) used 10 cm columns, both showing E2 transport. However, in larger columns like those of Casey et al., (2003) (15.2 cm) and Fan et al. (2008b) (30 cm), E2 transport was reduced or absent, demonstrating the impact of depth on estrogen retention and degradation.

4.5 Development of a Numerical Model for Steroid Hormone Transport in Soil

This numerical model was developed to simulate estrogen transport in soil, focusing on water flow, estrogen transport, and reaction processes. The model has three main parts: infiltration, water transport, and estrogen transport. Each part was designed to work together to capture the overall behaviour of estrogen in soil under dairy farm conditions in New Zealand.

1. **Infiltration Module:**

The model starts with the Green-Ampt (G&A) equation (Heber Green & Ampt, 1911) to simulate how rainfall infiltrates the soil. This provides the initial water transport needed for the next steps of the model.

2. Water Transport Module

Water flow through the soil is calculated using Richards' equation (Richards, 1931), which accounts for soil moisture dynamics and hydraulic properties. This step ensures that the model reflects how water moves through deeper soil layers.

3. Estrogen Transport Module

The movement of estrogen in the soil is simulated using the Convection-Dispersion Equation (CDE) (Barry & Sposito, 1989). This includes processes such as advection (transport with water flow), dispersion (spreading), and reactions such as sorption and degradation. Special pathways, such as preferential flow and transport with soil colloids, are also included to account for rapid movement.

The model uses finite difference methods for numerical solutions, applying a fully implicit approach to ensure stability and accuracy. Each module builds on the results of the previous one, creating a step-by-step simulation of the infiltration, water flow, and estrogen transport processes.

4.5.1 Development of Infiltration Module

The infiltration module simulates water entry into the soil profile, driven by rainfall and influenced by evapotranspiration. This process is modelled using the Green-Amp equation (G&A) (Heber Green & Ampt, 1911), which captures the infiltration dynamics under varying soil moisture conditions. The module integrates rainfall and evapotranspiration data to determine infiltration rates and cumulative infiltration over time (Whisler & Bouwer, 1970).

The infiltration process can be studied through three main approaches: in situ tests, physical models, and numerical models. In situ tests, while accurate, are often time-consuming and expensive. They require specialised equipment, favourable weather conditions, and extended testing periods, making them less practical for large-scale or frequent studies. In contrast, physical and numerical models have gained popularity due to their efficiency and versatility. These approaches can be used independently or in combination for infiltration studies (Whisler & Bouwer, 1970). Among physical models, rain simulators stand out for their ability to replicate precipitation under laboratory conditions. This allows the study of soil behavior under specific rainfall scenarios and physical conditions. Rain simulators are particularly useful for generating input data for numerical models and for calibrating these models, ensuring accuracy in simulations (Loch et al., 2001).

When studying infiltration, the key parameters are the cumulative infiltration (F) and the infiltration rate (f). These values are influenced by various factors, including the soil surface condition, vegetation cover, and the soil's physical, chemical, and biological properties. Parameters such as porosity, hydraulic conductivity, and moisture content play a significant role in determining infiltration rates

4.5.2 Description of Green-Amp Model

In numerical modelling, the Green-Ampt equation is widely used because of its simplicity and clear physical interpretation. The Green-Ampt equation assumes a homogeneous soil profile and applies Darcy's Law to estimate infiltration (Rawls et al., 1983; Whisler & Bouwer, 1970). It models the wetting front as a sharp boundary separating the unsaturated soil (with an initial moisture content θ_i from the saturated soil θ_s. Over time (t), the wetting front moves downward to a depth L, with water ponded at a depth h_0 on the soil surface.

The Green and Ampt approach represents a conservative and efficient method to calculate one-dimensional infiltration, but is limited to deep, well-drained, uniform, non-layered soils for a single rainfall event (Whisler & Bouwer, 1970). The original G&A model and subsequent advancements represent wetting fronts as discrete objects rather than discretising the model domain in space, yielding a computationally simpler model than the Richard equation. Infiltration is considered a complex physical process that is highly dependent on the characteristics of the soil through which water passes from the surface to the subsurface, connecting the surface flow with groundwater. The key component of infiltration in the implementation of rain-flow models, since this process is the main mechanism that affects the generation of runoff and seepage through soil. The Green-Ampt equation provides a straightforward framework for understanding infiltration, making it a valuable tool for numerical modelling in soil studies. The Green-Amp equation is also considered good when applied to non-uniform profiles with depth (Mein & Larson, 1973). To understand this concept, (Chow, 1965; Heber Green & Ampt, 1911; Mein & Larson, 1973; Rawls et al., 1983) provided the detailed calculation and development of the Green-Amp equation. Kale & Sahoo, (2011) summarized the different solutions of the Green-Ampt equation.

By assuming a vertical column of soil with a unit cross-sectional area. Initially, the soil has a uniform moisture content θ_i throughout. As the wetting front passes, the moisture content increases to the soil's porosity (η). The volume of water stored within this control volume,

from the surface to depth L, is equal to L(θ_s - θ_i) for a unit cross-sectional area. This volume corresponds to F, the cumulative depth of water infiltrated into the soil. The Green Amp representation in soil is shown in Figure 4.2.

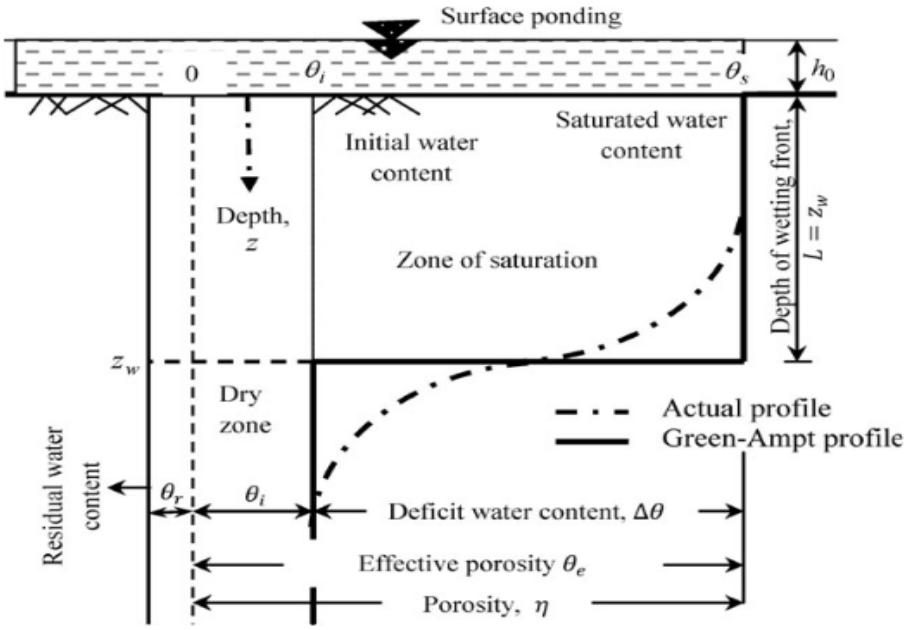

Figure 4-2: Infiltration profile by Green Amp equation (adopted from (Kale & Sahoo, 2011)

The infiltration rate $f(t)$ describes the rate at which water enters the soil surface. Based on Darcy's Law, the infiltration rate is:

$$f(t) = K_s \cdot \frac{\Delta H}{L} \tag{4.1}$$

Where, K_s saturated hydraulic conductivity (m/day), $\Delta H = \psi + h_0$ is total hydraulic head (m), where ψ is the suction head at the wetting front (This is the soil's ability to pull water into the unsaturated zone below the wetting front. It's a constant for a given soil type) and h_0 is the ponding depth (m), L is the depth of wetting front.

The wetting front depth L is related to the cumulative infiltration F(t) and the change in water content $\Delta\theta$ as

$$L = \frac{F(t)}{\Delta\theta} \tag{4.2}$$

Substituting L and ΔH relationship into Darcy's Law:

$$f(t) = K_s \cdot \frac{\psi + h_0}{F(t)/\Delta\theta} \tag{4.3}$$

Simplifying equation (4.3),

$$f(t) = K_s \cdot \frac{(\psi + h_0) \cdot \Delta\theta}{F(t)} \tag{4.4}$$

If the ponding depth h_0 is negligible, the equation (4.4) reduces to:

$$f(t) = K_s \cdot \frac{\psi \cdot \Delta\theta}{F(t)} \tag{4.5}$$

The cumulative infiltration F(t) represents the total volume of water that has infiltrated up to time t. As F(t) increases, the wetting front moves deeper into the soil. A deeper wetting front means more resistance to water flow: The longer the distance water must travel, the slower the infiltration rate becomes. Also, it reduced the impact of the suction head (ψ), as F(t) grows, the suction head is less effective at pulling water further into the soil. To model this dynamic interaction, F(t) is added to the numerator. Adding F(t) in the numerator to account for dynamic infiltration forces results in the final form:

$$f(t) = K_s \cdot \frac{(\psi + F(t))) \cdot \Delta\theta}{F(t)} \tag{4.6}$$

As infiltration progresses, at the Initial phase (t = 0), F(t) is small, so ψ+F(t) ≈ ψ. The infiltration rate is primarily driven by the suction head, and infiltration is fast. At the intermediate phase (t > 0), F(t) increases, making the denominator larger, and the infiltration rate decreases. This captures the natural slowing of infiltration as the soil becomes saturated and the wetting front deepens. At the steady state (F(t)→ infinity):

The infiltration rate approaches K_s, representing the saturated hydraulic conductivity, as suction forces diminish. A small threshold (1e-6) was applied to cumulative infiltration F(t) in the numerical implementation to prevent division by zero during early time steps.

4.5.2.1 Cumulative Infiltration

Cumulative infiltration F(t) represents the total amount of water infiltrated into the soil up to a given time. By definition:

$$f(t) = \frac{dF}{dt} \tag{4.7}$$

Substituting the infiltration rate equation (4.6) into equation (4.7):

$$\frac{dF}{dt} = K_s \cdot \frac{\big(\psi + F(t)\big) \cdot \Delta\theta}{F(t)} \tag{4.8}$$

Rearranging equation (4.8)

$$\frac{F(t)}{\big(\psi + F(t)\big) \cdot \Delta\theta}\, dF = K_s\, dt \tag{4.9}$$

Integrating both sides of the equation (4.9)

$$\int \frac{F(t)}{\psi + F(t)}\, dF = \int K_s \cdot \Delta\theta\, dt \tag{4.10}$$

For the left-hand side of the equation (4.10), use substitution,

$$u = \psi + F(t), \quad du = dF \tag{4.11}$$

Rearranging eq. (4.11)

$$\int \frac{F(t)}{\psi + F(t)}\, dF = \int \frac{u - \psi}{u}\, du \tag{4.12}$$

Split the integral and solve the equation (4.12) by re-substituting u = $\psi + F(t)$

$$\int 1\ du - \int \frac{\psi}{u}\, du = K_s \cdot \Delta\theta \cdot t \tag{4.13}$$

$$\big(\psi + F(t)\big) - \psi \cdot \ln\big(\psi + F(t)\big) = K_s \cdot \Delta\theta \cdot t + C \tag{4.14}$$

Where C is the constant in eq (4.14). To numerically compute the above equation for cumulative infiltration iteratively over small time steps

$$F(t+1) = F(t) + \frac{K_s \cdot (\Delta\theta \cdot \psi)}{1 + \frac{\Delta\theta \cdot \psi}{K_s \cdot t \cdot \Delta t}} \tag{4.15}$$

Where, F(t + 1) is cumulative infiltration at time t + 1 (m), F(t) is cumulative infiltration at time t (m), K_s is saturated hydraulic conductivity (m/day), $\Delta\theta$ is change in soil water content (θ_s-θ_i), ψ is suction head (m), Δt is time step size (days).

Equation (4.15) approximates infiltration based on physical soil properties and time, considering the balance between capillary suction (ψ) and hydraulic conductivity (K_s).

The Green-Ampt infiltration rate was computed at each time step, and cumulative infiltration was updated using an explicit forward Euler time-stepping scheme,

$$F(t+1) = F(t) + f(t) \cdot \Delta t \tag{4.16}$$

Where, $F(t+1)$ cumulative infiltration at time (t + 1), F(t) cumulative infiltration at time t, f(t) infiltration rate at time t, and Δt time steps in days. This approach avoids solving the implicit Green-Ampt equation directly and is commonly used for numerical implementations with small time steps.

$f(t)$ Infiltration rate was calculated using the Green-Ampt equation (4.6). By focusing on infiltration at the surface, the method seamlessly integrates with deeper water flow calculations (e.g., using Richards' equation). This alternative approach provides numerical stability, reduces dependency on steady-state assumptions, and improves model integration with variable rainfall and evapotranspiration inputs.

4.5.3 Application of Infiltration Equations in the Model

The infiltration equations derived from the Green-Ampt model are used to calculate the rate and cumulative amount of water entering the soil during the simulation period. Below is a step-by-step application of these equations within the numerical model.

4.5.3.1 Infiltration Rate and Cumulative Infiltration Equation Implementation

The infiltration rate f(t) is computed at each time step to determine how quickly water enters the soil surface from eq (4.6). Cumulative infiltration represents the total volume of water infiltrated into the soil up to time. It is iteratively updated using eq (4.16). In the model, soil parameters (K_s, ψ, θ_s, θ_i) are provided as constants based on the soil type (silt loam). Rainfall and evapotranspiration data are interpolated to match the simulation's time step (Δt). At each time step, the infiltration rate is calculated using the current cumulative infiltration F(t). The infiltration rate adjusts dynamically as the cumulative infiltration increases and the soil becomes wetter, reflecting decreasing infiltration over time.

F(0) is set to zero, assuming no infiltration at the start of the simulation. The infiltration rate $f(t)$ is used to increment F(t). Evapotranspiration is subtracted from F(t) to account for water loss during periods without rainfall.

$$F(t) = F(t) \text{ - evapotranspiration} \quad (4.17)$$

If F(t) becomes negative due to high evapotranspiration, it is reset to zero to avoid non-physical results.

4.5.3.2 Interaction with Rainfall and Evapotranspiration Data

Rainfall and evapotranspiration drive the infiltration process: Rainfall provides the primary water input for infiltration. If rainfall exceeds the soil's infiltration capacity, surface runoff is implied (though not modelled here in the model). Evapotranspiration reduces the amount of

infiltrated water by removing moisture from the soil, which depends on temperature, wind speed and humidity.

In the model, rainfall and evapotranspiration data are extracted from excel files for the 90-day simulation period (June, July, and August 2020) provided by NIWA New Zealand. The data is resampled to match the finer time steps of the simulation ($\Delta t=0.005$ days), ensuring temporal consistency. At each time step, rainfall is added to the soil as potential infiltration, and evapotranspiration is subtracted from F(t) to simulate water loss.

4.5.4 Overview of Workflow of Infiltration Model in MATLAB

1. Input Preparation:

- Load rainfall and evapotranspiration data.
- Define soil properties ($K_s, \psi, \theta_s, \theta_i$).
- Initialize $F(0)=0$.

2. Time Step Loop: For each time step:

- Compute $f(t)$ using the infiltration rate equation.
- Update $F(t+1)$ using the cumulative infiltration equation.
- Adjust $F(t)$ for evapotranspiration.
- Store results for visualization and analysis.

3. Output Generation:

- Plot infiltration rate over time.
- Plot cumulative infiltration over time.
- Compare rainfall, infiltration rate, and cumulative infiltration for insights into soil water dynamics.

The Green-Ampt model handles the surface infiltration dynamics, accurately representing the infiltration process in the upper soil layers (where most of the water enters the soil). Water redistribution in the soil profile (below 50 cm) can be modelled more effectively using Richards' equation. This accounts for vertical water flow driven by matric potential gradients and gravity. We use the Green-Ampt model to calculate infiltration flux at the surface (input to Richards' equation as a boundary condition). Richards' equation then distributes water through the soil profile, including depths below 50 cm. The 50 cm cap allows us to focus on the surface infiltration dynamics, which serve as the main driver for water redistribution in the soil profile and estrogen transport. Capping the wetting front prevents potential numerical

instability, such as unrealistically deep wetting fronts, particularly in conditions of long rainfall or low soil suction.

4.5.5 Data Cited in Literature for Green Amp Parameters

Green-Ampt parameters referenced in this study, including ponding time description, soil hydraulic properties and infiltration coefficients, are compiled in Appendix A. This appendix provides a summary of literature-sourced values for parameters such as saturated hydraulic conductivity, suction head, and moisture content variation for different soil types, which were cross-checked with our laboratory test for soil physical properties. These values serve as a baseline for the model development, ensuring numerical consistency with established hydrological studies. The data is compiled and used from published studies, including (Chow, 1965; Heber Green & Ampt, 1911; Kale & Sahoo, 2011; Mein & Larson, 1973; Rawls et al., 1983; Whisler & Bouwer, 1970). These references provide validated infiltration parameters widely used in hydrological modelling. A complete table of these parameters is included in Appendix A for reference.

4.6 Results and Analysis: Infiltration Dynamics

To better understand the infiltration dynamics captured by the Green Ampt model, this section presents a series of plots illustrating key outputs such as infiltration rate and cumulative infiltration over the 90-day simulation period. The plots integrate rainfall and evapotranspiration data, showcasing how these factors influence water movement into the soil. The visualisations highlight the temporal variations in infiltration and the interactions between soil hydraulic properties and environmental inputs. These results provide valuable insights into the behaviour of silt loam soil under New Zealand dairy pasture conditions.

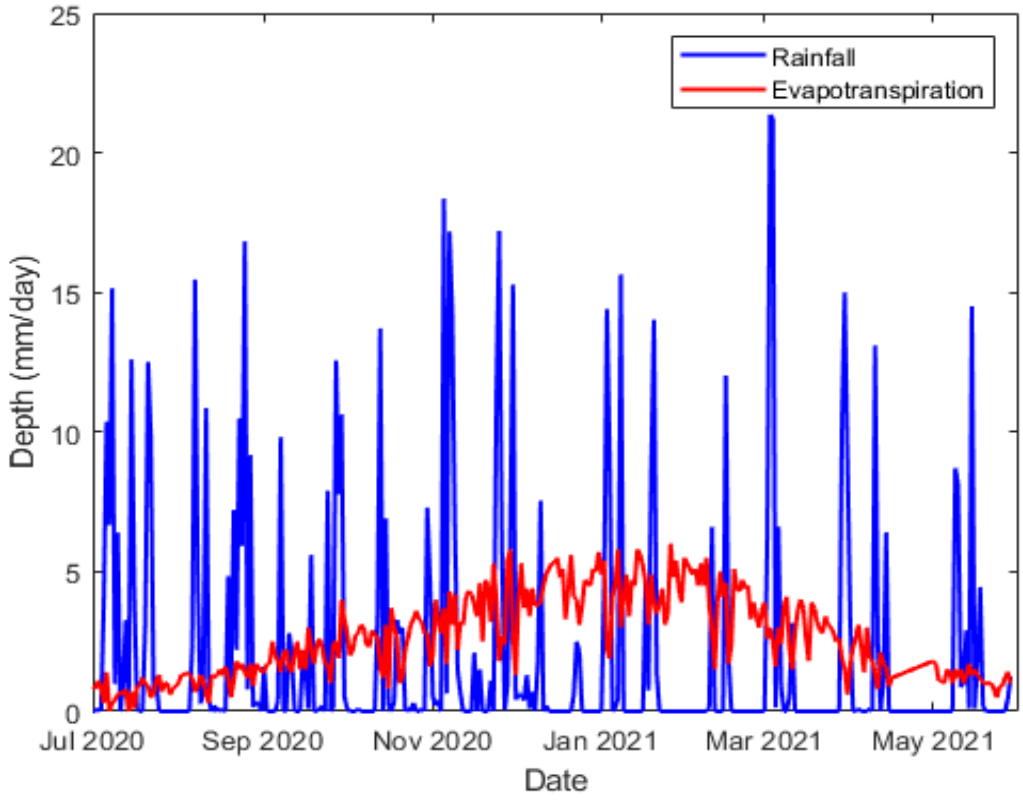

Figure 4-3: Daily rainfall and evapotranspiration rates over an entire year (July 2020- June 2021)

Figure 4.3 shows daily rainfall and evapotranspiration rates over an entire year (July 2020 to June 2021). Rainfall (blue line) displays substantial variability with frequent high-intensity events, particularly during winter and spring, while evapotranspiration (red line) shows a smoother seasonal trend, increasing during the warmer months (summer) and decreasing during winter. The plot captures the dynamic interaction between rainfall inputs and evapotranspiration losses, which are critical for understanding soil water balance and infiltration dynamics across different seasons.

Figure 4.4 illustrates the daily rainfall and evapotranspiration rates for the winter months (June, July, and August 2020). Rainfall is represented by sharp, irregular peaks (blue line), indicating intermittent, high-intensity rainfall events characteristic of New Zealand's winter season. Evapotranspiration (red line) remains relatively stable and low, reflecting reduced plant activity and lower evaporation rates during cooler months. The plot highlights the difference between rainfall and evapotranspiration, with rainfall dominating as the primary contributor to soil water during this period.

These graphs highlight the temporal variations in rainfall and evapotranspiration, which play a pivotal role in determining soil water availability and infiltration rates. During winter (June-August), high rainfall and low evapotranspiration create favourable conditions for infiltration, whereas in summer, increased evapotranspiration often leads to water deficits. The seasonal and annual trends in these graphs underscore the dynamic interplay between water inputs and losses. This data provides a foundation for the infiltration model by serving as time-dependent inputs that drive the simulation of soil water balance.

Moreover, Figure 4.5 illustrates the temporal variability of rainfall over the 90-day simulation period, represented as daily rainfall (bar chart) and cumulative rainfall (line). Rainfall serves as the primary driver of infiltration and subsequent estrogen transport in the soil. The stepwise increase in the cumulative rainfall curve reflects the discrete rainfall events, ranging from minor precipitation to peaks of approximately 25 mm/day.

This variability is important for modelling infiltration, as rainfall directly affects the soil water dynamics and the subsequent movement of estrogen within the soil profile. The rainfall data sets the initial boundary condition for water flux in the infiltration module, ensuring realistic inputs for simulating estrogen transport.

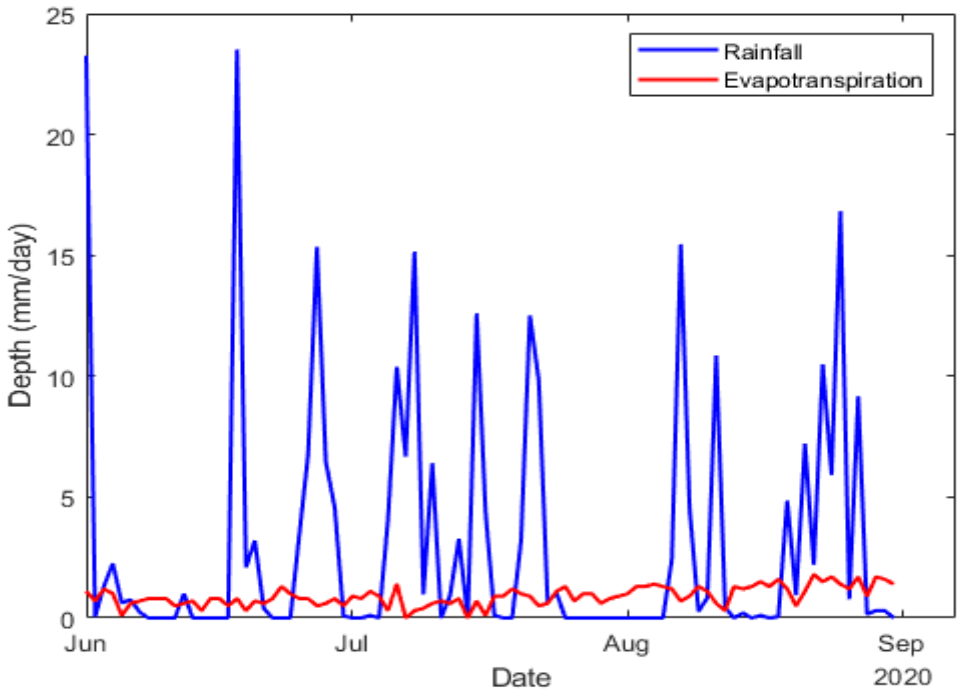

Figure 4-4: Daily rainfall and evapotranspiration rates during the winter months (June, July, August 2020)

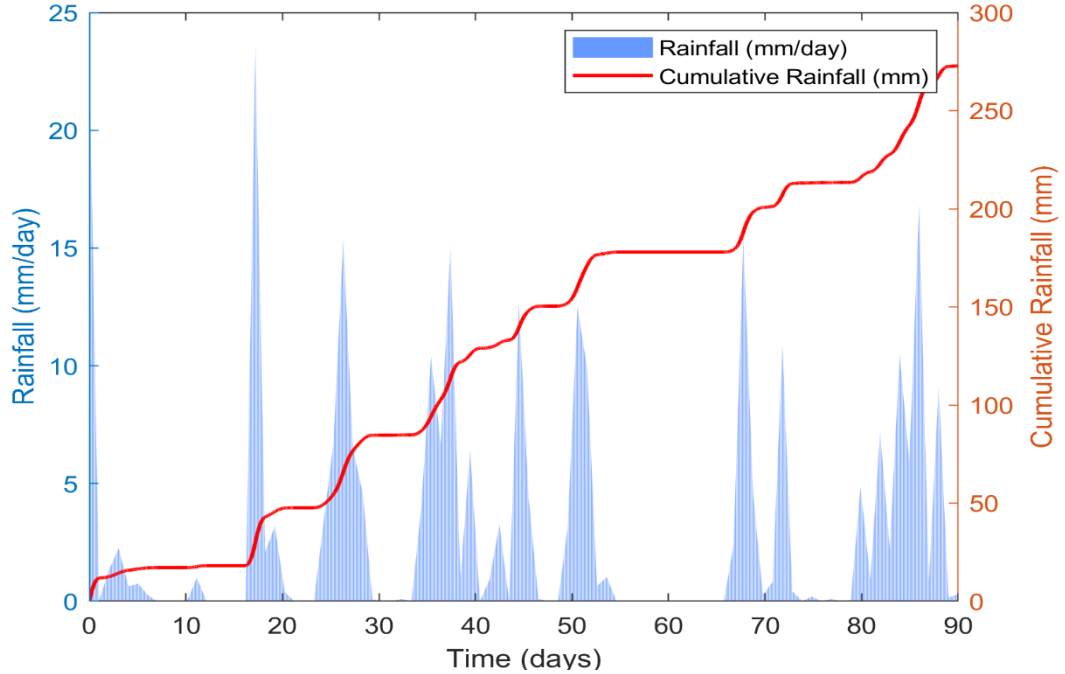

Figure 4-5: Daily rainfall and cumulative rainfall over the 90-day simulation period. The bar chart represents the daily rainfall intensity in mm/day, and the cumulative rainfall is shown as a line in mm, highlighting the contribution of individual rainfall events to total water input.

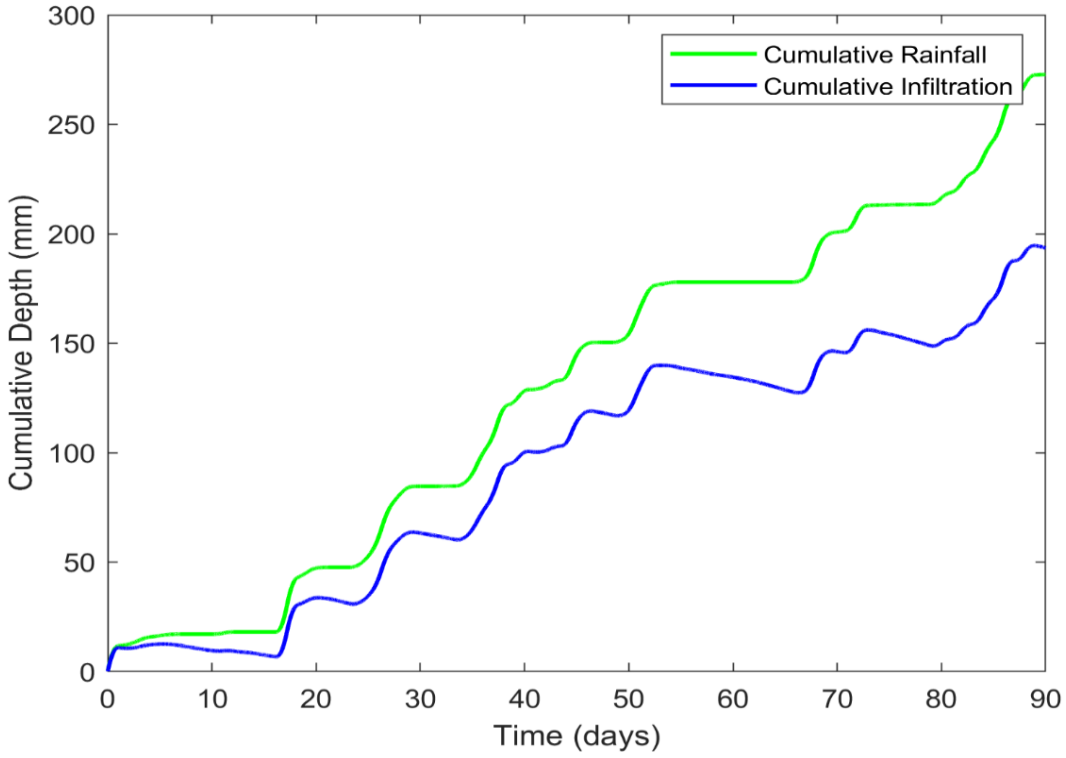

Figure 4-6: Comparison of daily rainfall and infiltration rate during the 90-day simulation period. The infiltration rate mirrors rainfall intensity, with infiltration occurring only during rainfall events. This relationship illustrates the dependence of infiltration dynamics on rainfall availability

Figure 4.6 demonstrates the relationship between cumulative rainfall and cumulative infiltration over the simulation period. The cumulative infiltration (blue line) closely tracks the cumulative rainfall (green line), indicating high infiltration efficiency under the given soil and climatic conditions. The slight gap between the two curves represents water lost to evapotranspiration, which is incorporated into the model to account for the removal of water from the soil system. This plot verifies the water balance within the infiltration module and shows that most of the rainfall infiltrates the soil, providing sufficient water for potential estrogen transport. Figure 4.7 compares the daily rainfall (blue line) and the corresponding infiltration rate (red line) in mm/day. The infiltration rate mirrors rainfall, with infiltration occurring only during rainfall events. The comparison demonstrates that infiltration rates do not exceed rainfall, consistent with the Green-Ampt infiltration model, and also emphasizes the impact of dynamic rainfall inputs on soil water infiltration.

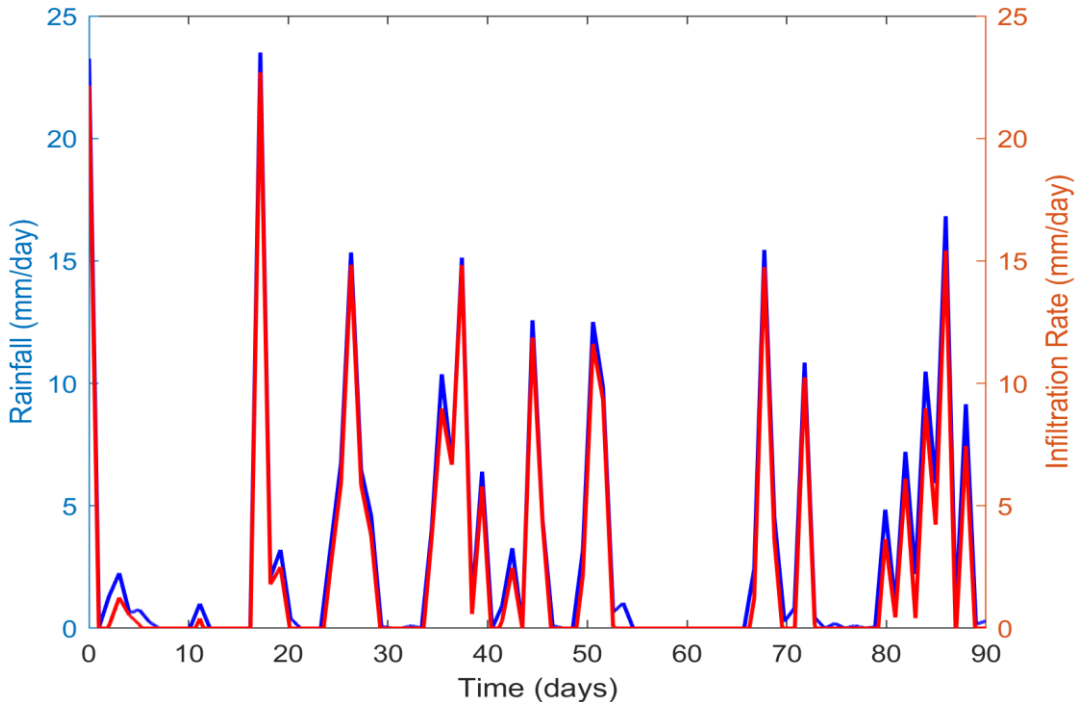

Figure 4-7: Rainfall and infiltration over the simulation period. The close alignment of the two curves indicates efficient infiltration, with minimal losses due to evapotranspiration and surface runoff. The gap between the curves reflects water retained.F

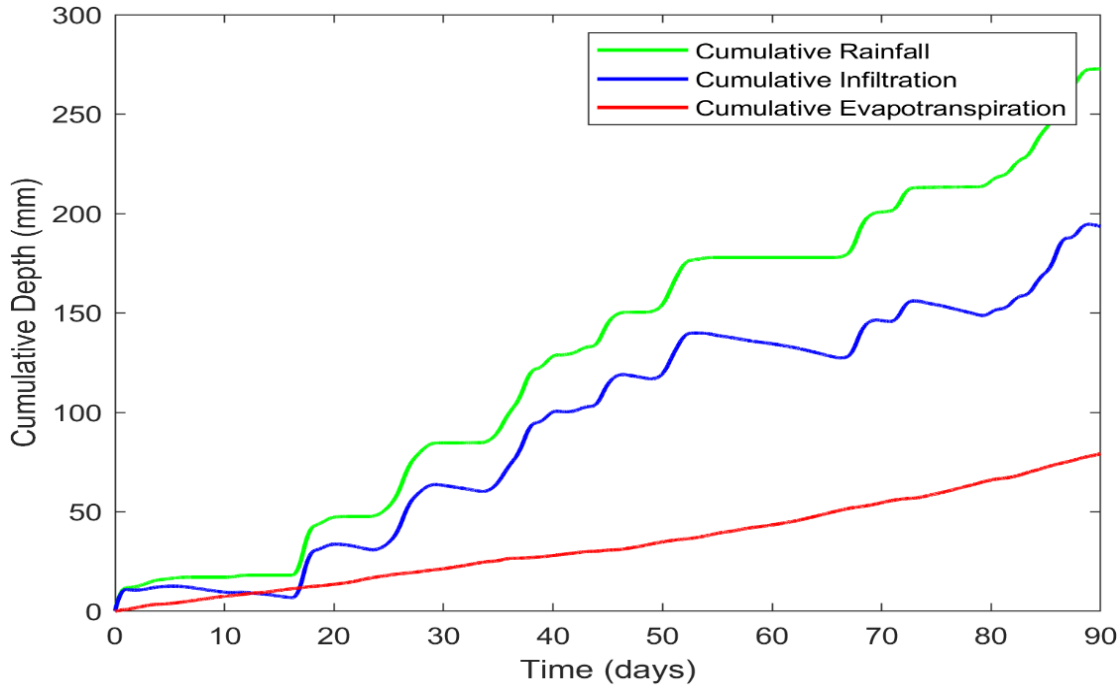

Figure 4-8: Cumulative rainfall, cumulative infiltration, and cumulative evapotranspiration over the 90-day simulation period. The plot illustrates the water balance in the infiltration module, highlighting how rainfall contributes to infiltration and ET over time.

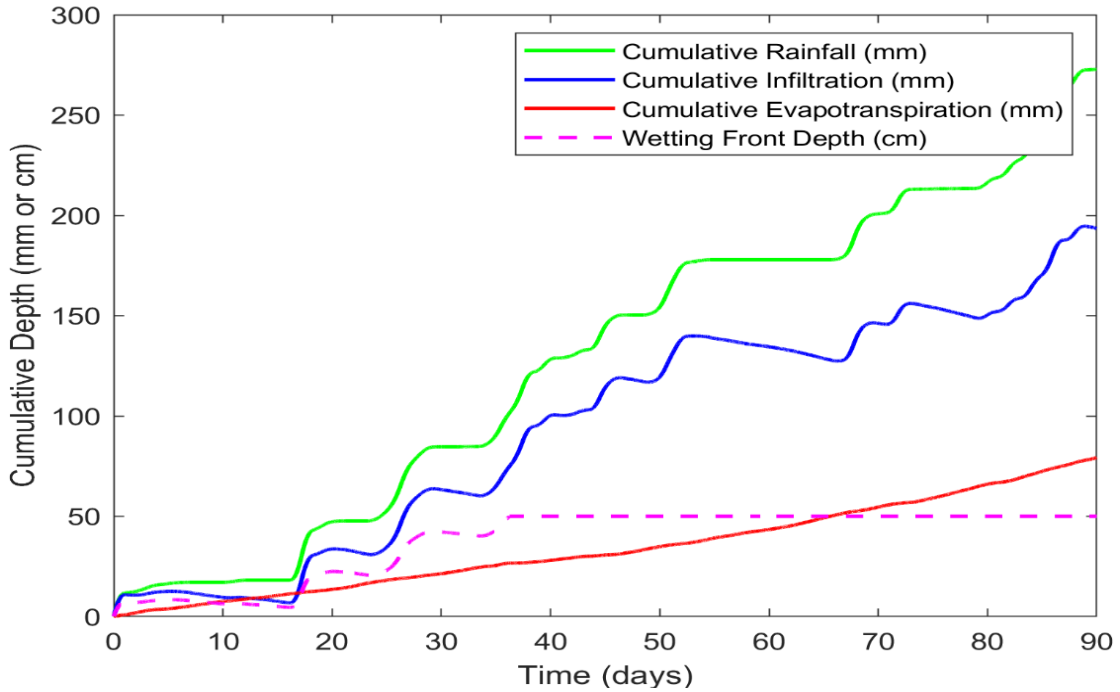

Figure 4-9: Comprehensive visualization of cumulative rainfall, cumulative infiltration, cumulative evapotranspiration, and wetting front depth during the simulation. The wetting front depth represents the progression of water into the soil, reaching a maximum of 50 cm as per the model assumptions. This figure summarises the water balance in the soil system over time.

Figure 4.8 shows the close alignment of cumulative infiltration with rainfall, demonstrating that most of the rainfall infiltrates the soil, with minimal losses to runoff. This is consistent with the Green-Ampt infiltration model and validates the water flux boundary conditions provided by the infiltration module. The cumulative evapotranspiration increases steadily, accounting for water loss due to atmospheric demand. The gap between cumulative rainfall and infiltration lines reflects the contribution of evapotranspiration to the overall water balance.
Figure 4.9 provides a comprehensive view of the water balance and wetting front progression in the soil profile. The cumulative rainfall (green line) drives the cumulative infiltration (blue line), while cumulative evapotranspiration (red line) represents water lost to the atmosphere. The wetting front depth (magenta dashed line) tracks the movement of water into the soil, reaching a maximum depth of 50 cm due to the Green-Ampt model's assumptions and the specific soil properties of silt loam. This cap ensures numerical stability while capturing the upper-zone dynamics where most estrogen sorption and degradation occur. This figure integrates all water fluxes in the system, emphasizing the dynamic interactions between rainfall, infiltration, evapotranspiration, and soil water redistribution. It highlights how the infiltration module prepares the initial conditions for estrogen transport, particularly by defining the spatial and temporal distribution of water available for solute movement.

4.6.1 Establishing Initial Conditions for the Water Model

This module establishes the initial conditions for water flow within the soil, as infiltration rates directly affect soil moisture distribution. The focus is on a 90-day winter period (June to August 2020), which requires for understanding of seasonal variations in soil infiltration and its impact on subsequent water and estrogen transport.

The infiltration module serves as the first component of the estrogen transport model, providing water fluxes and wetting front dynamics that show how estrogen is mobilised and transported in the soil. Rainfall drives infiltration, which in turn determines the depth and rate of estrogen movement through advection and dispersion. These plots validate the infiltration module, ensuring realistic water dynamics that will directly influence the coupled transport of estrogen.

The infiltration results, as visualised in these figures, establish:

1. Boundary Conditions for Water Flow: Rainfall and infiltration rates define the water flux at the soil surface.
2. Soil Water Availability: The cumulative infiltration sets the stage for water redistribution and solute transport.
3. Transport Zone Dynamics: The wetting front depth identifies the zone where estrogen transport processes (e.g., sorption and degradation) are most active.

4.7 Water Flow Module

The movement of water within the unsaturated zone plays a significant role in various applications, including agriculture, contaminant transport, and flood management. One of the most important processes this movement facilitates is groundwater recharge, which replenishes aquifers and sustains water availability. Groundwater recharge primarily occurs as precipitation infiltrates through the unsaturated zone (Farthing & Ogden, 2017; Richards, 1931).

The flow of water in unsaturated soils is commonly described mathematically using Richards' equation (Richards, 1931), which combines Darcy's law and the principle of mass conservation. Richards' equation provides a framework for simulating vertical water flow in unsaturated soils by accounting for soil hydraulic properties, pressure gradients, and water content variability in the soil profile. Richard's equation forms the foundation for modelling unsaturated water flow dynamics and serves as a critical component in understanding water transport processes in soils (Richards, 1931). In this study, Richards' equation was implemented to simulate water flow within the soil matrix, supporting the estrogen transport model by providing accurate predictions of water movement and availability.

To ensure a detailed and accurate representation of water dynamics in soil, two models were initially developed: Model 1 and Model 2, both built upon the Richards' equation. These models differ in how they handle the boundary flux at the soil surface and the integration with the infiltration process.

4.7.1 Model 1: Direct Rainfall and Evapotranspiration Inputs

Model 1 incorporates rainfall and evapotranspiration (ET) data directly into the surface boundary condition. The water flux at the surface is computed as:

$$q_{surface} = R(t) - ET(t) \quad (4.18)$$

Where R(t) is the rainfall rate and ET(t) is the evapotranspiration rate at time t. This flux drives the water movement into the soil and is used as the top boundary condition for Richards' equation. Free drainage is applied at the bottom boundary, ensuring realistic water flow at deeper soil layers.

Although Model 1 provides a straightforward approach by directly coupling rainfall and ET data, it does not account for the detailed infiltration processes, such as ponding or variability in infiltration rates due to soil saturation. Additionally, Model 1 leads to numerical instability due to the abrupt changes in boundary conditions, particularly under high rainfall or varying evapotranspiration scenarios. These limitations make it unsuitable for accurately modelling infiltration-driven transport processes under varying hydrological conditions.

4.7.2 Model 2: Coupling with Infiltration Module

In Model 2, the infiltration process is modelled using the Green-Amp equation and coupled with the Richards' equation. The surface flux $q_{surface}$ is derived from the Green-Ampt infiltration module, which provides a dynamic infiltration rate based on soil hydraulic properties and cumulative infiltration. This approach offers a more physically realistic representation of water entry into the soil by considering processes such as wetting front propagation. The Green-Ampt model accounts for the soil's saturated hydraulic conductivity (K_s), suction head (ψ), and the initial and saturated water content difference ($\Delta\theta$). By coupling this infiltration module with the water flow model, we integrate the effects of surface hydrology and subsurface flow.

Given the objectives of this study, which emphasize accurate water flow simulation for estrogen transport modelling, Model 2 provides the necessary framework for achieving reliable results. The instability issues associated with Model 1 further justify the decision to exclusively use Model 2.

4.8 Numerical Approach for Water Flow Module

The numerical solution of Richards' equation is implemented using the finite difference method (FDM) for spatial discretisation and the backward Euler method for temporal discretisation (Peskin & Schlick, 1989). The spatial grid is divided into discrete nodes, with Δx representing the distance between adjacent nodes, and Δt representing the time step size. As depicted in Figure 4.10, the pressure head h is calculated at each node i for successive time steps n and $n+1$. h_i^n denotes the pressure head at a spatial node i and time step n.

The implicit nature of the backward Euler scheme ensures numerical stability by solving for the pressure head values at the time step $n+1$ iteratively using the Picard method. This approach is particularly effective for handling the non-linearity of Richards' equation, especially when coupled with the Green-Ampt infiltration module to provide surface boundary conditions.

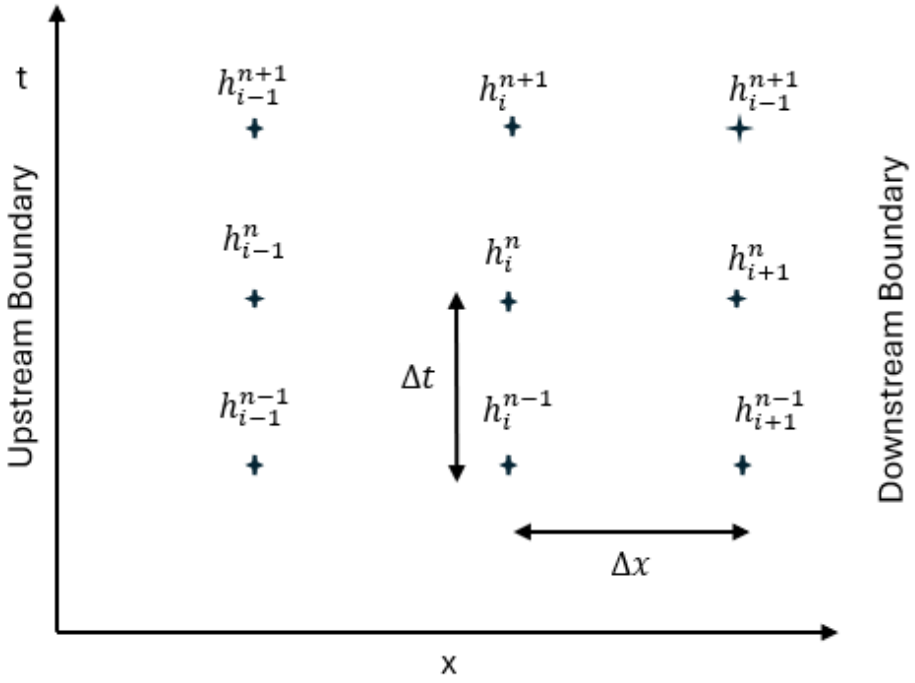

Figure 4-10: Schematic representation of the finite difference grid for solving Richards' equation using the backward Euler method. The grid illustrates spatial (Δx) and temporal (Δt) discretisation, with pressure head values (h_i^n) at various nodes and time steps.

4.8.1 Richards Equation

The Richards equation can effectively model water flow in unsaturated soils, which is important for understanding the movement of estrogen through both the vadose (unsaturated) and saturated zones of soil. It handles both saturation and unsaturation conditions by combining Darcy's law and the continuity equation, providing a more comprehensive detail of soil moisture dynamics. The Richard equation can be written in many forms, such as moisture

content, mixed moisture content capillary head (pressure head) and pressure head form (Celia et al., 1987; Farthing & Ogden, 2017; Ratha et al., 2023). The above Richard's equation forms are:

- Soil moisture form

$$\frac{\partial \theta}{\partial t} = \frac{\partial}{\partial z}\left(D(\theta)\frac{\partial \theta}{\partial z}\right) - \frac{\partial K(\theta)}{\partial z} \tag{4.19}$$

- Pressure head form

$$C(h)\frac{\partial h}{\partial t} = \frac{\partial}{\partial z}\left(K(h)\left(\frac{\partial h}{\partial z} - 1\right)\right) \tag{4.20}$$

- Mixed form

$$\frac{\partial \theta}{\partial t} = \frac{\partial}{\partial z}\left(K(\theta)\left(\frac{\partial h}{\partial z} - 1\right)\right) \tag{4.21}$$

Where, $D(\theta)$ is the soil moisture diffusivity coefficient, defined as $D(\theta)=K(\theta)(dh/d\theta)$, and $C(h) = \frac{\partial \theta}{\partial h}$ is the specific soil moisture content, θ is the volumetric water content of the soil (dimensionless), t is time, z is the spatial coordinate (vertical direction, positive downward), h is the pressure head $K(\theta)$ is the unsaturated hydraulic conductivity as a function of the water content.

The term $\frac{\partial h}{\partial z} - 1$ represents the hydraulic gradient due to gravity (since the gradient of the hydraulic head h includes both the pressure gradient and the gravitational potential. The Richard equation states that the change in water content over time $\frac{\partial \theta}{\partial t}$ is equal to the divergence of the flux, where the flux is the product of the hydraulic conductivity and the hydraulic gradient. This formulation captures the dynamics of water flow in soils that are not fully saturated, where both the hydraulic properties and water content can vary with depth and over time.

Richard's equation can be challenging to solve due to its non-linear nature, especially because $K(\theta)$ and the soil water retention curve (which relates θ to h) are both highly non-linear functions. Numerical methods, such as finite differences or finite elements (Kreiss & Scherer, 1974; Marfurt, 1984), are typically employed to find solutions under given initial and boundary conditions. The Richard equation contains both first and second-order derivatives, and finite-difference method techniques are commonly used to solve the equation.

The relationships between θ, K, and h were calculated using the Van Genuchten-Mualem (VGM) Model (Simunek & van Genuchten, 1999; Vereecken et al., 2010).

4.8.2 Van Genuchten Equation

The Van Genuchten model is widely used to describe the soil water retention curve, which defines the relationship between the soil's water content and its hydraulic properties. By linking hydraulic conductivity to the moisture content through the Van Genuchten parameters, we can more accurately simulate how changes in soil moisture affect the transport and fate of estrogen. The Van Genuchten model describes the soil water retention curve, linking volumetric water content (θ) to the pressure head (h). This relationship captures the soil's ability to retain or release water under varying moisture conditions. Additionally, the Van Genuchten hydraulic conductivity function connects soil moisture to hydraulic conductivity (K), enabling the simulation of water flow within the soil matrix. The Van Genuchten model is written as (Simunek & van Genuchten, 1999; Vereecken et al., 2010) :

$$\theta(h) = \theta_r + \frac{\theta_s - \theta_r}{(1 + (\alpha|h|)^n)^m} \tag{4.22}$$

$$h < 0, \theta_s, h >= 0$$

Where: $\theta(h)$ is the volumetric water content at pressure head h, θ_r is the residual water content, θ_s is the saturated water content, α is an air entry parameter (cm^{-1}), n is a pore size distribution parameter, and m is empirical fitting parameters with $m = 1 - 1/n$

Van Genuchten's hydraulic conductivity function can be written as:

$$K(\mathrm{h}) = K_r K_s = K_s[S_e]^{\lambda}\left[1 - \left(1 - (S_e)^{\frac{1}{m}}\right)^m\right]^2 \tag{4.23}$$

Where, $K(\theta)$ is unsaturated hydraulic conductivity, K_s is saturated hydraulic conductivity, S_e is effective saturation, λ is an empirical parameter (often taken as 0.5), and K_r is relative hydraulic conductivity. Where S_e can be calculated as:

$$S_e = \frac{\theta - \theta_r}{\theta_s - \theta_r} \tag{4.24}$$

4.8.3 Initial and Boundary Conditions

The initial and boundary conditions for the Richard equations are described as;

4.8.3.1 Initial Condition

The initial condition specifies the soil moisture profile (θ) or the pressure head (h) at each depth within the soil column at the start of the simulation (t = 0). This provides a baseline state for the model to simulate water movement.

$$\theta(z,0) = \theta_0(z), \qquad 0 < z < Z, \qquad t = 0$$

It sets up the initial state of the soil moisture before any infiltration begins. In the model, the pressure head is initialized with a slightly negative value (h = − 0.5 m) across the soil profile to represent the unsaturated conditions of the soil. The corresponding water content (θ) is calculated using the Van Genuchten water retention model:

The MATLAB representation:

```
h = -0.5 * ones(Nz, 1);      % Initial pressure head (m)
theta = theta_vG(h);         % Initial water content based on van Genuchten model
```

This initialization ensures that the soil is not fully saturated, which aligns with typical conditions in the unsaturated zone.

4.8.3.2 Top Boundary Condition (Surface)

The top boundary condition defines the water flux or pressure head at the soil surface (z = 0). Two approaches are used in the model:

Model 1: Surface flux is calculated directly from rainfall (R(t) and evapotranspiration ET(t),

$$q_{surface} = R(t) - ET(t) \qquad (4.25)$$

where, R(t) rainfall rate at time t, ET(t) evapotranspiration rate at time t.

Model 2: Surface flux is derived from the Green-Ampt infiltration module:

$$q_{surface} = f(t) \qquad (4.26)$$

Where f(t) is the infiltration rate calculated from the infiltration module.

The top boundary condition is applied in MATLAB as:

```
A(1, 1) = 1;
b(1) = q_surface / dz;infiltration_rate(t - 1);  % Surface flux from infiltration module or rainfall/evaporation
```

This boundary condition allows for dynamic interactions between surface water and soil, ensuring that the model captures the effects of infiltration, rainfall, and evapotranspiration.

4.8.3.3 Boundary Condition at the Bottom (Bottom Boundary)

The bottom boundary condition is applied at the deepest node (z = Z) of the soil column. It represents either free drainage or a saturated condition, depending on the pressure head (h):

- When $h < 0$, it implies unsaturated conditions and the gradient of the total head ($h + z$) with respect to z is zero. This is a free drainage condition. We apply this as the bottom boundary condition as:

  $\partial(h+z)/\partial z = 0$, if $h < 0$, $z = Z$, $t > 0$

- When $h \geq 0$, it implies saturated conditions and the pressure head h is zero, indicating that the bottom boundary is at the water table or a saturated zone.

  $h = 0$, if $h \geq 0$, $z = Z$, $t > 0$

  In the MATLAB code, we applied it as :

  A(Nz, Nz) = 1;

  b(Nz) = h(Nz-1); % Free drainage, % No pressure gradient at the bottom

For all simulations, the bottom boundary remained unsaturated, so the free drainage condition was applied consistently.

4.8.4 Numerical solution of the Richard equation

We used the mixed form of the Richard equation defined as;

$$\frac{\partial \theta(h)}{\partial t} = \frac{\partial}{\partial z}\left(K(h)\left(\frac{\partial h}{\partial z} - 1\right)\right) \tag{4.27}$$

The mixed form allows for more flexible and realistic boundary conditions that can use natural processes such as infiltration and evaporation. Additionally, the mixed form of Richard's equation effectively captures this nonlinearity by incorporating both θ and h, which allows for a more accurate representation of the flow dynamics in soil. Equation (4.27) contains the following components:

Temporal term:

$$\frac{\partial \theta(h)}{\partial t} \tag{4.28}$$

Flux term:

$$\frac{\partial}{\partial z}\left(K(h)\left(\frac{\partial h}{\partial z}\right)\right) \tag{4.29}$$

Gravity term:

$$-\frac{\partial}{\partial z}\left(K(h)\right) \tag{4.30}$$

4.8.5 Discretisation of the Flux and Gravity terms

The water flux q is given by Darcy's law:

$$\mathrm{q} = -\mathrm{K(h)}\frac{\partial \mathrm{h}}{\partial \mathrm{z}} \tag{4.31}$$

Where q is water flux (m/day), K(h) is hydraulic conductivity as a function of pressure head (h) (m/day), h is pressure head (m) and z is vertical depth (m).

At node i , the flux at the midpoint between nodes i and i+1 $q_{i+\frac{1}{2}}$ is approximated using central difference

$$\mathrm{q}_{\mathrm{i}+\frac{1}{2}} = -\mathrm{K}_{\mathrm{i}+\frac{1}{2}}\frac{\mathrm{h}_{\mathrm{i}+1} - \mathrm{h}_{\mathrm{i}}}{\Delta \mathrm{z}} \tag{4.32}$$

Where, $K_{i+\frac{1}{2}}$ is the hydraulic conductivity at the midpoint between nodes i and $i+1$, h_i and h_{i+1} are pressure heads at nodes i and $i+1$, Δz is the distance between adjacent nodes
The midpoint hydraulic conductivity $K_{i+\frac{1}{2}}$ is calculated as the arithmetic mean:

$$\mathrm{K}_{\mathrm{i}+\frac{1}{2}} = \frac{\mathrm{K}_{\mathrm{i}} + \mathrm{K}_{\mathrm{i}+1}}{2} \tag{4.33}$$

Similarly, the flux at the midpoint between nodes $i-1$ and $q_{i-\frac{1}{2}}$ is

$$\mathrm{q}_{\mathrm{i}-\frac{1}{2}} = -\mathrm{K}_{\mathrm{i}-\frac{1}{2}}\frac{\mathrm{h}_{\mathrm{i}} - \mathrm{h}_{\mathrm{i}-1}}{\Delta \mathrm{z}} \tag{4.34}$$

and,

$$\mathrm{K}_{\mathrm{i}-\frac{1}{2}} = \frac{\mathrm{K}_{\mathrm{i}-1} + \mathrm{K}_{\mathrm{i}}}{2} \tag{4.35}$$

The divergence of the flux at node i is approximated using finite difference.

$$\frac{\partial \mathrm{q}}{\partial \mathrm{z}} \approx \frac{\mathrm{q}_{\mathrm{i}+\frac{1}{2}} - \mathrm{q}_{\mathrm{i}-\frac{1}{2}}}{\Delta \mathrm{z}} \tag{4.36}$$

Submitting $q_{i+\frac{1}{2}}$ and $q_{i-\frac{1}{2}}$ in eq (4.36)

$$\frac{\partial \mathrm{q}}{\partial \mathrm{z}} \approx \frac{-\mathrm{K}_{\mathrm{i}+\frac{1}{2}}\frac{\mathrm{h}_{\mathrm{i}+1} - \mathrm{h}_{\mathrm{i}}}{\Delta \mathrm{z}} + \mathrm{K}_{\mathrm{i}-\frac{1}{2}}\frac{\mathrm{h}_{\mathrm{i}} - \mathrm{h}_{\mathrm{i}-1}}{\Delta \mathrm{z}}}{\Delta \mathrm{z}} \tag{4.37}$$

The gravity term is discretised as :

$$-\frac{\partial \mathrm{K}}{\partial \mathrm{z}} \approx -\frac{\mathrm{K}_{\mathrm{i}+\frac{1}{2}} - \mathrm{K}_{\mathrm{i}-\frac{1}{2}}}{\Delta \mathrm{z}} \tag{4.38}$$

4.8.6 Temporal discretisation

Temporal discretisation is used to approximate the time-dependent term in Richards' equation. In the implementation of the water flow module as shown in Figure 4.10, we utilise the backward Euler method (Peskin & Schlick, 1989), which is a fully implicit numerical scheme (Radu et al., 2004). This method is chosen because it ensures numerical stability, especially for nonlinear and stiff problems such as Richards' equation. The backward Euler method is unconditionally stable, meaning it remains stable for larger time step sizes (Δt), even when dealing with nonlinearities in the soil properties such as θ(h) and K(h).

In the implementation, the numerical model solves for the pressure head *h* iteratively using the Picard iteration method. Once the pressure head h is updated at each time step, the corresponding moisture content θ is calculated using the van Genuchten model $\theta = \theta(h)$.

Using the backward Euler method, the temporal derivative is approximated as:

$$\frac{\partial \theta}{\partial t} \approx \frac{\theta_i^{n+1} - \theta_i^n}{\Delta t} \tag{4.39}$$

Where, θ_i^{n+1} volumetric water content at node i at the new step $\mathrm{n}+1$, θ_i^n volumetric water content at node i and previous time step n, Δt is the time step size.

However, since the model solves for *h* rather than θ, the discretized form of Richards' equation is applied in the model as $\frac{\theta_i^{n+1}(h_i^{n+1}) - \theta_i^n(h_i^n)}{\Delta t} = \text{Flux Term} + \text{Gravity Term}$.

Richards' equation is nonlinear due to the dependence of θ(h) and K(h) on the pressure head h. The backward Euler method handles this nonlinearity by evaluating θ(h) and K(h) at the new time step $\mathrm{n}+1$, ensuring accurate solutions. Combining the spatial discretisation (finite difference) and temporal discretisation (backward Euler), the fully discretized Richards' equation at node i is

$$\frac{\theta_{\mathrm{i}}^{\mathrm{n}+1} - \theta_{\mathrm{i}}^{\mathrm{n}}}{\Delta \mathrm{t}} = \frac{\mathrm{K}_{\mathrm{i}+\frac{1}{2}}(\mathrm{h}_{\mathrm{i}+1}^{\mathrm{n}+1} - \mathrm{h}_{\mathrm{i}}^{\mathrm{n}+1}) - \mathrm{K}_{\mathrm{i}-\frac{1}{2}}(\mathrm{h}_{\mathrm{i}}^{\mathrm{n}+1} - \mathrm{h}_{\mathrm{i}-1}^{\mathrm{n}+1})}{\Delta \mathrm{z}^2} \tag{4.40}$$

Eq (4.40) it can be written as,

$$\frac{\theta_i^{n+1} - \theta_i^n}{\Delta t} = \frac{1}{\Delta z^2}\left[K_{i+1/2}^{n+1}(h_{i+1}^{n+1} - h_i^{n+1}) - K_{i-1/2}^{n+1}(h_i^{n+1} - h_{i-1}^{n+1})\right] + \frac{1}{\Delta z}\left[K_{i+1/2}^{n+1} - K_{i-1/2}^{n+1}\right] \quad (4.41)$$

The equations (4.40) and (4.41) represent a discretised version of Richards' equation for one-dimensional water flow in unsaturated soil, incorporating both flux and gravity terms and solved iteratively for all nodes at each time step. The equation (4.41) includes both flux divergence and gravity terms, making it a complete representation of Richards' equation in discretized form.

The gravity term from equation (4.41) $\frac{1}{\Delta z}\left[K_{i+1/2}^{n+1} - K_{i-1/2}^{n+1}\right]$ accounts for the influence of gravity on water movement. The equation is slightly more complex because it explicitly separates the gravity term. We used the equation (4.40) in the model, in which both the flux divergence and gravity terms are implicitly combined into a single term. The fluxes at the midpoints already account for the effects of gravity through the hydraulic conductivity values K(h). This form avoids separating the gravity term explicitly, assuming the combined K(h) behaviour adequately represents the effect of gravity.

Combining the flux and gravity terms reduces the complexity of the discretisation and matrix assembly. The effects of gravity are captured by the hydraulic conductivity K(h), which simplifies computation. The compact form reduces computational overhead while maintaining physical accuracy for typical unsaturated soil problems.

4.9 Iterative Solution of Richard's Equation: Picard Iteration

Since θ_i^{n+1} and $K(h_i^{n+1})$ depend on h_i^{n+1}, solving the discretized equation directly for h_i^{n+1} is not feasible. An iterative approach, such as Picard's iteration (Celia et al., 1987), is employed to handle the nonlinearity of the Richard equation. The Picard iteration method is a fixed-point iteration technique used to solve nonlinear systems of equations (Berinde, 2004; Celia et al., 1987). In the context of Richards' equation, the method is employed to solve for the pressure head h at each time step iteratively until convergence.

4.9.1 Picard Iteration Implementation

Initialisation: At the start of each time step n+1, initialise the pressure head $h^{(0)}$ (the initial guess) with the solution from the previous time step h^n

$$h^{(0)} = h^{n} \tag{4.42}$$

The Initial water content and hydraulic conductivity using the Van Genuchten model,

$$\theta^{(0)} = \theta\left(h^{(0)}\right), \quad K^{(0)} = K\left(h^{(0)}\right) \tag{4.43}$$

In MATLAB, h_old represents the initial guess for the pressure head at iteration k = 0, which corresponds to $h^{(0)}$ in the mathematical description. Similarly, the water content (θ) and hydraulic conductivity (K) are initialised using h_old.

% Initialize variables

h_old = h; % Initial pressure head from the previous time step (h^n)

theta = theta_vG(h_old); % Initial water content using van Genuchten model (θ^(0))

K = K_vG(theta); % Initial hydraulic conductivity (K^(0))

Matrix and RHS Assembly: Discretised Richard equation (4.40)

$$\frac{\theta_i^{n+1} - \theta_i^{n}}{\Delta t} = \frac{K_{i+\frac{1}{2}}(h_{i+1}^{n+1} - h_i^{n+1}) - K_{i-\frac{1}{2}}(h_i^{n+1} - h_{i-1}^{n+1})}{\Delta z^2}$$

Rearrange the above equation

$$\frac{\theta_i^{n+1}}{\Delta t} - \frac{K_{i+\frac{1}{2}}h_{i+1}^{n+1} - \left(K_{i+\frac{1}{2}} + K_{i-\frac{1}{2}}\right)h_i^{n+1} + K_{i-\frac{1}{2}}h_{i-1}^{n+1}}{\Delta z^2} = \frac{\theta_i^{n}}{\Delta t} \tag{4.44}$$

Tridiagonal matrix formation

$$A_{i,i-1}h_{i-1}^{n+1} + A_{i,i}h_i^{n+1} + A_{i,i+1}h_{i+1}^{n+1} = b_i \tag{4.45}$$

The tridiagonal coefficients for matrix formulation can be written as:

Lower diagonal:

$$A_{i,i-1} = -\frac{K_{i-\frac{1}{2}}}{\Delta z^2} \tag{4.46}$$

Main diagonal:

$$A_{i,i} = \frac{1}{\Delta t} + \frac{K_{i+\frac{1}{2}} + K_{i-\frac{1}{2}}}{\Delta z^2} \tag{4.47}$$

Upper diagonal:

$$A_{I,i+1} = -\frac{K_{i+\frac{1}{2}}}{\Delta z^2} \tag{4.48}$$

Right-hand side vector:

$$b_i = \frac{\theta_i^n}{\Delta t} + \frac{K_{i+\frac{1}{2}} - K_{i-\frac{1}{2}}}{\Delta z} \quad (4.49)$$

In MATLAB, h_old corresponds to $h^{(k)}$, which is the solution from the previous iteration. The matrix A and the right-hand side vector b are constructed iteratively using the current values of K.

```
% Loop over interior nodes to construct the matrix A and vector b
for i = 2:Nz-1
   A(i, i-1) = -K(i-1) / dz^2;  % Lower diagonal (A_{i,i-1})
   A(i, i) = 1/dt + (K(i+1) + K(i-1)) / dz^2;  % Main diagonal (A_{i,i})
   A(i, i+1) = -K(i+1) / dz^2;  % Upper diagonal (A_{i,i+1})
   b(i) = theta(i) / dt + (K(i+1) - K(i-1)) / dz;  % RHS vector (b_i)
end
```

Linear System Solution: The system of linear equations for $h^{(k+1)}$is

$$Ah^{(k+1)} = b \quad (4.50)$$

In each iteration, the matrix A and vector b are updated based on the current estimates of the hydraulic conductivity and pressure head. This iterative approach ensures convergence to a solution that satisfies the nonlinear Richard's equation.

To further elaborate on the matrix A the coefficient matrix A is constructed to capture the interactions between each node in the discretized domain based on the finite difference method. The diagonal elements account for the temporal changes and the fluxes due to hydraulic conductivity, while the off-diagonal elements represent the influence of adjacent nodes. This formulation ensures that the linear system accurately represents the physics of water transport in unsaturated soils according to Richards' equation.

The MATLAB backslash operator (\) is used to solve the system.

```
% Solve the linear system for the new pressure head
h_new = A \ b;  % h^(k+1)
```

Boundary conditions: For surface and bottom nodes we applied boundary conditions (surface flux from the infiltration module and rainfall/evapotranspiration, and free drainage at the bottom for Model 1 and Model 2). For top boundary condition (Node i = 1): At the surface, we impose a flux boundary condition (from infiltration module or rainfall minus evapotranspiration).

$$A_{1,1} = 1, \quad b_1 = \frac{q_{surface}}{\Delta z}$$

Here, $q_{surface}$ comes from the infiltration module or is derived as $q_{surface}$= R(t)−ET(t) for direct implimentaion. Bottom boundary conditions (Node i = Nz): Free drainage is applied (∂h/∂z=0)

$$A_{N_z,N_z} = 1, \quad b_{N_z} = h_{N_z-1}$$

Boundary conditions are directly imposed by setting the first and last rows of the matrix A and the vector b.

% Top boundary: Surface flux
A(1, 1) = 1;
b(1) = q_surface / dz; % Surface flux from infiltration module
% Bottom boundary: free drainage
A(Nz, Nz) = 1;
b(Nz) = h(Nz-1); % No pressure gradient at the bottom

Update Nonlinear Terms: Picard iteration updated water content and hydraulic conductivity for each iteration.

$$\theta^{(k+1)} = \theta\left(h^{(k+1)}\right), \quad K^{(k+1)} = K\left(h^{(k+1)}\right)$$

In MATLAB, implemented as:

% Update variables for the next iteration
h_old = h_new; % Update $h^{(k+1)}$ for the next iteration
theta = theta_vG(h_old); % Update water content
K = K_vG(theta); % Update hydraulic conductivity h_new is obtained, theta and K are updated for the next iteration.

Convergence Check: We use a pressure head for tolerance criteria.

$$|h^{(k+1)} - h^{(k)}| < \text{tolerance}$$

If the difference is smaller than the tolerance, the iterations stop, and $h^{(n+1)} = h^{(k+1)}$ is accepted as the solution for the current time step. If not, repeat the steps. In MATLAB, h_new corresponds to $h^{(k+1)}$, while h_old represents $h^{(k)}$

if norm(h_new - h_old) < tol% Check for convergence
break; % Exit the iteration loop if converged
end

Store Results: After convergence, store $h^{(n+1)}$, $\theta^{(n+1)}$, $K^{(n+1)}$. Results are stored in arrays for further analysis and visualization. In the code, we represented it as:

% Store the results for the current time step
h_all(:, t) = h_new;
theta_all(:, t) = theta;
K_all(:, t) = K;

Proceed to Next Time Step: Move to the next time step n + 2 and repeat the procedure until the end of the simulation using the previous steps.

In summary, the Picard iteration method is an efficient technique used to solve the non-linear Richards equation in our water flow model. By linearising the non-linear terms iteratively, the method ensures numerical stability and convergence within each time step. In Picard iteration, the pressure head (h) is updated iteratively until convergence is achieved. Starting with an initial guess for the pressure head h^0 the method computes the water content (θ) and hydraulic conductivity (K) using the Van Genuchten model. These values are used to assemble the tridiagonal matrix and the right-hand side vector of the discretized Richards' equation. The system of linear equations is then solved to obtain an updated estimate of the pressure head $h^{(k+1)}$. The process continues until the difference between consecutive iterations ($h^{(k+1)}-h^{(k)}$) is smaller than a predefined tolerance, indicating convergence. At this point, the solution for the current time step is accepted, and the model progresses to the next time step.

4.10 Results and Discussion: Water Flow

4.10.1 Soil Water Dynamics

This section explores the dynamics of soil water within a soil profile using Richards' equation outputs. The numerical model integrates real rainfall and evapotranspiration-based infiltration module data, offering insights into water movement across various depths over time. Key plots illustrating temporal and spatial variations in pressure head, hydraulic conductivity, and soil moisture are provided to describe the system's behaviour. The results are used for understanding soil water balance and serve as the foundation for subsequent analysis of estrogen transport in the soil.

Figure 4.11 shows the temporal variation of soil moisture (dimensionless) across different depths of the soil profile: surface (0 m), 0.10 m, 0.5 m, 1.0 m, and 1.5 m over a 90-day simulation period. The surface layer exhibits the most fluctuations in soil moisture over time. The sharp drops in soil moisture correspond to periods of high infiltration or lack of rainfall, highlighting the sensitivity of the surface layer to atmospheric conditions. The 0.10 m depth shows smaller fluctuations compared to the surface layer but still reflects short-term changes. This layer acts as a transition zone, buffering the effects of surface dynamics while still responding to infiltration and evapotranspiration processes. The soil moisture at 0.5 m, 1.0 m, and 1.5 m remains nearly constant throughout the simulation. These depths are less influenced by short-term surface conditions, suggesting limited infiltration beyond the upper layers due to low hydraulic conductivity or unsaturated conditions. Additionally, the sharp responses in the

surface and near-surface layers highlight the importance of these zones in processes like nutrient leaching and contaminant transport.

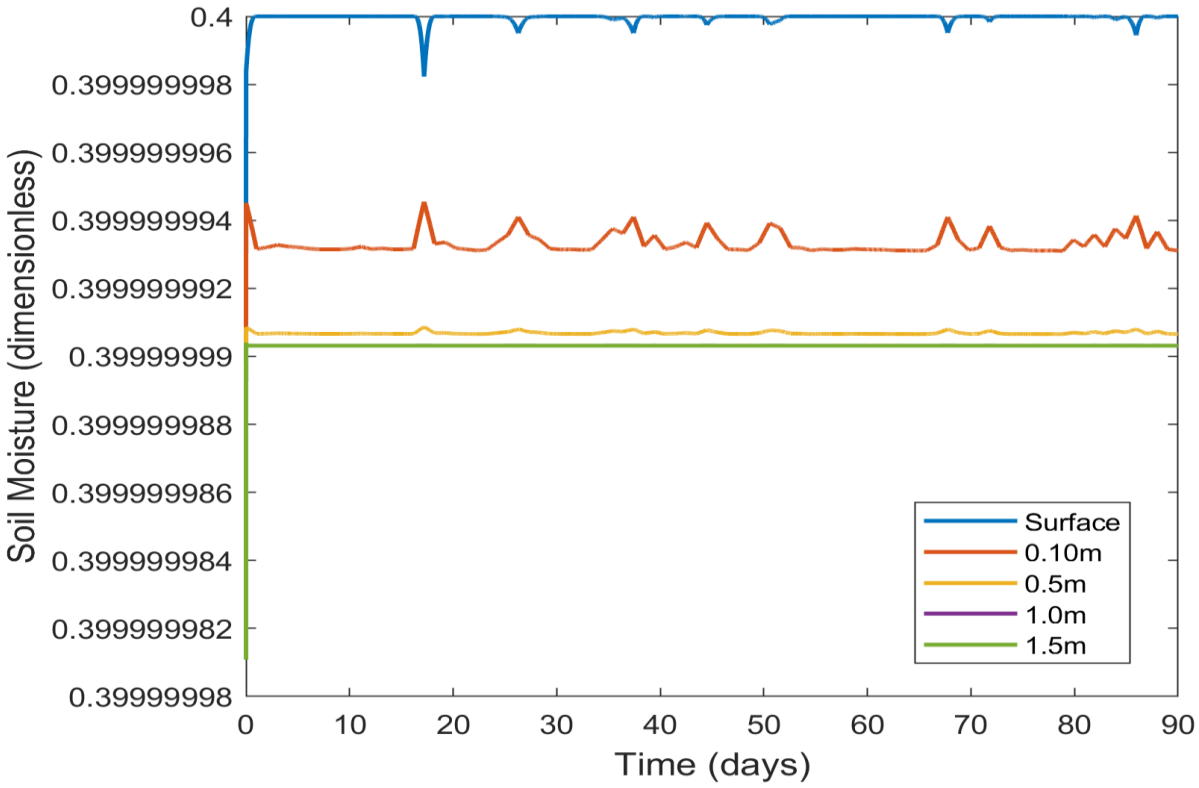

Figure 4-11: Temporal variation of soil moisture (dimensionless) across different depths (surface, 0.10 m, 0.5 m, 1.0 m, and 1.5 m) over a 90-day simulation period

4.10.2 Pressure Head Behaviour

Figure 4.12 illustrates the temporal variation of pressure head (in meters) at different soil depths (surface (0 m), 0.10 m, 0.5 m, 1.0 m, and 1.5 m) over a 90-day simulation period. The results presented here are obtained using the infiltration module (Model 2), where the surface flux is calculated using the Green-Ampt infiltration model, which dynamically accounts for infiltration rates based on soil hydraulic properties and cumulative infiltration.

The surface layer exhibits significant fluctuations in pressure head closely linked to infiltration events driven by rainfall, as simulated by the Green-Ampt module. Negative pressure head values (tension) dominate, indicative of unsaturated conditions in the topsoil. The sharp drops in pressure head correspond to increased infiltration rates following rainfall, where water infiltrates into the soil, causing a temporary decrease in pressure head before gradually recovering as the soil moisture redistributes.

At 0.10 m depth, pressure head fluctuations are present but dampened compared to the surface, reflecting the buffering effect of the soil profile. This depth still shows responsiveness to infiltration events calculated by the Green-Ampt model, though with reduced intensity.

In deeper layers (below 0.10 m), the pressure head remains relatively stable over time, with minimal to negligible fluctuations. These depths are largely unaffected by surface processes like rainfall and evapotranspiration during the simulated period, maintaining near-saturation conditions. This stability reflects the limited impact of surface infiltration on deeper soil layers over the 90-day simulation.

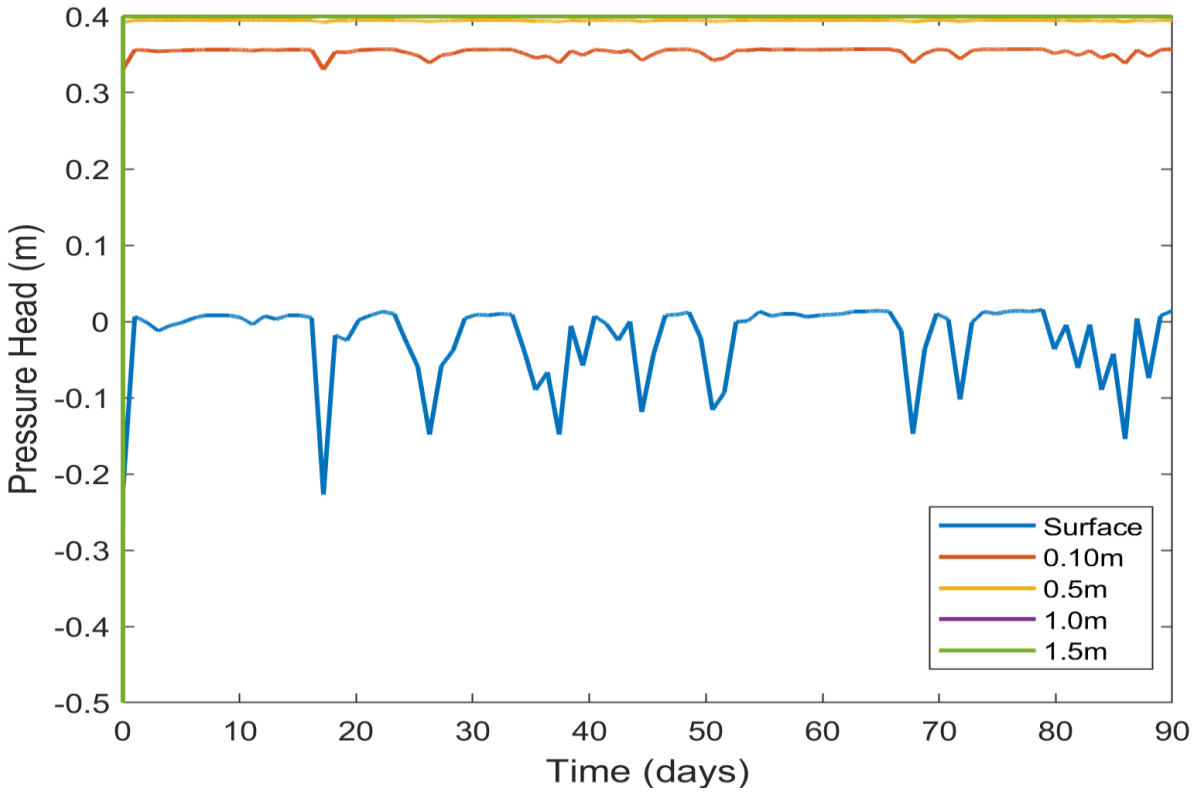

Figure 4-12: Temporal variation of pressure head at various soil depths for 90 days simulation

4.10.2.1 Implication of Pressure Head Dynamics

The dynamic pressure head at the surface shows its responsiveness to external environmental conditions. While, the stability of deeper layers suggests they serve as reservoirs with low hydraulic conductivity, restricting rapid water movement. This behaviour is important for understanding water availability for plant roots, as fluctuations are limited to the top 0.10-0.20 m, which coincides with the majority of root activity in many crops and dairy pastures. The

surface layer's high variability in the pressure head is critical for estrogen transport modelling, as it influences the movement of dissolved estrogens and colloid-bound particles. The deeper layers, being more stable, may contribute to long-term retention or slower vertical migration of estrogens.

4.10.3 Hydraulic Conductivity Dynamics

Figure 4.12 illustrates the temporal evolution of hydraulic conductivity at various depths (surface, 0.10 m, 0.50 m, 1.0 m, and 1.5 m) over a 90-day simulation period. The surface layer exhibits the most dynamic behaviour, with pronounced fluctuations in hydraulic conductivity corresponding to infiltration and drying cycles driven by rainfall and evapotranspiration.

These fluctuations are particularly evident in the steep drops in conductivity, which likely coincide with drying periods, reducing pore connectivity in the unsaturated zone.

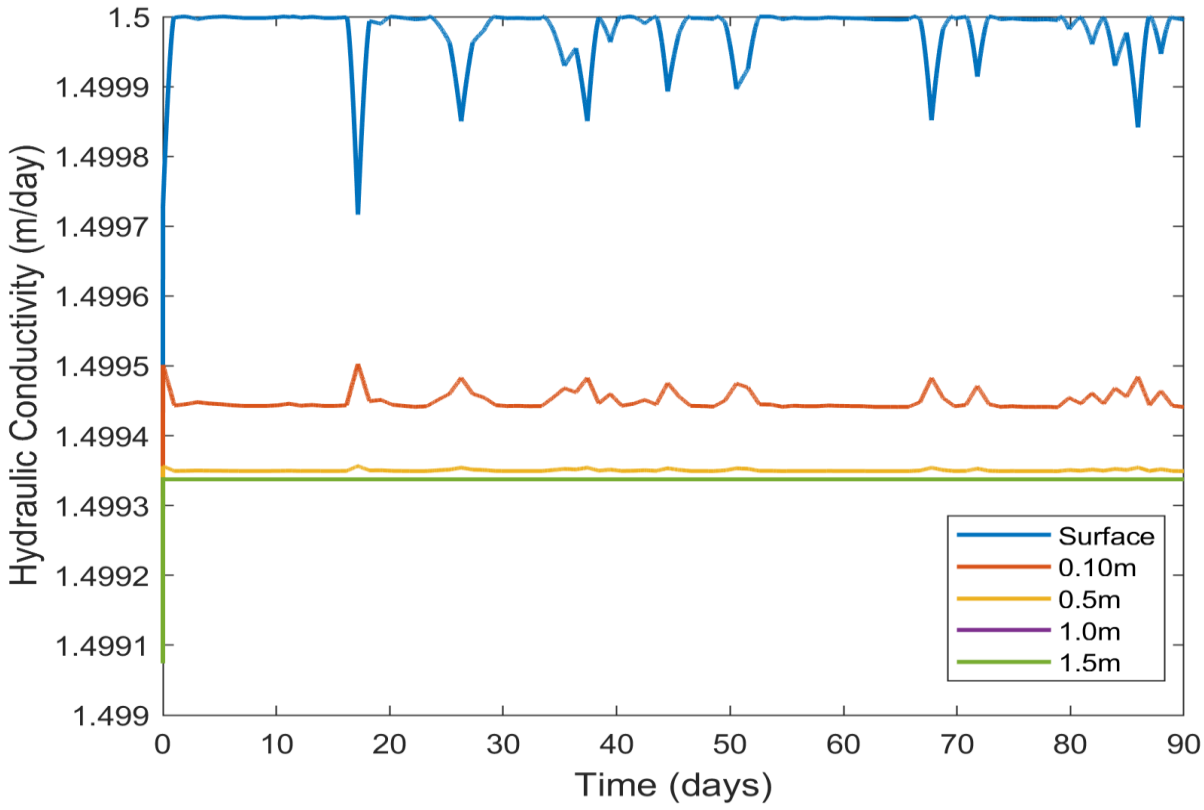

Figure 4-13: Hydraulic conductivity vs time for 90 days simulation time

At a depth of 0.10 m, smaller variations are observed compared to the surface, indicating a buffering effect of the soil profile. For depths below 0.50 m, the hydraulic conductivity

stabilizes and exhibits negligible temporal changes, reflecting the saturated or near-saturated conditions where water redistribution is slower and more uniform.

4.11 Estrogen Transport Model

4.11.1 Integration with Infiltration and Water Flow Modules

The estrogen transport model builds on the preceding infiltration and water flow modules to ensure that solute movement is driven by realistic soil water dynamics. In the earlier sections, surface water entry was modeled using the Green-Ampt infiltration model, providing a time-dependent infiltration flux $q_{surface}(t)$ and subsurface water movement was simulated with Richards' equation for variably saturated flow. These components supply the necessary hydrological inputs (soil water content $\theta(z,t)$ and Darcy flux q (z,t) as functions of depth z and time t) to the estrogen transport module. By coupling the water dynamics with the convection-dispersion equation for solute transport, the model achieves a more physically realistic representation of estrogen movement with the given water fluxes.

The water flow module predicts how water (and thus any dissolved estrogen) percolates through the soil profile, accounting for rainfall, evapotranspiration, and soil hydraulic properties, and the estrogen transport module uses these predictions as inputs to govern the advective and dispersive transport of estrogen.

4.11.2 Mathematical Formulation

In this section, we present the governing equations and mathematical formulation of the estrogen transport model, encompassing advection, dispersion, degradation, sorption, and colloidal transport processes. We also describe the discretisation approach used to solve these equations numerically.

4.11.3 Advection-Dispersion Equation (dissolved phase)

The core equation for solute (dissolved estrogen) transport in one dimension is the advection-dispersion-reaction equation (Kaluarachchi & Morshed, 1995; Tzatchkov et al., 2002).

Ignoring sorption and colloids for the moment, the equation for the dissolved concentration $C_d(z,t)$ (mg/L) in the soil water is:

$$\frac{\partial C_d}{\partial t} = D\,\frac{\partial^2 C_d}{\partial z^2} \;-\; v\,\frac{\partial C_d}{\partial z} \;-\; \lambda_d\, C_d \qquad (4.51)$$

Where, z is depth (with $z = 0$ at the soil surface, positive downward), t is time. The term with D represents hydrodynamic dispersion, which combines diffusion and mechanical dispersion. The term with v (m/day). represents advection, describing convective downward transport with pore water velocity. The decay of the dissolved phase is characterized by λ_d (day^{-1}). This is a first-order decay constant for the dissolved phase.

4.11.4 Sorption via Freundlich Isotherm

Sorption introduces a storage term and modifies the previous transport equation. We use a Freundlich isotherm to describe the equilibrium partitioning of estrogen between the aqueous phase and the soil solid phase (Das et al., 2004; Z. Yu et al., 2004). The Freundlich model is a nonlinear sorption relationship commonly applied to organic contaminants(L. Lee et al., 2003; Sarmah et al., 2010).

At equilibrium, the sorbed concentration S, (mg/kg) is related to the dissolved concentration C_d (mg/L)by

$$S = K_f C_d^n \tag{4.52}$$

K_f is the Freundlich sorption coefficient in (L^n kg^{-1} mg^{1-n}). n is the Freundlich exponent (dimensionless).

Assuming local equilibrium, the sorption effect enters the transport equation as a retardation factor R from (Coles, 2007),

$$R = 1 + \frac{\rho}{\theta}\frac{dS}{dC_d} \tag{4.53}$$

For a Freundlich isotherm, the derivative $\frac{dS}{dC_d}$ is

$$\frac{dS}{dC_d} = K_f n C_d^{n-1} \tag{4.54}$$

Therefore, the retardation factor becomes

$$R = 1 + \frac{\rho K_f n C_d^{n-1}}{\theta} \tag{4.55}$$

For a Freundlich isotherm including retardation factor,

$$R(C_d) = 1 + \frac{\rho\, K_f\, n\, C_d^{n-1}}{\theta} \tag{4.56}$$

This R multiplies the time derivative in the governing equation, yielding

$$R(C_d)\,\frac{\partial C_d}{\partial t} = D\,\frac{\partial^2 C_d}{\partial z^2} - v\,\frac{\partial C_d}{\partial z} - \lambda_d\,C_d \tag{4.57}$$

When $n = 1$ (linear sorption), the retardation factor R is constant. However, when $n \neq 1$, R varies with C_d, making the equation nonlinear. Sorption slows down the transport by a factor of R and reduces peak concentrations since some mass is held on solids. Mass conservation is ensured by tracking the sorbed mass in parallel with C_d.The Freundlich parameters $K_f$and n are provided from experimental isothermal data from the literature.

4.11.5 Degradation of estrogen

The degradation of estrogen in the dissolved phase in the above equation is represented by: $-\lambda_d C_d$ (Fan et al., 2008b; C.-P. Yu et al., 2013) where λ_d is the first-order decay rate constant (1/day).

The decay rate can be derived from a half-life $t_{1/2}$ using (Sinkkonen & Paasivirta, 2000),

$$\lambda_d = \frac{\ln 2}{t_{1/2}} \tag{4.58}$$

Degradation in the sorbed phase is considered; an additional term is added to the sorbed mass balance $\rho\lambda_s S$ Where, λ_s is the decay rate for the sorbed phase (often assumed equal to λ_d)

Using the retardation approach, an effective decay rate in the liquid phase can be adjusted to account for sorbed-phase degradation. For simplicity, it is often assumed: $\lambda_s = \lambda_d$

4.11.6 Preferential Flow and Colloidal Transport Considerations

Real-field estrogen transport is often faster than what a single-porosity equilibrium model predicts, due to preferential flow through macropores and colloid-facilitated transport (Steiner et al., 2010a). Preferential flow implies that a fraction of water (and solute) bypasses the fine soil matrix and travels quickly via large pores or cracks, greatly reducing contact time with the soil matrix. Field evidence of deep estrogen leaching up to 1 meter (Laegdsmand et al., 2009), indicates that conventional matrix-only models would severely underestimate transport distance in such cases.

While preferential flow pathways such as macropores are not explicitly modeled, the use of the Green-Ampt infiltration module for the top 50 cm enables simulation of rapid infiltration

during high-intensity events. This approach approximates the initial conditions under which preferential flow might occur but does not capture the distinct flow domain interactions typically associated with dual-permeability models.

Colloid-facilitated transport is another mechanism by which estrogen mobility is enhanced (Harvey, 2019; Prater et al., 2015, 2016). Estrogens can sorb onto mobile colloidal particles (such as dissolved organic matter or fine suspended clays) which then travel with the water flow, effectively shielding the estrogen from immobile soil sorption sites. This results in a reduction of effective retardation. Laboratory studies (Chambers et al., 2014; J. Prater, 2012a) have shown that the presence of dissolved organic carbon (DOC) and colloids can decrease sorption of estrogens onto stationary soil particles, thereby increasing estrogen mobility.

We model the dynamics of colloids in the soil using first-order attachment and detachment processes. Attachment refers to colloids being immobilized by sticking to soil grains (filtering out of the flowing water), while detachment is the process of previously attached colloids becoming resuspended and mobile in the pore water.

We introduce variables for colloid-facilitated contaminant transport such as:

$C_c(z,t)$: The concentration of estrogen bound to mobile colloids (mg/L in the water phase, $C_a(z,t)$: The concentration of estrogen on attached (immobile) colloids (mg per kg soil, or a proportional measure).

The mobile colloid-associated estrogen C_c is transported by advection–dispersion similarly to C_d but with potentially different velocity and dispersion. Its governing equation is:

$$\frac{\partial C_c}{\partial t} = -v_c \frac{\partial C_c}{\partial z} + D_c \frac{\partial^2 C_c}{\partial z^2} - k_{\text{att}} C_c + k_{\text{det}} C_a - \lambda_c C_c \tag{4.59}$$

Where. v_c is pore water velocity for colloid-associated estrogen (m/day). D_c is the dispersion coefficient for colloid-associated estrogen (m^2/day). k_{att} is attachment rate coefficient (day^{-1}). k_{det} is the detachment rate coefficient (day^{-1}). λ_c Degradation rate for colloid-associated estrogen (day^{-1}).

The last two terms represent the exchange between mobile and immobile colloid phases. The $-k_{\text{att}} C_c$ a sink term due to attachment. This represents mobile colloids leaving the mobile phase, taking their associated estrogen with them. $+k_{\text{det}} C_a$ a source term due to detachment. This represents previously attached colloids releasing estrogen back into the mobile phase. This

equation assumes that the concentration of colloidal estrogen is dilute enough that processes like colloid-colloid interactions or blocking are negligible.

4.12 Numerical Implementation

For numerical stability, the CFL (Courant-Friedrichs-Lewy) number (De Moura & Kubrusly, 2013) for one-dimensional flow is calculated as:

$$\text{CFL} = \frac{v\Delta t}{\Delta z} \leq 1 \tag{4.60}$$

which essentially measures how far the advective front moves in one time step relative to grid spacing. For an explicit upwind scheme, stability (and avoiding oscillations) generally requires CFL ≤ 1. If CFL > 1 the simulation would be attempting to add information more than one grid cell per step, which can lead to numerical instability and unphysical results (like negative concentrations or overshoots. We also checked the numerical stability against diffusion stability. The core of the numerical model is the time-stepping loop that updates the concentration profiles for both matrix and colloidal phases. At each time step, we compute the changes in concentration due to advection, dispersion, degradation, and phase exchanges (sorption, attachment, detachment). We use finite difference approximations for spatial derivatives and a forward Euler time integration (KREISS & SCHERER, 1974; LeVeque, 1998; Marfurt, 1984, 1984; Peskin & Schlick, 1989; Radu et al., 2004) .

Pseudocode for one time step (updating from time t to $\mathrm{t} + \Delta\mathrm{t}$) is as follows.

Using the current dissolved-phase concentration array $\mathrm{C_d^n}$ (where the superscript n indicates the value at the current time step), calculated spatial derivatives. For advection, used an upwind scheme (since the flow is downward, we use backward differences)

$$\frac{\partial C_d}{\partial z}\,|_i \approx \frac{C_{d,i}^n - C_{d,i-1}^n}{\Delta z}, \text{for } i = 2, \dots, N \tag{4.61}$$

Index 1 is the top cell. This assumes $C_{d,0}$ (just above the top boundary) is known from the boundary condition, e.g C_{inflow}

For Dispersion Term Approximation, which applies to interior cells

$$\frac{\partial^2 C_d}{\partial z^2}\,|_i \approx \frac{C_{d,i+1}^n - 2C_{d,i}^n + C_{d,i-1}^n}{\Delta z^2}, \text{for } i = 2, \dots, N-1 \tag{4.62}$$

Using these derivatives, we compute the rate of change from advection and dispersion

$$\left(\frac{\partial C_d}{\partial t}\right)_{\text{adv},i} = -\frac{v(t)}{\Delta z}\left(C_{d,i}^n - C_{d,i-1}^n\right) \tag{4.63}$$

$$\left(\frac{\partial C_d}{\partial t}\right)_{\text{disp},i} = D(t)\,\frac{C_{d,i+1}^n - 2C_{d,i}^n + C_{d,i-1}^n}{\Delta z^2} \tag{4.64}$$

We then account for degradation and sorption in the matrix phase. For degradation, the first-order decay gives a sink term

$$\left(\frac{\partial C_d}{\partial t}\right)_{\text{decay},i} = -\lambda_d \, C_{d,i}^n \tag{4.65}$$

For sorption, since we assume local equilibrium, we do not have an explicit kinetic term in the C_d equation; instead, sorption is implicitly handled via the retardation effect. In our code, we handle sorption by an iterative approach within each time step.

We predict an intermediate C_d^* using only advection, dispersion, and decay (ignoring sorption uptake during that sub-step). Then we calculate the new sorbed concentration $S^* = K_f(C_d^*)^n$ at equilibrium with C_d. We enforce mass balance: the total estrogen in cell i at the new time should equal the old total plus any gains/minuses. The total includes both dissolved and sorbed

For each cell, we combine the terms,

$$\Delta C_{d,i} = \left[\left(\frac{\partial C_d}{\partial t}\right)_{\text{adv}} + \left(\frac{\partial C_d}{\partial t}\right)_{\text{disp}} + \left(\frac{\partial C_d}{\partial t}\right)_{\text{decay}}\right]_i \Delta t \tag{4.67}$$

We perform a similar finite difference update for the mobile colloid-associated estrogen concentration C_c. Advection and dispersion for useC_c v_c and Dc in place of v and D, and we use an upwind scheme as well

$$\left(\frac{\partial C_c}{\partial t}\right)_{\text{adv},i} = -\frac{v_c(t)}{\Delta z}\left(C_{c,i}^n - C_{c,i-1}^n\right) \tag{4.68}$$

$$\left(\frac{\partial C_c}{\partial t}\right)_{\text{disp},i} = D_c(t)\,\frac{C_{c,i+1}^n - 2C_{c,i}^n + C_{c,i-1}^n}{\Delta z^2} \tag{4.69}$$

In addition to advection-dispersion, the colloid phase has attachment/detachment terms:

The attachment removes mobile colloid-bound estrogen and transfers it to the immobile phase. This process is modelled as a first-order sink term in the Cc equation

$$\text{Attachment Term} = -k_{\text{att}} C_{c,i}^n \tag{4.70}$$

Detachment adds estrogen to the mobile colloid phase from the immobile reservoir. This process is represented as

$$\text{Detachment Term} = +k_{\text{det}} C_{a,i}^n \tag{4.71}$$

Where,$C_c$is the concentration of mobile colloid-bound estrogen at cell i, C_a is the concentration of attached-colloid estrogen at cell i, k_{att} is the attachment rate coefficient, k_{det} is the detachment rate coefficient.

also include degradation

$$\Delta C_{c,i} = \left[\left(\frac{\partial C_c}{\partial t}\right)_{\text{adv}} + \left(\frac{\partial C_c}{\partial t}\right)_{\text{disp}} - k_{\text{att}} C_{c,i}^{n} + k_{\text{det}} C_{a,i}^{n} - \lambda_c C_{c,i}^{n}\right] \Delta t \tag{4.72}$$

then update

$$C_{c,i}^{n+1} = C_{c,i}^{n} + \Delta C_{c,i} \tag{4.73}$$

The attached colloidal estrogen C_a in each cell changes due to attachment and detachment (opposite to the changes in C_c) and degradation. The following equation was implemented.

$$\frac{\partial C_{a,i}}{\partial t} = +k_{\text{att}} C_{c,i}^{n} - k_{\text{det}} C_{a,i}^{n} - \lambda_c C_{a,i}^{n} \tag{4.74}$$

when mobile colloid-bound estrogen attaches, it increases the immobile store Ca, and when immobile colloids detach, Ca decreases. We integrate this with a forward step

$$\Delta C_{a,i} = \left(k_{\text{att}} C_{c,i}^{n} - k_{\text{det}} C_{a,i}^{n} - \lambda_c C_{a,i}^{n}\right) \Delta t \tag{4.75}$$

and update $C_{a,i}^{n+1} = C_{a,i}^{n} + \Delta C_{a,i}$.

4.12.1 Boundary and Initial Conditions

Appropriate boundary conditions are enforced in the discretisation. Based on these studies Rouleau & Osterle, (1955) Simunek & van Genuchten, (1999) and Weinan & Liu, (1996) initial and boundary conditions implemented in the model. The top boundary at the soil surface (z = 0) is handled as a Dirichlet (fixed concentration) condition in this model setup. We assume a continuous source of estrogen at the surface (for example, irrigation or rainfall containing estrogen (such as dairy farm effluent) maintaining an estrogen concentration at z = 0. This is implemented by fixing the concentration at the first node: $\mathrm{C_1(t) = C_0}$ for all (t). The bottom boundary at z = L (e.g. 2.0 m depth) is taken as a no-flux (zero concentration gradient) boundary since we assume no estrogen initially in the groundwater below and we want to prevent artificial loss of solute out of the domain. The zero-gradient Neumann condition $\partial \mathrm{C}/\,\partial \mathrm{z}|z = L = 0$. With this boundary condition, any estrogen that reaches the bottom boundary will simply exit the domain by advection if pushed by water flux (since the concentration gradient is zero, there is no diffusive influx from below to counter it, so it behaves like a free outflow for advection).

The initial condition for the simulation is that the soil profile is estrogen-free prior to the surface application. We set $\mathrm{C(z, 0) = 0}$ for all $0 < \mathrm{z} \leq \mathrm{L}$, and assume a small initial concentration at

the surface node to initiate the simulation (in our case, $C_1(0) = C_0$ at the very start, representing an immediate application at t = 0). The initial water content profile $\theta(z, 0)$and pressure head profile $h(z, 0)$ are taken from the steady-state or antecedent condition given by the Richards' module.

The complete MATLAB code used to develop and simulate the estrogen transport model is publicly available on GitHub. This includes all scripts for implementing the Green-Ampt infiltration, Richards' equation using Picard iteration, advection-dispersion processes, sorption, and degradation modules. The repository can be accessed at:

https://github.com/madnan376/NumericalModellingForEstrogenTransport

4.13 Results and discussion (Estrogen Transport)

The results of the estrogen transport model are presented and discussed in this section. The model outputs include concentration profiles, mass balance assessments, and colloidal transport dynamics of Estrone (E1) and Estradiol (E2) under various conditions; some of the plots are presented in Appendix A. The concentration profiles of E1 and E2 demonstrate the advective-dispersive transport processes integrated with degradation and sorption over time. Figure 4.14 shows the vertical concentration profiles of estrone (E1) and estradiol (E2) at 9, 45, and 81 days, corresponding to early, mid, and late stages of the 90-day simulation. At 9 days, both hormones exhibit peak concentrations in the upper 0.2–0.4 m of the soil, with E2 concentrations consistently higher than E1, reflecting its lower sorption affinity. By 45 days, both compounds have migrated deeper, with attenuated concentrations near the surface and more dispersed profiles. At 81 days, the concentration gradients have further flattened, and the profiles appear more uniform, indicating progressive degradation and sorption. Across all timepoints, E2 penetrates deeper than E1, confirming its relatively greater mobility under identical flow conditions. Figure 4.15 shows that the highest concentrations remain near the surface in early stages, followed by gradual downward migration. E2 maintains higher relative concentrations at greater depths than E1 throughout the simulation, indicating its greater mobility. By day 60–90, both hormones exhibit attenuated concentration fronts beyond 0.6 m depth, with limited movement below 1.2 m. The smooth, continuous fronts suggest matrix-dominated transport under steady infiltration without sharp preferential breakthroughs.

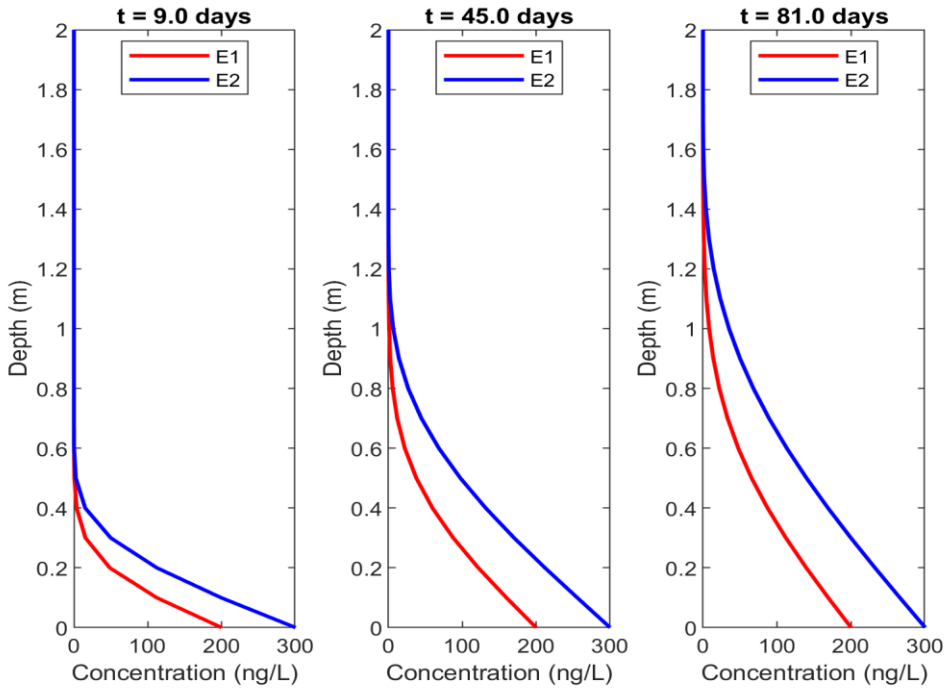

Figure 4-14: Concentration profiles of dissolved estrogen E1 (red) and E2 (blue) at selected times: 10% (9 days), 50% (45 days), and 90% (81 days) of the total simulation period. Concentrations are plotted as a function of depth (0–2 m) in the soil profile

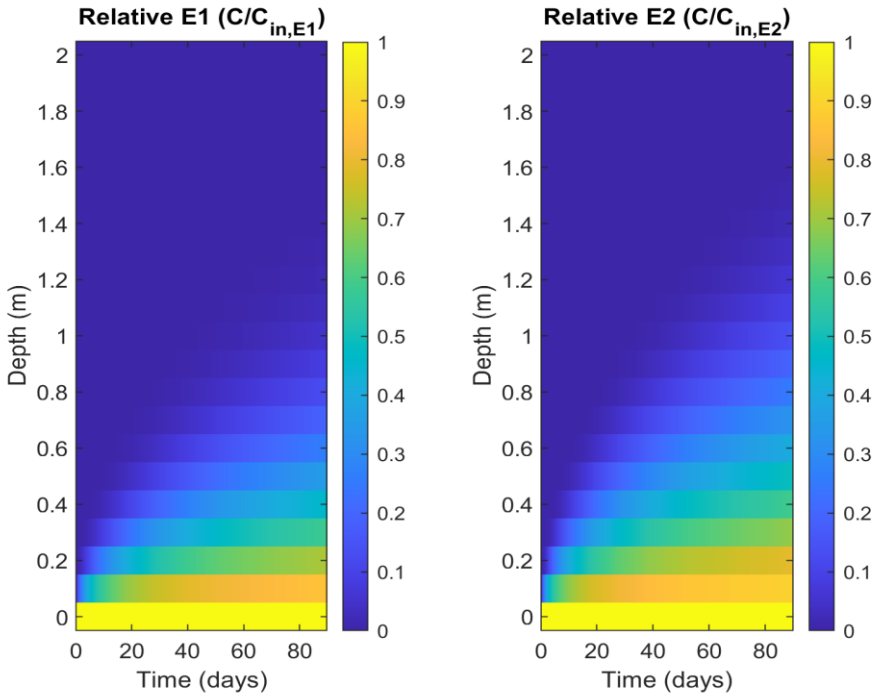

Figure 4-15: Contour maps of normalized concentration (C/C_in) for estrone (E1) and estradiol (E2) over 90 days within a 2 m soil column

The normalized concentration fronts predicted by our 2-m numerical model closely align with published column-scale measurements of estrogen transport in natural soils. Sangsupan et al, (2006) reported that only 27 % of applied 17β-estradiol (E2) mass leached through a 30-cm undisturbed soil column, with breakthrough concentrations (Ct/C0) peaking near 0.3 at ~0.3 m depth under saturated flow conditions and mostly sorbed at top 10 cm soil layer. In comparison, our model under unsaturated conditions shows a relative concentration of ~0.7 at 0.35 m after 30 days, higher due to slower infiltration and limited percolation. Casey et al, (2005) measured linear sorption coefficients (log K_{oc} ≈2.94 for E2 vs 2.99 for estrone (E1)), indicating slightly lower sorption and greater mobility of E2; these values predict penetration depths and attenuation trends very similar to those in our model (E2 advancing deeper than E1, and C/Cin falling below 0.1 beyond ~1 m).

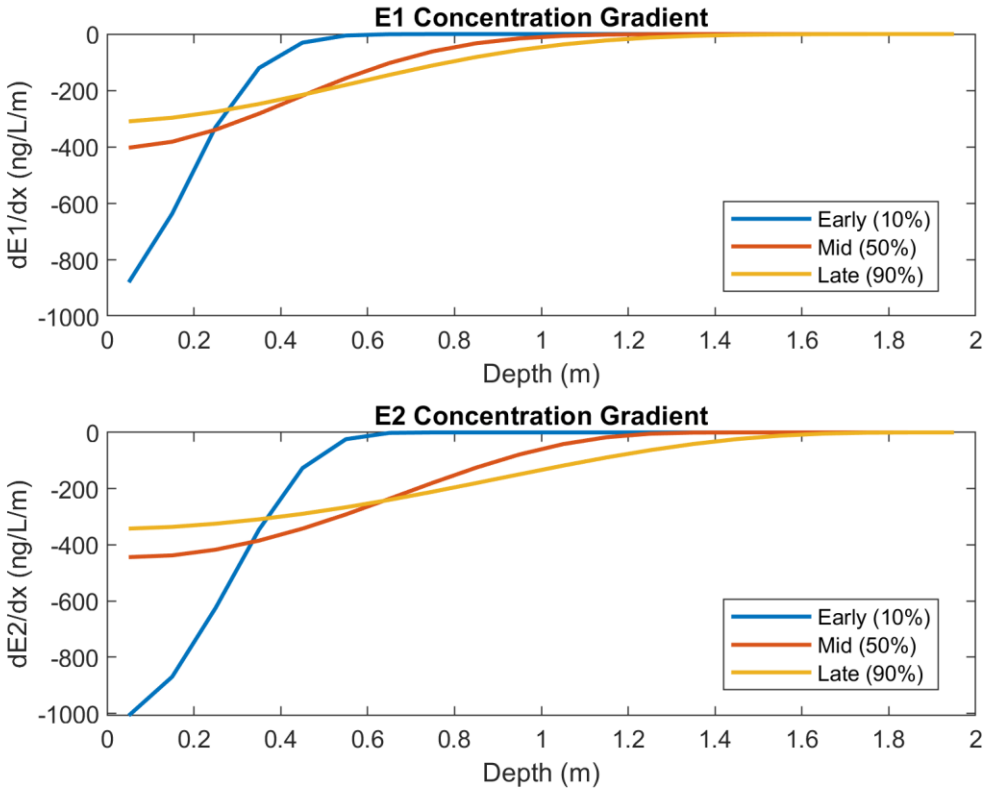

Figure 4-16: Vertical concentration gradients (dC/dx) of estrone (top) and estradiol (bottom) plotted against depth at 10%, 50%, and 90% cumulative breakthrough.

Figure 4.16 shows the vertical concentration gradients (dC/dx) of estrone (E1) and estradiol (E2) at early (10%), mid (50%), and late (90%) stages of the simulation. At the early stage, both hormones exhibit steep negative gradients in the top 0.3 m, indicating rapid concentration drop immediately below the surface. By the mid-point, gradients become less steep and shift deeper (around 0.5–0.7 m), reflecting downward movement of the concentration front. At the late stage, the gradients flatten across the entire profile, especially below 1.5 m, indicating strong attenuation and limited further transport. Across all time points, E2 gradients are consistently shallower than E1's, confirming greater mobility and deeper migration of E2 under identical flow and reactive conditions.

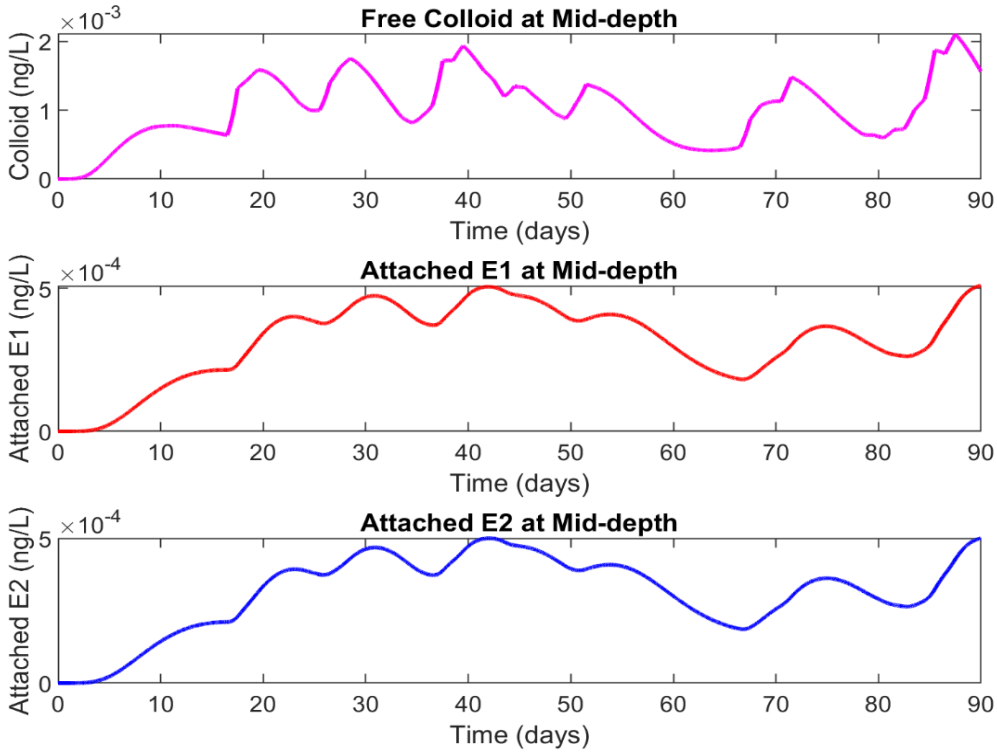

Figure 4-17: Time series of free colloid concentration and colloid attached estrone (E1) and estradiol (E2) at 0.5 m depth over 90 days

At mid-depth (0.5 m), the time-series of free colloid concentration (top panel) exhibits recurrent pulses (peaks ≈1.5–2.0×10^{-3} ng L^{-1}) roughly every 15-20 days, reflecting episodic infiltration events driving colloid mobilization. Corresponding concentrations of colloid-attached estrone (middle panel) and estradiol (bottom panel) are an order of magnitude lower (peak ≈4-5×10^{-4} ng L^{-1}) but display the same temporal pattern, indicating that hormone transport is

tightly coupled to colloid flux. Peak attached E2 slightly exceeds attached E1 at most times, consistent with E2's greater colloidal affinity or slower desorption. The near-synchronous timing of free colloid and attached hormone maxima with minimal lag supports a transport mechanism in which colloids serve as vectors for estrogen movement. Between pulses, all three signals decline toward low baseline values, reflecting periods of limited colloid delivery and ongoing sorption/degradation.

Wang et al., (2022) found that natural colloids (silica, illite, and humic acid) increased E1 transport by 11–26% and E2 transport by 20-36% in saturated sand columns. Lucas & Jones, (2009) observed that under simulated urine infiltration in intact soil cores, colloid flux peaks aligned with spikes in attached estradiol concentration at ~0.5 m depth, confirming synchronous transport pulses. They showed that 17β-estradiol leaches earlier and at higher concentrations when added via artificial urine than via water, consistent with the mobilization of colloids and reduced degradation. Although they do not explicitly use the phrase "colloid-facilitated," they cite colloid mobilization and dissolved organic carbon as reasons for enhanced estrogen transport. Sangsupan et al., (2006) showed breakthrough curves for E2 and Testosterone in undisturbed columns. They observed that the total hormone flux is dominated by short pulses in the effluent that appear at or near the same time as potential colloid pulses and that these pulses could be "colloid-facilitated E2 transport. The combination of preferential flow and colloid transport explains the earlier arrival of E2 in some columns. They estimate that up to 20-30% of E2 was recovered in early effluent pulses, presumably attached to mobile colloids.

To provide a more detailed view of the simulation results and confirm the consistency of our main findings, we include several supplementary plots in Appendix A.

4.14 Conclusions

The model results and literature data indicate that estrone (E1) and estradiol (E2) rapidly sorb in the upper soil and are attenuated by microbial degradation. This leads to steep concentration declines with depth. E2 typically shows greater mobility than E1, likely due to its lower sorption affinity or slower degradation.

Colloid-facilitated transport enhances the vertical movement of E1 and E2, particularly during infiltration events that mobilize colloids. This is reflected in transient hormone peaks at depth.

While the model does not explicitly simulate macropore flow, rapid infiltration in the Green-Ampt framework can approximate some preferential flow effects.

Overall, these findings highlight the roles of soil sorption, microbial activity, and colloid mobility in controlling estrogen leaching. Management practices that limit colloid mobilization and control infiltration dynamics may reduce the risk of groundwater contamination.

Chapter 5

Modelling Estrogen Transport in Dairy Farms: Integrating Hydrological and Environmental Data Using a Watershed Model

5.1 Introduction

This chapter details the processing and integration of environmental data and associated equations for simulating estrogen transport in a New Zealand dairy farm watershed using the Soil and Water Assessment Tool (Arc SWAT) (Neitsch et al., 2011) . Estrogens such as estrone (E1) and estradiol (E2) are significant contaminants in agricultural runoff, primarily from livestock manure and effluent, and their transport through surface runoff and sediment is a major concern for environmental health (Adeel et al., 2017; Ying et al., 2002; Zhao et al., 2019). Effective modelling of their movement requires a hydrological model that can simulate runoff, sediment transport, and estrogen dynamics across the farm landscape (J. B. Gadd, Tremblay, et al., 2010; Jenkins et al., 2006; Zhao et al., 2019).

The data required for this simulation include high-resolution topographic data (LiDAR DEM), soil properties, and land use/land cover (LULC) information, all of which were pre-processed to ensure compatibility with the Arc SWAT model. As described in Chapters 6 and 7, the DEM was used for watershed delineation and to establish flow networks, while the soil and LULC datasets were reclassified to match the model's specifications. This chapter also outlines the use of key equations to calculate parameters for the Arc SWAT model, particularly those related to runoff generation, sediment yield, and the transport of estrogens in both dissolved and sediment-bound forms.

This chapter lays the groundwork for the model results presented in Chapters 6 and 7, where the simulation outcomes and their implications for managing estrogen contamination on dairy farms will be discussed in detail.

5.2 Runoff Generation Using the SCS Curve Number Method

Runoff generation is fundamental to hydrological modelling, particularly when assessing soil erosion and contaminant transport in agricultural landscapes such as dairy farms. The Soil Conservation Service (SCS) Curve Number (CN) Method, developed by the United States Department of Agriculture (USDA) (Boughton, 1989; United States Department of Agriculture, Soil Conservation Service, 1954), provides an empirical approach to estimating direct runoff

from rainfall events. This method integrates land use, soil type, and hydrological conditions to predict runoff volume, serving as a critical input for subsequent sediment yield estimation using the Modified Universal Soil Loss Equation (MUSLE) and estrogen transport modelling.

The SCS Curve Number Method estimates the direct runoff (Q) resulting from a specific rainfall event (P) by considering the land's capacity to absorb rainfall before runoff begins. The method is grounded in two primary concepts (Bosznay, 1989; Boughton, 1989):

1. **Potential Maximum Retention (S)**: This represents the maximum amount of rainfall that can be retained on the ground through processes like infiltration, evaporation, and transpiration before runoff starts.
2. **Initial Abstraction (I_a)**: Accounts for all losses before runoff begins, including water intercepted by vegetation, surface storage, and initial infiltration.

These components are incorporated into the Curve Number (CN), a dimensionless parameter ranging from 0 to 100 that reflects the combined effect of land use, soil type, and antecedent moisture conditions on runoff generation. A lower CN indicates higher infiltration and lower runoff potential, whereas a higher CN signifies reduced infiltration and increased runoff.

5.2.1 Method Assumptions

The SCS CN Method operates under the following key assumptions:

- Homogeneous Land Characteristics: Land use, soil type, and hydrological conditions are uniform within each hydrologic unit.
- Event-Based Estimation: Runoff is calculated for individual storm events without accounting for prior moisture conditions unless explicitly adjusted.
- Steady-State Infiltration: The method assumes a uniform infiltration rate throughout the rainfall event.

5.2.2 Runoff Estimation

The following equations for estimating runoff using the SCS Curve Number Method are used (Uwizeyimana et al., 2019)

For Runoff depth,

$$Q = \frac{(P - I_a)^2}{(P - I_a) + S} \quad \text{if } P > I_a \tag{5.1}$$

Where Q is runoff depth (mm), P is rainfall depth (mm), I_a is initial abstraction (mm) and S is the potential maximum retention after runoff begins (mm). S represents the potential maximum retention after runoff begins. Indicates the capacity of the soil to retain rainfall before runoff occurs.

$$S = \left(\frac{1000}{CN} - 10\right) \times 25.4 \quad (5.2)$$

S is the potential maximum retention after runoff begins (mm), and CN is the curve Number (dimensionless) given in Table 5.2 and Table 5.3.

The portion of rainfall that is retained on the surface and does not contribute to runoff. Acts as a threshold to determine whether a rainfall event will generate runoff. Ia can be calculated as:

$$I_a = 0.05 \times S \quad (5.3)$$

Where. I_a initial abstraction (mm) S is potential maximum retention after runoff begins(mm). This equation is modified for Waikato region runoff calculation, contrasting the standard I_a=0.2S (Shaver, 2020). Based on these equations we can calculate S and I_a for specific CN as described in Table 5.1.

Table 5-1: Potential maximum retention and initial abstraction calculated based on equations 5.2 and 5.3

Curve Number (CN)	Potential Maximum Retention (S) [mm]	Initial Abstraction (Ia) [mm]
60	169.33	8.47
70	108.86	5.44
75	84.67	4.23
80	63.5	3.18
85	44.82	2.24

Table 5-2: Runoff Curve Numbers for Urban Lands(Shaver, 2020)

Cover Description	Condition	GroupA	Group B	Group C	Group D
Open space (lawns, parks, reserves, etc.)	Poor (grass cover < 50%)	68	79	86	89
	Fair (grass cover 50% - 75%)	49	69	79	84
	Good (grass cover > 75%)	39	61	74	80
Impervious areas	Paved parking lots, roofs, driveways, etc.	98	98	98	98
Streets and roads*	Paved; kerbing and catchpits (excluding right-of-way)	98	98	98	98
	Paved; open ditches (including right-of-way)	83	89	92	93
	Gravel (including right-of-way)	76	85	89	91
	Dirt (including right-of-way)	72	82	87	89

Table 5-3: Runoff Curve Numbers for Rural Lands (Shaver, 2020)

Cover Description	Condition	Group A	Group B	Group C	Group D
Pasture, grassland, continuous forage for grazing	Poor	68	79	86	89
	Fair	49	69	79	84
	Good	39	61	74	80
Straight row crops	Poor	72	81	88	91
	Good	67	78	85	89+
Bush – grass combination (orchard)	Poor	57	73	82	86
	Fair	43	65	76	82
	Good	32	58	72	79
Bush*	Poor	45	66	77	83
	Fair	36	60	73	79
	Good	30	55	70	77
Farmsteads – buildings, lanes, driveways,	N/A	59	74	82	86

* Bush condition:
Poor (forest litter, small trees, and bush are destroyed by heavy grazing or regular burning)
Fair(woods are grazed but not burned, and some forest litter covers the soil)
Good(woods are protected from grazing, and litter and bush adequately cover the soil)

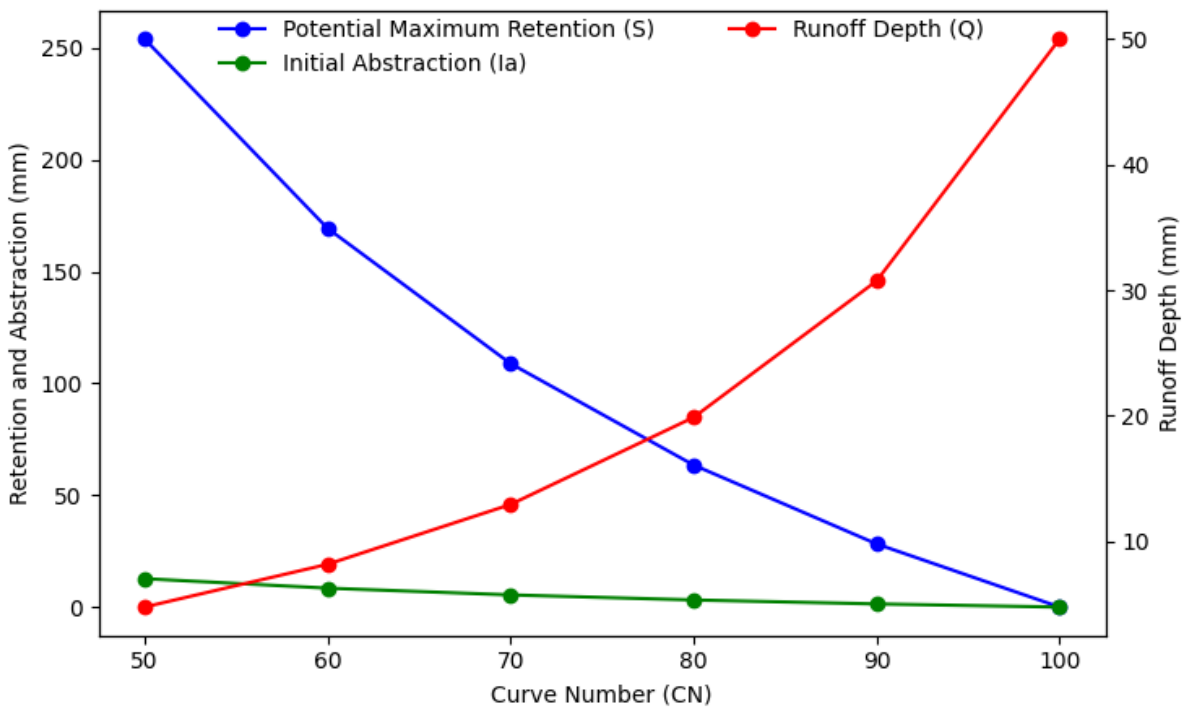

Figure 5-1: Conceptual relationships between Curve Number (CN), potential maximum retention (S), initial abstraction (Ia), and runoff depth (Q)

Figure 5.1 shows, the SCS CN method demonstrates the potential maximum retention (S) decreases as CN increases, meaning soils with higher CN values retain less water before generating runoff. Initial Abstraction (I_a) also declines slightly with increasing CN, indicating that surfaces with higher CN (e.g., compacted soils and impervious areas) lose less water before runoff initiation. Also, runoff depth (Q) increases significantly with higher CN values, showing that land surfaces with low infiltration capacity (urbanized or degraded areas) contribute more to surface runoff.

This conceptual framework provides a basis for integrating runoff calculations with sediment yield and estrogen transport modelling in subsequent analyses.

5.3 Hydrological Soil Groups (HSGs)

Understanding Hydrological Soil Groups (HSGs) is important for accurately estimating runoff and sediment yield using the SCS Curve Number Method. The Natural Resources Conservation Service (NRCS) classifies soils into four groups (A, B, C, and D) based on infiltration rates, runoff potential, soil texture, and depth to impermeable layers (U.S.Department Agriculture & Natural Resource Conservation, 2009). These classifications directly impact hydrological modelling and runoff prediction. Classification of Hydrological Soil Groups.

5.3.1 Classification of Hydrological Soil Groups

The four primary Hydrological Soil Groups (HSGs) are:

Group A – Low Runoff Potential

- High infiltration capacity, leading to minimal runoff.
- Texture: Mostly sand or gravel with less than 10% clay.
- Saturated Infiltration Rate: >40.0 μm/s in all soil layers.
- Examples: Deep, well-drained sandy soils.

Group B – Moderately Low Runoff Potential

- Moderate infiltration, generating more runoff than Group A soils.
- Texture: Loamy sand or sandy loam, with 10-20% clay.
- Saturated Infiltration Rate: 10-40 μm/s.
- Examples: Well-drained loamy soils.

Group C – Moderately High Runoff Potential

- Restricted water movement, leading to higher runoff.
- Texture: Clay loam, silty clay loam, or sandy clay loam, with 20-40% clay.
- Saturated Infiltration Rate: 1.0-10.0 μm/s.
- Examples: Soils with moderate clay content affecting infiltration.

Group D – High Runoff Potential

- Very limited infiltration, producing significant runoff.
- Texture: Clayey soils with >40% clay and <50% sand.
- Saturated Infiltration Rate: ≤1.0 μm/s.
- Examples: Shallow or compacted clay soils with poor drainage.

The above soil groups are summarised in Table 5.4.

The saturated vertical soil coefficient of permeability is also an important parameter in hydrological modelling and can be assumed to be equal to the soil infiltration rate. This assumption simplifies the modelling process by directly linking infiltration characteristics to soil permeability. Further details about soil groups can be found from (Bosznay, 1989; Boughton, 1989; Shaver, 2020; U.S.Department Agriculture & Natural Resource Conservation, 2009).

Table 5-4: Summary of Hydrological Soil Groups

Hydrological Soil Group	Runoff Potential	Typical Clay Content (%)	Typical Sand Content (%)	Key Characteristics
Group A	Low	<10	>90	High infiltration, gravel or sand textures, well-aggregated
Group B	Moderately Low	Oct-20	50-90	Moderate infiltration, loamy sand or sandy loam textures
Group C	Moderately High	20-40	<50	Restricted infiltration, loam or clay loam textures
Group D	High	>40	<50	Very restricted infiltration, clayey textures, high shrink-swell potential

5.4 Study Site Hydrological Soil Group Classification

The dairy farm study site consists of pasture fully covered with grass and two primary soil types:

- Clay over Loam: High clay content with loamy sublayers.
- Silt over Loam: Significant silt content with underlying loam.

Based on soil characteristics, the site is classified as Hydrological Soil Group C due to:

1. Soil Texture & Composition: 20-40% clay, <50% sand.
2. Infiltration Capacity: Moderate runoff potential due to restricted water movement.
3. Depth to Water Table & Impermeable Layers: No shallow impermeable layers or high-water tables within 0.5 meters, meeting Group C criteria.

5.4.1 Curve Number (CN) Assignment for the Study Site

The Curve Number (CN) is a dimensionless value (0-100) representing runoff potential based on soil type, land use, and hydrological condition. Higher CN values indicate higher runoff potential. For Group C soils with grassland (>75% cover), the assigned CN value is 74. Using this value, we calculate the Potential Maximum Retention (S) and Initial Abstraction (Ia) for the study site, Table 5.5.

Table 5-5: Summary of Soil Classification and CN Assignment for Dairy Farm Site

Characteristic	Description
Land Use Type	Pasture fully covered with grass (good condition)
Soil Types	Clay over loam and silt over loam
Hydrological Soil Group (HSG)	Group C
Curve Number (CN)	74
Potential Maximum Retention (S)	89.2 mm
Initial Abstraction (I_a)	4.46 mm

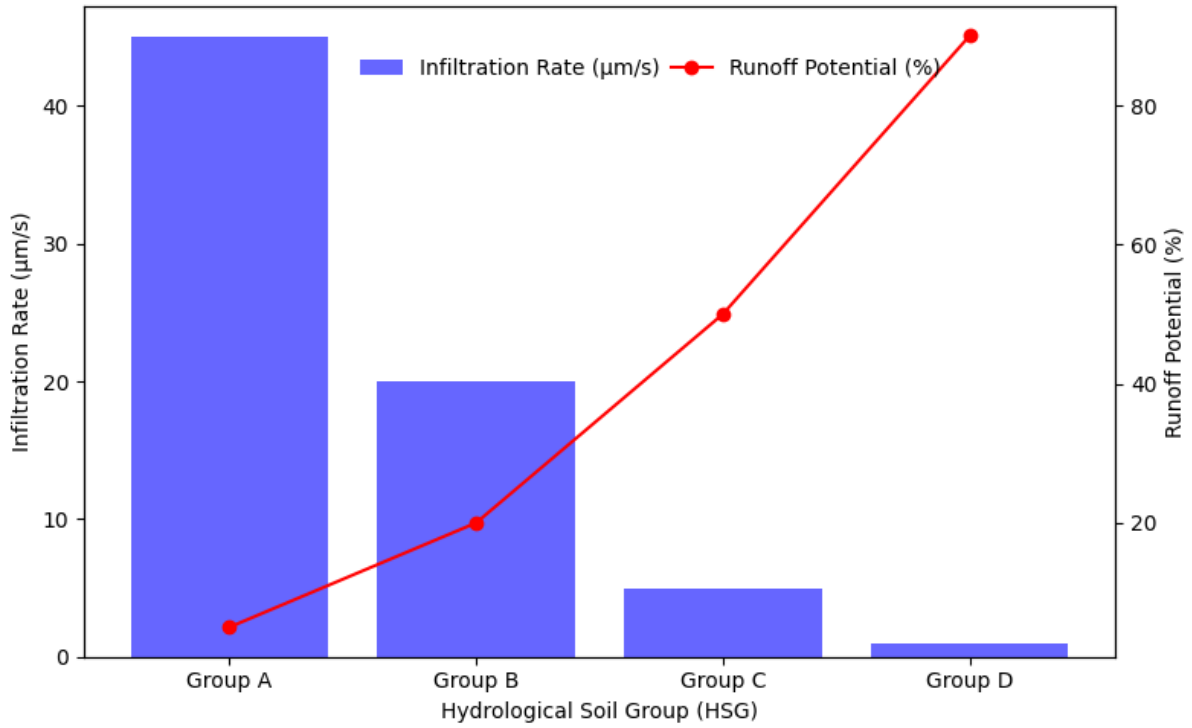

Figure 5-2: Relationship between infiltration rate(µm/s) and runoff potential (%) across hydrological soil groups (HSGs)

Figure 5.2 represents the relationship between infiltration rate and runoff potential for the four Hydrological Soil Groups (HSGs), classified based on USDA NRCS standards (U.S.Department Agriculture & Natural Resource Conservation, 2009). The blue bars indicate infiltration capacity, while the red line shows the corresponding runoff potential.

The data used for this plot are based on typical infiltration rates and runoff potential values for each soil group. The data visualization is derived from empirical soil classification values, aligning with hydrological modelling principles used in SCS Curve Number methodology.

5.5 Sediment Yield Estimation

Soil erosion from agricultural and pastoral landscapes is a global concern, with direct impacts on food security, landscape stability, water quality, and ecosystem functions (Borrelli et al., 2017; ITPS, 2015; Smetanová et al., 2020). Accelerated erosion rates in these areas often exceed natural soil production by multiple orders of magnitude, particularly under intensive land-use practices like grazing (Hancock et al., 2020; R. Monaghan et al., 2008).

In New Zealand, the effects of livestock grazing on surficial soil erosion are well-documented but rarely integrated into high-resolution predictive models (Donovan & Monaghan, 2021).

The Modified Universal Soil Loss Equation (MUSLE) enhances traditional models by incorporating runoff variables, offering improved event-based sediment yield predictions. Within the ArcSWAT modelling framework, MUSLE estimates sediment yield for each Hydrologic Response Unit (HRU) using the equation. The Revised Universal Soil Loss Equation (RUSLE) and its predecessor, the Universal Soil Loss Equation (USLE), are empirical models designed to estimate mean annual soil loss due to surface erosion. These models were developed using data from agricultural plots and have since become widely applied in various contexts, from field to global scales (Borrelli et al., 2017; Renard, 1997).

5.5.1 ArcSWAT Model Overview

To estimate event-based sediment yield, the Modified Universal Soil Loss Equation (MUSLE) (Williams J.R, 1975) is employed within the Arc SWAT framework, replacing the Revised Universal Soil Loss Equation (RUSLE) (Renard, 1997) used for annual soil loss predictions. MUSLE enhances soil erosion modelling by incorporating runoff volume and peak discharge, improving event-scale sediment yield predictions (Neitsch et al., 2011). MUSLE is a modified version of the Universal Soil Loss Equation (USLE) (Wischmeier, 1978).

The Arc SWAT model is a GIS-based interface facilitating watershed-scale hydrological and erosion simulations (Arnold et al., 1998; Chiang et al., 2010; Neitsch et al., 2011). Arc SWAT enables spatially explicit modelling by utilizing Digital Elevation Models (DEM), soil, and land use datasets to parameterize hydrological processes. This model has been extensively applied in agricultural watershed management to evaluate runoff, sediment transport, and nutrient dynamics (Teshager et al., 2016).

ArcSWAT simulates hydrological response units (HRUs), which represent unique land cover-soil combinations within a watershed, ensuring detailed representation of erosion-prone areas. The Modified Universal Soil Loss Equation (MUSLE) is incorporated within ArcSWAT to estimate event-based sediment yield based on surface runoff and peak flow conditions.

RUSLE includes key factors influencing soil loss, including seasonal rainfall erosivity (R), slope length (L), slope steepness (S), soil erodibility (K), and cover management (C), each of which plays an important role in determining erosion potential (Selby, 1993).

The Modified Universal Soil Loss Equation (MUSLE) can be written as:

$$S = 11.8(Q.q.A)^{0.56} \cdot K \cdot LS \cdot C \cdot P.CFRG \quad (5.4)$$

Where, S is predicted soil loss (t ha^{-1} day^{-1}), Q is surface water runoff in mm/ha per day, q is peak runoff rate (m^3/s), A is the area of HRU (ha) K is soil erodibility factor (metric ton m^2 h / (m^3 metric ton cm)) LS is topographic factor (dimensionless), a product of slope length (L) and slope steepness (S), C is cover and management factor (dimensionless), representing the effect of vegetation cover and land management practices on erosion rates, P is support practice factor (dimensionless), accounting for the impact of conservation practices such as contouring, strip cropping, or terracing. CFRG is the coarse fragment factor (dimensionless).

5.5.2 Components of MUSLE for the Study Area

5.5.2.1 Runoff-Based Energy in MUSLE

Rainfall erosivity (R) reflects the energy of rainfall to detach soil particles, considering both rainfall intensity and volume. It is particularly sensitive to short, intense storm events (Nearing et al., 2005). For New Zealand, R is calculated using region-specific seasonal rainfall data derived from linear and power functions based on high-resolution meteorological records (Klik et al., 2015; NIWA, 2012). Unlike RUSLE, the Modified Universal Soil Loss Equation (MUSLE) does not use the rainfall erosivity factor (R). Instead, MUSLE relies on runoff volume (Q) and peak runoff rate (q) to estimate sediment detachment and transport (Chiang et al., 2010; Neitsch et al., 2011; Teshager et al., 2016). This approach ensures the model captures spatial and temporal variations in erosive rainfall.

5.5.2.2 Soil Erodibility (K) and Grazing-Adjusted Erodibility (Ktr)

Soil erodibility quantifies a soil's susceptibility to erosion under standard conditions, accounting for texture, organic matter, permeability, and structural stability(Renard, 1997). However, traditional methods for determining K in New Zealand were found to inadequately represent soil texture and other critical parameters (Dymond et al., 2010). Recent reviews (Benavidez et al., 2018) have advocated for incorporating additional soil physical and chemical properties, including the structural vulnerability index (Hewitt, 1993; Hewitt & Shepherd, 1997), particle size fractions, surficial gravel content, drainage classes, and phosphate retention. These refinements enhance the precision of K-factor calculations, improving soil loss estimates for various land uses and providing the values for (K_{tr}).

In ArcSWAT, the K-factor is predefined and is not calculated dynamically. Instead, precomputed values specific to New Zealand soils were used (Donovan, 2022). Adjustments were made to account for grazing impacts on soil structure and permeability, which influence runoff-driven sediment transport in the MUSLE framework. The following Table 5.6 presents precomputed K-values for North and South Island soils, including adjustments for livestock grazing and soil texture variations

Table 5-6: Soil Erodibility (K) Values for New Zealand Pastoral Lands (Donovan, 2022)

Parameter	South Island	North Island	Key Observations
Mean Ktr Value	0.029	0.02	Higher mean K_{tr}-value for the South Island, indicating slightly greater susceptibility to erosion.
Standard Deviation (σ)	0.018	0.014	Moderate spatial variability with bimodal distributions.
Permeability Relationship	Inversely related	Inversely related	Soils with lower permeability are more erodible.
Particle Size Relationship	Directly related	Directly related	Coarser particle size corresponds to higher erodibility.
Effect of Grazing (Ktr)	+3.3–9% (seasonal)	+3.3-9% (seasonal)	Livestock treading increases erodibility, especially in winter due to intensive forage crop grazing.

These values reflect erosion risks associated with dairy pasture systems**,** where livestock reduces soil structure stability and increases surface runoff, leading to higher sediment transport during storm events in MUSLE-based sediment yield calculations**.**

5.5.2.3 Slope Length (L) and Steepness (S)

These factors capture the impact of terrain on soil erosion. L represents the distance over which runoff occurs, while S reflects the gradient of the slope. High-resolution DEMs and GIS techniques improve the calculation of L and S, ensuring an accurate representation of New Zealand's complex topography (P. Bircher et al., 2019; Desmet & Govers, 1996).

Table 5-7: Terrain Slope Length and Steepness Factors (LS) for Aotearoa, New Zealand

Region	Mean LS-Factor	Standard Deviation (σ)	Key Observations
North Island	1.62	1.83	Majority of land has low LS-factor values.
South Island	1.29	1.91	Southern Alps contribute to more intermediate to high LS-factor values.
Comparison	South Island has 25% higher LS-factor than the North Island.		Average susceptibility to erosion is 25% greater in the South Island due to topographic differences.
Global Context	Comparable to central tendency of European Union LS-factor (μ = 1.63) (Panagos et al., 2015a).		

For our ArcSWAT model, the terrain characteristics of the Waikato region align with North Island LS-factors Table 5.7, confirming moderate erosion susceptibility. These values supported DEM-based LS-factor calibration in ArcSWAT, ensuring realistic sediment yield predictions under the MUSLE framework. While ArcSWAT computes these values internally, the standard LS-factor equations are based on (Desmet & Govers, 1996; Renard, 1997; H. Zhang et al., 2017).

5.5.2.4 Cover Management (C) and Grazing-Adjusted Ground Cover (C_{gr})

The C-factor accounts for the protective effects of vegetation on soil erosion. Grazing-adjusted values (C_{gr}) reflect reductions in ground cover caused by livestock grazing, which can double soil loss susceptibility compared to ungrazed conditions. This is particularly relevant for high-producing grasslands where intensive grazing significantly affects ground cover (Donovan & Monaghan, 2021; Wischmeier, 1978).

5.5.2.5 Support Practice Factor (P)

The P-factor represents the influence of soil conservation practices, such as contouring and terracing, on reducing erosion. While less commonly applied in pasture-based systems, this factor can be adjusted for localized land-use practices in New Zealand.

5.5.2.6 Grazing-Adjusted Factors (K_{tr} and C_{gr})

The inclusion of grazing impacts, such as stock treading and grazing intensity, into MUSLE represents an advancement in erosion modelling. Grazing-adjusted soil erodibility (K_{tr}) and ground cover (C_{gr}) incorporate the effects of hoof pressure, grazing density, and soil moisture, which influence permeability and structural stability (Donovan & Monaghan, 2021). These

refinements have greatly improved soil loss estimates for pastoral systems, especially in New Zealand, where pastoral lands account for over 40% of the national land area (Environment & NZ, 2019). Grazing significantly alters soil structure and permeability, both of which influence the K-factor used for estimating soil erodibility. In this study, the impact of livestock grazing was incorporated as a percentage change in soil permeability (P) and soil structure (S), based on grazing-related parameters such as livestock hoof pressure, grazing density and duration, and historical grazing intensity. These factors were informed by extensive studies on macroporosity, bulk density, and permeability before and after grazing (Climo & Richardson, 1984; Drewry, 2006; Drewry et al., 2008; Gradwell, 1960; Houlbrooke et al., 2009; Houlbrooke, Paton, et al., 2011). Macroporosity is particularly sensitive to grazing intensity, affecting soil aeration, water infiltration, and solute transport (Greenwood & McKenzie, 2001a).

ArcSWAT does not directly incorporate grazing-induced soil compaction effects in its default setup. To address this, a grazing-adjusted soil erodibility (K_{tr}) factor was derived from published datasets and site-specific adjustments. The grazing impact was modeled as a reduction in soil permeability and structural stability, following empirical studies on livestock treading effects (Delage & Lefebvre, 1984; Hu et al., 2018; Katou et al., 1987).

5.6 Climate Zones and Rainfall Patterns in New Zealand

New Zealand exhibits a diverse range of climatic zones due to its unique geography and weather systems. The New Zealand Institute of Water and Atmospheric Research (NIWA) (NIWA, 2012) divided the country into nine climate zones, with four zones located in the North Island and five in the South Island. These zones reflect distinct precipitation patterns driven by topography, prevailing winds, and regional climate dynamics. Table 5.8 represents these regions and rainfall characteristics.

For Region 2 Central North Island (Waikato), moderate precipitation due to sheltering effects from mountains to the south and east and less windy compared to other regions in New Zealand. Annual rainfall ranges from 1,000 to 1,300 mm, increasing with altitude. At higher elevations, such as Mount Ruapehu and Tongariro National Park, rainfall reaches 3,000 mm annually.

Table 5-8: Rainfall Characteristics of New Zealand's Climate Zones (NIWA, 2012)

Region	Locations	Characteristics	Mean Annual Rainfall
Northern North Island	Kaitaia, Whangarei, Auckland, Tauranga	Warm, humid summers; mild winters. Tropical storms from the east or north-east occur in summer and autumn.	1,100–1,300 mm
Central North Island	Hamilton, Taupo, Rotorua	Sheltered by mountains to the south and east; less windy compared to other parts.	1,000–1,300 mm; up to 3,000 mm at higher altitudes (Mount Ruapehu/Tongariro National Park).
South-West North Island	New Plymouth, Wanganui, Palmerston North, Wellington	Very exposed to weather fronts from the Tasman Sea; highly windy.	~1,000–1,200 mm; peaks at 1,500 mm (New Plymouth) and up to 8,000 mm (Mount Taranaki).
Eastern North Island	Gisborne, Napier, Masterton	Dominated by north-east winds; relatively dry.	770–1,000 mm
Northern South Island	Takaka, Nelson, Blenheim	Sunniest region of New Zealand. Peaks occur in areas like Golden Bay.	700–1,000 mm; peaks at 2,000 mm.
Western South Island	Westport, Hokitika, Milford Sound	High variability due to exposure to Tasman winds; heaviest rainfall occurs here.	Up to 10,000 mm (Southern Alps).
Eastern South Island	Kaikoura, Christchurch, Timaru	Low precipitation; common long dry spells in summer.	600–700 mm
Inland South Island	Lake Tekapo, Alexandra, Manapouri, Queenstown	High east-to-west rainfall gradient.	350 mm (Alexandra); up to 3,000 mm (Manapouri).
Southern New Zealand	Dunedin, Invercargill	Influenced by south-east weather fronts; precipitation spread throughout the year.	700 mm (Dunedin); up to 1,200 mm (Invercargill).

Table 5-9: Seasonal Ccrop and Fcover Values for Grasslands and Forage Crops (Donovan, 2022; Donovan & Monaghan, 2021).

Land Use Class	Subclass Description	September–November (Spring)	December–February (Summer)	March–May (Autumn)	June–August (Winter)
Grassland with Woody Biomass	Grassland with matagouri and sweet briar, broadleaved hardwood shrubland, manuka/kanuka shrubland, coastal and woody shrubland	C=0.01, F=1.0	C=0.009, F=1.0	C=0.008, F=1.0	C=0.01, F=1.0
Grassland High-Producing	Grassland with high-quality pasture species				
	Grazing, dairy - Ungrazed	C=0.02, F=0.95	C=0.01, F=0.99	C=0.01, F=0.95	C=0.03, F=0.90
	Grazing, dairy - Grazed	C=0.04, F=0.80	C=0.03, F=0.75	C=0.03, F=0.78	C=0.05, F=0.78
	Grazing, non-dairy - Ungrazed	C=0.02, F=0.95	C=0.01, F=0.99	C=0.01, F=0.95	C=0.03, F=0.90
	Grazing, non-dairy - Grazed	C=0.04, F=0.90	C=0.03, F=0.85	C=0.03, F=0.88	C=0.05, F=0.87
Grassland Low-Producing	Low fertility grassland and tussock grasslands; mostly hill country				
	Grazing, dairy - Ungrazed	C=0.03, F=0.95	C=0.02, F=0.99	C=0.02, F=0.95	C=0.04, F=0.90
	Grazing, dairy - Grazed	C=0.05, F=0.80	C=0.04, F=0.75	C=0.04, F=0.78	C=0.06, F=0.78
	Grazing, non-dairy - Ungrazed	C=0.03, F=0.95	C=0.02, F=0.99	C=0.02, F=0.95	C=0.04, F=0.90
	Grazing, non-dairy - Grazed	C=0.05, F=0.90	C=0.04, F=0.85	C=0.04, F=0.88	C=0.06, F=0.87
Winter-Forage Crops	Grazed, intensive, Brassica species (e.g., fodder beet, swede, kale)				
	Ungrazed	C=0.05, F=0.80	C=0.04, F=0.75	C=0.04, F=0.78	C=0.06, F=0.78
	Grazed	C=0.4, F=0.0	C=0.36, F=0.3	C=0.33, F=0.6	C=0.3, F=0.0

Table 5.9 provides a detailed breakdown of the Cover and Management Factor **(**C and F) values across different land-use classes, accounting for both seasonal variations and specific land-management practices.

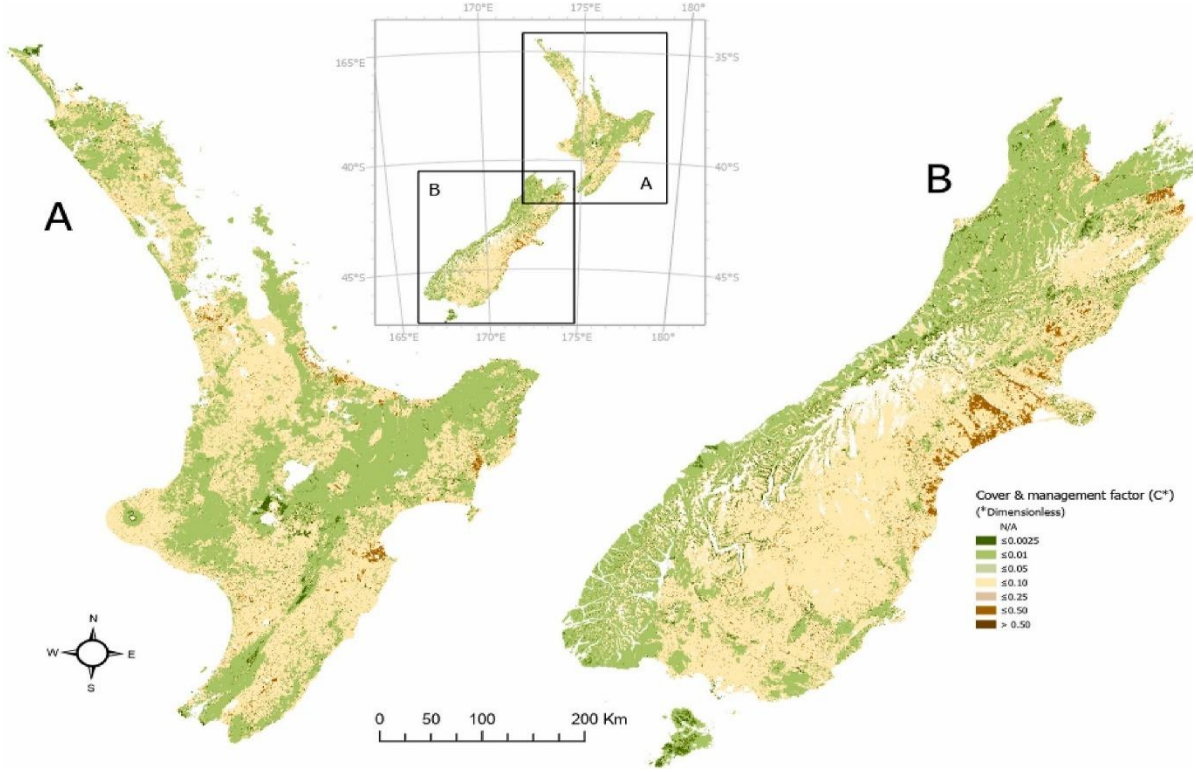

Figure 5-3: Cover and management factor for the (A) North and (B) South Islands of Aotearoa, New Zealand. The values illustrated are for Winter. C-factor values for each vegetation type (Donovan, 2022)

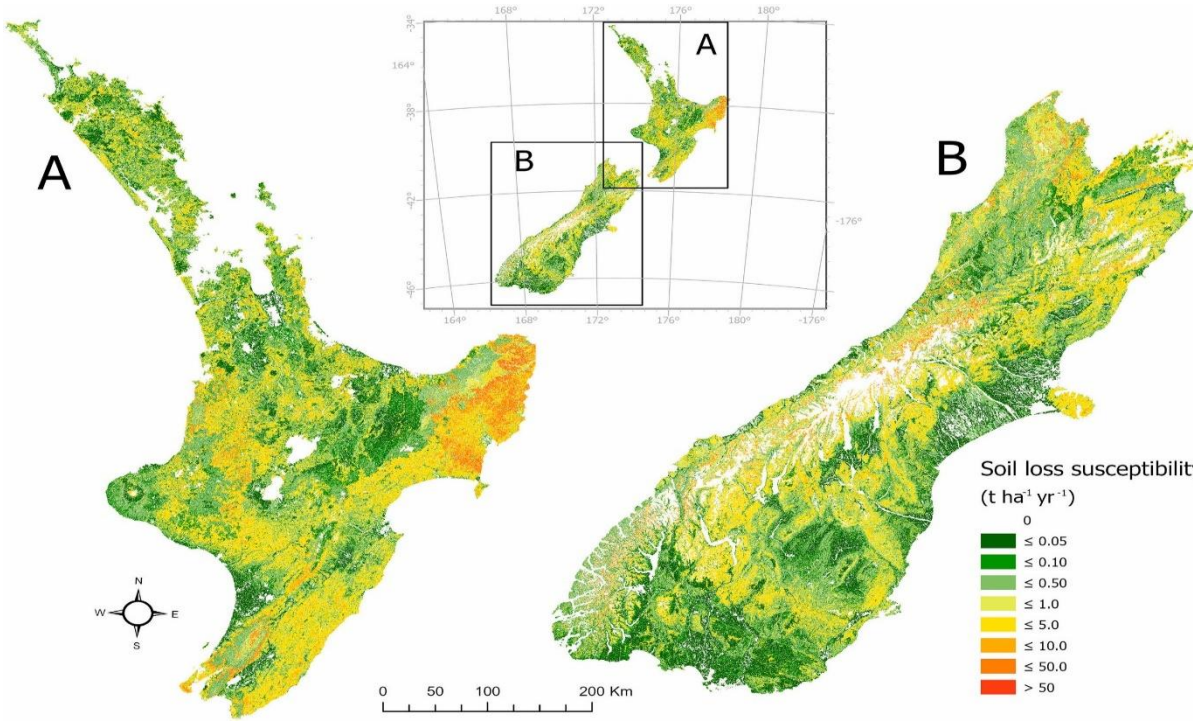

Figure 5-4: A national map depicting modeled soil loss from surface erosion across Aotearoa, New Zealand. The rates represent gross soil losses and do not consider sediment transport, redeposition, or the ultimate fate of the eroded soil (Donovan, 2022).

5.7 National Soil Loss Estimates in New Zealand

Soil loss from surface erosion varies significantly across New Zealand, influenced by land use, topography, and climate(Donovan, 2022). The North Island experiences higher variability in erosion rates, while the South Island generally has greater total soil loss due to its steeper terrain**.**

Table 5-10: Soil Loss from Surface Erosion Across Aotearoa, New Zealand (Donovan, 2022)

Region	Total Soil Loss (t/year)	Erodible Area (ha)	Soil Loss Yield (t/ha/year)	Percentage of Total Soil Loss (%)
North Island	5.56 - 16.03 million	10.82 million	0.51 - 1.45	34 - 55%
South Island	10.93 - 13.16 million	13.58 million	0.80 - 0.95	45 - 66%
Total (NZ)	16.49 - 29.19 million	24.40 million	0.68 - 1.17	100%

For the 22 catchments analyzed by (Donovan, 2022). The average soil loss due to surface erosion from pastoral grasslands was 0.84 t ha^{-1} yr^{-1}, with a range of 0.02 to 2.5 t ha^{-1} yr^{-1} . These values are notably lower than the average soil loss reported for the European Union (2.02 t ha^{-1} yr^{-1}) and the global average (1.70 t ha^{-1} yr^{-1}) (Doetterl et al., 2012; Panagos et al., 2015).

5.8 Assessing Grazing Effects on Soil Erosion in Dairy Pasture

In New Zealand, the challenge of soil erosion is compounded by the intensification of pastoral farming systems, particularly dairy farming, which exerts substantial pressure on soil structure and hydrological processes (Dymond et al., 2016; R. M. Monaghan et al., 2017). The interaction between livestock grazing, soil compaction, and sediment loss is well-documented, with grazing practices known to increase soil vulnerability to erosion through mechanisms such as hoof treading and vegetation removal (Drewry et al., 2008; Greenwood & McKenzie, 2001a). These processes intensify surface runoff, reduce infiltration, and mobilize sediment into waterways, contributing to water quality degradation (Houlbrooke et al., 2009; R. W. McDowell et al., 2003).

5.8.1 Soil Texture and Organic Matter Influence

Dairy pasture soils in Waikato are predominantly loamy (L) and silty (Z), which are moderately erodible. Organic matter (OM) content was measured from surface soil samples (0 - 0.2 m depth) and is known to enhance soil stability by reducing K-factor values.

Table 5-11: Particle size fractions for each class are defined in the New Zealand Fundamental Soils Layer (Clayden & Webb, 1994)

NZLRI Particle Size Class	Particle Size Description	Particle Size Distribution (e.g., Clayden & Webb, 1994; p. 12)		
		Sand (%)	Silt (%)	Clay (%)
S	Sandy	80%	10%	10%
Z	Silty	20%	60%	20%
C	Clayey	20%	20%	60%
L	Loamy	50%	25%	25%

5.8.2 Permeability Class (p) Adjustments in ArcSWAT

Soil permeability (p) influences water infiltration and drainage rates, affecting runoff and sediment transport in ArcSWAT. Instead of detailed calculations, we used NZ Fundamental Soils Layer (FSL) database classifications to assign permeability classes (Hewitt, 1993; Newsome et al., 2008):

- Rapid permeability: 72–288 mm/h
- Moderate permeability: 4–72 mm/h
- Slow permeability: <4 mm/h

The dairy farm soils in Waikato fall within the moderate permeability range, meaning they allow infiltration but are prone to saturation under prolonged rainfall.

5.8.3 Soil Structure (s) and Grazing Impact Adjustments

Soil structure influences water infiltration, runoff, and erosion resistance. In ArcSWAT, soil structure is predefined based on soil texture and land use. For grazed pasturelands, soil structure is adjusted for livestock impacts to account for:

- Stock treading reducing aggregate stability and permeability

- Increased compaction in winter due to wetter soil conditions
- Soil texture and organic matter influencing erosion resistance

5.8.3.1 Soil Data Sources for Erosion Modelling in Arc SWAT

To accurately assess soil erosion within the study site, soil characteristics were obtained from the New Zealand Fundamental Soil Layer (FSL) database (Clayden & Webb, 1994; Hewitt, 1993; Newsome et al., 2008) and supplemented with laboratory analyses. The FSL database provides a comprehensive record of soil properties from over 1,500 locations across New Zealand, offering key attributes for erosion modelling.

The primary soil parameters incorporated into Arc SWAT included: Microporosity (0 – 0.6 m depth), particle size distribution, gravel content, drainage class, and permeability, essential for determining infiltration and runoff potential. Phosphate retention and organic carbon content, with carbon serving as a proxy for organic matter to assess soil stability and erodibility (Clayden & Webb, 1994; Webb & Wilson, 1995) Site-specific laboratory analysis to validate soil texture, bulk density, and erodibility (K-factor) for model calibration.

These datasets were essential in defining soil erodibility (K) and were integrated into Arc SWAT to refine erosion predictions for the dairy farm site.

5.8.3.2 Grazing Intensity

The grazing intensity (i) is a critical parameter used to assess the impact of livestock on soil erosion, as it captures the combined effects of grazing density (d, head per hectare) and stock-specific constants (c). These constants vary depending on feed allocation and utilization patterns for different livestock types (DairyNZ, 2020a; Parker, 1998).

$$i = \frac{d \cdot c}{1000} \tag{5.5}$$

Where: i: grazing intensity (RSU per square meter) d: grazing density (head per hectare) c: livestock constant, reflecting feed allocation and utilization

Standard value of c for dairy cattle on pasture **is** 8 RSU (Relative Stock Units) per head, as this reflects typical feed allocation and utilization for dairy cows on high-producing pastures. If farm management involves intensive grazing or higher feed allocation (e.g., supplementary feed), may consider increasing c slightly to reflect higher pressure per cow. For instance, c = 8.5 or c = 9 could be appropriate for more intensive systems. Conversely, if grazing is more extensive, c could be slightly reduced to 7.5 RSU

Table 5-12: Typical range of grazing density and equivalent values of intensity (i) for pasture (Donovan & Monaghan, 2021)

Livestock	Typical grazing density (d; head/ha) (Pasture)	Grazing intensity equivalents (i; RSU/m²) (Pasture)	Livestock constant (c)
Sheep	<5 - 300	0.001 - 0.041	1.35
Beef cattle	<1 - 50	0.001 - 0.03	6.9
Dairy cattle	40 - 100	0.03 - 0.08	8

Higher grazing intensity increases soil pressure, compaction, and erosion risk. These values were used in Arc SWAT for grazing impact parameterization.

5.8.3.3 Soil Susceptibility to Compaction and Pugging

The risk of soil degradation under grazing depends heavily on the soil's susceptibility to compaction and pugging, which are influenced by two key factors: clay content (ϕ) and soil water content (SWC, σ). These interactions are captured through two modelled factors: compaction susceptibility (ωc) and pugging susceptibility (ωp). These models based on empirical data on soil responses to grazing pressures (Donovan & Monaghan, 2021; Finlayson et al., 2002; Greenwood & McKenzie, 2001a; Houlbrooke et al., 2009).

The soil susceptibility to these processes is vital for dairy farming operations, particularly in areas prone to high rainfall or grazing pressure. Both compaction and pugging reduce soil porosity, water infiltration, and root penetration, ultimately affecting pasture productivity and increasing the risk of surface runoff and erosion.

Compaction susceptibility (ωc) reflects the risk of soil compaction due to grazing and is strongly influenced by SWC. At a critical water content (CWC), soil compressibility peaks moisture levels are high enough to reduce resistance to pressure but not so high as to lose structural cohesion (Donovan & Monaghan, 2021). This behaviour is modelled as:

$$\omega_c = 0.003 \cdot \phi \cdot \left(75 \cdot \sigma - 20 \cdot (\phi + 1)\right)^2 + 8 \cdot \phi + 2 \qquad (5.6)$$

Where, ϕ: clay content (0–100%), σ: Soil water content (expressed as a fraction, 0-1).

This equation provided values we used to adjust soil properties in ArcSWAT to better reflect grazing-induced degradation. This equation highlights that soils with intermediate SWC are

most susceptible to compaction, as excessive dryness increases soil strength, while high saturation reduces compressibility. This pattern aligns with studies on soil deformation under grazing (Drewry, 2006; Greenwood & McKenzie, 2001a). For example, clay-rich soils in New Zealand pastures may experience heightened compaction risk during spring or early summer when soil moisture levels are moderate.

Pugging susceptibility (ωp) reflects the soil's vulnerability to deep hoof imprints, which can severely disrupt soil structure. This susceptibility is particularly high in clay soils under saturated conditions. The following equation models this behaviour (Donovan & Monaghan, 2021; Finlayson et al., 2002):

$$\omega_p = 1 - e^{-500 \cdot \phi \cdot \left(\max\left(0, \sigma^3 - 0.25 \cdot \phi\right)\right)^2} \quad (5.7)$$

Where, ϕ: clay content (0–100%), σ: soil water content (expressed as a fraction, 0-1).

This equation shows that soils with high clay content and near-saturated moisture levels are most vulnerable to pugging. The exponential component reflects how rapidly pugging risk increases as SWC approaches saturation. This behaviour is consistent with findings on soil responses to livestock grazing during wet periods, particularly on New Zealand's dairy farms (Finlayson et al., 2002; Greenwood & McKenzie, 2001a).

5.9 Conclusion

This chapter presented the integration of hydrological, soil, and grazing parameters into the Arc SWAT model to assess runoff generation, soil erosion, and sediment transport in a dairy farm setting. The SCS Curve Number method was applied to estimate runoff potential, while the MUSLE framework was adapted to incorporate grazing-induced soil degradation. Key modifications included: Adjusting soil erodibility (K) to account for grazing pressure, incorporating livestock intensity, hoof pressure, and compaction effects. Modifying permeability (P) and structural integrity (S) to simulate grazing-induced compaction and its influence on infiltration and runoff generation. By incorporating high-resolution soil data, rainfall erosivity values, and grazing parameters, this study improves erosion predictions and estrogen transports with runoff and sediment transport at the farm scale. The results highlight the importance of land-use management in mitigating soil degradation and sediment transport, particularly under intensive dairy grazing systems.

Future work may involve further refinement of dynamic soil parameters, validating model outputs with field observations, and assessing the long-term sustainability of current grazing practices to minimize erosion risks in New Zealand dairy farms

Chapter 6
Modelling Sediment Yield and Estrogen Transport in a Dairy Farm Using ArcSWAT

6.1 Introduction

Dairy farming is a cornerstone of agricultural productivity in New Zealand, contributing significantly to the economy. However, it is also associated with environmental challenges, particularly the loss of sediments and the transport of steroid hormones such as estrone (E1) and estradiol (E2) into surface water systems. These hormones, originating from livestock manure and effluent application, pose a serious ecological risk due to their endocrine-disrupting properties, even at trace concentrations(Ying et al., 2002). Additionally, sediment loss from pastureland contributes to water quality degradation and acts as a carrier for bound estrogens, exacerbating their impact on aquatic environments (Yang et al., 2012).

Understanding the mechanisms of sediment yield and estrogen transport in agricultural landscapes is important for mitigating their environmental impact. Studies (Jenkins et al., 2006; Zhao et al., 2019; Zhao & Lung, 2017) have shown that estrogens in manure and soil systems undergo runoff-driven transport, influenced by rainfall events, land use, and hydrological processes. Research conducted in the South River watershed (Virginia, USA) revealed that E2 on the land surface is transported into streams primarily through storm-induced runoff, with dilution occurring during high-flow conditions (Zhao & Lung, 2017). These findings align with previous work indicating that estrogens are mobilized by surface water movement and exhibit variable persistence in aquatic environments (Colucci et al., 2001; Writer et al., 2011).

This chapter focuses on modelling these processes within a New Zealand dairy farm using the Soil and Water Assessment Tool (SWAT) (Neitsch et al., 2011). SWAT provides a framework for simulating sediment dynamics and pollutant transport, making it a suitable tool for assessing the environmental footprint of intensive agricultural practices. The modelling approach adopted in this study builds upon established methodologies for tracking hormone transport and degradation in watersheds (Pagsuyoin et al., 2012; Zhao & Lung, 2017; Zheng et al., 2012)

The objectives of this chapter are:

1. To simulate sediment yield from a dairy farm.
2. To model the transport of estrogens (E1 and E2) in dissolved and sediment-bound forms through surface runoff.
3. To identify critical source areas (hotspots) for sediment and estrogen losses, guiding targeted management practices.

This study integrates detailed hydrological and management data, including effluent application, grazing, and manure management, to provide a comprehensive simulation of sediment and estrogen dynamics. By coupling sediment yield and estrogen transport in a single modelling framework, the research aims to deliver insights into the pathways and magnitudes of these environmental stressors, informing sustainable management practices for dairy farming.

The findings of this study are expected to contribute to the development of mitigation strategies, such as Wetlands, Riparian buffer zones, optimised Effluent management, and reduced Grazing intensities, to minimize sediment and estrogen losses from dairy farms while maintaining agricultural productivity.

6.2 Study Site

Most of the detailed information about the study site, including the farm's layout, management practices, and hydrological features, is provided in Chapter 3 of this thesis. The farm, located in rural Waikato, New Zealand, consists of effluent and non-effluent blocks, a well-established effluent management system, and critical infrastructure such as an effluent pond, cowshed, and raceways. The site also includes key natural features like the Maungatea stream and on-farm small drains, making it an ideal case study for modelling sediment yield and estrogen transport.

6.3 Data Processing for SWAT Modelling

To accurately simulate sediment yield and estrogen transport using the SWAT model, various input datasets were obtained and prepared. The datasets used in this SWAT modelling study, including the Digital Elevation Model (DEM), soil layers, and Land Use/Land Cover (LULC) data, have been described in detail in Chapter 5. In this chapter, we provide a brief overview of these datasets as they form the foundation for our modelling framework. Further elaboration

on how each dataset was processed and utilised in the SWAT model will be provided in the subsequent sections of this chapter. The datasets were pre-processed to ensure compatibility with the SWAT model.

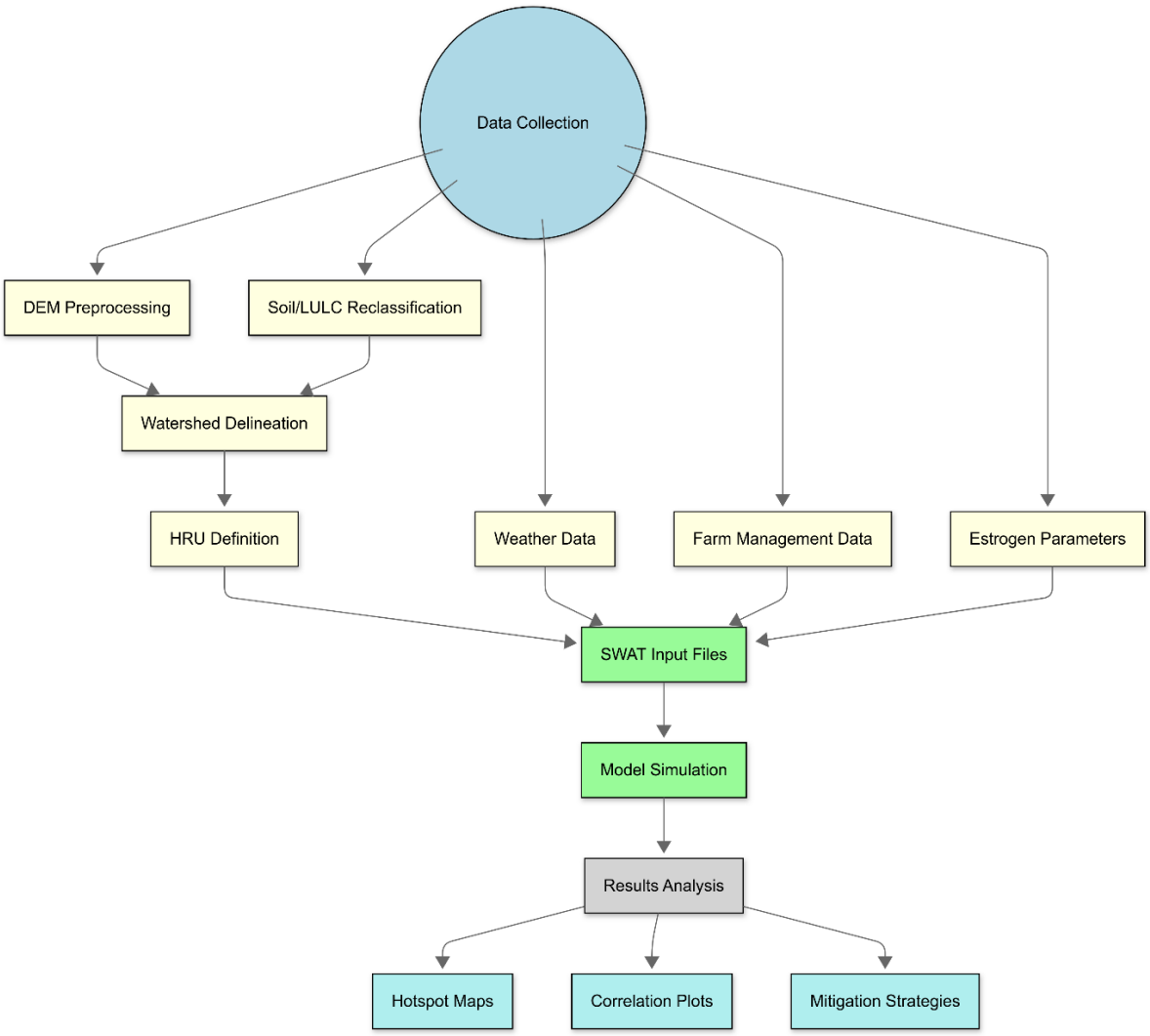

Figure 6-1: A flowchart depicting the ArcSWAT model workflow for simulating sediment and estrogen transport in agricultural landscapes

Figure 6.1 illustrates a flowchart of the ArcSWAT model setup and simulation process for sediment and estrogen transport. It shows how various data sources (DEM preprocessing, soil/LULC reclassification, weather, farm management, and estrogen parameters) are combined into SWAT input files, followed by model simulation and results analysis, culminating in hotspot identification, correlation plots, and recommended mitigation strategies.

6.3.1 Digital Elevation Model (DEM)

A high-resolution 1-meter LiDAR DEM was obtained from the Waikato Regional Council which was captured between January 5 and March 26, 2021. The dataset includes Digital Elevation Models (DEM) and Digital Surface Models (DSM) in NZTM2000 projection, with 1:1,000 tiling. The point cloud data is in LAS format with a pulse density of 4 pulses/m², and accuracy specifications of ±0.2m vertical and ±1.0m horizontal. The data, managed by Waikato Regional Council and Co-Lab, was captured by Ocean Infinity Ltd and is distributed by Toitū Te Whenua Land Information New Zealand under a Creative Commons Attribution 4.0 license. It can be downloaded freely from (https://data.linz.govt.nz/layer/113203-waikato-lidar-1m-dem-2021/) This recently generated dataset provides detailed elevation information, enabling precise delineation of watershed boundaries, slope gradients, and hydrological pathways. The high spatial resolution of the DEM enhances the accuracy of runoff and sediment transport simulations. The DEM was processed to derive essential topographic features.

1. Projection: The DEM was reprojected to match the SWAT model's coordinate reference system, ensuring spatial alignment with other input layers. A standard projected coordinate system (NZTM 2000) was used.
2. Clipping: The DEM was clipped to the study site boundary using the dairy farm's shapefile extracted from Google Earth to focus on the area of interest and reduce computational load.
3. Hydrological Conditioning: Sinks and depressions in the DEM were filled using the hydrology toolbox in ArcGIS Pro (Licensed by The University of Waikato). This step ensured continuous flow paths for accurate stream network delineation.
4. Flow Direction and Accumulation: Flow direction and flow accumulation grids were generated to support watershed delineation in Arc SWAT. These outputs were critical for defining stream networks and subbasins.

6.3.2 Soil Layers

Soil data were sourced from the LRIS Portal (https://lris.scinfo.org.nz/layer/48066-nzlri-soil/) which provides free access to national soil databases managed by Landcare Research New Zealand. The soil dataset includes attributes such as texture, bulk density, and organic matter content, used for calculating soil erodibility, water infiltration, and nutrient retention. The soil data were prepared as follows:

1. **Attribute Selection**: Soil attributes relevant to SWAT, such as texture, bulk density, organic matter, and hydrological group, were extracted from the original dataset.
2. **Reclassification**: Soil types were reclassified to match SWAT's predefined soil database categories. A lookup table was created to map local soil types (silt loam, clay loam) to SWAT-compatible classifications.
3. **Rasterization**: The soil data, originally in vector format (shapefile), were converted to a raster format with the same resolution and extent as the DEM. This ensured seamless integration into the HRU definition process in Arc SWAT.

6.3.3 Land use/Land cover (LULC)

The Land Use/Land Cover data were also acquired from the LRIS Portal (https://lris.scinfo.org.nz/). This dataset, developed by Landcare Research, categorizes the study area into specific land use types, such as pasture and native vegetation. The LULC data were instrumental in defining HRUs (Hydrological Response Units) and assessing the impacts of land management practices on sediment yield and estrogen transport. The LULC data were processed to represent land use patterns accurately:

1. **Reclassification**: LULC classes were reclassified to align with SWAT's land use classification system. For instance, pastureland was mapped to SWAT's “PAST” class.
2. **Rasterization**: Similar to soil data, the LULC dataset was rasterized to ensure compatibility with the DEM and soil layers of site.
3. **Spatial Alignment**: All raster’s (DEM, soil, and LULC) were aligned to the same spatial resolution and extent to avoid discrepancies during HRU delineation.

Once the layers were prepared, they were imported into the Arc SWAT interface:

1. The DEM was loaded first for watershed delineation, creating subbasins and defining stream networks.
2. The Soil and LULC layers were added to classify subbasins into Hydrological Response Units (HRUs). The HRU definition process included:
    - Thresholding to eliminate minor land use and soil classes (e.g., below 10% of subbasin area).
    - Overlaying land use, soil, and slope raster’s to define HRUs accurately.

3. The finalized layers were saved as SWAT-compatible feature classes and tables, which were then used for subsequent model parameterization.

6.4 Soil and Hydrological Mapping

6.4.1 Slope Mapping

The slope map, as shown in Figure 6.2, was generated using a high-resolution 1-meter LiDAR Digital Elevation Model (DEM). The slope was calculated in ArcGIS Pro using the Slope tool from the Spatial Analyst toolbox, which derives the steepness or gradient of the farm in percentage format. The calculated slope values were then categorized into five distinct slope classes, ranging from 0 - 3.2% to 29 -62%, to highlight spatial variations in slope across the dairy farm.

The slope tool processes the DEM by analysing elevation changes between neighbouring cells. The slope values are expressed as percentages, where flat terrain corresponds to low values and steep terrain corresponds to high values. While the high-resolution DEM ensures accurate slope calculation, localized variations in soil compaction and vegetation cover, which also influence runoff and erosion, are not represented in the slope map. We calculated the slope layer directly from the DEM rather than using a pre-existing soil slope layer from the LIRS portal. The high-resolution LiDAR DEM provided a more precise representation of the topography compared to generalised soil slope layers available online.

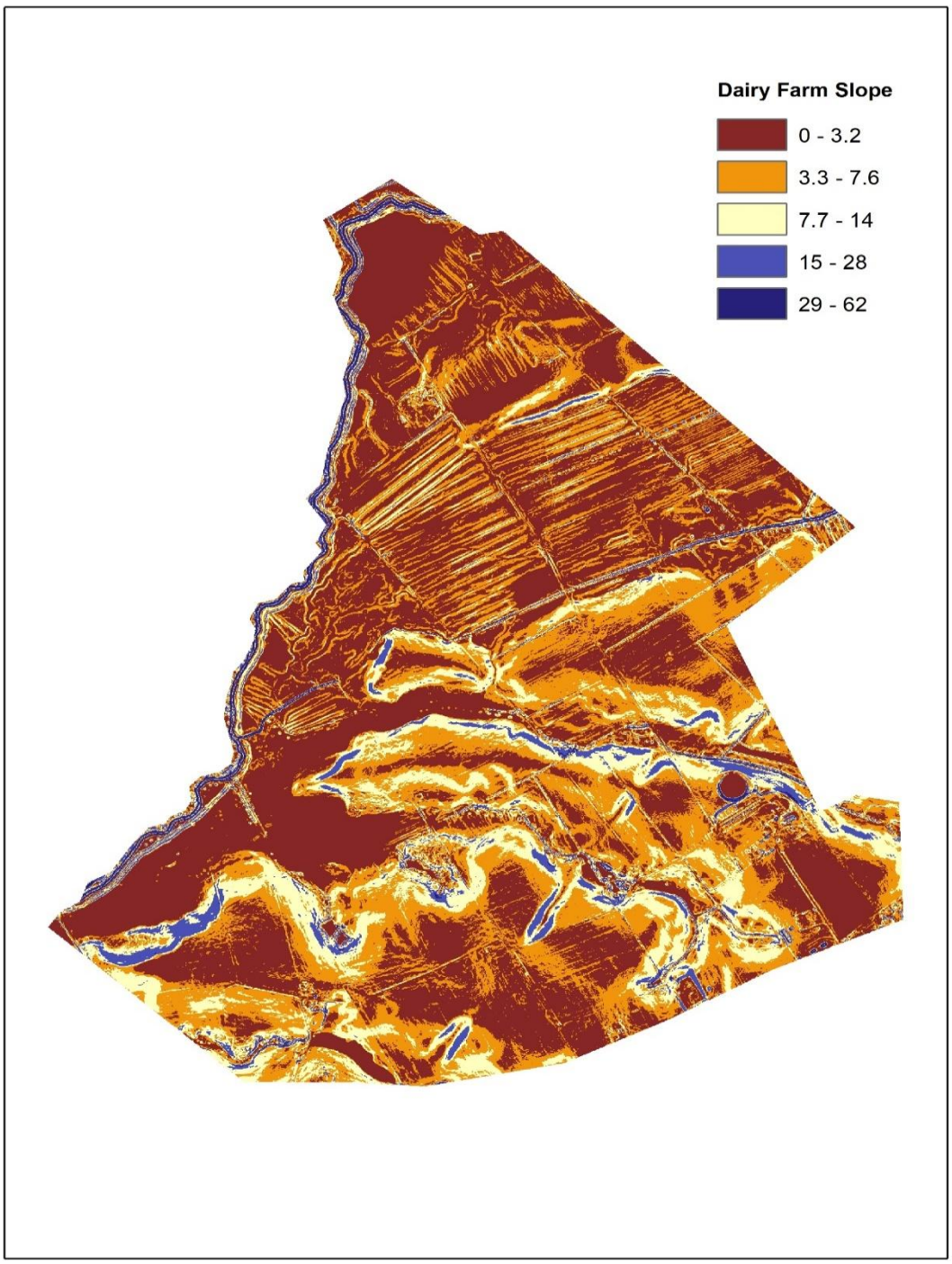

Figure 6-2: Slope Map of the Dairy Farm Showing Gradient Variations Derived from the SWAT Model for Hydrological and Erosion Analysis

6.4.2 Flow Directions Analysis

The flow direction map, as shown in Figure 6.3, was generated using the Flow Direction tool in the ArcGIS Map Spatial Analyst toolbox. This map shows the direction of water flow across the landscape, derived from the 1m LiDAR Digital Elevation Model. Each cell in the map is assigned a specific flow direction based on the steepest descent to its neighbouring cell, allowing for the identification of hydrological pathways within the study site.

The flow direction is computed using the D8 (deterministic eight-direction) method. This method assigns one of eight possible flow directions (represented by integers 1, 2, 4, 8, 16, 32, 64, and 128) to each grid cell. These values correspond to cardinal and diagonal directions (e.g., north, northeast, east, etc.). The direction is determined by identifying the neighbouring cell with the steepest downward slope.

The map highlights the natural flow patterns across the dairy farm, providing insights into water movement from high-elevation areas to low-lying regions. Flow direction aids in understanding how runoff contributes to streamflow and how pollutants, such as sediment and estrogens, are transported within the watershed. Flow direction influences the spatial distribution of sediment yield and the transport of dissolved and sediment-bound estrogens.

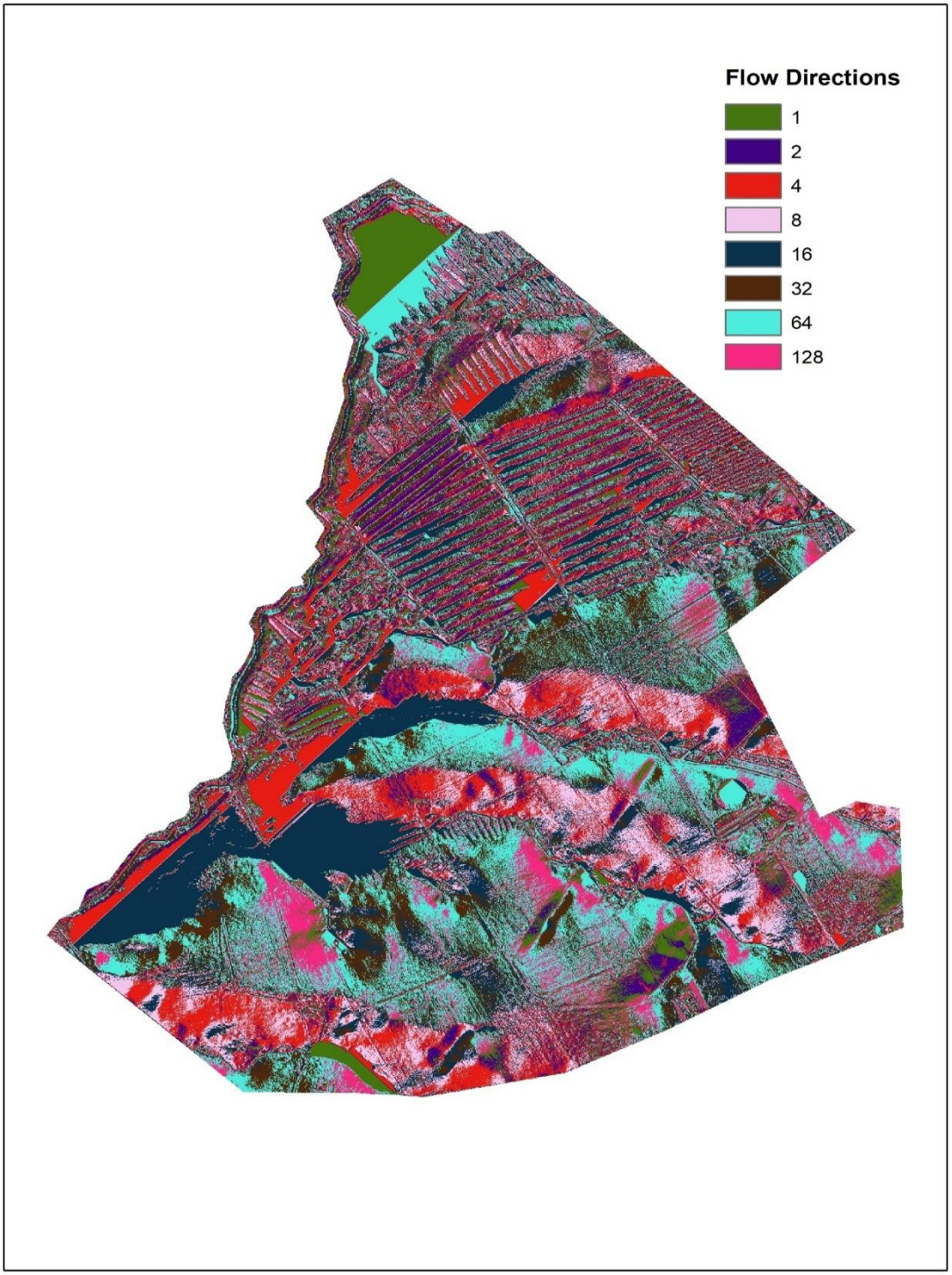

Figure 6-3: Flow Direction Map of the Dairy Farm Generated Using a High-Resolution LiDAR DEM in ArcGIS Map

6.4.3 Flow Accumulation Analysis

The flow accumulation map as shown in Figure 6.4. This map highlights the locations across the study area where surface runoff converges and accumulates, forming drainage pathways and potential stream networks. The flow accumulation values are derived by summing the number of cells contributing runoff to a given cell, with higher values indicating areas where more water converges.

The flow accumulation tool uses the flow direction data to trace the movement of water across the terrain. For each cell, the number of upstream cells contributing water flow is counted and assigned as the flow accumulation value.

Cells with no upstream contributors are classified as 0 (shown in tan colour), representing areas with no flow accumulation (e.g., hilltops, ridges). Cells with upstream contributions are assigned values of 1 or higher (shown in blue), representing cells receiving runoff from multiple upstream sources having higher accumulation values, forming potential drainage pathways or stream channels.

Interpretation and Implications:

- Low Accumulation Areas: Represent hilltops or flat regions where water disperses rather than accumulates.
- High Accumulation Areas: Indicate natural drainage channels, stream networks, or areas prone to erosion and runoff concentration.
- Critical Source Areas (CSAs): Regions with high flow accumulation values that may serve as primary transport pathways for sediment and dissolved pollutants, including estrogens.

The flow accumulation map is essential for identifying key hydrological pathways within the dairy farm, guiding effective watershed management strategies. This information supports the placement of mitigation measures, such as riparian buffer zones and sediment traps, to minimize nutrient and estrogen transport to surface waters.

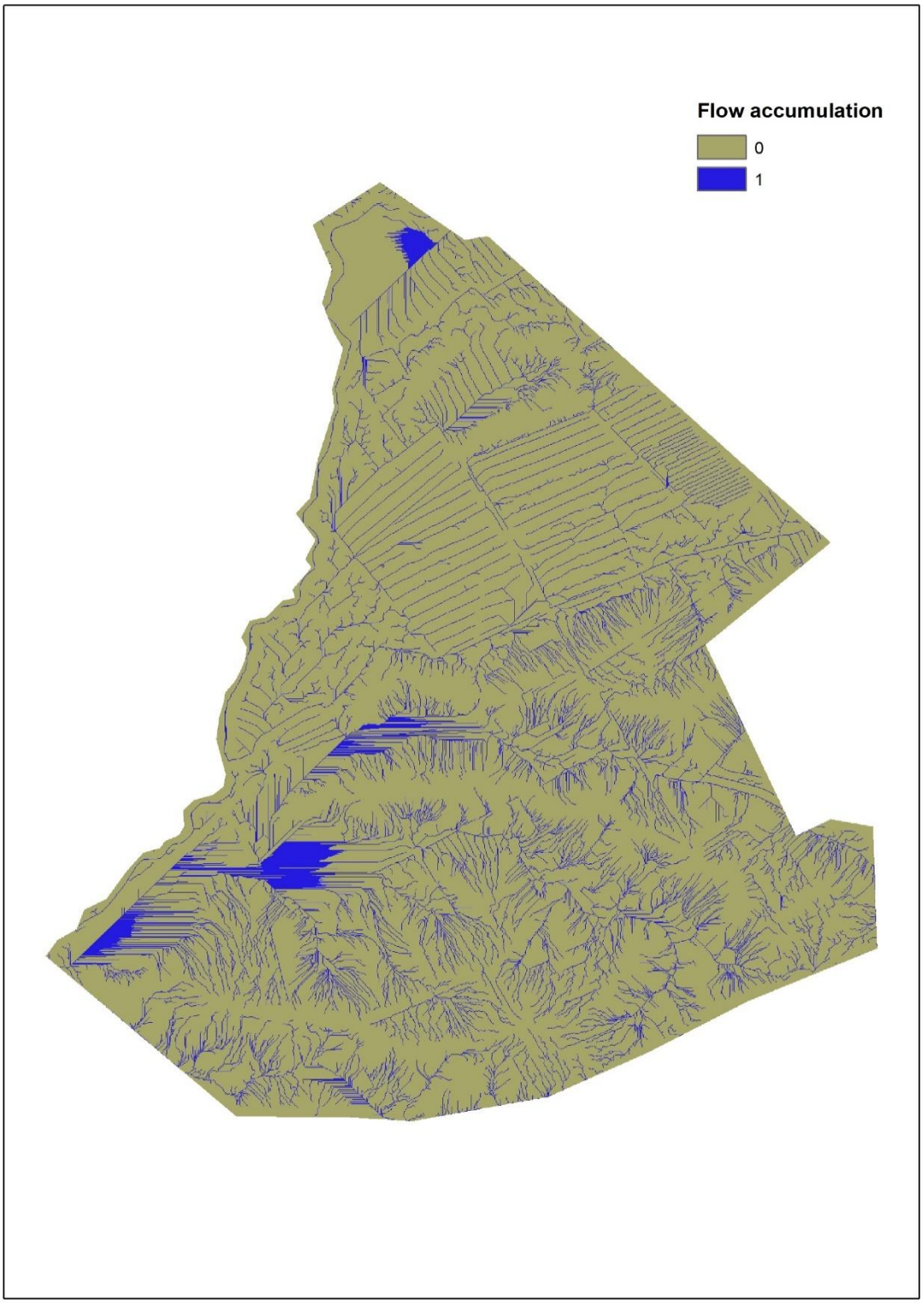

Figure 6-4: Flow Accumulation Map of the Dairy Farm Showing Hydrological Convergence Zones and Drainage Pathways

6.5 Watershed Delineation and Stream Network

Figure 6.5 represents the watershed delineation and associated hydrological features, including basins, streams, reaches, and outlet points. It is a critical output from the Arc SWAT model, which integrates the previous Flow Direction and Flow Accumulation layers with DEM data to identify hydrological connectivity and define watershed boundaries.

The red boundary marks the extent of the watershed, derived using flow accumulation thresholds and outlet points. It defines the catchment area that contributes runoff to specific outlet points within the dairy farm. The stream network (blue lines) is extracted based on flow accumulation values, representing areas of concentrated flow. This network highlights major drainage pathways and is key to modelling sediment and pollutant transport.

The watershed is divided into smaller subbasins (purple polygons), each contributing to a specific part of the stream network. Subbasins are defined to capture local hydrological processes and are used in spatially distributed modelling of runoff, sediment yield, and estrogen transport. Reaches (blue lines) represent the channelised flow within the stream network and are critical for modelling sediment and nutrient transport. Outlet points (green circles) indicate locations where water exits a subbasin and contributes to downstream flow. Yellow lines represent the longest path that water takes to exit the watershed or subbasin, providing insights into flow dynamics and sediment transport potential.

The delineation accurately captures the hydrological connectivity within the dairy farm, including natural drainage patterns and the relationship between subbasins and the stream network. The stream network ensures that surface runoff, sediment, and dissolved pollutants are routed appropriately across the landscape.

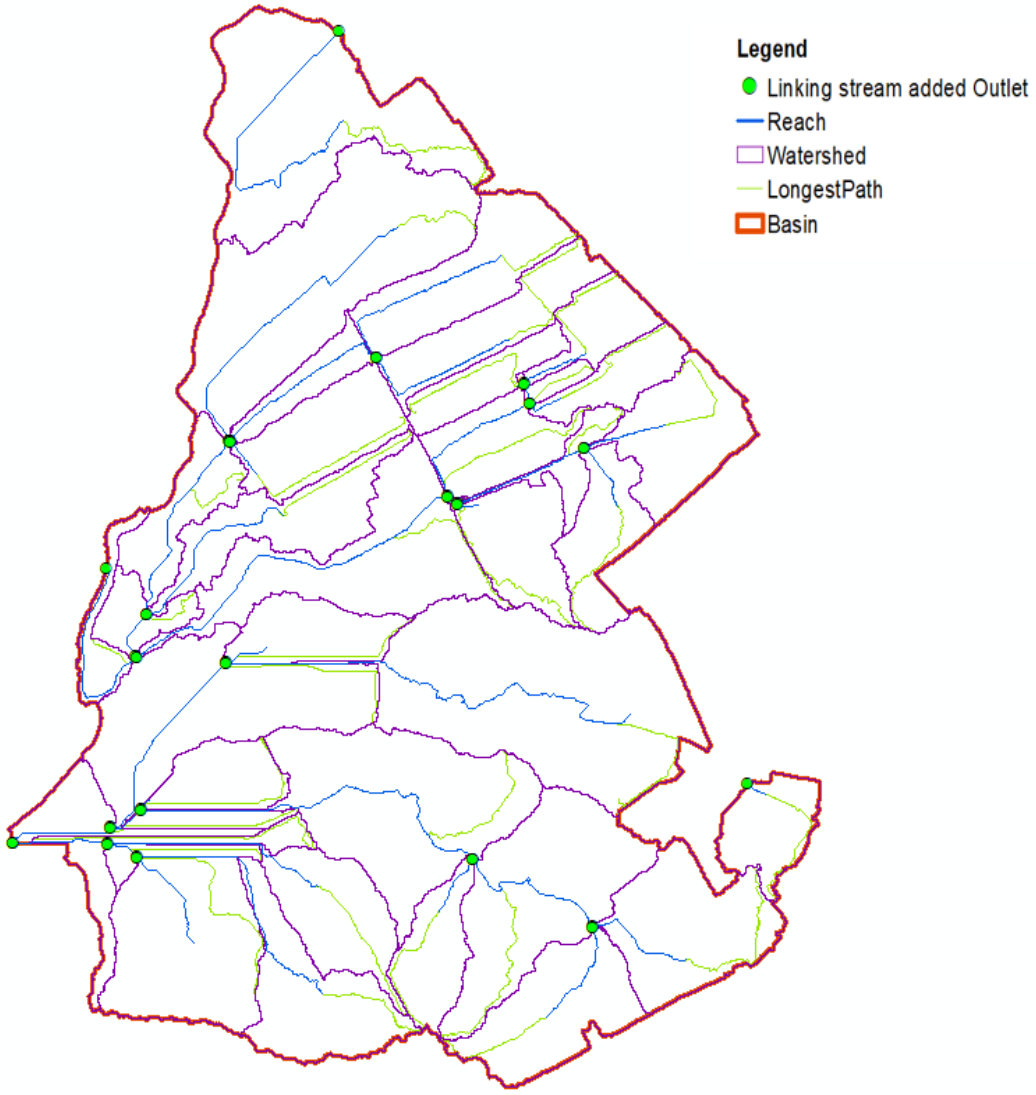

Figure 6-5: Watershed Delineation and Stream Network of the Dairy Farm, Derived from High-Resolution LiDAR DEM

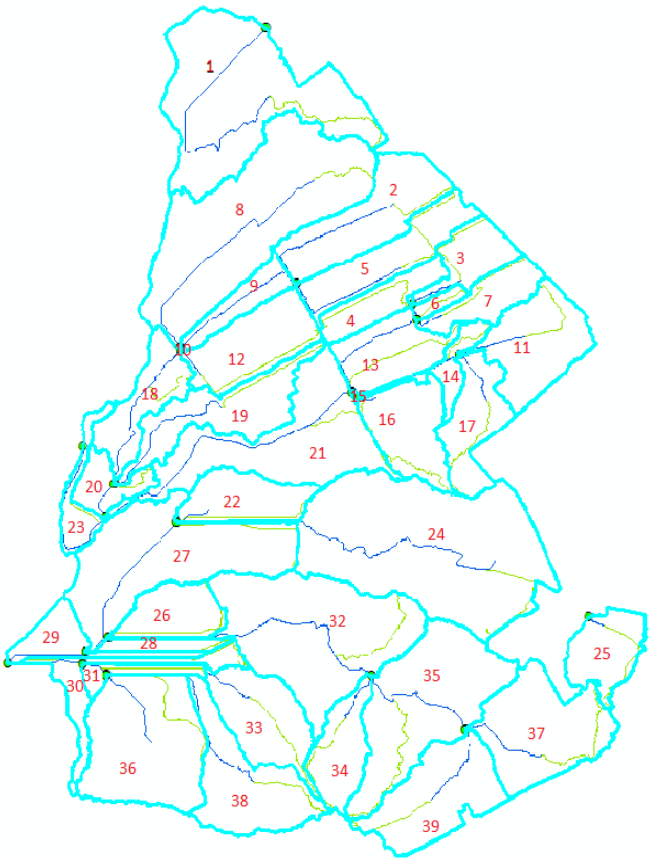

Figure 6-6: Numbered Subbasins in the Dairy Farm Watershed, Classified as Pastureland for Hydrological and Estrogen Transport Analysis

The map in Figure 6.6 shows the delineated subbasins within the dairy farm, each assigned a unique identifier for analysis and model parameterization. These subbasins were generated during the watershed delineation process in Arc SWAT**,** representing hydrologically independent units that contribute runoff, sediment, and nutrient and estrogen loads to specific outlet points.

6.5.1 Land Use and Soil Characteristics

For this study site, we considered the land use and soil data to be uniform across the majority of the dairy farms (Reference back to Chapter 3). Approximately 98% of the area is covered by pasture**,** which is typical for dairy farming operations in the region. Similarly, the soil is predominantly classified as clay loam and silt loam, reflecting the farm's dominant soil types. This uniformity simplifies the modelling process by focusing on the primary land use and soil

type, which are the most significant contributors to runoff, sediment yield, and estrogen transport. The assumptions align with field observations and available data, ensuring a realistic representation of the site while minimizing unnecessary complexity.

6.5.2 Defining Watershed Boundaries

The flow direction and flow accumulation layers were generated from the DEM to define the hydrological pathways and watershed boundaries. A flow accumulation threshold of 1000 cells was applied, equivalent to 1 hectare, to identify drainage areas and define the stream network accurately. This threshold ensured the exclusion of minor flow paths while focusing on major drainage channels critical for sediment and nutrient transport.

6.5.3 Stream Network Extraction

The stream network was derived from areas with flow accumulation values exceeding the set threshold. The network highlights major drainage pathways and natural flow patterns, serving as the foundation for routing sediment and estrogens during runoff events.

6.5.4 Outlet Points and Subbasins

Initially, 42 outlet points were automatically generated to segment the watershed. These were refined by manual adjustments to 39 to avoid redundancy and better represent key hydrological locations as shown in Figure 6.5. A balance was maintained between capturing spatial variability and ensuring computational efficiency. Each outlet point delineates a subbasin, contributing to the stream network and serving as hydrologically independent units for modelling.

The longest flow paths within each subbasin were calculated to understand the hydrodynamics of water and sediment transport. These paths show the maximum distance water travels before exiting a subbasin, providing insights into potential sediment deposition and transport times.

6.5.5 Hydrological Response Unit (HRU) Definition

The Hydrological Response Units (HRUs) in the SWAT model were generated by overlaying spatial layers of land use, soil, and slope. HRUs represent unique combinations of these factors within each subbasin, allowing spatially distributed simulation of hydrological and sediment transport processes. The following thresholds were applied to ensure computational efficiency and to define the HRUs for this study;

- Land Use Threshold: 20% of the subbasin area.

- Soil Threshold: 10% of the land use area.
- Slope Threshold: 20% of the soil area.

These thresholds ensured that only dominant HRUs were retained while normalizing their areas to represent 100% of the total subbasin area. A total of 127 HRUs were generated across the study area, reflecting the variability in slope and hydrological processes within the dairy farm.

Each HRU represents a unique combination of:

- Land Use: Pasture (98% of farm area)
- Soil Type: Clay loam and silt loam
- Slope Class: Five slope categories ranging from 0-3.2% to 29-62%

These HRUs form the basis for distributed hydrological modelling, allowing SWAT to capture variations in runoff generation, sediment transport, and estrogen movement within the watershed.

6.6 Input Data for ArcSWAT Model

All datasets were synchronized to ensure compatibility with the daily timestep of the SWAT model. Inputs were converted into SWAT-compatible text files, including .wgn (weather generator), .mgt (management operations), and .sol (soil database). Custom management operations (e.g., effluent irrigation and grazing) were created to reflect farm-specific practices.

Daily precipitation, maximum and minimum temperatures, relative humidity, wind speed, and solar radiation. Other data were obtained from the New Zealand National Climate Database (NIWA), supplemented with site-specific measurements where necessary. A custom weather generator file (.wgn) was prepared to provide synthetic data for filling gaps in variables like solar radiation and wind speed.

In managing dairy effluent applications to pastures in New Zealand, it is essential to adhere to specific guidelines by respective Regional Councils to optimize nutrient utilization and minimize environmental impacts. The nutrient content of dairy effluent can vary; for instance, liquid effluent typically contains approximately 0.62 kg of nitrogen per cubic meter. In contrast, separated solids have higher nutrient concentrations, with total nitrogen levels around 3.59 kg per tonne (Houlbrooke, Longhurst, et al., 2011). To mitigate environmental risks, it is recommended to limit nitrogen application from effluent to 150 kg N/ha/year on grazed

pastures. For cropping systems, higher rates may be permissible based on crop requirements and soil conditions (Houlbrooke, Longhurst, et al., 2011). The depth of effluent application should align with soil risk categories. For high-risk soils, such as those with artificial drainage or coarse soil structure, it is advised to apply effluent at a depth less than the soil water deficit to prevent ponding and runoff. For high-rate application tools, a maximum depth of 10 mm is recommended, while low-rate application tools can apply up to 25 mm, provided a suitable soil water deficit exists (DairyNZ, 2011). It ensures that the application rate of effluent is less than the soil's infiltration rate to prevent ponding. For sloping land, the instantaneous application rate should be less than the soil infiltration rate to avoid runoff (DairyNZ, 2011). Adequate effluent storage is essential to manage applications during unsuitable weather conditions. The required storage volume depends on factors such as herd size, milking frequency, yard wash-down procedures, and local rainfall patterns. For example, tools like the Dairy Effluent Storage Calculator can assist in determining appropriate storage needs (Bay Plenty Regional Council).

In our study, we utilized data collected from direct visits to dairy sites, interviews with dairy owners, and documents provided by them detailing stock density, fertilizer usage, and annual soil health assessment reports. Additionally, we incorporated guidelines from authoritative sources such as the (Arable Research; Taranki Regional Council; DairyNZ, 2011, 2020, ; Houlbrooke et al., 2011; Bay of Plenty Regional Council,; Resource Management) to inform our model inputs.

6.6.1 Effluent Irrigation Parameters

Effluent irrigation practices were incorporated into the model based on regional council guidelines and documentation provided by dairy owners. Effluent from the farm’s effluent pond was considered the primary source of irrigation, aligning with standard dairy farm management practices.

Irrigation was added as a management operation within the HRU settings of the SWAT model. Key parameters, such as irrigation amount (IRR_AMT), irrigation source (effluent pond), and irrigation schedule (e.g., monthly applications), were defined based on regulatory recommendations and on-farm records.

The impact of irrigation on soil water balance, nutrient movement, and estrogen transport was explicitly modelled by incorporating effluent nutrient loads, estrogen concentrations, and soil

infiltration rates. Table A1 (Appendix A) summarizes key parameters related to effluent irrigation, including irrigation amount, nutrient load, and efficiency factors.

6.6.2 Fertilizer Application Data

Fertilizer application parameters were integrated into Arc SWAT based on regional council guidelines and dairy farm management records to ensure an accurate representation of nutrient cycling, microbial transport, and estrogen fate. The .mgt file was configured to capture the timing, rate, and method of manure application, optimizing process-based simulations of nitrogen, phosphorus, and estrogen transport. Appendix A listed these parameters.

Manure applications were scheduled monthly to reflect on-farm practices while minimizing the overestimation of nutrient leaching in wet conditions. Surface spreading was set as the application method, ensuring spatial consistency with HRUs and linking nutrient mobilization to hydrological response. Mineralization and microbial decomposition rates were adjusted to capture ammonification, nitrification, and organic matter turnover, preventing overaccumulation in the soil. To model runoff-driven transport, manure application was coupled with erosion-based nutrient loss functions, ensuring that phosphorus and nitrogen fluxes align with sediment dynamics.

This implementation ensures that nutrient cycling, pollutant fate, and hydrological interactions in ArcSWAT remain process-driven and consistent with observed dairy pasture management practices.

6.6.3 Grazing and Livestock Management

Grazing and livestock were implemented as a management operation in Arc SWAT's .mgt file with parameters such as grazing days (GRZ_DAYS), biomass consumed (BIO_EAT), and biomass trampled (BIO_TRMP), ensuring that biomass consumption, manure deposition, and estrogen transport align with monthly pasture rotations, a standard dairy farm practice. Grazing was scheduled as a recurring management event within the HRU schedule. Every 30 days, cows were moved between pastures for rotational grazing. Nutrient and estrogen release from manure was time-dependent, with first-order decay coefficients applied to dissolved and sediment-bound fractions. The table A3 and A4 summarized the Grazing and Livestock management within the SWAT model.

Continuous grazing and trampling affect soil compaction and erosion susceptibility, altering hydrological connectivity and nutrient fluxes. Uniform grazing intensity and manure deposition were applied across the pasture due to the predominance of dairy cattle and homogeneous management practices. The dairy farm under study encompasses 110 hectares, systematically divided into 39 subbasins, each averaging approximately 2.82 hectares. Implementing a rotational grazing system, the entire herd of 180 cows grazes one subbasin per day, proceeding sequentially through all subbasins. This management practice results in a 39-day grazing cycle for each subbasin, comprising 1 day of grazing followed by 38 days of rest.

Stocking density, influencing pasture utilization and nutrient deposition, is calculated as follows:

$$\text{StockingDensity} = \frac{\text{Number of Cows}}{\text{Area of Subbasin}} = \frac{180 \text{ cows}}{2.82 \text{ hectares}} \approx 63.83 \text{ cows/hectare}$$

This high stocking density necessitates management to prevent overgrazing and ensure sustainable pasture regrowth during rest periods.
For further guidance on setting these parameters in SWAT, the SWAT theoretical documentation (Chiang et al., 2010; Neitsch et al., 2011), which provides detailed explanations of model inputs related to land management and agricultural practices.

6.6.4 Estrogen Parameters:

The transport and fate of estrone (E1) and estradiol (E2) were incorporated into Arc SWAT using pesticide input files, a process-based simulation of dissolved and sediment-bound estrogen transport, farm manure composition records, and literature-reported degradation rates. Since SWAT does not have built-in estrogen handling, E1 and E2 were implemented as pesticide analogs, allowing simulation of their sorption, degradation, and runoff transport mechanisms. Estrogen inputs were dynamically linked to grazing and effluent irrigation operations within Arc SWAT's management (.mgt) file, such as estrogen release corresponds to manure deposition and effluent application events. First-order decay rates were used to model estrogen degradation.

Estrone (E1) is the primary degradation product of E2 in manure and soil systems, exhibiting moderate hydrophobicity (Log KOW = 3.1-3.4) and a variable water solubility range of 0.8–12.4 mg/L. Due to its strong affinity for sediment, E1 has an extended persistence in soil and

runoff events, influencing long-term estrogen cycling in pastureland. Manure-derived E1 concentrations can reach 16.1 ng/g dry solids (DS) in dairy farming systems (L. S. Lee et al., 2003; Sarmah et al., 2006b). Estradiol (E2) is the biologically active estrogen excreted by dairy cattle, with a higher hydrophobicity (Log KOW ~4.0) compared to E1, leading to stronger sediment adsorption. E2 is less stable in the environment, with rapid microbial oxidation converting it to E1. Its water solubility (13 mg/L) allows dual transport modes dissolved-phase leaching and sediment-bound mobility-during runoff events. Fresh dairy manure typically contains 16.6 ng/g DS of E2 (Wei et al., 2011).

6.6.4.1 Estrogen Excretion Estimation

Dairy cows excrete natural estrogens, primarily estrone (E1) and 17β-estradiol (E2), through urine and feces. The concentration of these estrogens in manure is a pivotal factor in environmental modelling. Studies have reported average concentrations of 17β-estradiol and estrone in dairy feces to be approximately 104.4 μg/kg and 262 μg/kg, respectively (Wei et al., 2011).

6.6.4.2 Total Estrogen Deposition per Subbasin

The total daily estrogen deposition in each subbasin during grazing is calculated by:

$$\begin{aligned}\text{TotalDailyEstrogenDeposition} &= \text{Number of Cows} \times \text{Manure Production per Cow} \\ &\times \text{Total Estrogen Concentration in Manure}\end{aligned}$$

This section outlines the methodologies and calculations used for estimating estrogen loads across the study area, integrating grazing operations, manure application, and surface runoff processes.

6.6.4.3 Pathways of Estrogen Loading in Arc SWAT

The spatial and temporal distribution of estrogen inputs was explicitly modelled in ArcSWAT by linking estrogen fluxes to manure deposition (grazing and effluent application), runoff dynamics, and hydrological connectivity.

6.6.4.4 Direct Deposition During Grazing and Manure Application

Cows excrete E1 and E2 directly onto pastures, with estrogen loading rates influenced by:

- Daily manure production per cow
- Estrogen content in manure, varying with diet and seasonal conditions
- Time spent grazing, influencing manure deposition spatial patterns

The daily estrogen excretion (Qc) was computed using (Zhao & Lung, 2017),

$$Q_c = W \times S \times E \quad (6.1)$$

Where: Q_c is daily estrogen excretion (ng/day), W is daily manure production (kg/day). S is solid content in manure (%). E is estrogen content in solid manure (ng/g).

The application of dairy manure to pastureland introduces both E1 and E2 into the environment. Based on studies (DairyNZ, 2020b) dairy manure application rates of up to 1200 g/m²/year to pastureland are common in New Zealand. The hormone content in applied manure, combined with precipitation and irrigation practices, determines the extent of estrogen leaching and runoff.

Estrogen deposition onto cropland occurs through the application of manure generated by dairy cows. This pathway is important in agricultural systems where manure is regularly applied to enhance soil fertility. The monthly E1 and E2 loads to cropland were calculated using the equation (Zhao & Lung, 2017)

$$M = R\ C\ F \quad (6.2)$$

Where M is the monthly E1/E2 loads to cropland from manure application (kg/month), R is the annual manure application rate to cropland (kg/ha). C is the estrogen content in manure (mg/kg). F is the fraction of manure applied to cropland in a specific month.

The deposition of E2 and E1 onto pastureland arises primarily from cattle grazing and manure application. The monthly estrogen load to pastureland is calculated using the equation

$$M = RCF + PQ_c\ TD \quad (6.3)$$

Where M is the monthly estrogen load to pastureland from cows (kg/month). R is the annual manure application rate to pastureland (kg/ha). C is the estrogen content in manure (mg/kg). F is the fraction of manure applied to pastureland in a specific month. P is the population of cows. Q_c is the daily estrogen production per cow (mg/day). T1 is the fraction of time cows spend grazing on pastureland. D is the number of days in that month.

Both E1 and E2 are transported in dissolved and sediment-bound forms during surface runoff events. Research shows that approximately 18% of E2 from manure can desorb and mobilise into runoff water, while E1 demonstrates a similar behaviour under varying soil moisture and pH conditions.

The total estrogen load in runoff (L_{runoff}) can be expressed as:

$$L_{runoff} = 0.18 \cdot M_{total} \quad (6.4)$$

- **Direct Deposition into Stream**

Cows grazing near streams may excrete wastes directly into the waterways, contributing to estrogen (E2) contamination in streams. Approximately 18% of the E2 from cattle manure can desorb into water, amplifying the estrogen load in the hydrological system. This direct deposition of E2 into streams is calculated using the equation:

$$L = P\ Q_c\ T_2 \times 18\% \quad (6.5)$$

L is the daily E2 load into streams from cattle manure directly excreted into streams (mg/day). P is the population of cows, Q_c is daily E2 production per cow (mg/day) mg/day average = 0.27 mg/day. T2 is the fraction of time cows spend in or near streams (T2 =0.1, assuming 10% of grazing time near streams). 18% is the fraction of E2 desorbed from manure into the stream water, as observed in studies.

This equation (6.5) models the direct contribution of grazing cattle to E2 contamination in streams. It highlights the importance of grazing management practices, such as restricting cattle access to waterways through fencing or alternative watering systems, to mitigate the direct deposition of estrogen into streams. This was parameterized as a non-point-source input in ArcSWAT, ensuring hydrologically consistent pollutant fate modelling.

This process-based estrogen modelling approach in ArcSWAT provides a high-resolution, mechanistic framework **for** assessing estrogen transport and environmental risks in dairy farm systems**.**

6.7 Results and Discussion

6.7.1 HRU Analysis

This section presents the results from the SWAT model simulations, which explore the dynamics of estrogen transport in runoff and sediment within the study area. The focus is on understanding the relationship between runoff, sediment yield, and the concentrations of estrone (E1) and estradiol (E2) across different Hydrological Response Units (HRUs) and subbasins. Figures 6.7 through 6.15 illustrate key findings, such as the correlation between runoff and estrogen concentrations, as well as the impact of sediment transport on estrogen mobilization. These results provide valuable insights into the hydrological and soil processes that govern estrogen transport, revealing both predictable patterns and complex interactions influenced by multiple factors, including runoff intensity, soil characteristics, and management practices.

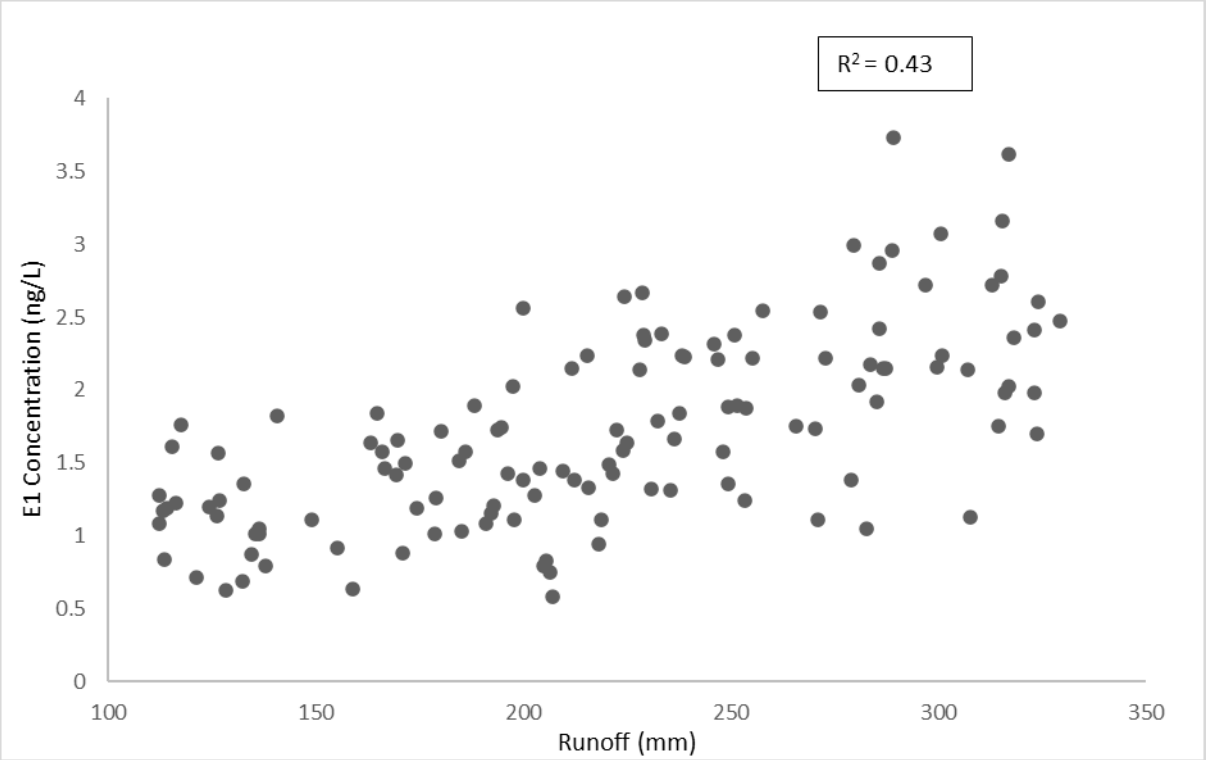

Figure 6-7: Correlation between runoff (mm) and E1 concentration (ng/L) at the HRU scale

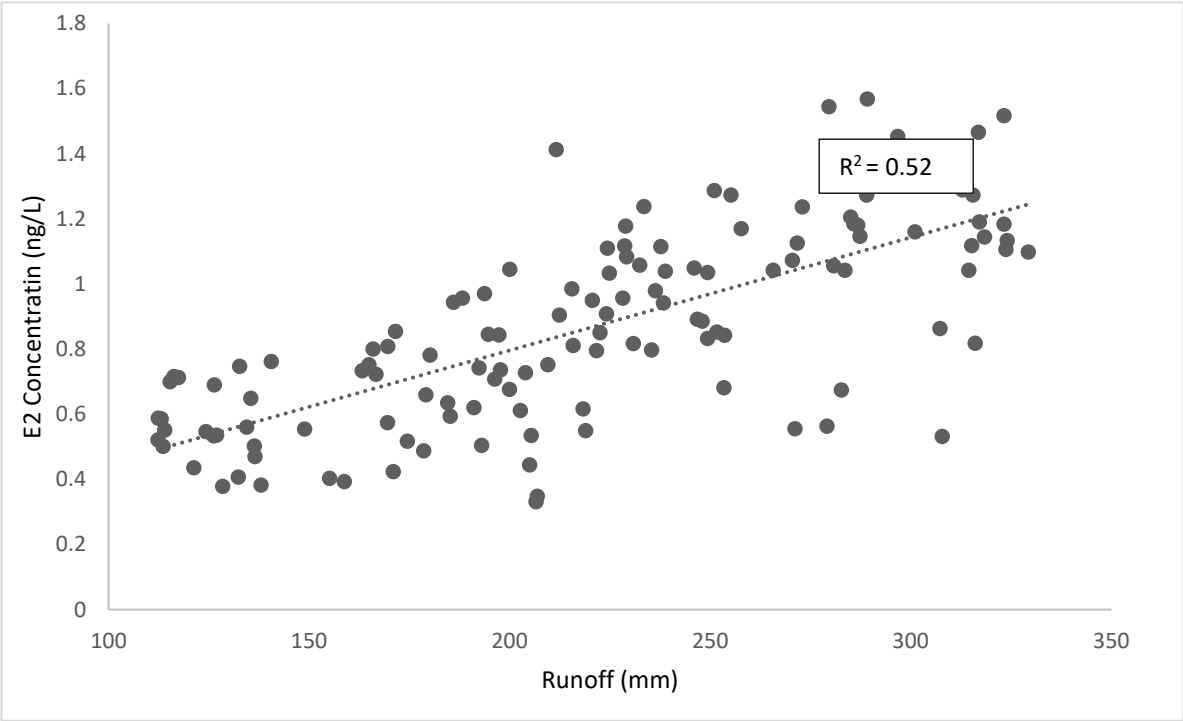

Figure 6-8: Relationship between annual runoff (mm) and E2 concentration (ng/L) at the HRU scale

The relationship between runoff and E1 concentration presented in Figure 6.7 illustrates a moderately positive correlation (R^2 = 0.43). This observation points toward a hydrological dependency of E1 mobilization, where increased runoff likely enhances the transport of sorbed and dissolved E1 fractions. However, the relatively low R^2 suggests variability that cannot be fully explained by runoff alone. This variability likely reflects the influence of soil characteristics, such as organic matter content and texture, which govern sorption dynamics, and site-specific hydrological pathways, such as infiltration versus overland flow. Additionally, the observed trend might be moderated by the distinct physicochemical properties of E1 compared to other estrogens. E1's higher sorption potential and potentially slower degradation rates in certain soil conditions may result in greater retention within the soil matrix, thereby creating non-linear or localized transport responses to runoff.

Figure 6.8 illustrates the relationship between runoff (mm) and E2 concentration (ng/L) at the HRU scale. The data show a clear positive correlation, with an R^2 value of 0.52, suggesting that runoff explains approximately 52% of the variation in E2 concentrations across HRUs.

The observed trend aligns with the fundamental understanding that higher runoff volumes are associated with increased mobilization of estrogen. As water flows overland or through the soil, it interacts with surface particles, mobilizing both dissolved and particle-bound estrogen. However, the moderate correlation coefficient reflects the complexity of this process, where multiple factors beyond runoff contribute to E2 dynamics.

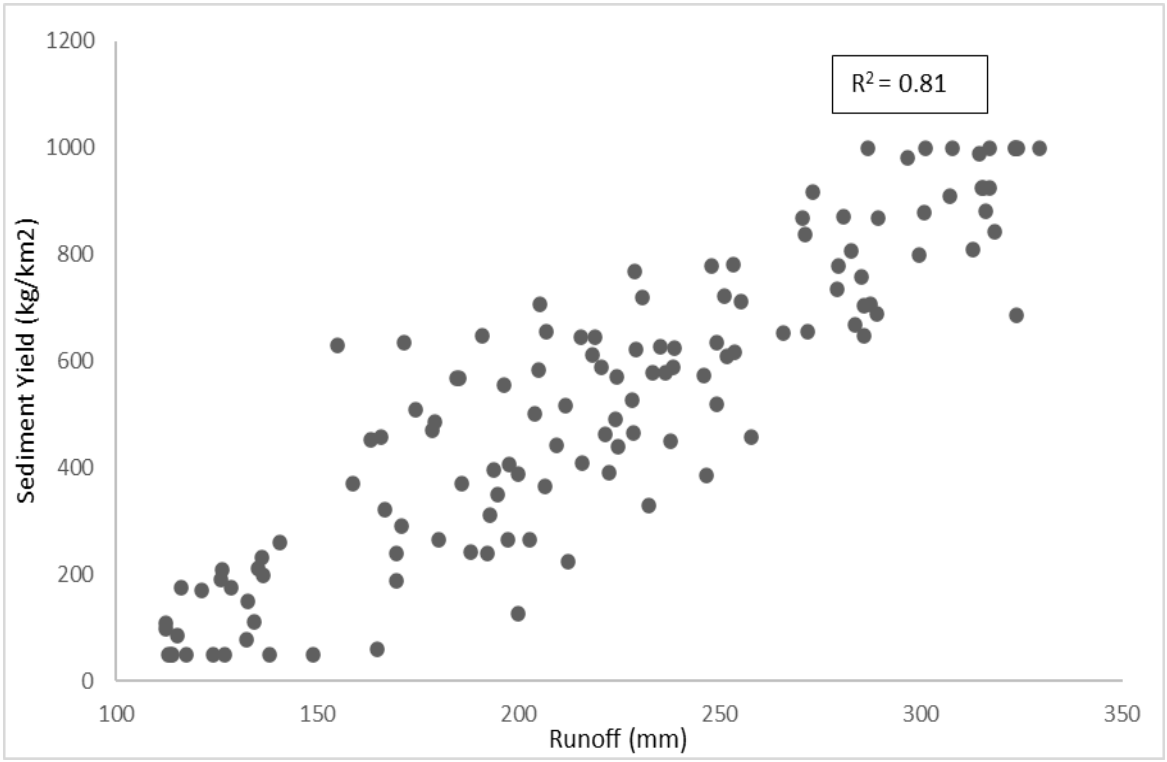

Figure 6-9: Correlation between Annual runoff (mm) and sediment yield (kg/km²) at the HRU scale

The relationship between runoff and sediment yield, as demonstrated in Figure 6.9, shows a strong positive correlation (R^2 = 0.81), suggesting a dominant hydrological influence on sediment transport processes. The linearity of this trend suggests that, within the studied HRUs, the relationship is relatively uniform and less affected by secondary processes such as soil cohesion or vegetation cover, which often introduce variability in sediment dynamics. The strength of this correlation likely reflects the coupling of overland flow intensity with sediment mobilization. As runoff increases, it generates greater shear forces capable of detaching soil particles, especially in areas with low vegetation cover or weak soil structure. Furthermore, this trend good fit with hydrological theory, where sediment yield is proportional to both the volume and velocity of surface runoff. Furthermore, the strong relationship at the HRU scale

provides a basis for scaling these processes to subbasins and assessing cumulative impacts on downstream sediment transport and water quality.

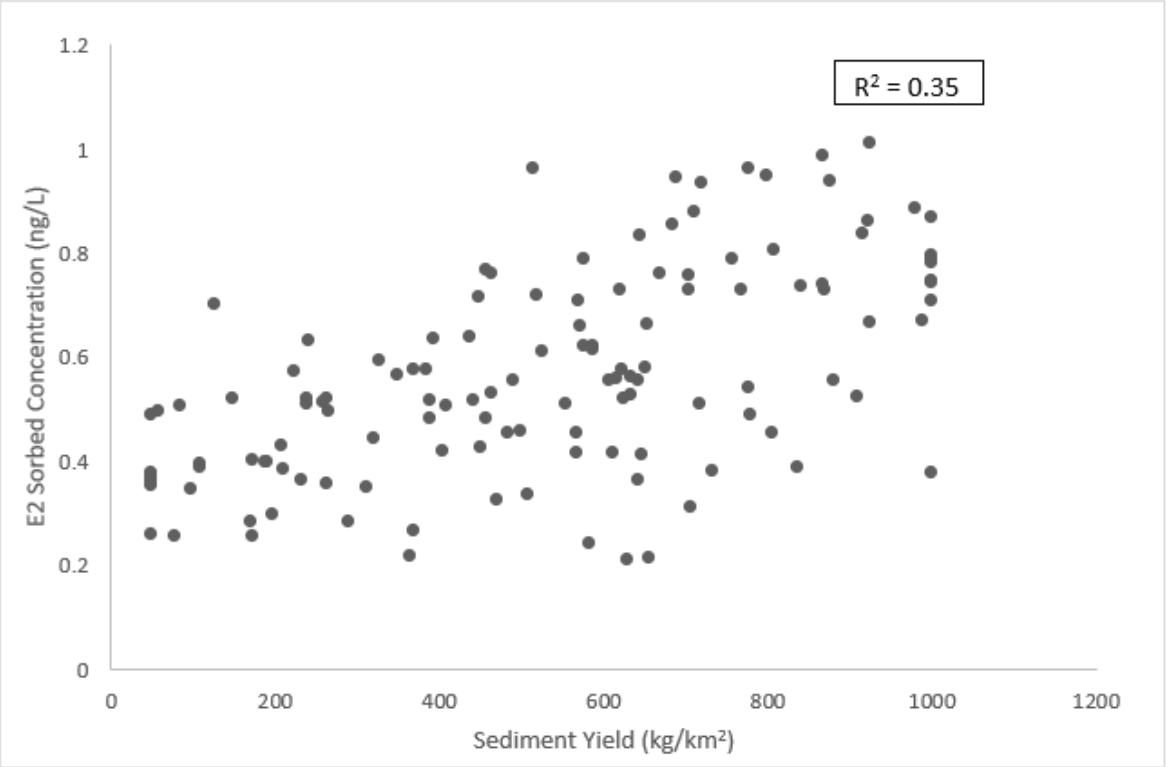

Figure 6-10: Relationship between Annual sediment yield (kg/km2) and E2 sorbed (ng/L)

Figures 6.10 and 6.11 show the relationship between sediment yield (kg/km2) and the sorbed concentrations of E2 and E1 (ng/L) across different hydrological response units (HRUs). These analyses evaluate how sediment transport impacts the binding and distribution of estrogen compounds, particularly in agricultural landscapes where sediment acts as a vehicle for contaminant transport. As sediment yield increases, the E2 sorbed concentration tends to rise. The differences in R^2 values between the two plots highlight the dynamics of sediment-bound estrogen transport. E2, being more persistent, demonstrates a stronger sediment association compared to E1. The dominance of E2 in sediment-sorbed forms aligns with the stronger correlation between sediment yield and E2-sorbed concentrations observed in plots. The weaker correlation for E1 further supports the understanding that E1 is less likely to bind to sediments and instead exists predominantly in the soluble phase or undergoes rapid degradation.

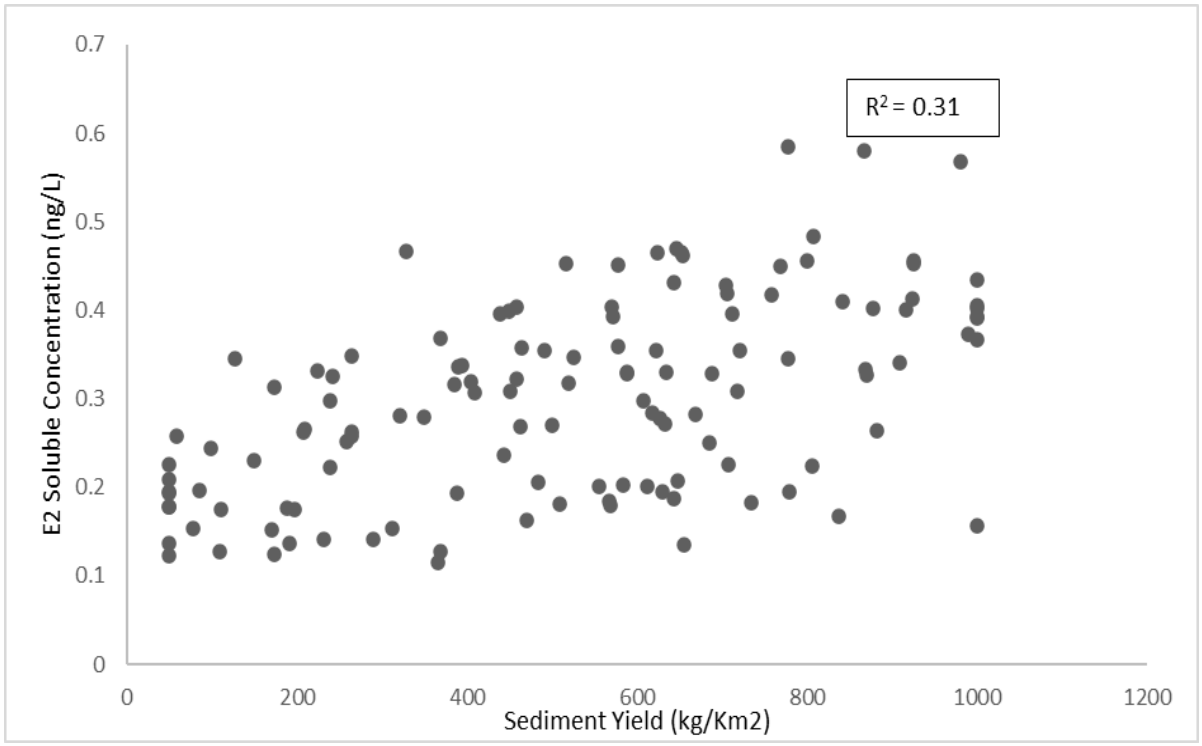

Figure 6-11: Relationship between sediment yield (kg/km2) and soluble concentrations (ng/L) of E2

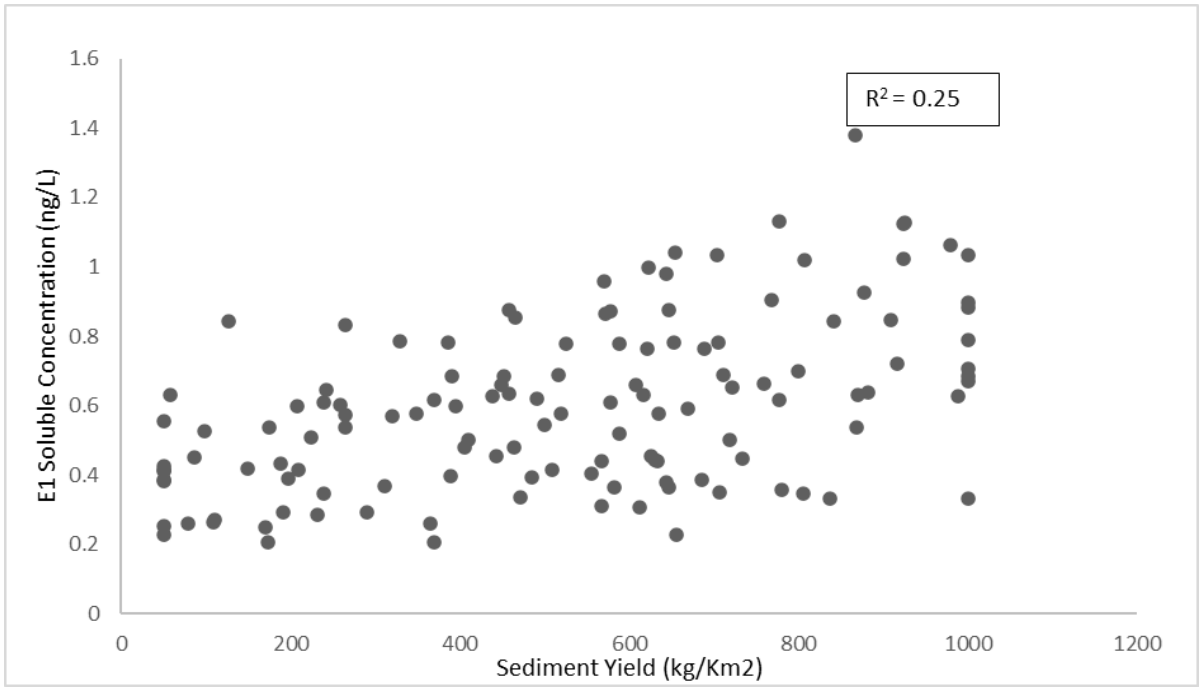

Figure 6-12: Relationship between sediment yield (kg/km2) and soluble concentrations (ng/L) of E1

Figures 6.11 and 6.12 show a weak positive correlation ($R^2 = 0.31$ and $R^2 = 0.25$) between sediment yield (kg/km^2) and the soluble concentration of E2 (ng/L). While there is an upward trend, the spread of data points indicates substantial variability in soluble E2 concentrations for a given sediment yield. This variability can be attributed to hydrological and chemical processes, such as preferential flow paths or the degree of saturation, which influence the transport and partitioning of E2 in the dissolved phase. Additionally, the weak correlation suggests that factors other than sediment yield, such as soil organic matter or E2 degradation rates, may play significant roles in controlling E2 concentrations in the dissolved phase. Both E2 and E1 exhibit sorption to soils and sediments, with their sorption affinities influenced by factors such as organic carbon content and sediment properties. Studies have shown that the sorption coefficients for these estrogens can vary depending on the characteristics of the soil or sediment (Bai et al., 2015).

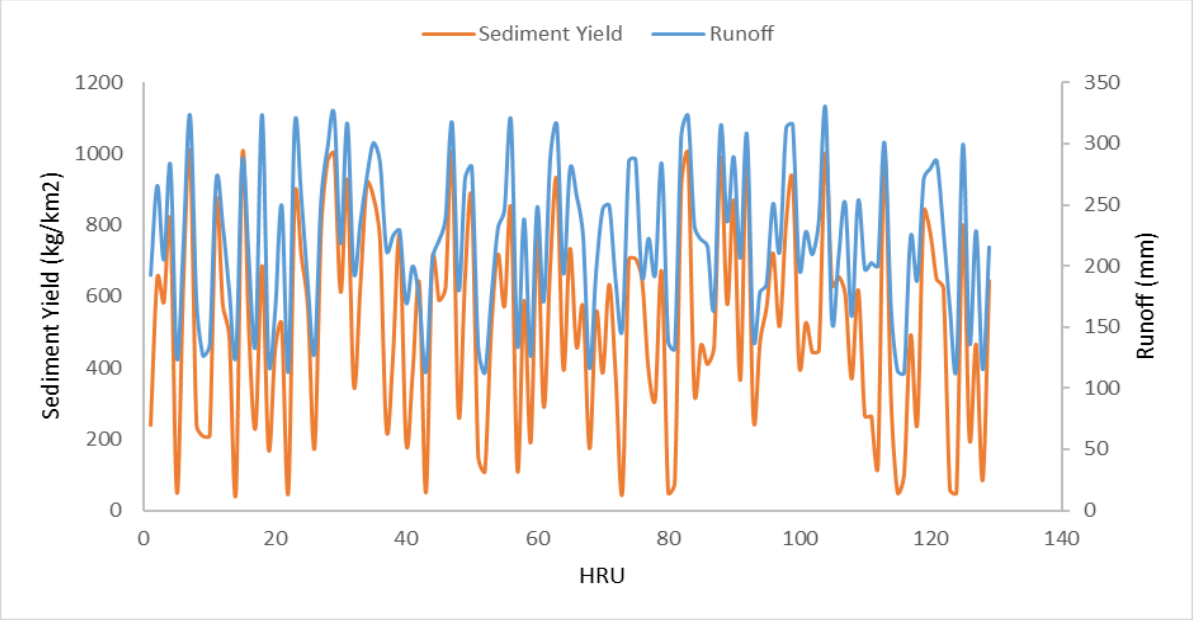

Figure 6-13: The relationship between sediment yield and runoff across various HRUs. The orange line represents sediment yield (kg/km²), while the blue line runoff (mm)

Both sediment yield and runoff exhibit oscillatory behaviour across the HRUs Figure 6.13, indicating variability in hydrological and sediment transport processes. The patterns of sediment yield closely follow those of runoff, suggesting a strong dependence of sediment yield on runoff. Some HRUs may have low erodibility (K) due to cohesive soils (e.g., clayey soils) or high organic matter, which resists detachment despite significant runoff. Conversely, sandy

or loamy soils (high erodibility) may detach easily with lower runoff volumes. In flatter areas, runoff velocity is lower, meaning it lacks the energy to detach and transport sediment. Steep slopes generate higher detachment rates, even with moderate runoff. The highest sediment yield exceeds 1000 kg/km² at multiple HRUs, with specific peaks aligning with high runoff values, such as around HRUs 20, 45, and 90. Runoff reaches its maximum of approximately 350 mm at similar HRUs, confirming a correlation between the two variables. The sediment yield drops below 200 kg/km² at several HRUs, notably around HRUs 10, 60, and 100, which correspond to lower runoff values of approximately 50-100 mm**.** Key HRUs, such as 20, 45, and 90, stand out for their high sediment yield and runoff values. These HRUs likely represent areas with higher erosion potential or steeper slopes. Conversely, HRUs 10, 60, and 100 show low sediment yield and runoff, potentially indicating flat or less erodible regions.

HRUs with peak sediment yield and runoff, such as 20, 45, and 90, could be targeted for sediment management practices, such as vegetation cover enhancement or erosion control measures.

6.7.2 Subbasin Analysis

The subbasin-level analysis provides a broader perspective on hydrological and sediment transport dynamics by aggregating data from individual HRUs. This section evaluates runoff, sediment yield, and associated estrogen transport metrics across the subbasins to understand spatial patterns and identify critical areas for intervention. Figure 7.14 highlights subbasin-level analysis on hydrological and sediment transport dynamics by aggregating data from individual HRUs.

- **High Runoff Subbasins**:

Subbasins 9, 25, and 31 stand out with runoff values exceeding 1400 mm, reflecting areas of concentrated hydrological activity. These subbasins are likely influenced by factors such as high rainfall or impervious surfaces, contributing to enhanced surface runoff. Runoff trends are consistently high in subbasins 13 and 20 to 24, which may also coincide with their proximity to water-contributing topographies.

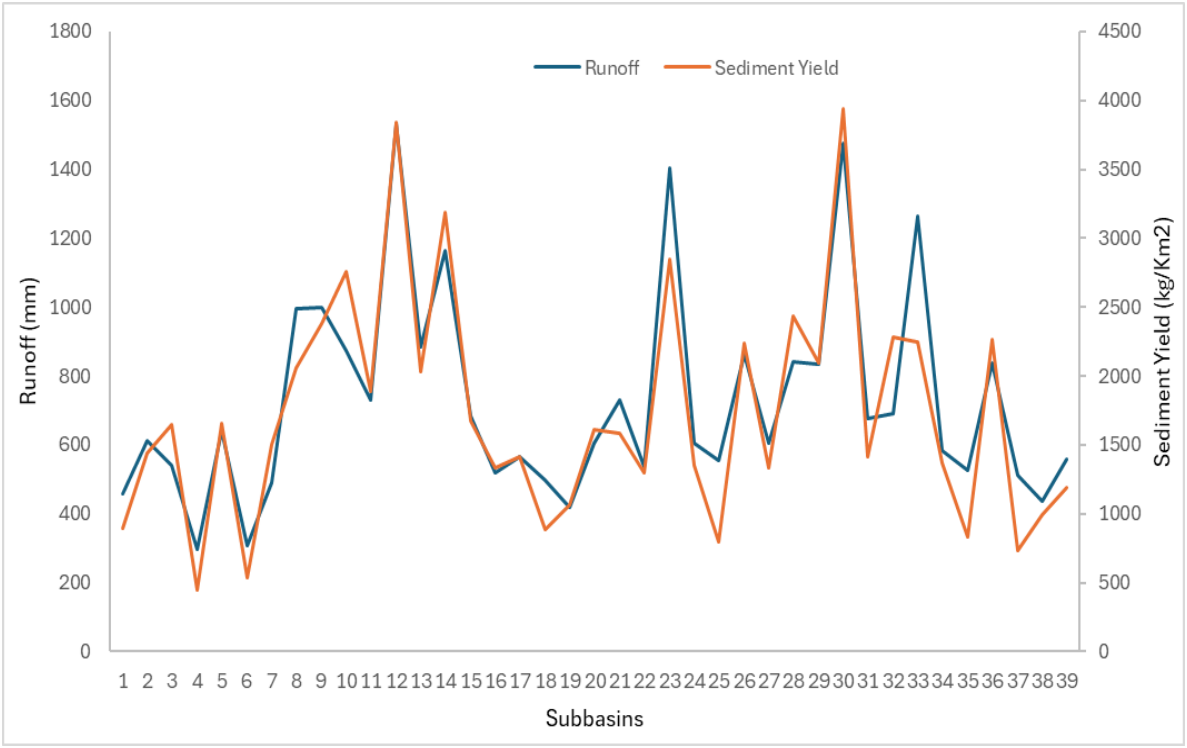

Figure 6-14: Aggregated runoff (mm) and sediment yield (kg/km²) for each subbasin

High Sediment Yield Subbasins:

Subbasins 12, 25, and 31 exhibit sediment yields exceeding 3000 kg/km², strongly correlating with their elevated runoff. This highlights the dual impact of hydrological intensity and soil erosion processes. Subbasins such as 7 and 11 demonstrate moderately high sediment yields, suggesting areas where erosion control practices may require reinforcement. Subbasins such as 17 and 21 consistently exhibit lower runoff (<500 mm) and sediment yields (<1000 kg/km²), indicating more stable or vegetative cover-dominated regions with minimal erosion and controlled hydrological activity. The strong correlation between runoff and sediment yield highlights the interconnectedness of surface flow and erosion. High runoff areas inevitably mobilize more sediment, exacerbating downstream sedimentation and contaminant transport.

Runoff, as a dominant hydrological driver, appears to efficiently transport dissolved E2 through surface flow pathways. The linear relationship reflects a scenario where higher runoff volumes carry proportionally greater E2 concentrations due to increased mobilization from soil or surface residues (Figure 6.15). However, the linearity may also indicate a uniform source of E2 across subbasins (e.g., livestock excretion or agricultural inputs), coupled with consistent

hydrological connectivity. Data points at the upper runoff range (>1200 mm) align well with the trend, suggesting that even under extreme runoff conditions, the relationship holds steady. This consistency predicts the reliability of runoff for estimating E2 concentrations. Subbasins with high runoff (>1000 mm) are evidently hotspots for dissolved E2 transport. Mitigation strategies should focus on reducing runoff through practices such as buffer zones, grassed waterways, and reduced tillage, which can intercept surface flows and minimize estrogen export.

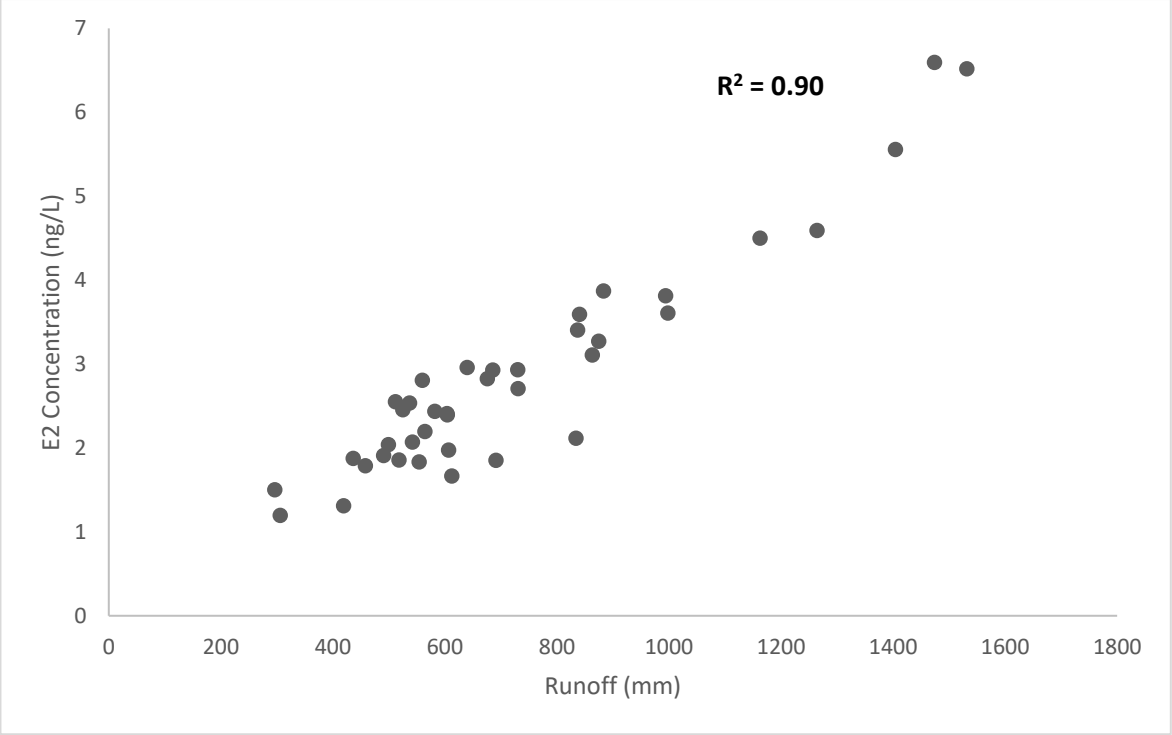

Figure 6-15: Relationship between E2 concentration (ng/L) and runoff (mm) at the subbasin scale

The strong correlation mirrors the behavior observed with E2, highlighting runoff as a primary driver of dissolved E1 mobilization across subbasins. The slightly lower R^2 value compared to E2 (0.90) may suggest the marginally greater influence of additional processes (e.g., sorption or degradation) on E1 transport R^2 0.86 (as shown in Figure 6.16). However, its stronger tendency to sorb to sediments could also moderate its concentration in runoff compared to E2.

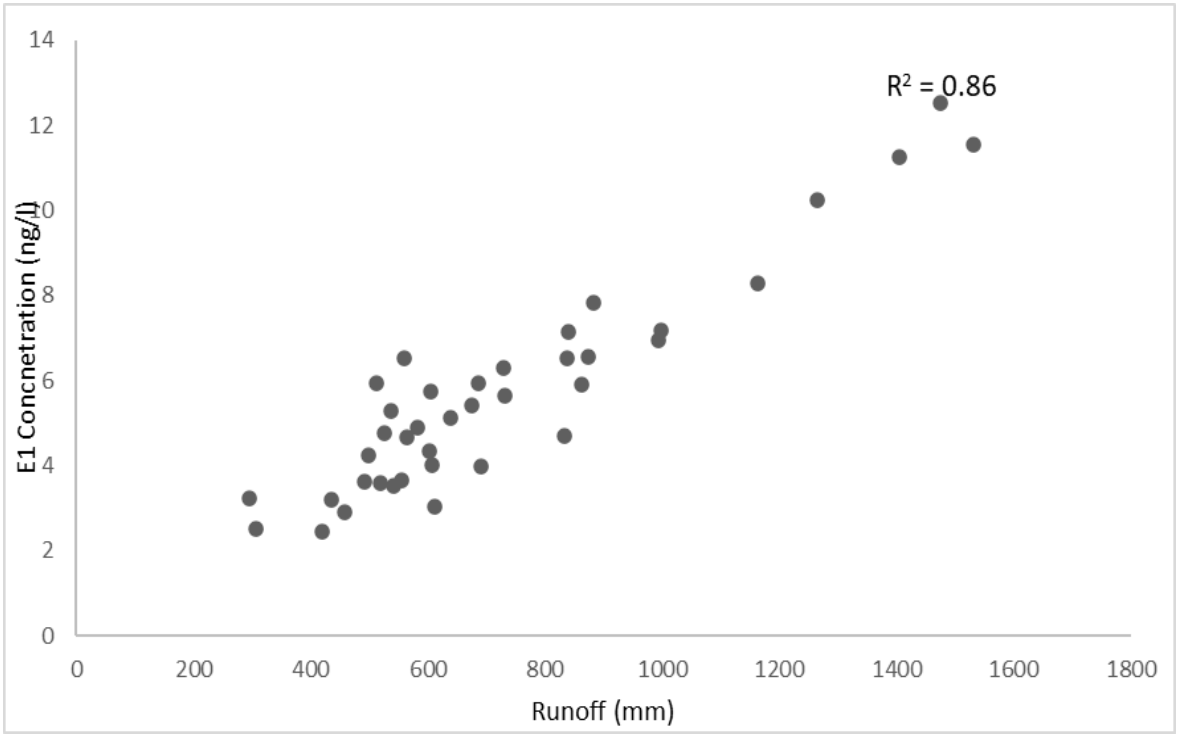

Figure 6-16: Relationship between E1 concentration (ng/L) and runoff (mm) at the subbasin scale

The subbasin-level analysis provided a more aggregated perspective compared to the HRU-level evaluation, revealing stronger correlations between runoff, sediment yield, and estrogen concentrations. While at the HRU level, the relationships between sorbed and soluble estrogens versus surface runoff and sediment yield demonstrated weak correlations, the subbasin-scale results exhibit improved linear trends. These enhanced correlations underscore the impact of spatial aggregation in smoothing out localized variability and capturing broader hydrological patterns.

However, it is critical to acknowledge that the improved correlations may also reflect the inherent limitations of aggregating data. While subbasin-level trends simplify spatial patterns, they may obscure micro-scale processes and localized heterogeneities observed at the HRU level. For example, localized sorption or degradation effects, which may dampen the correlation at the HRU scale, are less discernible when averaged at the subbasin scale. Therefore, both scales of analysis are complementary, with HRU-level capture fine-scale variability and subbasin-level trends offering a broader, cumulative perspective. The stronger correlations at the subbasin scale serve as a foundation for identifying high-priority areas for intervention for best management practices, while HRU-level details ensure the granularity required for targeted management strategies.

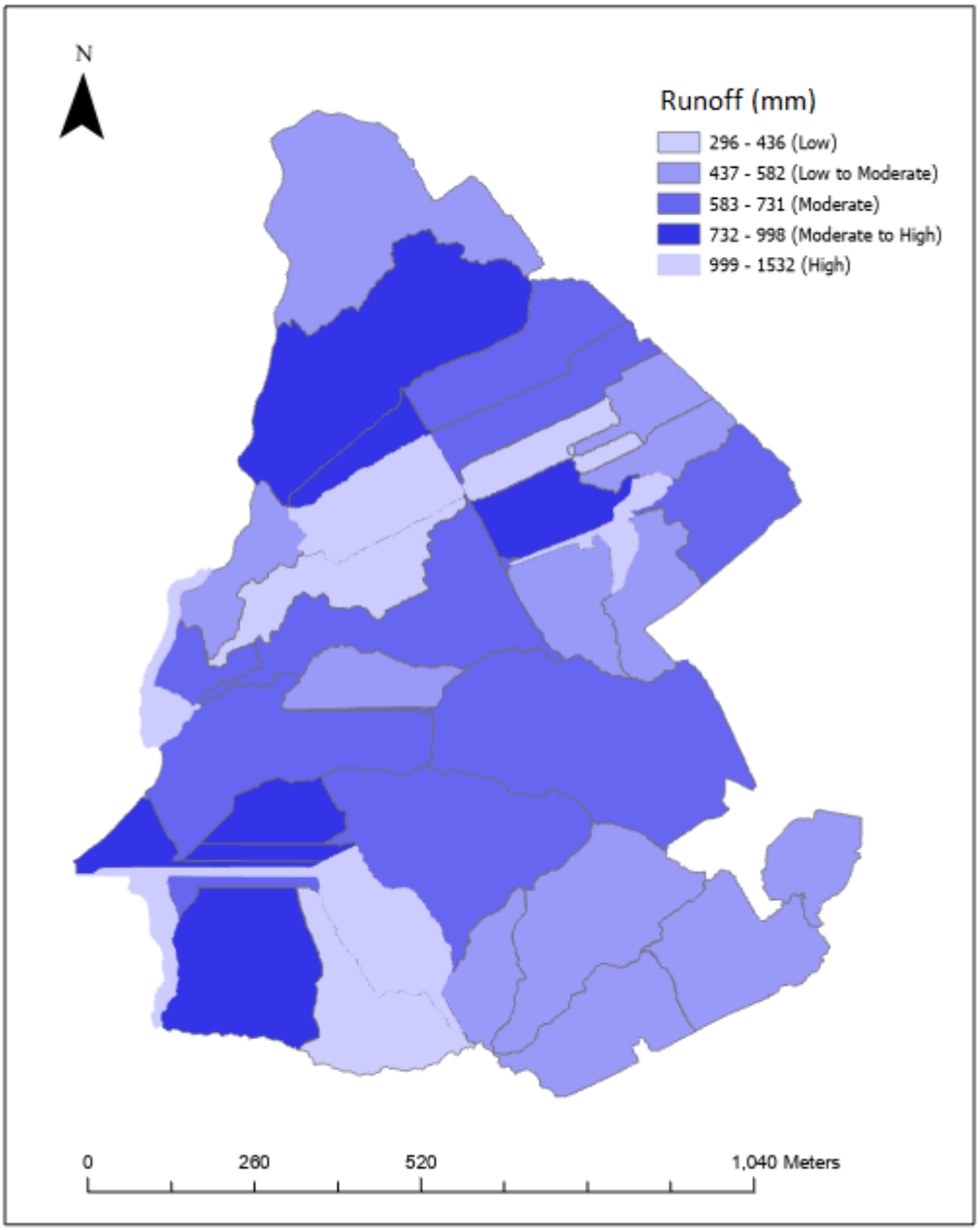

Figure 6-17: Spatial Distribution of Runoff (mm) Across Subbasins, Indicating Areas with High Surface Water Flow

Figure 6.17 illustrates the distribution of runoff across subbasins, identifying hydrologically active zones where surface flow is highest. These areas exhibit strong connectivity with stream networks, making them critical zones for sediment and pollutant transport.

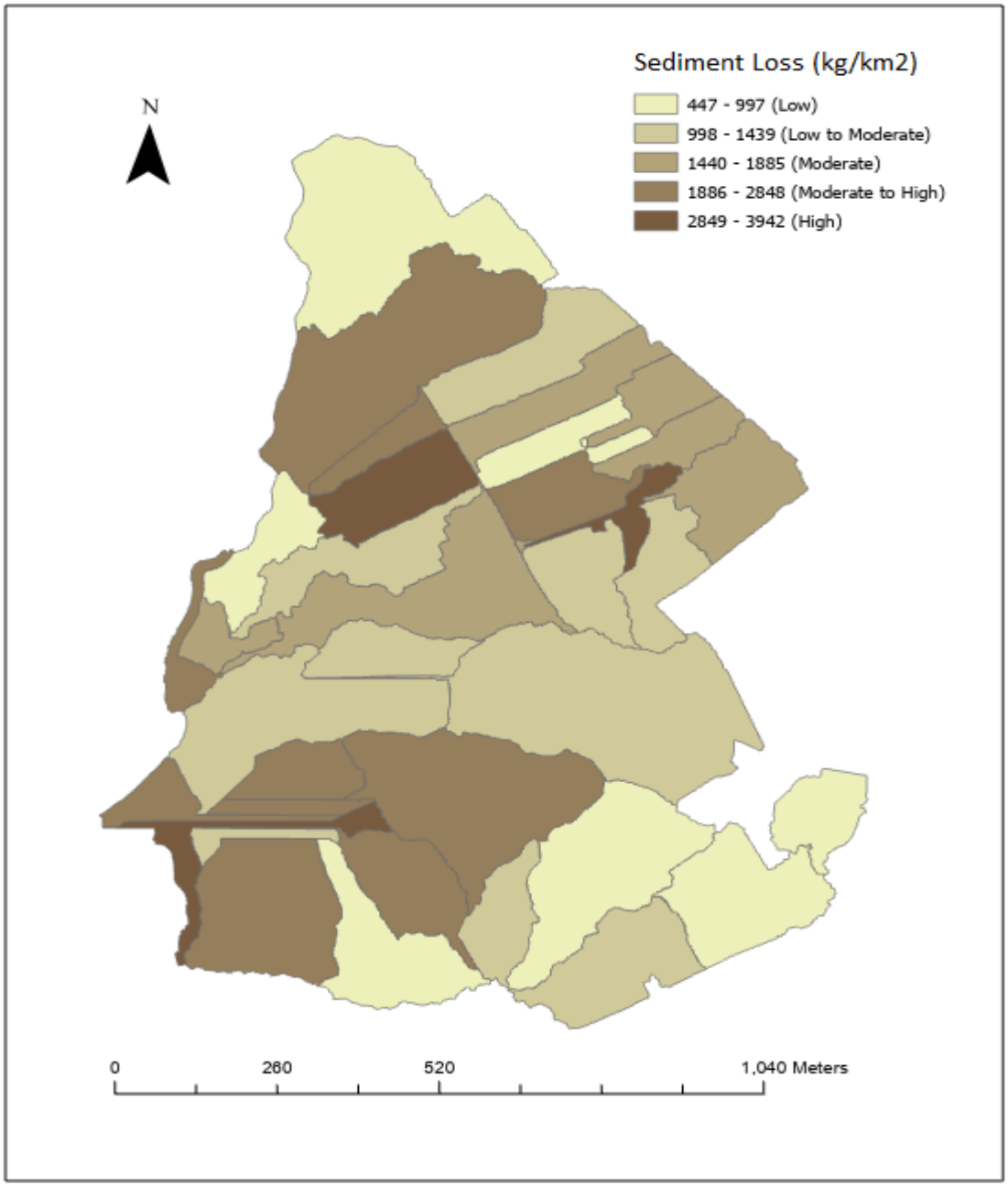

Figure 6-18: Annual Sediment Loss (kg/km²) Across Subbasins, Highlighting Erosion-Prone Areas

Figure 6.18 highlights subbasins with the highest sediment yield. A strong correlation is observed between sediment loss and high-runoff subbasins, reinforcing the role of overland flow in sediment loss processes.

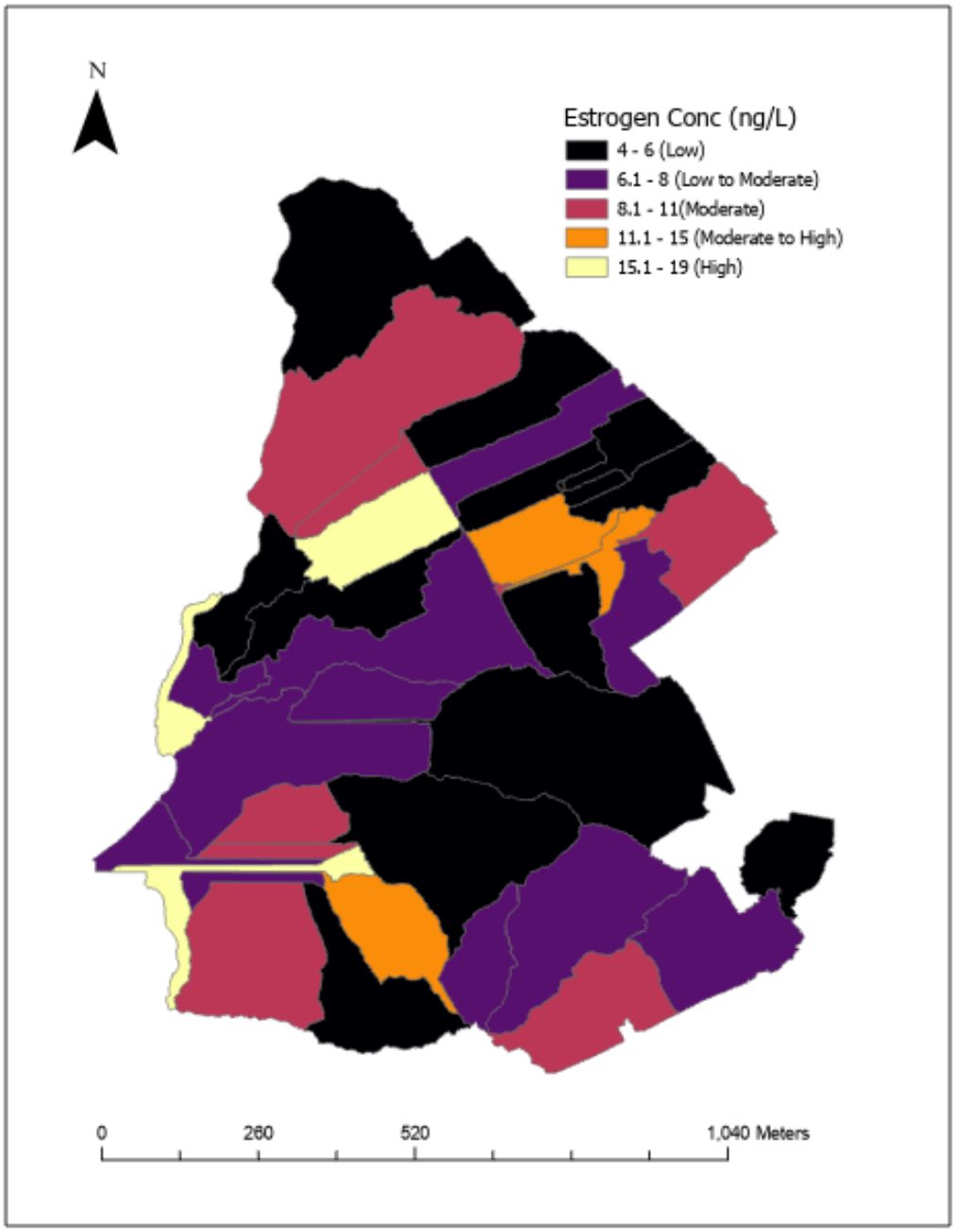

Figure 6-19: Spatial Distribution of annual Estrogen Concentrations (ng/L) Across the Subbasins

Figure 6.19 presents the spatial variation of estrogen concentrations in surface runoff. The highest estrogen levels are observed in subbasins where runoff and sediment loss are most pronounced (Figures 6.17 and 6.18), demonstrating the dual role of overland flow and erosion in estrogen mobilization.

Some areas with high sediment and runoff (dark brown & dark blue) also show high estrogen concentrations (yellow & orange on the estrogen map). However, some high-estrogen areas do

not have extremely high sediment loss, meaning estrogen transport is not only sediment-bound but also moves in dissolved form in runoff. Some low sediment loss areas still show moderate or high estrogen concentrations. This suggests that in some subbasins, dissolved estrogen transport via runoff is dominant, rather than sediment-bound transport. Some high runoff areas do not always correspond to high sediment loss, indicating that certain land covers or soil structures resist erosion despite high runoff.

Overall, there is a strong correlation between high sediment loss, high runoff, and high estrogen concentrations. However, some subbasins with high estrogen levels have lower sediment loss, showing that dissolved estrogen transport plays a role. These differences suggest that management strategies need to target both sediment-bound and dissolved transport of estrogens.

6.8 Validation of Arc SWAT Output from Previous Studies

6.8.1 Estrogen Concentrations in Runoff

Our results show that estrone (E1) and estradiol (E2) concentrations in runoff follow a similar trend to those reported by (Fan et al., 2007a; J. B. Gadd, Tremblay, et al., 2010; Zhao & Lung, 2017). The concentration of estrone (E1) in our study ranged from 0.8 ng/L to 25.0 ng/L, while estradiol (E2) concentrations were lower, peaking at 7.0 ng/L during storm events. In our study, estrogen concentrations in runoff fluctuated significantly, with estrone (E1) consistently being the most dominant estrogen. This aligns with Yang et al., (2012), who reported similar concentration ranges in runoff from biosolid-amended agricultural plots, where multiple estrogens such as E1 and E2 levels ranged from 0.8 ng/L to 2 ng/L and up to 25 ng/L. The E1 concentrations frequently exceeded those of E2, in line with (Sarmah et al., 2006b, 2008b; Tremblay et al., 2018b), who observed estrone as the dominant estrogenic compound in agricultural runoff. Moreover, Tremblay & Northcott, (2003) also observed estrone concentrations in the Waikato River in the range of 0.8 to 2.23 ng/L, reinforcing the relevance of our study area and the magnitude of estrogen concentrations typically found in agricultural runoff. Our results show that 17β-estradiol (E2) concentrations were lower than estrone, with peak concentrations of up to 7.0 ng/L during storm events. We also noted that estrogen concentrations decreased significantly in runoff days after heavy rainfall, which could be attributed to sorption to sediment particles or biodegradation processes, consistent with (Scherr et al., 2009), who reported estrone concentrations decreasing by over 50% within 24 hours in the presence of active soil microbial populations.

The SWAT model simulates estrogen transport through surface runoff, taking into account factors such as manure application, grazing, and effluent irrigation. We observed that effluent application resulted in elevated estrogen concentrations in runoff, similar to findings by (Jenkins et al., 2006; Yang et al., 2012), who highlighted the role of manure-derived estrogen in waterway contamination. The SWAT output further validated these results by showing that high runoff events were associated with increased estrone (E1) concentrations, supporting the concept that storm-induced runoff is a key driver of estrogen mobilization (Fan et al., 2008a; J. B. Gadd, Tremblay, et al., 2010).

The results indicated that stormwater runoff triggered by intense rainfall events following manure application was associated with the highest estrogen concentrations in runoff. These observations suggest that manure management strategies should account for seasonal rainfall patterns to minimize estrogen export (Dutta et al., 2010, 2012).

Yang et al., 2012 also observed E2 was also found at relatively low concentrations (< 2 ng/L) in runoff, and E1 concentrations were higher on day 35, exceeding 10 ng/L. This increase in E1 concentrations is likely attributable to two main factors: the release of estrone from the biosolids applied to the field and, to a lesser extent, the biodegradation of E2 to E1. The concentration profiles of E2 followed a similar trend to E1, suggesting that estrone may have been formed from the degradation of estradiol compounds, supporting the degradation pathways proposed by (Yang et al., 2012). In addition to these findings, the sorption behavior of the estrogens in our study was also consistent with (L. S. Lee et al., 2003; Yang et al., 2012), who reported that estrone (E1) exhibited a higher sorption coefficient (K_d = 33 L/kg) compared to E2 (K_d = 23 L/kg). Similarly, our study found that estrone had a stronger affinity for soil organic carbon than estradiol, making it more likely to be retained in the soil and reducing its mobility in runoff. The K_{oc} values reported by Yang et al, (2012) for E1 (1557 L/kg) were also higher than those for E2 (1082 L/kg), further supporting the idea that estrone is more readily sorbed by soil compared to estradiol.

6.8.2 Impact of Manure Management and Grazing Practices

Manure management influenced the estrogen concentrations in runoff. For raw manure applications, we observed estrone concentrations in runoff as high as 25 ng/L, which is in line with (Dutta et al., 2010), who found E2 estrogen concentrations up to 26.4 to 77 ng/L from fields receiving raw poultry manure. This is significantly higher than when pelletized manure

was applied, where estrone concentrations were reduced to below 5 ng/L, reflecting the impact of manure treatment on estrogen export. Agricultural management practices, particularly those related to manure application and grazing management, played an important role in estrogen export. Manure, particularly when applied during high rainfall periods, was identified as a major contributor to estrogen loading in runoff. This is consistent with findings from (R. M. Monaghan et al., 2017), who observed that grazing in winter significantly increased the export of nutrients and contaminants, including estrogens, from dairy pastures. Moreover, (R. W. McDowell et al., 2003, 2011; R. McDowell & Wilcock, 2008) demonstrated that the presence of livestock exacerbates sediment and phosphorus losses from agricultural fields, further facilitating estrogen transport into surface waters. They demonstrated that nutrient and sediment losses, including estrogen, were significantly higher in grazed pastures (up to 75% increase in sediment loss) compared to ungrazed fields, which further validates our observation that grazing increases estrogen export into surface waters, especially under high rainfall conditions.

6.8.3 Sorption and Degradation of Estrogens in Soil

The correlation between sediment yield and estrone (E1) and estradiol (E2) sorbed concentrations showed a clear trend, with sediment yield increasing as the concentration of estrone sorbed to sediments rose. The SWAT model output highlighted a significant positive correlation ($R^2 = 0.81$) between sediment yield and runoff, confirming that runoff volume is a major factor influencing sediment transport in the study area. This result supports findings by (Yang et al., 2012; Zhao et al., 2019) who observed that surface runoff is strongly linked to sediment mobilization, which, in turn, acts as a vehicle for estrogen transport.

At the HRU level, the SWAT output showed that estrone concentrations were moderately correlated with runoff ($R^2 = 0.43$), and estradiol concentrations had a stronger positive correlation ($R^2 = 0.52$) with runoff. The moderate to strong correlations suggest that runoff is a primary driver for estrogen transport; however, factors like soil organic content, soil texture, and hydrological pathways also influence estrogen concentrations. These findings align with Zhao & Lung, (2017), who observed similar trends in estrogen transport in their agricultural modelling.

6.9 Critical Source Areas (CSAs) and Hotspot Identification

The SWAT model was effective in identifying Critical Source Areas (CSAs) for sediment and estrogen losses on the dairy farm. From Figures 6.17, 6.18 and 6.19, we can find the critical hotspots that needed urgent attention.

The subbasins 8, 13, 26, 28, 29, and 36 exhibit runoff values around 1000 mm, indicating moderate to high surface flow activity. Subbasins 26 and 28 show direct connectivity to stream networks, increasing the risk of pollutant transport into surface water. The subbasins 12, 19, 4, 6, 33, 38, and 30 exhibit the highest recorded runoff values, exceeding 1500 mm, making them the primary contributors to hydrological connectivity. The extreme runoff levels suggest low infiltration capacity, likely due to compacted soils, high rainfall intensity, and surface sealing.

The subbasins 12, 14, and 30 experience the highest sediment loss (>2800 kg/km²), indicating areas with severe soil erosion. These subbasins not only have high sediment yield but also overlap with high runoff zones, increasing the risk of sediment-bound pollutant transport. Runoff in these areas carries not just sediments but also nutrients, organic matter, and potential contaminants. Subbasin 30 is particularly vulnerable as it experiences both high runoff (>1500 mm) and sediment loss, making it one of the most erosion-prone areas in the study site.

The subbasins 12, 14, 19, 26, 28, 30, 33, and 38 exhibit the highest estrogen concentrations in surface runoff (>15 ng/L), indicating major estrogen transport zones. Subbasins 12, 26, and 30 overlap with high sediment loss and high runoff areas, suggesting that both dissolved and sediment-bound estrogen transport mechanisms are at play. Subbasin 30 is the most critical and requires a combination of runoff reduction, sediment control, and estrogen mitigation measures.

Subbasins with both high runoff and high sediment loss are the most critical zones for estrogen transport, as they facilitate both dissolved and sediment-bound estrogen movement. Based on this criterion, the highest-priority areas for management interventions are subbasins 12, 14, 19, 26, 28, 30, 33, and 38.

6.10 Maungatea Stream: Estrogen and Sediment Transport Analysis

The Maungatea Stream, a major water stream located on the western side of the dairy farm, plays a crucial role in draining surface runoff, receiving sediment loads, and transporting dissolved and sediment-bound estrogens from the farm's hydrological network. As Maungatea

Stream flows beyond the dairy farm, any contaminants entering it can spread estrogens further downstream, increasing the environmental footprint of estrogen pollution beyond the farm's boundary.

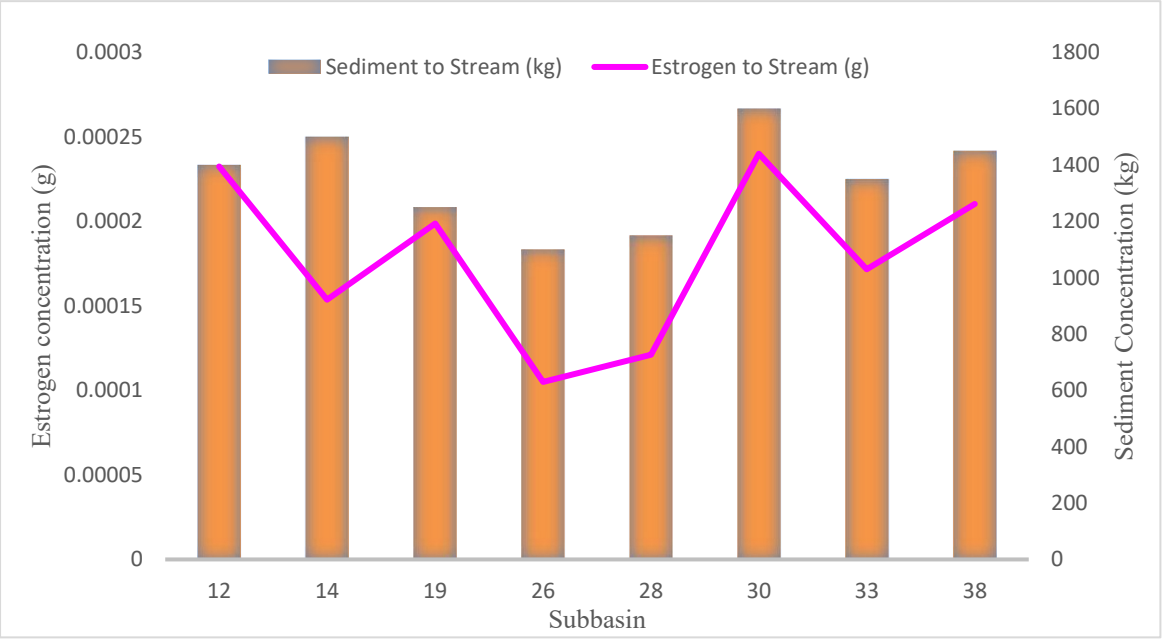

Figure 6-20: Estimated sediment and estrogen contributions to Maungatea Stream from high-risk subbasins. The brown bars represent the sediment transported to the stream (kg), while the pink line shows the total estrogen load reaching the stream (g). Subbasin 30 exhibits the highest contribution of both sediment and estrogen, highlighting its critical role in pollution transport. Subbasins 12, 14, and 38 also show significant contributions, necessitating targeted management strategies to reduce erosion and estrogen mobility

The eight subbasins (12, 14, 19, 26, 28, 30, 33, and 38) were selected based on high runoff (>1000 mm) and high sediment loss (>2800 kg/km²) because:

- Runoff is the primary driver of estrogen movement (both dissolved and sediment-bound).
- High sediment loss increases the risk of sediment-bound estrogen transport.These subbasins have direct or indirect connectivity to Maungatea Stream, making them critical sources of estrogen contamination.

We assumed the selected eight subbasins (12, 14, 19, 26, 28, 30, 33, 38) contribute to estrogen loads in Maungatea Stream, we rely on hydrological connectivity, transport pathways, and flow accumulation patterns, and we also assumed 50% sediment reached to the Maungatea stream from the subbasins. The hydrological and sediment transport analysis confirms that Maungatea Stream receives estrogen and sediment loads from multiple subbasins, primarily those with

high runoff and erosion potential. Figure 6.20 shows that subbasins 30, 12, 14, and 38 require immediate erosion and estrogen control measures.

6.11 Management Strategies to Reduce Estrogen Transport in Surface Water

To effectively reduce estrogen contamination in dairy farm streams, a combination of runoff control, erosion prevention, and pollutant filtration is required. Since estrogen moves both as a dissolved contaminant in runoff and bound to eroded sediments, management practices must address both hydrological and soil erosion processes, such as Wetlands, Riparian zones, Effluent Management, and Grazing management. These Management Practices are thoroughly evaluated in Chapter 7.

6.12 Assumptions and Limitations of the Study

1. **Uniform Hydrological Conditions Within Each HRU**
   Each Hydrological Response Unit (HRU) is assumed to have homogeneous soil, land use, and slope characteristics. Variability within an HRU (e.g., microtopography or minor soil patches) is not explicitly modelled.
2. **Daily Timestep Sufficiency**
   The model runs on a daily timestep, considered sufficient to capture key runoff and erosion events that govern estrogen mobilization and sediment transport.
3. **SCS Curve Number Validity**
   We adopt the SCS Curve Number (CN) method for runoff estimation, including the region-specific modification $I_a=0.05\times S$. This approach is presumed valid for Waikato conditions.
4. **DEM Accuracy**
   The 1 m LiDAR DEM is assumed to accurately represent subbasin boundaries, slopes, and flow paths. Minor artifacts (e.g., unfilled sinks) are deemed negligible after sink-filling and preprocessing.
5. **Representative Soil and LULC Data**
   Soil and LULC reclassification to SWAT-compatible categories is assumed to match real-world conditions. Local anomalies, such as very small soil patches or mixed land use below threshold percentages, are excluded.

6. **Single Erodibility (K_{tr}) and crop cover C_{gr} Value per Soil Type**
   Soil type is assigned one erodibility factor (K or grazing-adjusted K_{tr}) and crop cover Cgr in MUSLE. We assume no significant seasonal or microscale changes in soil structure within a given HRU.
7. **First-Order Decay for Estrogen**
   Estrogen species (E1, E2) are modeled as pesticide analogs with a constant, first-order decay rate, without accounting for temperature or microbe-related variations in degradation.
8. **Dissolved and Sediment-Bound Transport**
   The model partitions estrogens into dissolved and sediment-bound phases based on literature-derived sorption coefficients. It is assumed these coefficients remain accurate across different soil moisture and pH levels.
9. **Uniform Manure and Effluent Application**
   Manure and effluent are applied uniformly according to the farm's management schedule, with no substantial spatial variability in application intensity within each HRU.
10. **No Major Subsurface Drainage**
    We do not explicitly simulate tile drainage or other deep subsurface flow pathways, assuming overland flow is the principal route for sediment and estrogen movement.
11. **Static Grazing and Management Routines**
    Grazing rotations, stocking densities, and effluent application rates remain as recorded. Any temporal changes outside the modelling period are not simulated.
12. **No Field Validation**
    Due to time constraints, we did not validate the model's output (e.g., simulated flow, sediment, or estrogen concentrations) against field observations at the study site. While the model uses established methodologies, future work would benefit from comparing predictions with local measurements.

6.13 Conclusion

This concluding section synthesises the modelling results of Chapter 6 to provide context for the BMP scenario analysis presented in Chapter 7.

Our findings suggest that best management practices (BMPs), such as riparian buffer zones, Wetlands, controlled grazing, and optimized effluent management, are essential for reducing estrogen transport. The SWAT model confirmed the role of effluent management and grazing

in controlling the release of estrogens into surface water. Furthermore, the subbasin-level analysis confirmed the importance of spatial aggregation in capturing broader hydrological patterns and making management decisions, similar to the approach outlined by (Zhao & Lung, 2017). By incorporating estrogen fluxes into manure management, grazing, and irrigation schedules, we can identify the most effective interventions to reduce estrogen contamination. Houlbrooke et al. (2009 and Houlbrooke & Longhurst, et al. (2011) who highlighted the role of effluent irrigation in controlling nutrient and pollutant transport in dairy farming systems.

Chapter 7
Evaluating Best Management Practices for Reducing Estrogen in Surface Runoff

7.1 Introduction

In the previous Chapters 5 and 6, the modelling framework for estrogen transport in surface runoff was developed using ArcSWAT. Key processes influencing estrogen movement, such as hydrology, erosion, sorption, and degradation, were parameterized based on field data and literature. Chapter 6 provided a detailed assessment of baseline conditions, identifying hotspots of estrogen contamination, sediment yield, and high runoff areas in the dairy watershed. These findings formed the foundation for the Best Management Practices (BMPs) simulations conducted in Chapter 7.

This chapter focuses on the implementation and assessment of BMPs to mitigate the transport of estrogen, sediment, and runoff in agricultural landscapes, particularly dairy farms. The ArcSWAT model was used to simulate the impact of different BMPs, including wetlands, grazing management, effluent management, and riparian buffer zones, on hydrological and contaminant transport processes. The objective is to evaluate the effectiveness of these strategies in improving water quality and reducing estrogen pollution in surface runoff.

Building upon the previous analysis, this chapter aims to:

1. Evaluate the effectiveness of BMPs in reducing runoff, sediment transport, and estrogen loads across the dairy farm.
2. Use spatial analysis and graphical representation to illustrate the impact of BMPs across various subbasins.
3. Provide insights into policy and management strategies that could enhance water quality while maintaining sustainable dairy farming practices.

7.2 Wetlands as a Best Management Practice

Constructed wetlands are a key management practice for mitigating sediment, nutrient, and estrogen transport from dairy farm operations (Tousignant et al., 1999). Effective integration of constructed wetlands into the ArcSWAT model demands specific considerations based on recommendations provided in Tanner et al. (2005, 2022). The essential parameters for

constructing effective wetlands in a dairy farm context are described below from the New Zealand guide for Wetlands by Tanner et al. (2022).

7.2.1 Wetland Size and Catchment Area

A practical wetland size typically ranges from 1% to 5% of the contributing drainage catchment area (Tanner et al., 2022). Given that the subbasins on the studied dairy farm range between 3 to 6 hectares, suitable wetland sizes would be approximately 300 to 3000 m² (0.03-0.3 ha). Optimal wetland locations include low-lying areas near drainage outlets or critical subbasins identified with high runoff, sediment yield, and estrogen concentrations.

7.2.2 Hydrological Design and Flow Management

Constructed wetlands should ensure a minimum water retention period of 10 to 15 days to maximize contaminant removal efficiencies (Tanner et al., 2022). Properly designed inflow structures, such as sediment forebays or inlet pools, are used to avoid clogging and ensure effective sediment deposition. Additionally, wetlands should be equipped with a high-flow bypass system to handle excess stormwater and adjustable outlet structures like weirs or standpipes to manage water levels effectively.

7.2.3 Wetland Zonation and Depth Profile

A three-zone wetland system is recommended by Tanner et al. (2022) to enhance the treatment efficiency of sediment, nutrient, and contaminant removal. This system includes:

- Sedimentation Pond (Deep Pool): Depth greater than 1.5 meters, covering approximately 20% of the total wetland area, dedicated to capturing coarse sediment.
- Deep Water Zone (Open Water): Around 0.5 meters deep, representing about 30% of the total area, facilitating fine sediment settlement and microbial nutrient transformation.
- Shallow Vegetated Zone: Approximately 0.3 meters deep, occupying 50-70% of the total area, where significant plant uptake and microbial processes occur.

7.2.4 Vegetation Selection

The shallow vegetated zone should predominantly comprise emergent macrophytes known for effective nutrient and estrogen uptake, such as Carex secta (Sedge), Schoenoplectus tabernaemontani (Lake Clubrush), and Typha orientalis (Raupo).

Additionally, planting riparian buffer vegetation like Harakeke (Flax), Toetoe, Ti kouka (Cabbage Tree), and Manuka around the wetland edges enhances bank stability and provides shading (S. Bircher et al., 2015; Card et al., 2012; Tanner et al., 2022).

Constructed wetlands designed according to these guidelines can achieve sediment removal efficiencies ranging from 50% to 90%, nitrogen removal of 20% to 50%, phosphorus removal efficiencies of 25% to 50%, and other contaminants removal efficiencies of approximately 30% to 70%, depending on the retention time and vegetation established and highly effective in reducing E. coli, with some achieving over 99.99% reductions (Tanner et al., 2005, 2022).

7.3 Wetland Performance in Dairy Farm Management

Constructed wetlands have demonstrated high efficiency in mitigating contaminants, particularly estrogenic hormones (E1 and E2), sediment, and runoff in agricultural settings. This section examines the effectiveness of wetlands in reducing estrogen loads, trapping sediment, and regulating runoff volumes within dairy farm landscapes. Table 7.1 summarises some wetland performances across New Zealand.

Table 7-1: Summary of Wetland Performance Across Dairy Farms in New Zealand (Tanner et al., 2022)

Case Study	Location	Wetland Size (% of Catchment)	Nitrogen Reduction (%)	Phosphorus Reduction (%)	Sediment Reduction (%)	Fecal Bacteria Reduction (%)
Titoki	Northland	1.60%	18-38%	Variable (small-moderate increase)	Not monitored	Small increases, but >99.99% during accidental effluent inflow
Whangamaire	Waikato	0.60%	Minimal (initial stage)	>50%	Not monitored	Not reported
Toenepi	Waikato	1.10%	30%	Small-moderate increase	Not measured	Small-moderate increase
Owl Farm	Waikato	4.50%	50%	15%	45%	Increase due to resident wildlife
Baldwins	Waikato	1.20%	60%	20%	70%	80%
Okaro	Bay of Plenty	0.70%	12-41% (77-80% nitrate-N)	12-60%	71-88%	89-96%
Awatuna	Taranaki	2.20%	Monitoring in progress	Monitoring in progress	Monitoring in progress	Monitoring in progress
Ashley Clinton	Hawke's Bay	0.90%	Monitoring in progress	Monitoring in progress	Monitoring in progress	Monitoring in progress
Kaiwaiwai	Wairarapa	0.5ha wetland	38% (Total-N), 56% (Nitrate)	21% (Export), 24% (Dissolved P Export)	6%	Not analyzed
Fish Creek	Golden Bay	1.00%	Minimal (initial stage)	>50% (early stage)	Not monitored	Not reported
Warnock's Farm	Southland	1.90%	51% (Total-N), 32% (Nitrate-N)	92% (DRP), 71% (Total P)	90% (Duckpond), not detectable post-wetland	95%

7.3.1 Removal of Estrogenic Hormones (E1 and E2) in Wetland Treatment Systems

Constructed wetlands have been shown to attenuate steroid hormones, often achieving high removal efficiencies. A recent review of livestock wastewater treatments found that wetlands can remove up to about 90% of influent estrogen compounds, effectively reducing estrogenic activity in the effluent (Gomes et al., 2022). Similarly, a comprehensive analysis of various

wetland systems reported average removal rates for steroidal hormones ranging from roughly 55% to 95% (Hakk et al., 2018)**.** These high percentages indicate that with appropriate design and conditions, wetlands typically eliminate well over half and, in many cases, the majority of E1 and E2 from agricultural runoff. In practice, hormone removal in wetlands is facilitated by a combination of biological and physical mechanisms, which together yield substantial reductions in estrogen loads.

Studies highlight several mechanisms and design features that enable effective estrogen removal in wetlands. Microbial biodegradation (particularly under aerobic conditions) is often the dominant pathway for breaking down E1/E2; accordingly, wetland configurations that promote oxygenation tend to perform best (Hakk et al., 2018). Vertical flow or hybrid wetlands, which periodically expose water to air, generally outperform surface-flow wetlands for estrogen removal (Hakk et al., 2018).

Studies indicate that up to 42% of estrone (E1) mass is absorbed by wetland vegetation such as duckweed, while 17% is retained in the sediment layer. This uptake and adsorption, combined with metabolic transformation of E1 to less harmful metabolites (e.g. estriol), only a small fraction of estrogenic compounds (~5%) remaining in the effluent, reinforcing wetlands as an effective tool for reducing endocrine-disrupting contaminants in dairy farm runoff (Hakk et al., 2018).

7.3.2 Sediment Trapping Efficiency of Farm Wetlands

Wetlands are highly effective at capturing sediment from agricultural runoff. As runoff water spreads out and slows through wetland vegetation, suspended particles settle out, often yielding substantial reductions in sediment load. Field studies on dairy farm wetlands have documented total suspended solids (TSS) removal efficiencies on the order of ~65-80% (Sukias & Tanner, 2023). For example, a constructed wetland receiving dairy runoff in New Zealand removed about 80% of incoming sediment during a wet year and around 65% in a drier year with lower flow volumes (Sukias & Tanner, 2023). Several design and operational factors affect sediment trapping in wetlands. A key consideration is providing zones for settling, such as sediment forebays at inlet points, which can capture coarse particles and prevent excessive sediment accumulation or resuspension in the main wetland (Mean & Efficiencies, 2006). Dense vegetation cover (emergent plants) throughout the wetland further enhances sedimentation by reducing flow velocity and stabilizing deposited sediments. Sufficient hydraulic residence time is important: wetlands that detain runoff longer allow more particles to settle out before water exits. Conversely, very high flow events can temporarily decrease efficiency if short-circuiting

or resuspension occurs, though wetlands often still retain a large sediment fraction even during storms (Mathew, 2021). Guidelines from DairyNZ/NIWA suggest that a wetland sized around 1% of the catchment might remove ~50% of incoming sediment, while a larger wetland (~5% of catchment) could achieve up to 90% sediment reduction in the long term (Tanner et al., 2022).

7.3.3 Wetland Runoff Volume Reduction in Agricultural Settings

Constructed wetlands in agricultural landscapes (such as on dairy farms) typically provide only a modest reduction of runoff volume. Unlike infiltration-focused practices, surface-flow wetlands primarily attenuate flows rather than permanently removing water. Design manuals often assume essentially zero net annual volume retention in constructed wetlands (Mean & Efficiencies, 2006; Tanner et al., 2022; Tousignant et al., 1999). Overall, reported runoff volume reductions range from negligible in most cases up to perhaps ~10 - 30% under favourable conditions, with higher losses only possible if significant infiltration or evaporation occurs over extended periods (Mathew, 2021). Several factors influence the degree of volume reduction achieved by farm wetlands. Soil permeability beneath the wetland is critical. The wetlands situated on coarse-textured, sandy soils can infiltrate more water, whereas those on clay or compacted soils have virtually no infiltration (Hirschman et al., 2008). Residence time matters as well; a longer hydroperiod allows more time for infiltration and evaporation of stored water. In practice, however, constructed wetlands are sized to detain runoff and reduce peak flows rather than eliminate volume, so they can delay and slowly release drainage water (Hirschman et al., 2008).

7.3.4 Wetland Implementation for Dairy Farm Subbasins in ArcSWAT

For a dairy farm of ~110 hectares, implementing a wetland is a well-established best management practice to improve water quality. Common guidelines recommend sizing the wetland as a few percent of the catchment area (often 1–5% of the farm's area draining into it) to achieve meaningful contaminant reductions (Tanner et al., 2005). In our dairy farm, this means on a 110-ha farm, a wetland on the order of 1-5 hectares (or multiple smaller wetlands totalling that area) would be installed at strategic locations (e.g. intercepting farm drains or runoff from critical source areas). Estrogen reductions, while not usually measured on farms, are estimated with sediment outcomes because estrogens bind to sediments and also degrade over time. The wetland is structured to optimize retention time (10-15 days), enhance sediment trapping (50-90%), and promote nutrient and estrogen removal (30-70%) through both physical

and biological processes (Tanner et al., 2005). Figure 7.1 illustrates the component and layout of a wetland recommended for New Zealand dairy pastures.

Wetlands were simulated in ArcSWAT by modifying the .pnd (pond/wetland) files to adjust storage capacity, surface area, and retention time based on wetland size and location in each subbasin. Key model parameters were adjusted, including wetland fraction (WET_FR), nutrient settling rates (NSETLW, PSETLW), sediment trapping efficiency (SEDTRAP), and flow routing modifications to ensure runoff passes through the wetland before entering streams. These parameter values were determined based on hydrological, chemical, and biological processes documented in wetland treatment studies (Mean & Efficiencies, 2006; J. P. Sukias & Tanner, 2023b; Tanner et al., 2005, 2022; Tousignant et al., 1999). The wetland parameters are provided in Appendix A.

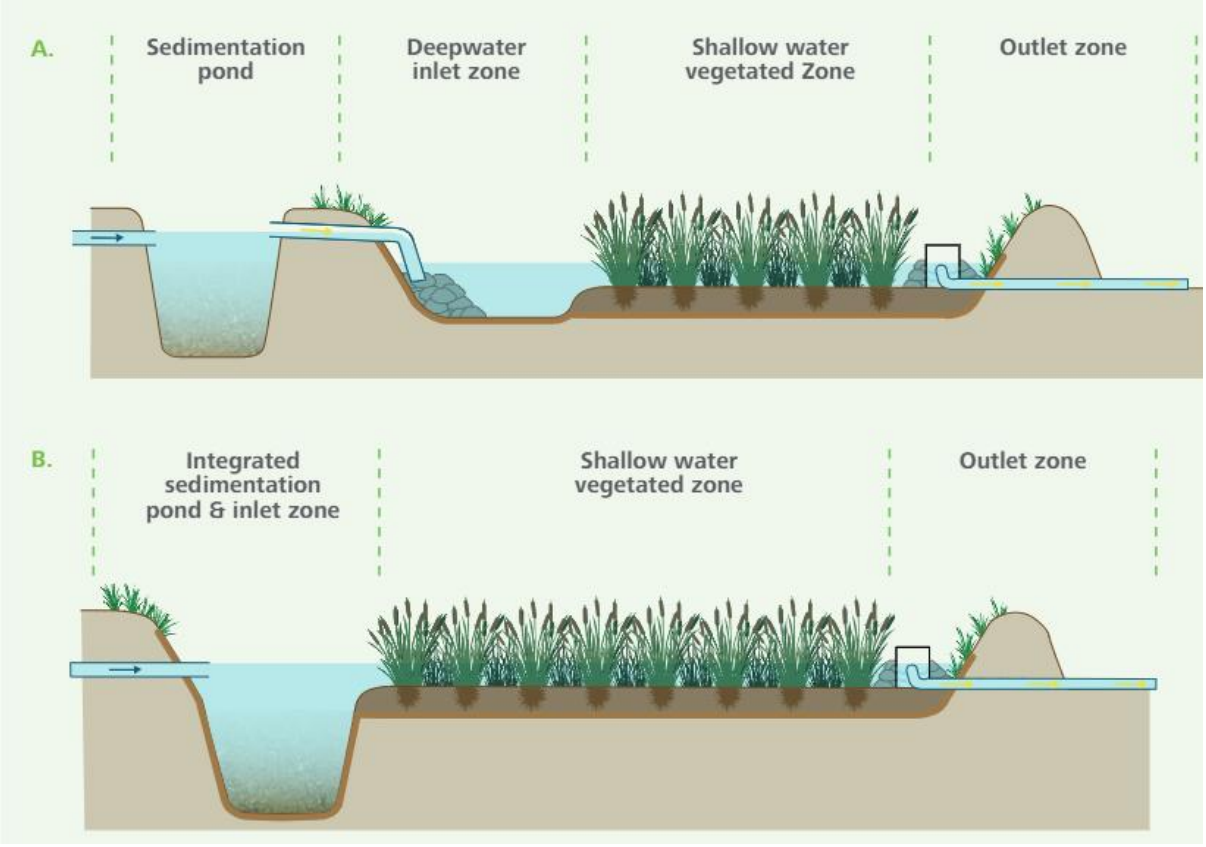

Figure 7-1: Surface flow constructed wetland treatment designs illustrating distinct zones. Option (A) presents separate sedimentation, deepwater inlet, shallow vegetated, and outlet zones. Option (B) integrates sedimentation and inlet zones with a shallow vegetated zone for simplified construction and effective contaminant removal (adapted from (Tanner et al., 2022)

7.4 Wetland Placement and Performance in Dairy Farm Management

7.4.1 Wetland Placement and Contributing Subbasins

The placement of wetlands within the dairy farm was determined based on flow accumulation, runoff volume, sediment yield, and estrogen concentrations. The objective was to position wetlands at strategic locations where they could intercept and treat surface runoff before entering the main water channels. Using the hydrological analysis and watershed delineation in ArcSWAT, four potential wetland locations were identified, as shown in Figure 7.3. These wetlands are expected to improve water quality by reducing sediment transport, nutrient loading, and estrogen concentrations from contributing subbasins.

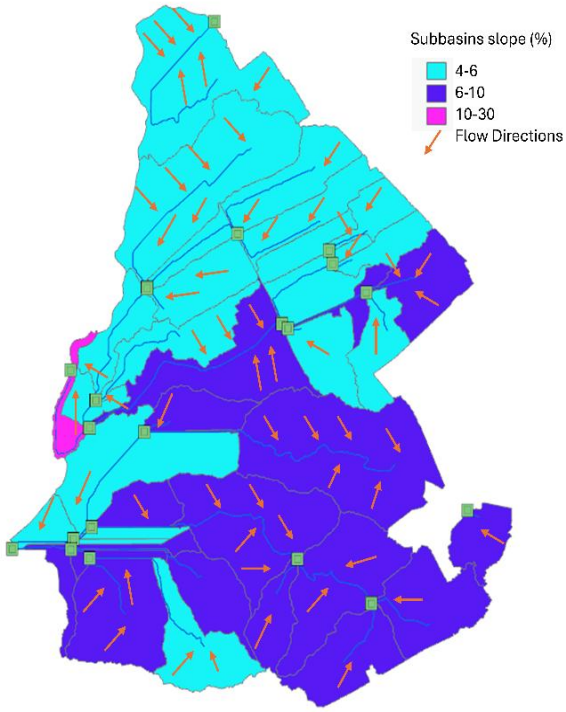

Figure 7-2: The slope classification of subbasins within the study area, categorized into three slope ranges: 4-6%, 6-10%, and 10-30%. Arrows indicate the predominant flow directions, aiding in identifying potential critical source areas for estrogen transport.

Each wetland was assigned specific contributing subbasins based on flow accumulation patterns and hydrological connectivity. Wetland 1 is positioned in the northernmost part of the farm and receives runoff primarily from Subbasin 1. This subbasin contributes directly to the wetland and is characterized by moderate flow accumulation. Wetland 2 is located in the central part of the watershed and is influenced by runoff from Subbasins 3, 7, 11, 14, and 6. Wetland

3 is situated downstream of multiple high-runoff subbasins, receiving contributions from Subbasins 8, 2, 5, 9, 10, 12, 19, 21, 13, 17, 18, 20, 23, 15, 16, and 4. Wetland 4 is located in the southern section of the dairy farm and receives runoff from Subbasins 25, 37, 35, 32, 38, 33, 36, 30, 31, 28, 29, 24, 39, 27, 22, 26, and 34.

These locations were selected to maximize contaminant reduction potential by intercepting high runoff and sediment-contributing areas while ensuring hydrological connectivity within the watershed. The flow direction map presented in Figure 7.2 shows the movement of surface water through the subbasins, with arrows indicating predominant flow paths.

7.4.2 Wetland Management Practices and Contaminant Reductions

To evaluate the effectiveness of wetland management practices on reducing runoff, sediment yield, and estrogen concentrations (E1 and E2), results were obtained using the ArcSWAT model. Four different wetlands were modeled based on their respective subbasins, sizes, and hydrological characteristics relevant to dairy farming practices, typically suited to a farm area of approximately 110 ha.

Wetland 1, covering Subbasin 1, exhibited a moderate reduction in runoff volumes, achieving approximately 10% runoff reduction. Sediment yield in this wetland was effectively reduced by around 60%, reflecting its good sediment retention capabilities. Estrogen (E1 and E2) concentrations averaged a 35% reduction, indicating effective biochemical and sedimentation processes within this wetland system.

Wetland 2, spanning Subbasins 3, 6, 7, 11, and 14, achieved runoff volume reductions averaging 15%, reflecting its enhanced detention capacity. Sediment yield was notably reduced by approximately 70%, and estrogen concentrations showed an average 50% reduction. These results align well with literature expectations for mid-sized constructed wetlands commonly implemented on dairy farms.

Wetland 3, the largest management practice covering Subbasins 2, 4, 5, 8–10, 12, 13, 15–21, and 23, showed substantial runoff attenuation, reducing runoff volume by approximately 30%. Sediment trapping efficiency was particularly high, averaging around 90% reduction. Estrogen removal was also highly effective, with a 70% average reduction observed across the modeled subbasins. Wetland 4, comprising Subbasins 22, 24–39, presented minimal runoff volume

reduction (about 7%), reflecting its limited infiltration or evaporation capability. However, the sediment trapping efficiency remained high, averaging approximately 75%, and estrogen

concentration decreased by approximately 60%. These results underscore that even wetlands with limited hydrological modification capacity can effectively reduce contaminants through sedimentation and biochemical interactions.

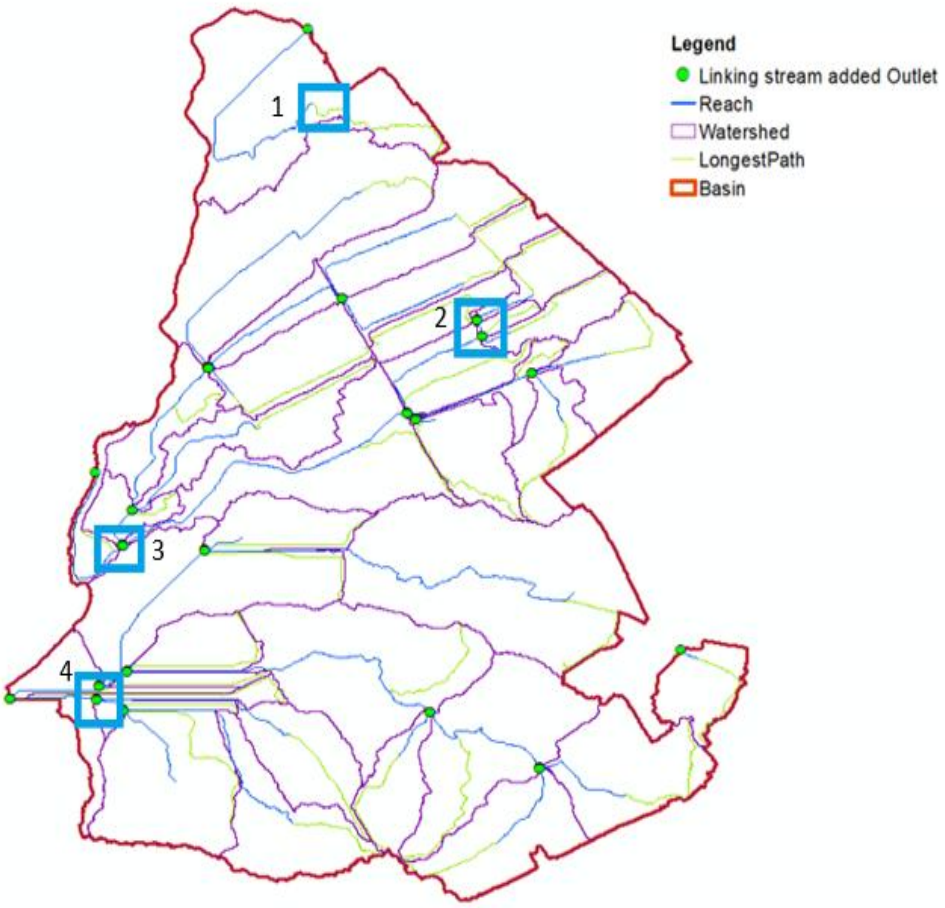

Figure 7-3: The wetland locations on the dairy watershed map

7.5 Effectiveness of Wetland Implementation

The maps in Figure 7.3 and Figure 7.4 presented below compare the current conditions of runoff, sediment yield, and estrogen concentrations with the expected outcomes after wetland implementation. These spatial representations help identify critical source areas for contaminant loading and support strategic wetland placement for maximum efficiency

7.5.1 Current Conditions vs. Wetland Implementation Outcomes

Figure 7.4 provides a combined spatial visualization of key hydrological and water quality parameters under existing dairy farm management practices. The sediment loss map highlights erosion-prone subbasins where particulate-bound estrogen transport is most significant, with values ranging from 447 to 3,942 kg/km². The runoff map displays areas with high hydrological loading, contributing to increased mobilization of contaminants, with runoff values varying between 296 and 1,532 mm. The estrogen concentration map identifies critical regions where E1 and E2 levels range from 4 to 19 ng/L, indicating substantial estrogen transport risk.

These maps reveal that the highest estrogen concentrations correlate with runoff exceeding 1,000 mm and sediment losses surpassing 2,800 kg/km², emphasizing the interconnectedness of hydrological and contaminant transport processes. The spatial distribution suggests that subbasins with elevated runoff and sediment loss should be prioritized for wetland intervention to improve water quality outcomes.

Figure 7.5 illustrates the projected reductions in these parameters following the implementation of wetlands. By comparing these datasets, the effectiveness of wetlands in reducing hydrological and contaminant transport processes can be evaluated. Following the application of wetlands, significant reductions in sediment loss, runoff volumes, and estrogen concentrations are observed. The wetland-integrated model results indicate that these constructed treatment systems effectively reduce hydrological loading and contaminant transport. Following wetland application, significant improvements were observed, which are also mentioned in the previous section.

- A 50-90% reduction in sediment loss, lowering values from up to 3,942 kg/km² to below 1,500 kg/km² in the most affected areas.
- A 30-70% decrease in estrogen concentrations, reducing values from a peak of 19 ng/L to below 8 ng/L in critical subbasins.
- A 10-30% reduction in runoff volumes, bringing peak values down from 1,532 mm to under 1,000 mm in targeted regions.

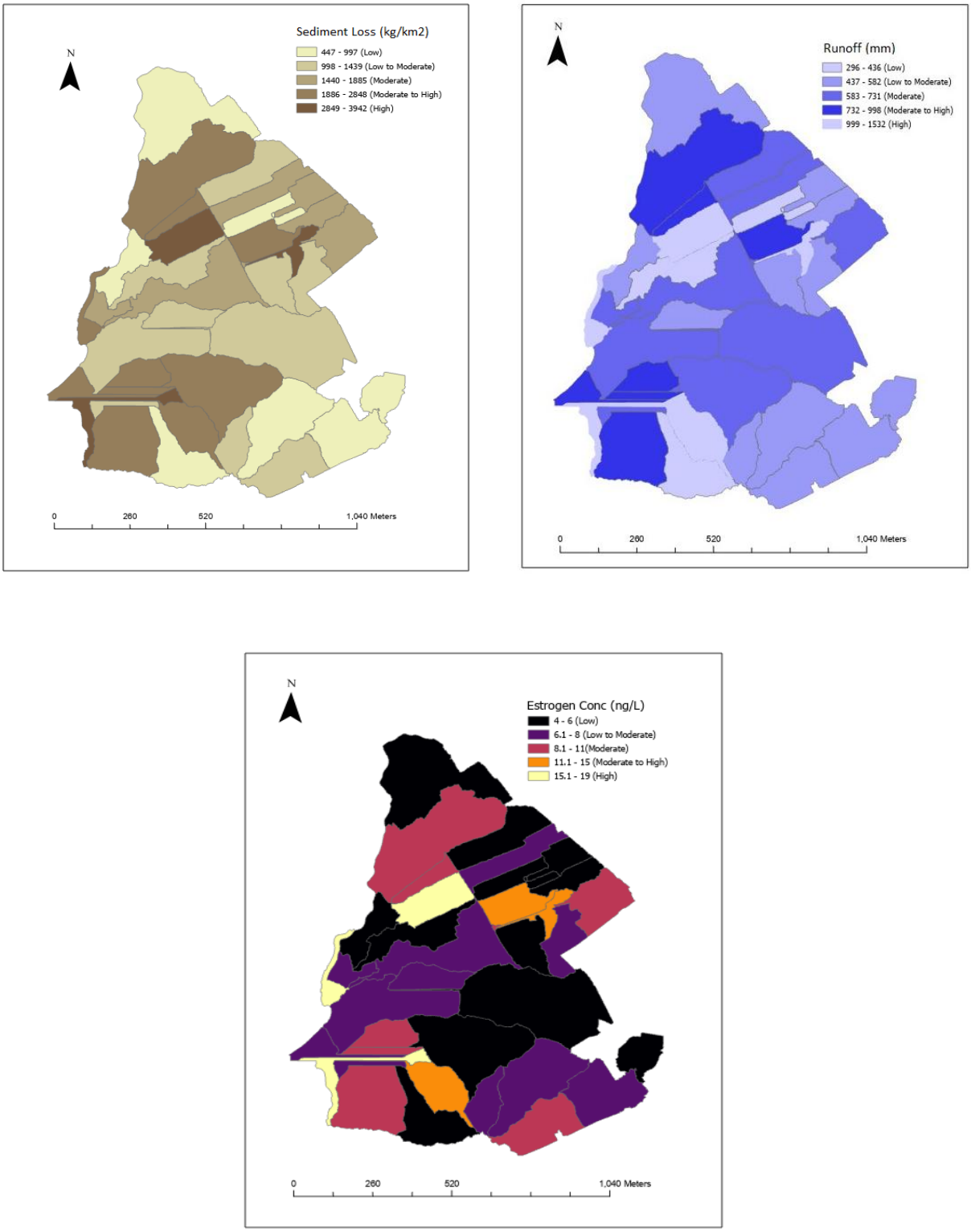

Figure 7-4: Spatial Distribution of annual Sediment Loss (top left) (kg/ha), Runoff (mm) (top right), and Estrogen Concentrations (ng/L) (bottom) under current dairy farm management practices.

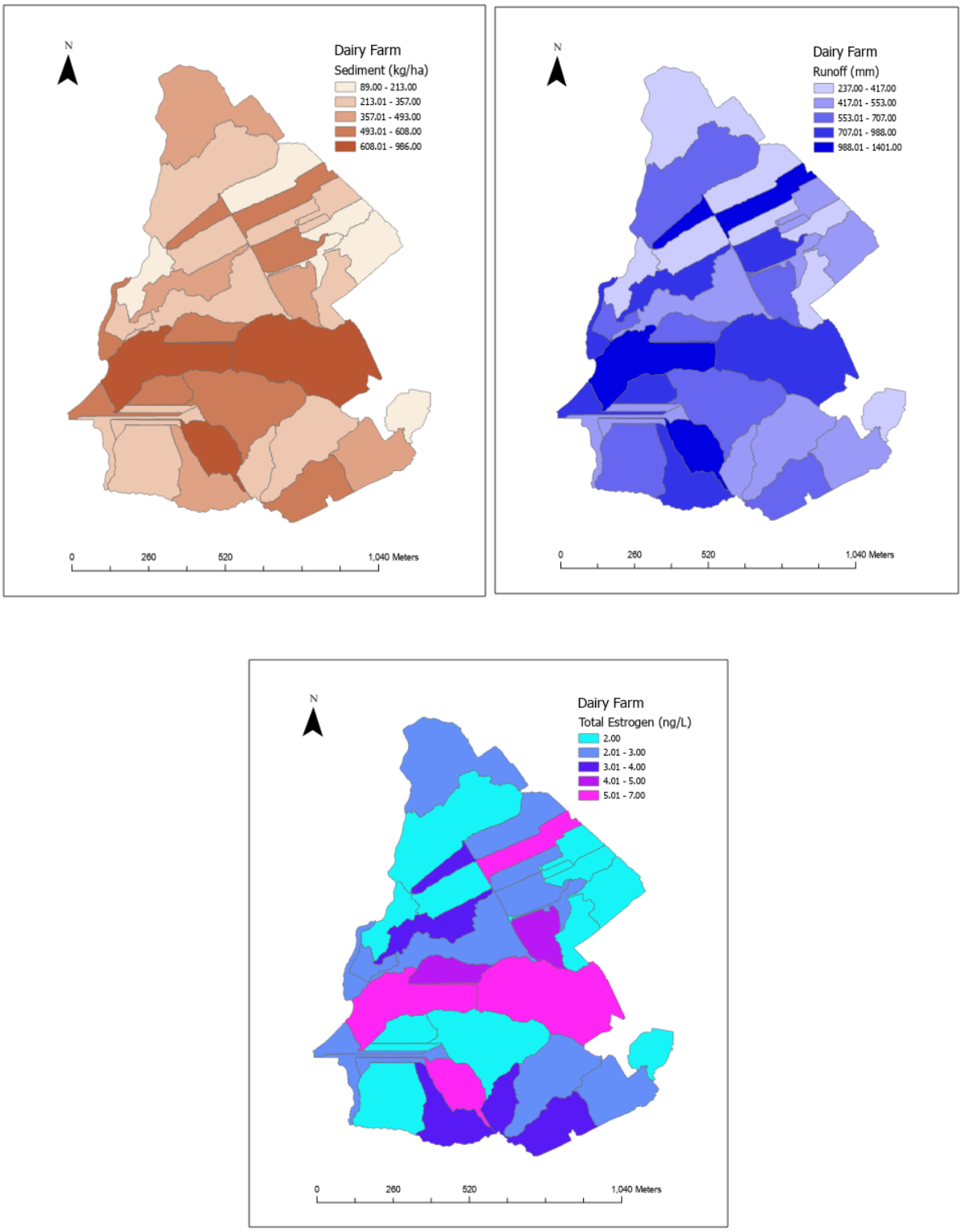

Figure 7-5: Projected Spatial Distribution of annual Sediment Loss (top left) (kg/ha), Runoff (mm) (top right), and Estrogen Concentrations (ng/L)(bottom) After Wetland Implementation

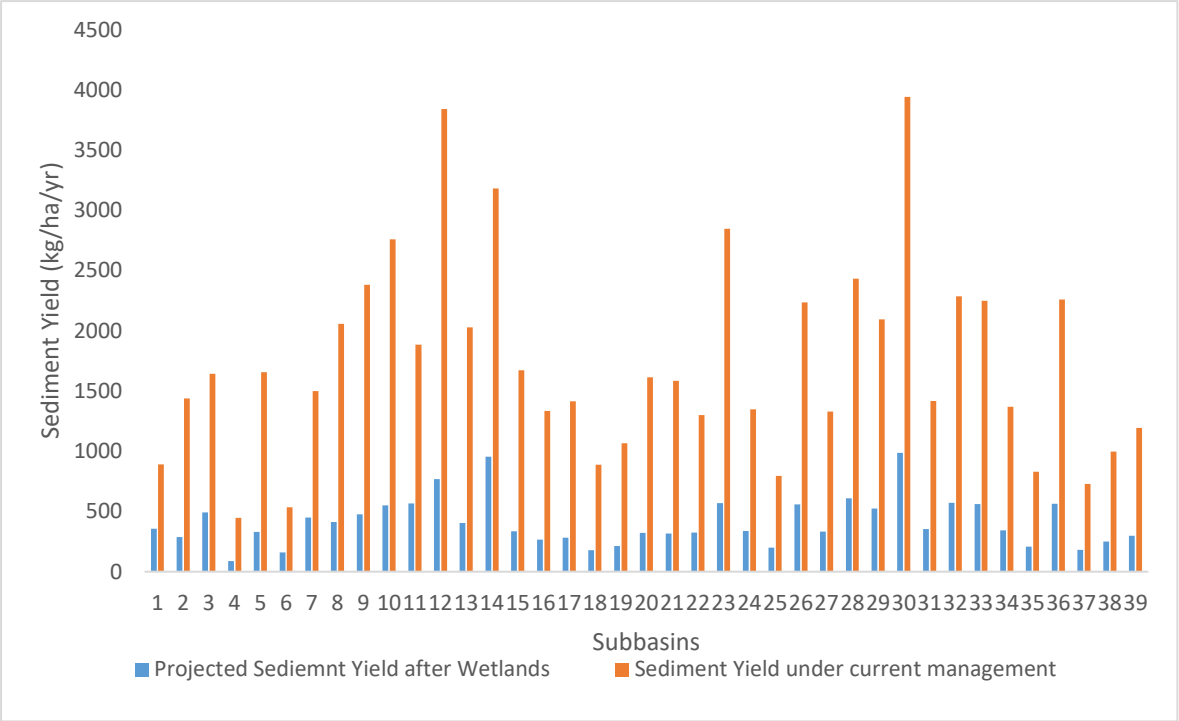

Figure 7-6: Sediment Yield (kg/ha/year) before and after Wetland implementation

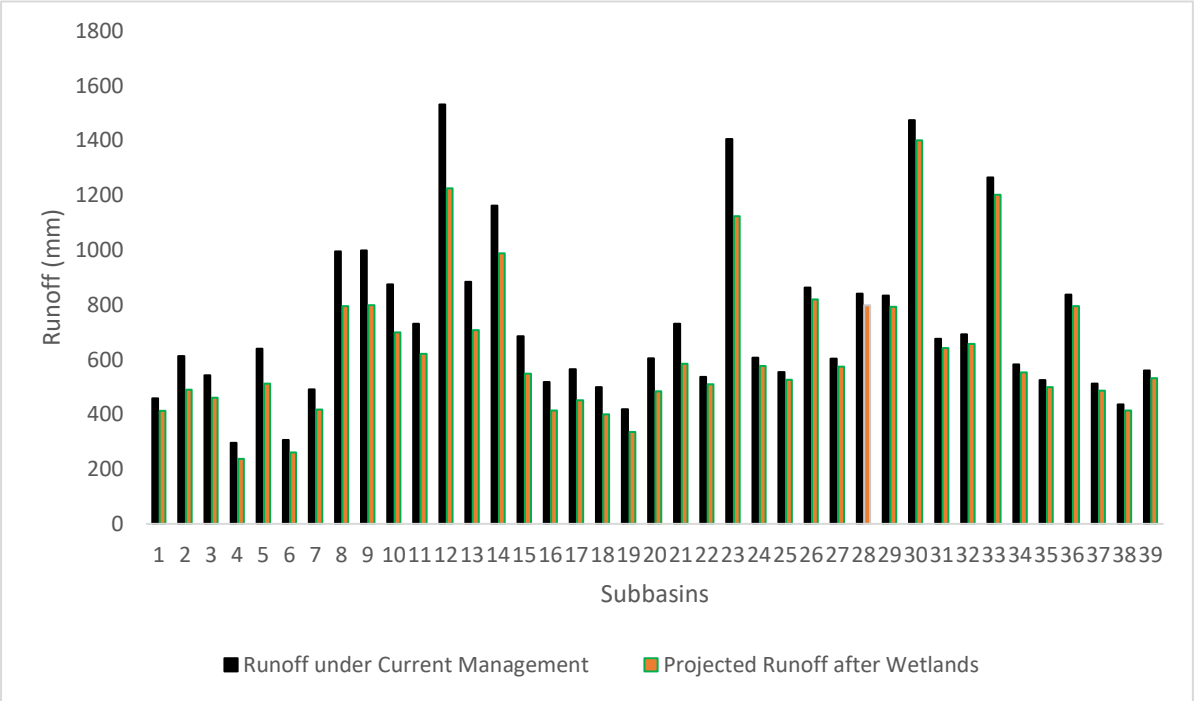

Figure 7-7: Runoff (mm) before and after Wetland implementation

The graphical representation in Figures 7.6, 7.7, and 7.8 provides a quantitative comparison of the reductions achieved through wetland implementation. Figure 7.8 shows the total estrogen concentrations (E1 and E2) before and after wetland treatment, highlighting significant reductions in high-risk subbasins. Figure 7.7 presents runoff volumes across all subbasins, demonstrating a notable decrease in peak runoff levels due to improved retention and flow attenuation. Figure 7.6 illustrates sediment yield reductions with substantial declines in erosion-prone areas, reinforcing the role of wetlands in sediment trapping and contaminant mitigation. These figures complement spatial analysis by providing clear numerical evidence of wetland effectiveness.

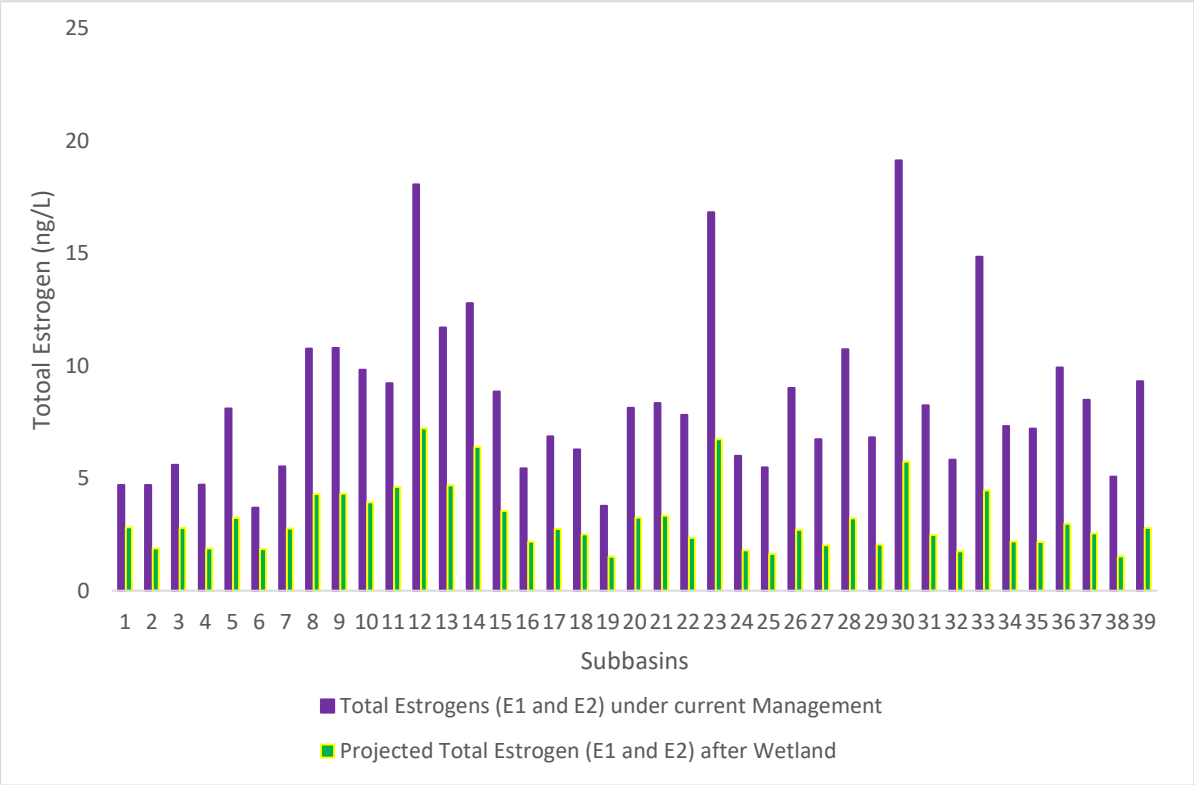

Figure 7-8: Total Estrogen Concentrations (ng/L) before and after Wetland implementation

7.6 Grazing Management

7.6.1 Impact of Overgrazing on Hydrological and Sediment Transport Processes

Overgrazing and continuous stocking contributed to increased sediment transport and gully erosion, especially in areas with high stocking densities (e.g., >2.5 livestock units/ha). These areas exhibited elevated sediment delivery rates up to 500 kg/ha/year, whereas areas with well-managed rotational grazing had significantly lower erosion rates (Minea et al., 2022). One of the key findings is that structured grazing management practices, such as rotational grazing, can reduce runoff and sediment losses when compared to continuous grazing. The management of stocking density also influences runoff, such as half-stocking density has been shown to lead to an 18% reduction in runoff compared to full stocking densities (Kumar et al., 2010).

Sanjari et al., (2009) demonstrated that time-controlled (TC) grazing reduces runoff and sediment loss compared to continuous grazing. Their study found that TC grazing increased ground cover up to 90%, which improved infiltration and reduced soil erosion. Runoff reductions were most pronounced for small rainfall events (<50 mm), while sediment concentration decreased by 25% in steeper areas and over 50% in lower slope areas. Furthermore, a minimum of 70% ground cover was required to effectively reduce sediment loss, reinforcing the importance of rest periods and reduced trampling in pasture management.

The study by Schwarte et al., (2011) found that continuous grazing systems resulted in 24-38% higher runoff volumes compared to rotational stocking systems. In contrast, rotational grazing reduced runoff by 10-30% due to improved vegetative cover, which enhanced soil infiltration and decreased surface water flow velocity. A similar study by Minea et al., (2022) reported that stocking density reductions led to a 15-25% decrease in runoff, particularly in hilly terrain where overland flow was dominant. These studies provided a foundational basis for simulating grazing management interventions in Arc SWAT.

7.6.2 Integration of Spatial Analysis for Management Practices

A spatially explicit analysis of grazing management was conducted using ArcSWAT model outputs, evaluating the impact of reducing grazing pressure on sediment, runoff, and estrogen transport. The following management parameters were adjusted in the model to reflect the effects of grazing interventions:

- Reduction in Grazing Days (365 to 330 days/year): Allowed for soil recovery, leading to an estimated 10–20% reduction in sediment transport.

- Biomass Consumption Reduction (BIO_EAT: -20%): Improved forage availability, which enhanced root structures, promoting higher infiltration rates and lower runoff coefficients.
- Trampling Reduction (BIO_TRMP: -20%): Reduced soil compaction, increasing infiltration by up to 15% and decreasing total sediment loads as mentioned by Sanjari et al., (2009).

Additionally, restricting livestock access to waterways has proven to be an effective strategy. Studies have shown that rotational grazing with limited stream access reduces sediment yield and phosphorus transport, whereas unrestricted grazing leads to higher contaminant loads. Schwarte et al., (2011) found that rotational grazing reduced sediment losses by approximately 40%, while phosphorus transport was also minimized due to improved vegetation cover and decreased soil disturbance. Figure 8.8 illustrates the projected reductions in these parameters following the implementation of grazing management.

7.6.3 Comparison of Grazing Management Implementation Outcomes

Figures 7.9, 7.10, 7.11 and 7.12 present the current management scenario and the projected reductions in sediment loss, runoff volumes, and estrogen concentrations after the implementation of grazing management practices. These modifications primarily focused on rotational grazing, reducing overgrazing, and improving vegetative cover, which collectively enhanced soil stability and water retention. Figure 7.9 illustrates the projected spatial distribution of sediment yield, runoff and estrogens.

Sediment Loss: Initially reaching values above 3,900 kg/km², sediment loss has been reduced by approximately 17.5% on average, with reductions ranging from 4.9% to 50.0% across subbasins. Most subbasins now show values below 1,000 kg/km² post-implementation (Figure 7.10). Runoff Volumes: Previously exceeding 1,500 mm in peak areas, runoff has decreased by around 11.9% on average, with reductions varying from 4.9% to 30.0%, leading to peak values dropping below 900 mm due to improved infiltration and vegetative cover (Figure 7.11). Estrogen Concentrations: Originally reaching 19 ng/L in critical areas, grazing management has led to approximately 13.3% reductions on average, with individual subbasins experiencing reductions between 4.9% and 35.0%, with most subbasins showing levels below 6 ng/L after implementation (Figure 7.12).

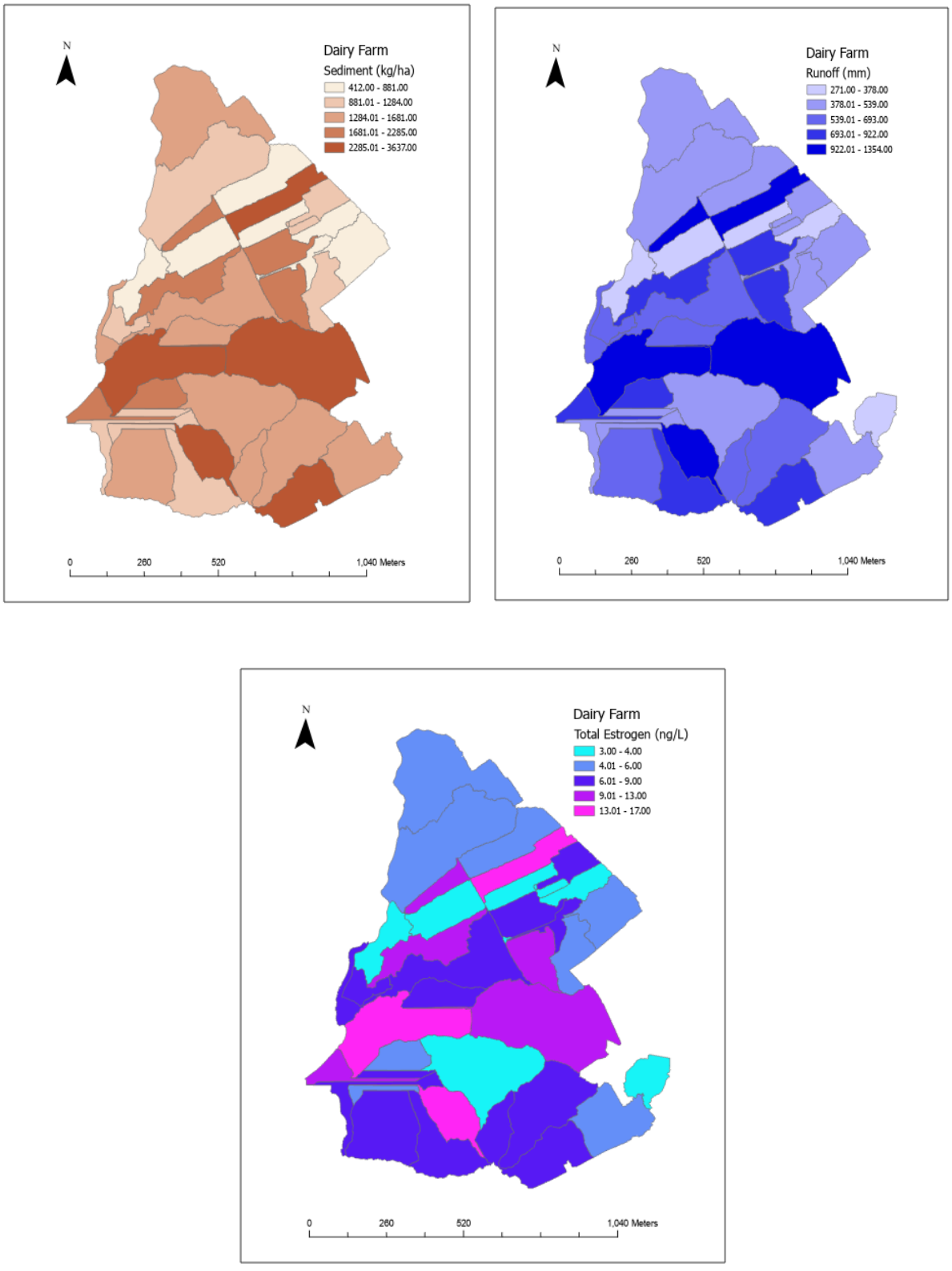

Figure 7-9: Projected Spatial Distribution of annual Sediment Loss (top left) (kg/ha), Runoff (mm) (top right), and Estrogen Concentrations (ng/L)(bottom) after grazing implementation

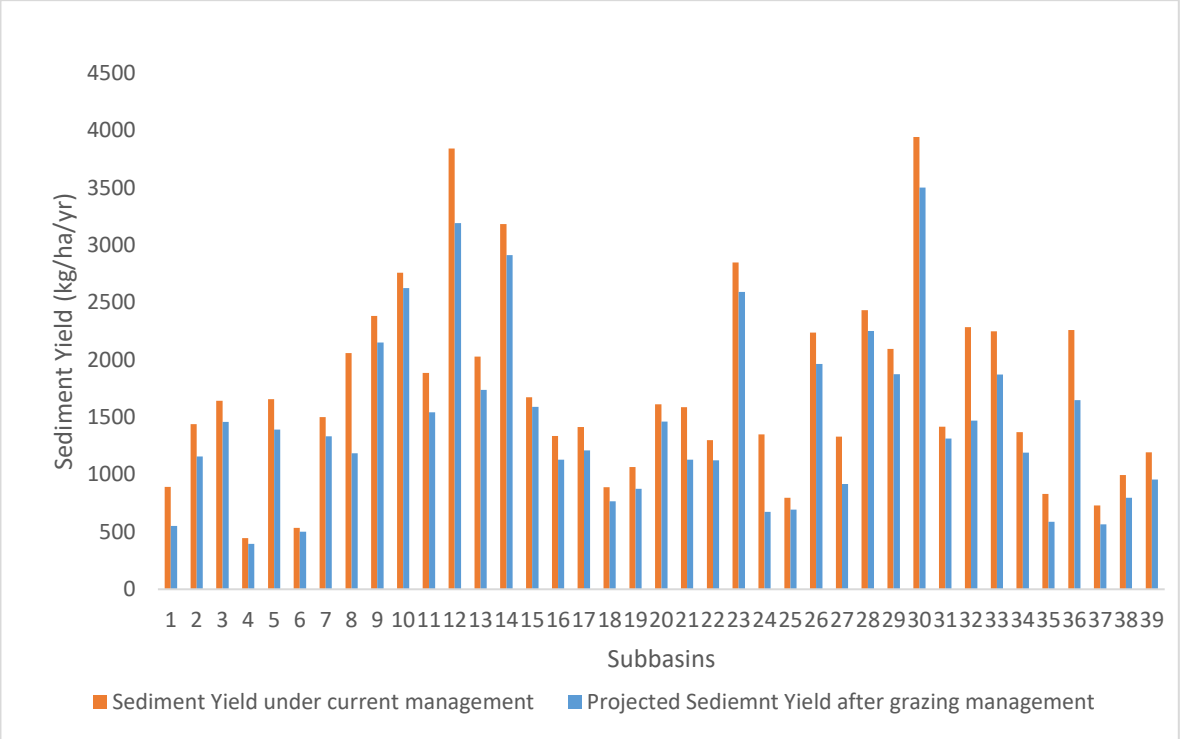

Figure 7-10: Comparison of sediment yield (kg/ha/yr) before and after grazing management

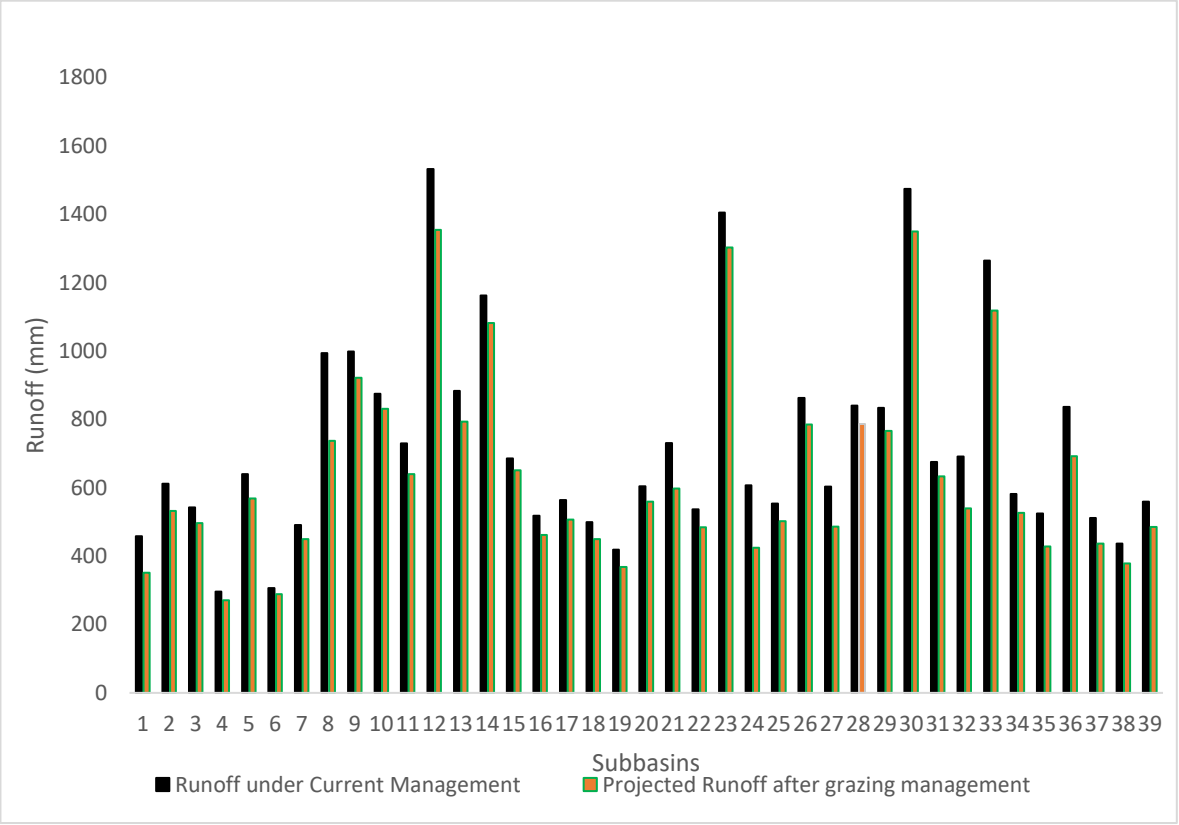

Figure 7-11: Comparison of Runoff (mm/ha/yr) before and after grazing management

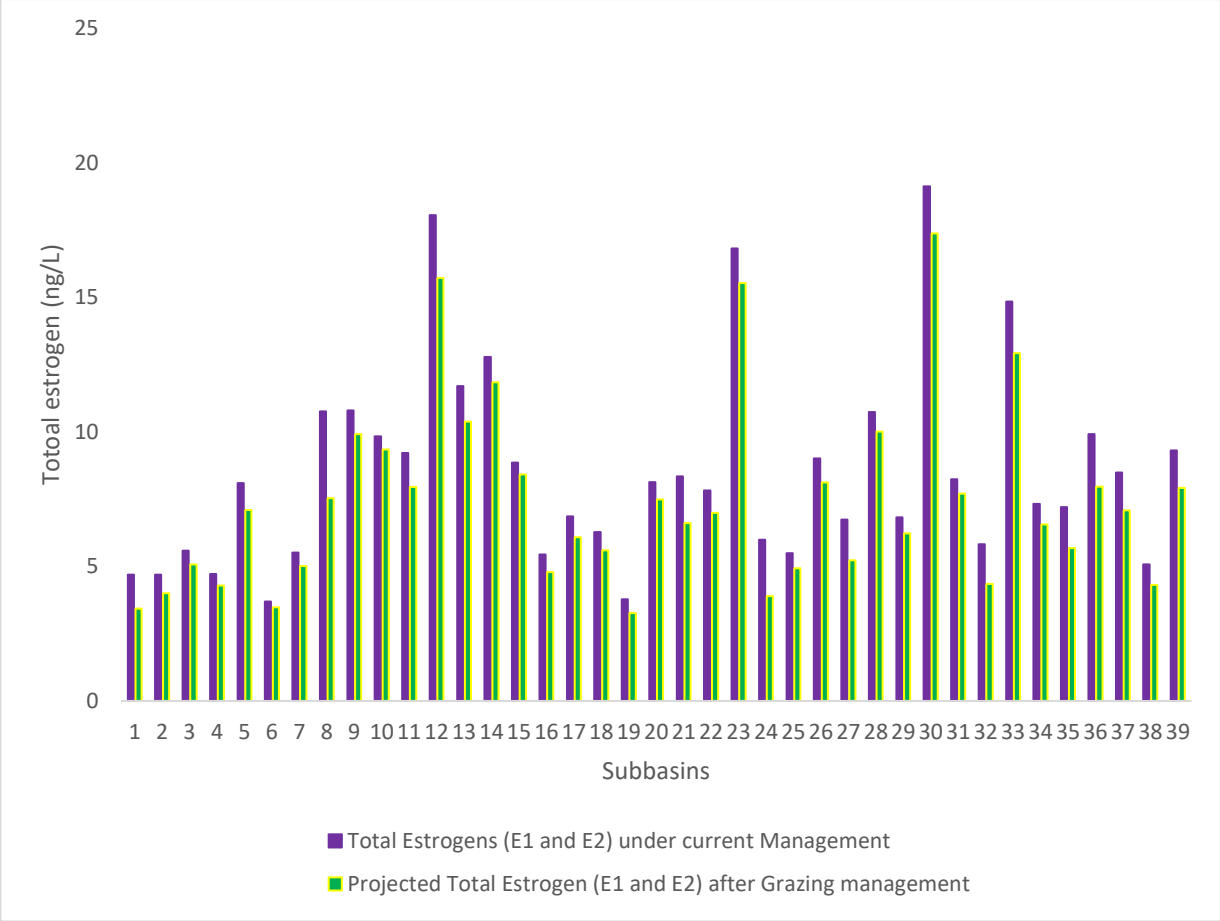

Figure 7-12: Comparison of Total Estrogen (E1 and E2) (ng/ha/yr) before and after grazing management

7.7 Effluent Management Modifications in ArcSWAT

Effluent management plays a crucial role in minimizing estrogen transport, runoff, and sediment loss in dairy farming systems. The study by Sanders et al., (2019) evaluated the effects of fertilizer source and two irrigation depths on nutrient leaching. This study found that higher irrigation depths increased nutrient leaching, emphasizing the importance of optimizing irrigation practices to minimize environmental impacts. Lowering irrigation not only reduced overall water use by 50% but also resulted in 39% and 35% reductions in cumulative inorganic nitrogen (N) and dissolved total phosphorus (DTP) losses.

7.7.1 ArcSWAT Effluent Application Modifications

Effluent management modifications in ArcSWAT were implemented to reduce estrogen transport, runoff, and sediment loss while maintaining surface application. The effluent irrigation depth was reduced from 10 mm to 8 mm per application, ensuring less surface runoff and improved infiltration. Additionally, the number of irrigation events was reduced from 12 to 8 per year, with no applications during June-August, the months with the highest rainfall in New Zealand. This scheduling adjustment aimed to prevent overland flow during wet conditions, reducing the risk of estrogen and sediment transport to waterways.

Despite continuing surface spreading, the controlled application timing and reduced depth led to lower runoff potential and better absorption in the soil. No changes were made to nutrient content, ensuring that nitrogen and phosphorus inputs remained consistent. However, estrogen concentrations in the applied effluent were assumed to be 40% lower, reflecting natural degradation in effluent ponds before application. These modifications resulted in an estimated 30-50% reduction in estrogen transport (E1 and E2), 15-30% reduction in total runoff, and 15-30% lower sediment loss.

Effluent is the primary source of estrogens (E1 & E2) in dairy farms, and stopping application in wet months means zero estrogen input during high-runoff periods. The natural degradation of estrogens in stored effluent ponds further lowers estrogen concentrations before application. Reducing the number of application months (by 33%) directly reduces estrogen losses, along with the effects of treatment and soil retention. The effluent contains particulate matter that contributes to sediment transport, especially when applied in wet conditions. By eliminating

winter applications, sediment-bound pollutants from effluent are not washed away during peak runoff months. This enhances the overall sediment reduction effect, but since effluent is not the primary source of erosion. Effluent irrigation contributes to direct surface runoff when applied in wet months. Stopping application in June-August means runoff from effluent sources is entirely prevented during these months

Effluent management practices have demonstrated reductions in sediment loss, runoff, and estrogen concentrations across the watershed. The simulations show that sediment loss, which previously peaked at 3,942 kg/km², was reduced by an average of 10.55%, with reductions varying from 4.94% to 25% across different subbasins. Runoff, which initially exceeded 1,500 mm in some areas, decreased by an average of 11.5%, with reductions ranging from 10% to 30%. Estrogen concentrations, which reached 19.1 ng/L in critical areas, were reduced by an average of 17.49%, with individual subbasins showing reductions between 4.87% and 50%. These results highlight the role of effluent management in reducing contaminant transport by enhancing infiltration and limiting runoff-driven pollution. When combined with grazing management and wetland interventions, effluent management further strengthens watershed sustainability and water quality improvement by reducing the source contribution of pollutants.

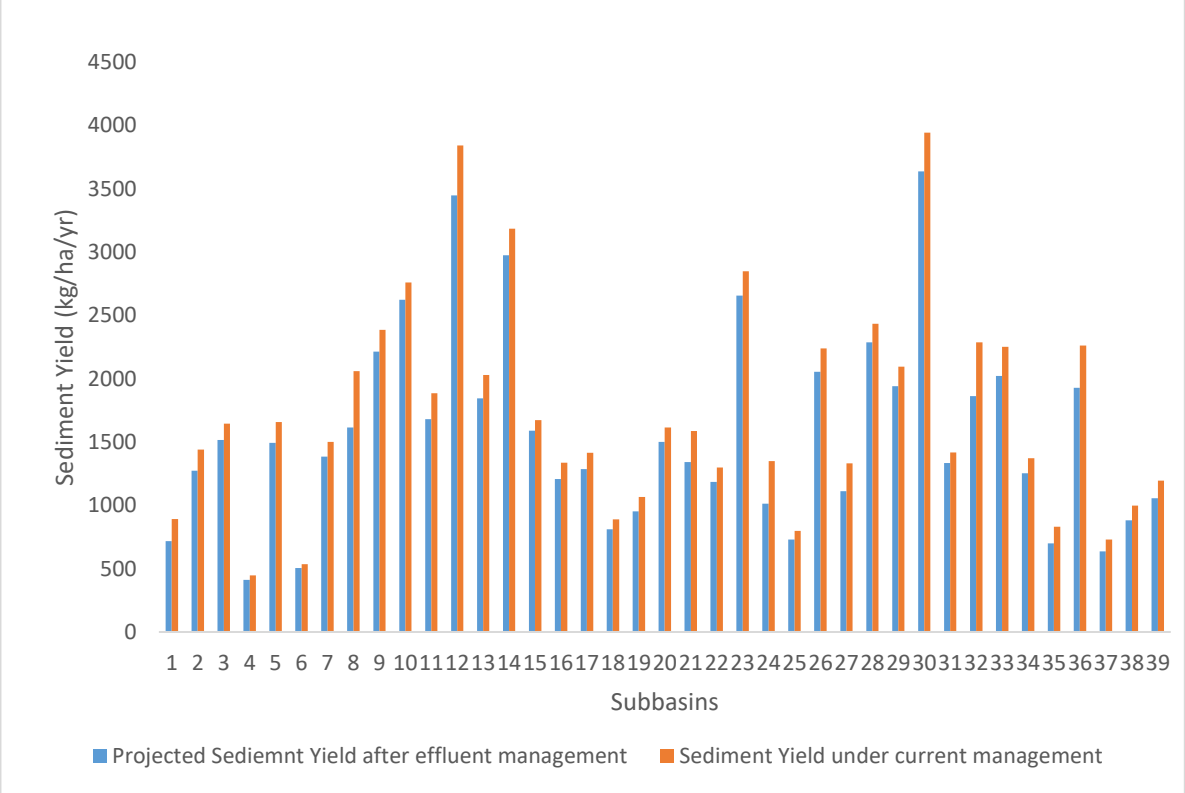

Figure 7-13: Sediment Yield reduction after Effluent Management implementation

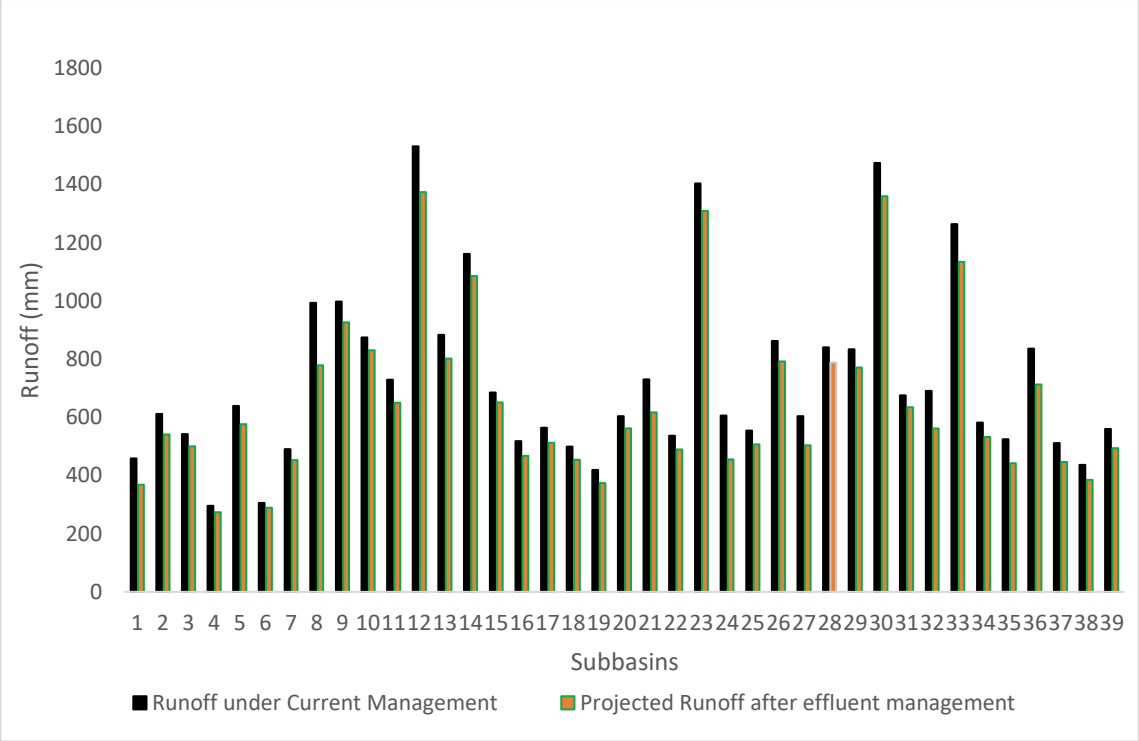

Figure 7-14: Runoff reduction after Effluent Management Implementation

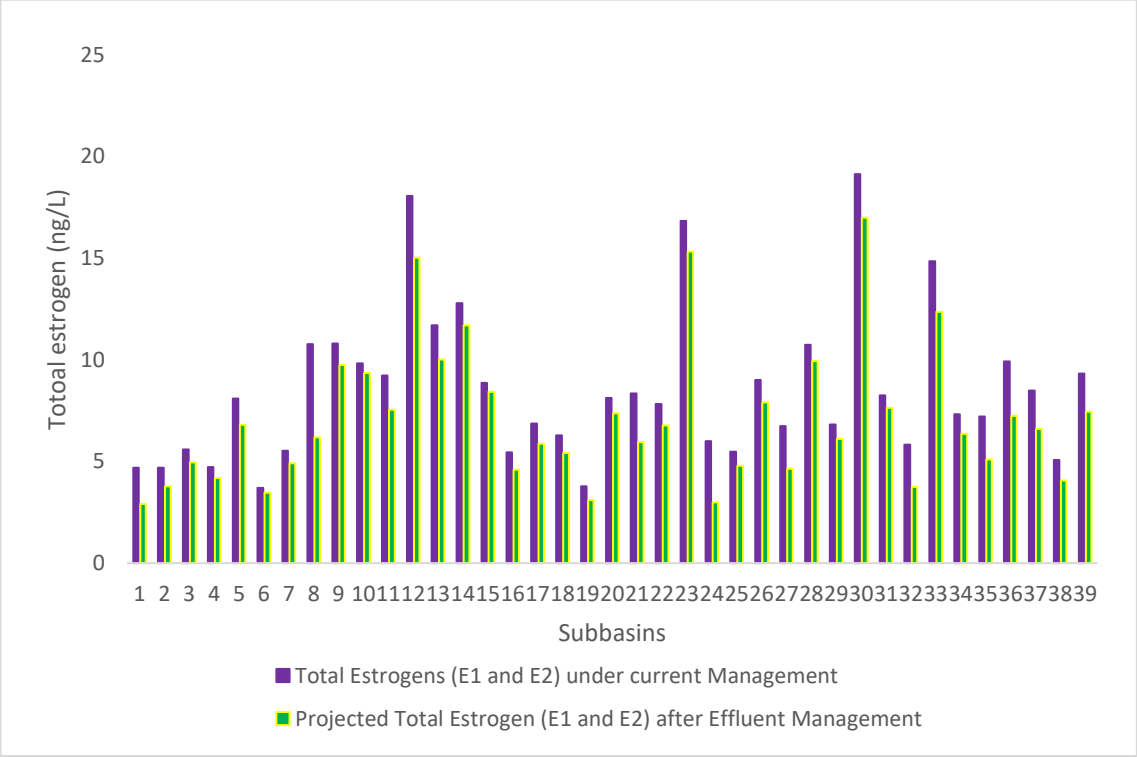

Figure 7-15: Estrogen Concentration Reduction After Effluent Management Implementation

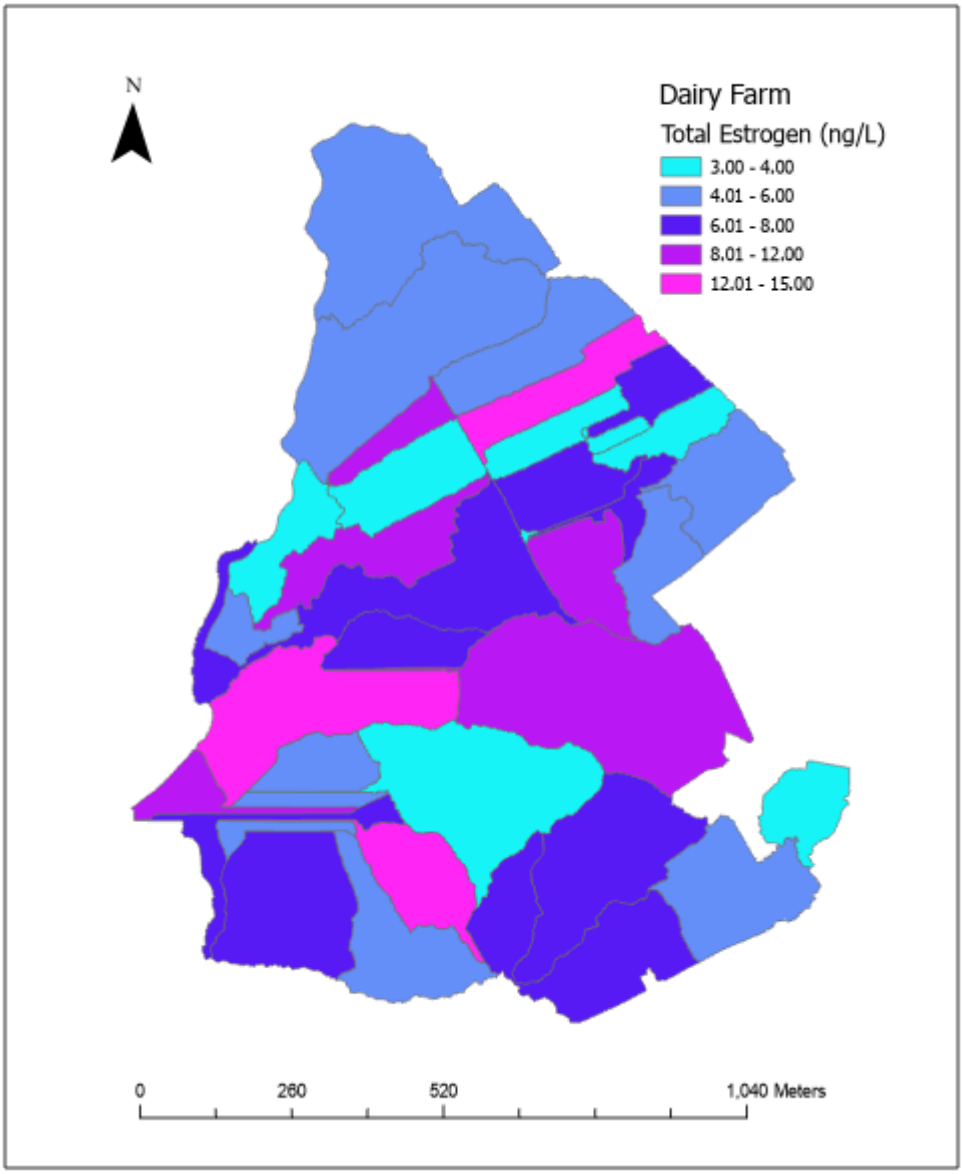

Figure 7-16: Projected Total Estrogen Concentration (ng/L/yr) after Effluent Management implementation

The numerical representation of these reductions is presented in Figures 7.13, 7.14, and 7.15. Unlike wetlands and grazing management, runoff and sediment reductions remained relatively minor, as effluent modifications primarily influenced estrogen transport rather than overall hydrological processes. The spatial distribution of estrogen concentrations before and after effluent management implementation is illustrated in Figure 7.16. This map highlights subbasins where estrogen transport was most pronounced under current conditions and demonstrates the effectiveness of the modified application schedule in reducing estrogen losses.

The highest estrogen concentrations, previously exceeding 12 ng/L, were reduced to levels below 8 ng/L in critical subbasins following effluent management intervention.

7.8 Riparian Buffer Strips

Riparian buffer strips are vegetated areas (grasses, shrubs, or trees) along waterways that help reduce runoff, sediment, nutrients, and estrogen transport by trapping sediments before they reach streams and filtering runoff by slowing down water movement, absorbing nutrients & estrogens in soil and vegetation. Enhancing infiltration and groundwater recharge (Tomer et al., 2005).

Figure 7.17 illustrates the key hydrological and biogeochemical processes occurring within a riparian buffer zone, highlighting its role in contaminant filtration, sediment deposition, and nutrient transformation. As runoff and shallow groundwater pass through the buffer, various mechanisms contribute to pollutant attenuation, such as Deposition & Infiltration, Uptake & Transformation, Mineralization & Volatilization, Streambank Stabilization, Shade & Temperature Regulation. These combined processes enhance water quality by reducing sediment loss, nutrient leaching, and contaminant transport into adjacent streams.

Dosskey et al., (2010) reported that vegetated riparian buffers improve infiltration and reduce surface runoff by 20-60%, depending on buffer width and vegetation type. Arora et al., (2003) confirmed that riparian vegetation enhances organic matter content, which promotes higher estrogen sorption capacity, reducing dissolved pesticide loads. Another study by Zhang et al.,(2017) found that buffer zones with grasses and trees reduced curve number CN values by 5-15%, improving infiltration and reducing peak flow rates. Furthermore, Mayer et al., (2007) demonstrated that riparian vegetation increases surface roughness, slowing overland flow velocity and allowing greater infiltration and groundwater recharge. Wide buffers (>50 m) more consistently removed significant portions of nitrogen entering a riparian zone than narrow buffers (0-25 m).

Kuok et al. (2013) studied utilizing the Buffer Zone Calculator for sediment removal efficiency, demonstrated that higher crop cover coefficient values lead to increased TSS at the outfall, signifying the importance of vegetation cover in erosion control. The most effective land use types for reducing TSS were forests with undergrowth, mixed dipterocarp forests, and cultivated grasses, whereas cleared land and settlements exhibited the highest sediment losses.

This highlights the necessity of maintaining a dense vegetative cover in riparian buffer zones to minimize erosion and sediment loss.

To evaluate the effectiveness of riparian buffer zones in reducing sediment transport, surface runoff, and estrogen loading, buffers are applied to all selected dairy farm subbasins that are directly connected to streams within the farm. This selection criterion ensures that the subbasins contributing the highest pollutant loads have direct hydrological pathways to water bodies, where mitigation measures can have the most impact.

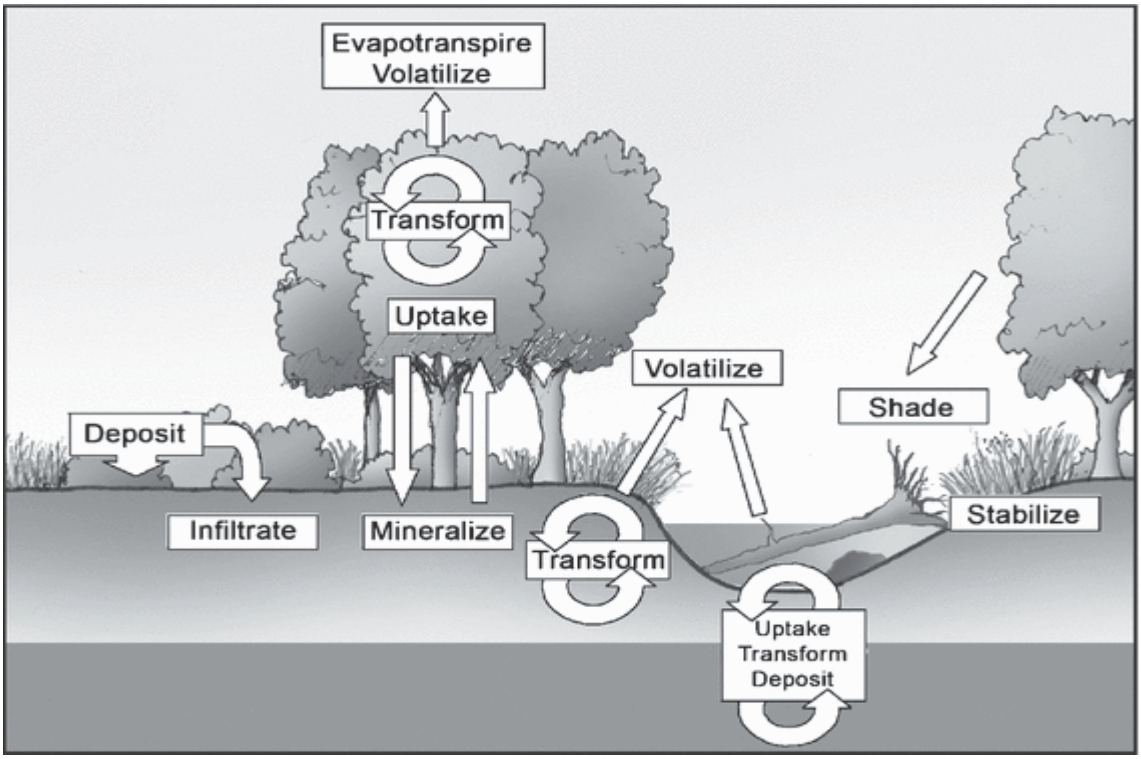

Figure 7-17: Processes of Riparian Buffer Zones in Contaminant Retention and Transformation- (Adapted from Dosskey et al., (2010))

The selection process was based on three key parameters: High sediment loss (kg/km²), indicating areas prone to erosion and sediment transport. High surface runoff (mm), contributing to the mobilization of sediments and dissolved pollutants. High estrogen concentrations (ng/L), including both sorbed and soluble fractions, which are transported via runoff and sediment movement.

7.8.1 Riparian Buffer Implementation and Subbasin Selection

High-Priority Subbasins (Identified Across All Three Parameters & Stream Connectivity) are 12, 14, 23, 30, and 1. These subbasins exhibit high sediment detachment, elevated runoff, and substantial estrogen transport, posing a significant risk of pollution to downstream water bodies and the Maungatea water stream, which flows along the dairy farm. As they are directly connected to farm streams, riparian buffers will play a crucial role in trapping sediments, filtering dissolved pollutants, and reducing direct estrogen input into surface waters.

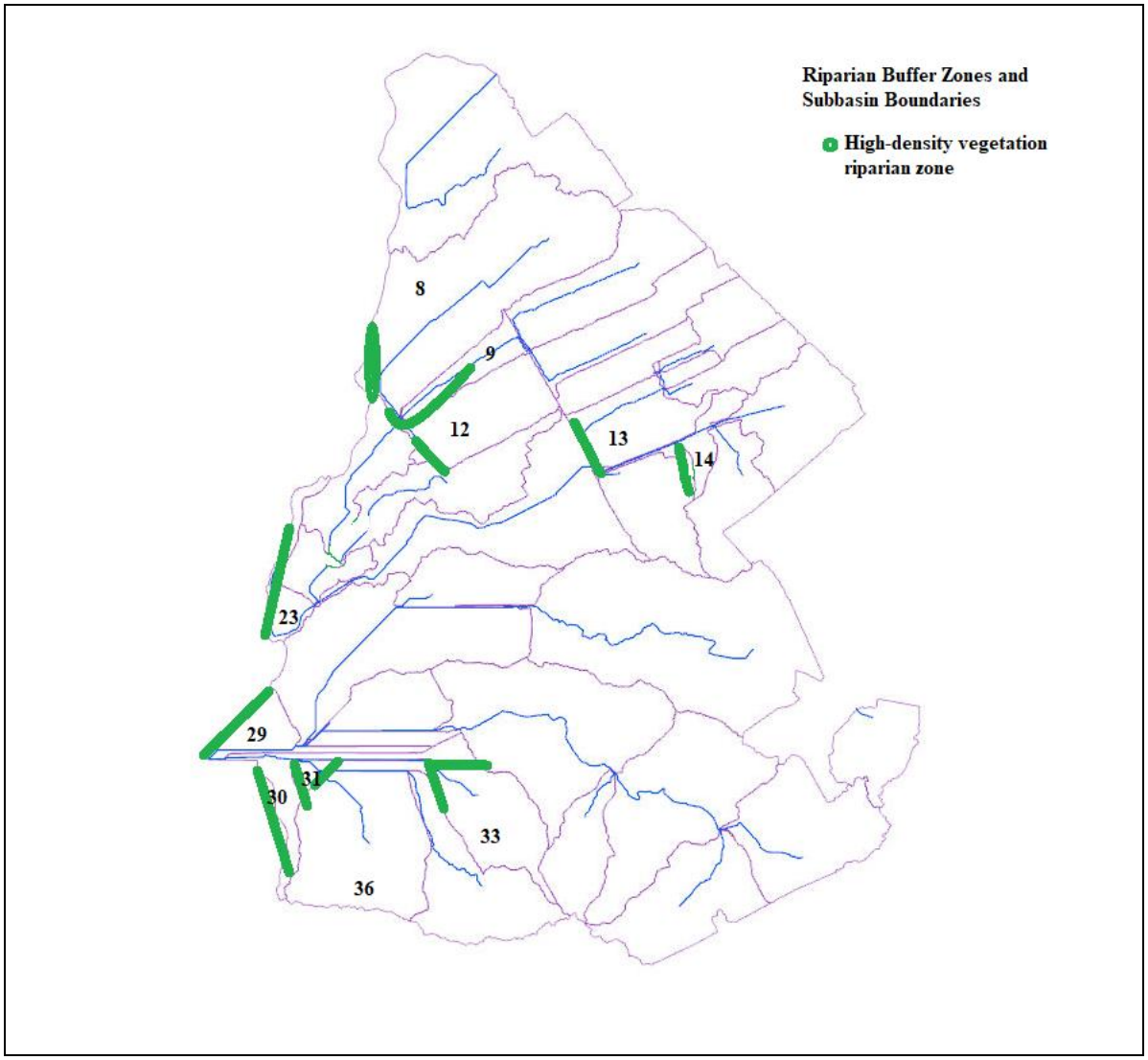

Figure 7-18: Spatial representation of riparian buffer zones applied to selected subbasins within the dairy farm watershed. The green-highlighted areas indicate high-density vegetation buffers strategically placed along stream networks to reduce sediment transport, enhance infiltration, and mitigate estrogen and nutrient runoff.

Medium-Priority Subbasins (Identified in Two Parameters & Stream Connectivity) are 29, 8, 9, 33, and 31. These subbasins contribute high sediment or runoff volumes but moderate

estrogen transport, or vice versa. Their stream connectivity makes them suitable for riparian buffer application to assess localized effects on pollutant attenuation.

Low-Priority Subbasin (Selected for Hydrological Characteristics & Stream Connectivity) is 36. This subbasin was identified due to high runoff contribution, although sediment and estrogen levels are lower. Buffers in this area will help evaluate their role in runoff attenuation and flow velocity reduction, indirectly supporting erosion control.

Riparian buffers were incorporated into the land-use classification of the selected subbasins. This was done by converting sections of HRUs (Hydrologic Response Units) to riparian vegetation, which included grass, shrubs, and tree-based buffers. This modification ensured that buffer zones were modeled as a distinct land use category, influencing surface runoff, infiltration, and sediment trapping. As illustrated in Figure 7.18, these buffers were placed along key hydrological pathways where erosion and runoff risks were highest, ensuring effective pollutant attenuation before reaching downstream water bodies.

7.8.2 Riparian Buffer Modifications in ArcSWAT

The curve number (CN2), which controls runoff potential, was reduced in riparian areas to account for the higher infiltration capacity of vegetated buffers. The reduction varied depending on the vegetation type and soil properties, ensuring a more realistic representation of runoff attenuation. To reflect the erosion-reducing effect of riparian buffers, the parameters in the Universal Soil Loss Equation (USLE) were modified. USLE_P (Support Practice Factor) was reduced to account for the effectiveness of riparian vegetation in controlling erosion and sediment transport. USLE_C (Crop Management Factor) was adjusted to represent the lower erosion susceptibility of riparian vegetation compared to pasture or cropland. The slope length factor (SLSUBBSN) was adjusted to reflect the role of riparian buffers in slowing overland flow and reducing sediment detachment. Channel Erodibility Factor (CH_EROD) and Channel Cover Factor (CH_COV) were modified to reflect enhanced bank stabilization provided by riparian vegetation, reducing sediment loading in stream networks (Sirabahenda et al., 2020).

Riparian zones trap sediments before they reach the water bodies, requiring changes to sediment transport parameters:

- SPCON (Linear Coefficient for Sediment Reentrainment) and SPEXP (Exponent for Sediment Reentrainment): Adjusted to simulate the effect of buffer zones in trapping and reducing sediment loads before they enter the main channel.
- BIOMIX (Biological Mixing Efficiency): Increased to account for higher organic matter accumulation in buffer areas, which stabilizes soil structure and reduces erosion.
- Riparian vegetation increases surface roughness and slows runoff velocities, requiring modification of OV_N (Manning's Roughness Coefficient for Overland Flow).

HRUs in riparian-connected subbasins were modified to explicitly differentiate buffer zones from adjacent pasturelands. This ensured that land use-specific runoff and erosion characteristics were accounted for in model simulations.

7.8.3 Impact of Riparian Buffers on Runoff, Sediment, and Estrogen Transport

Riparian buffer zones were implemented in selected critical subbasins to mitigate runoff, sediment transport, and estrogen loads in the study area. The final selected subbasins for the Riparian buffer implementation were 8, 9, 12, 13, 14, 23, 29, 30, 31, 33, and 36, ensuring targeted mitigation in priority areas.

Riparian zones contribute to estrogen retention and degradation by enhancing sorption, microbial breakdown, and plant uptake. The reductions varied based on the estrogen fraction and its transport mode. Sorbed Estrogen (E1 and E2 bound to sediments) showed the highest removal efficiencies, with 50-90% reduction observed due to sediment filtration and deposition in the buffer zones. Soluble Estrogen (dissolved E1 and E2) experienced 30-70% reduction, attributed to adsorption onto organic matter and microbial degradation within the riparian soil profile. The simulation results demonstrate that riparian buffers effectively reduced hydrological and water quality impacts in critical subbasins. The combined effects of reduced runoff, sediment filtration, and estrogen removal highlight the importance of riparian management as a nature-based solution for improving water quality in agricultural landscapes.

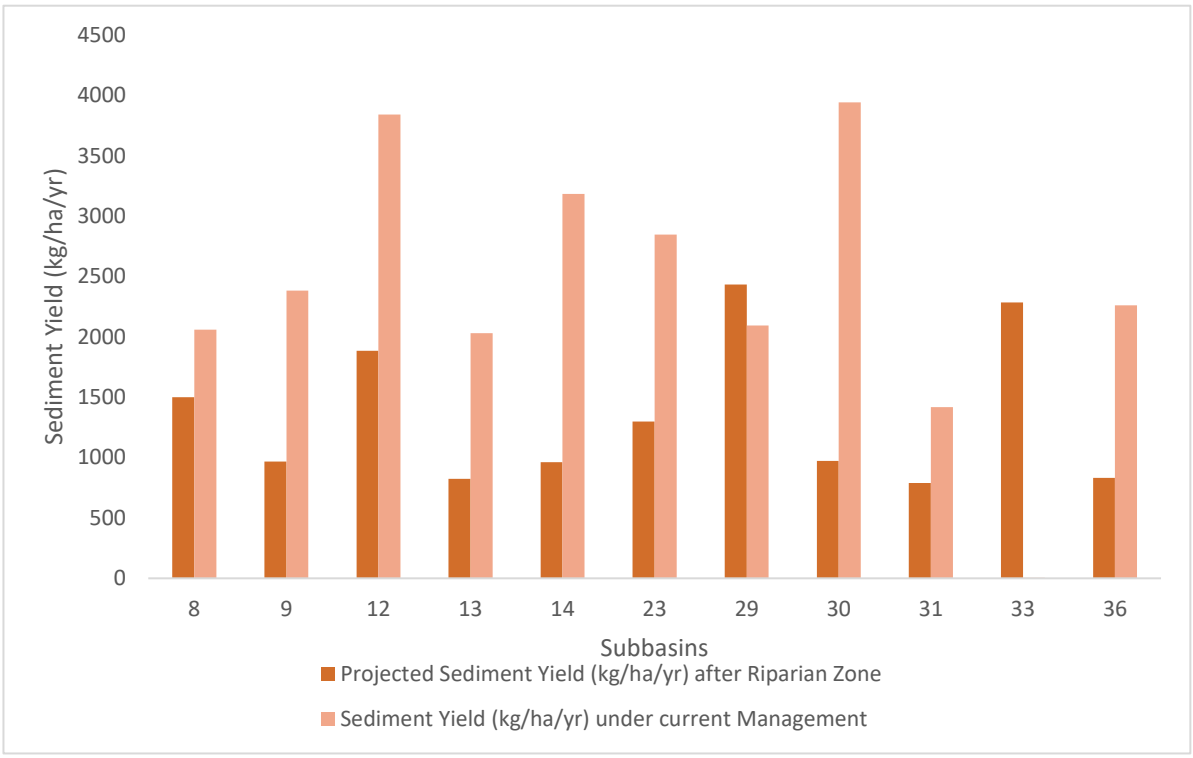

Figure 7-19: Comparison of sediment yield (kg/ha/yr) before and after riparian management in selected subbasins

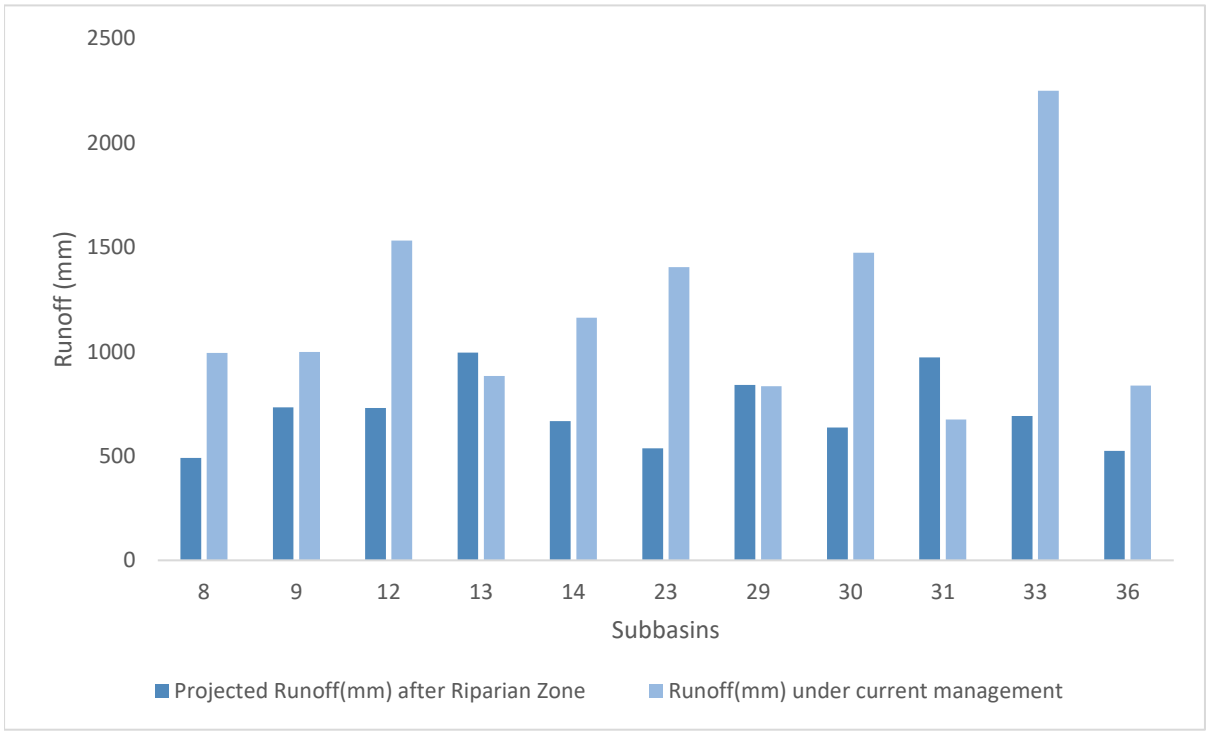

Figure 7-20: Comparison of runoff (mm) before and after riparian management implementation in selected subbasins

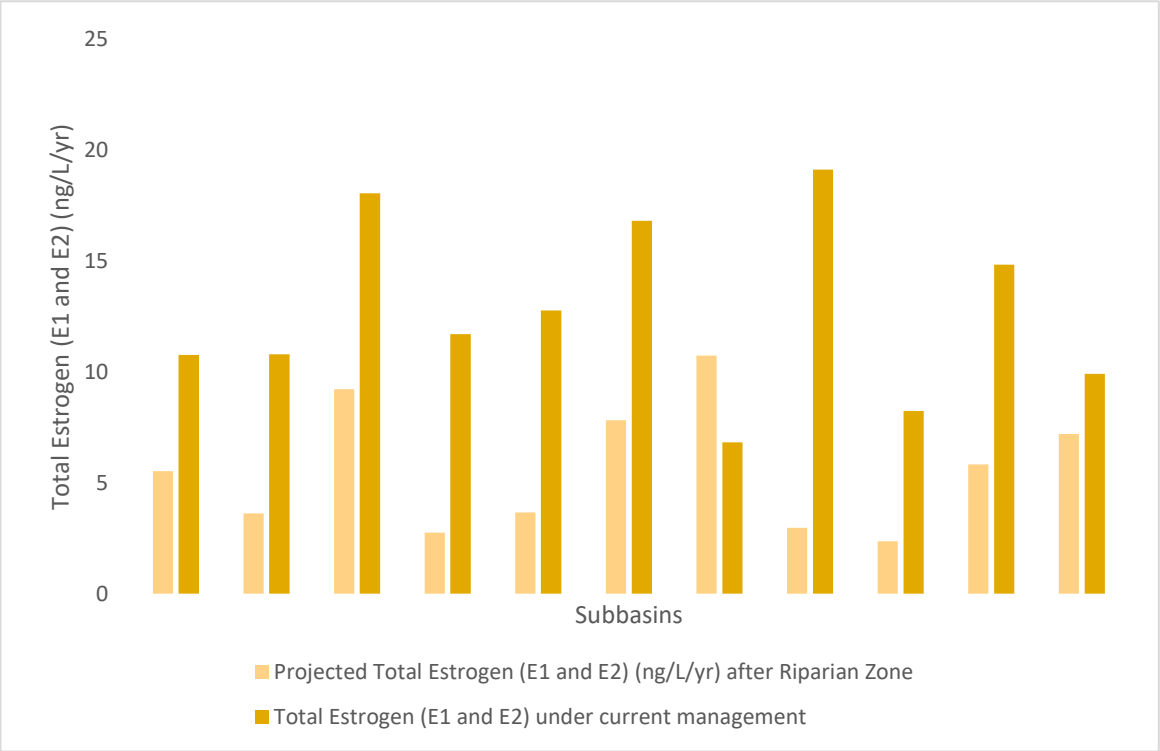

Figure 7-21: Comparison of total estrogen concentrations (ng/L) before and after riparian management implementation in selected subbasins

Figure 7.19 demonstrates that sediment loss was reduced by an average of 41.8%, with variations across subbasins ranging from 16.3% to 79.8%. The effectiveness of riparian zones in sediment trapping and stabilization contributed to this outcome, particularly in subbasins with initially high sediment loads.

Riparian management practices led to significant reductions in runoff, sediment yield, and estrogen concentrations in the selected subbasins. As shown in Figure 7.20, runoff volumes exhibited an average reduction of 39.2%, with decreases ranging from 25.3% to 56.2%. This decline reflects the improved infiltration and reduced surface flow due to enhanced vegetation and buffer strips along watercourses.

Estrogen concentrations (Figure 7.21) showed the highest reduction, with an average decrease of 54.7%, and reductions across subbasins ranging from 30.1% to 84.5%. This indicates that riparian buffers play a critical role in reducing estrogen transport by limiting surface runoff and increasing soil filtration capacity.

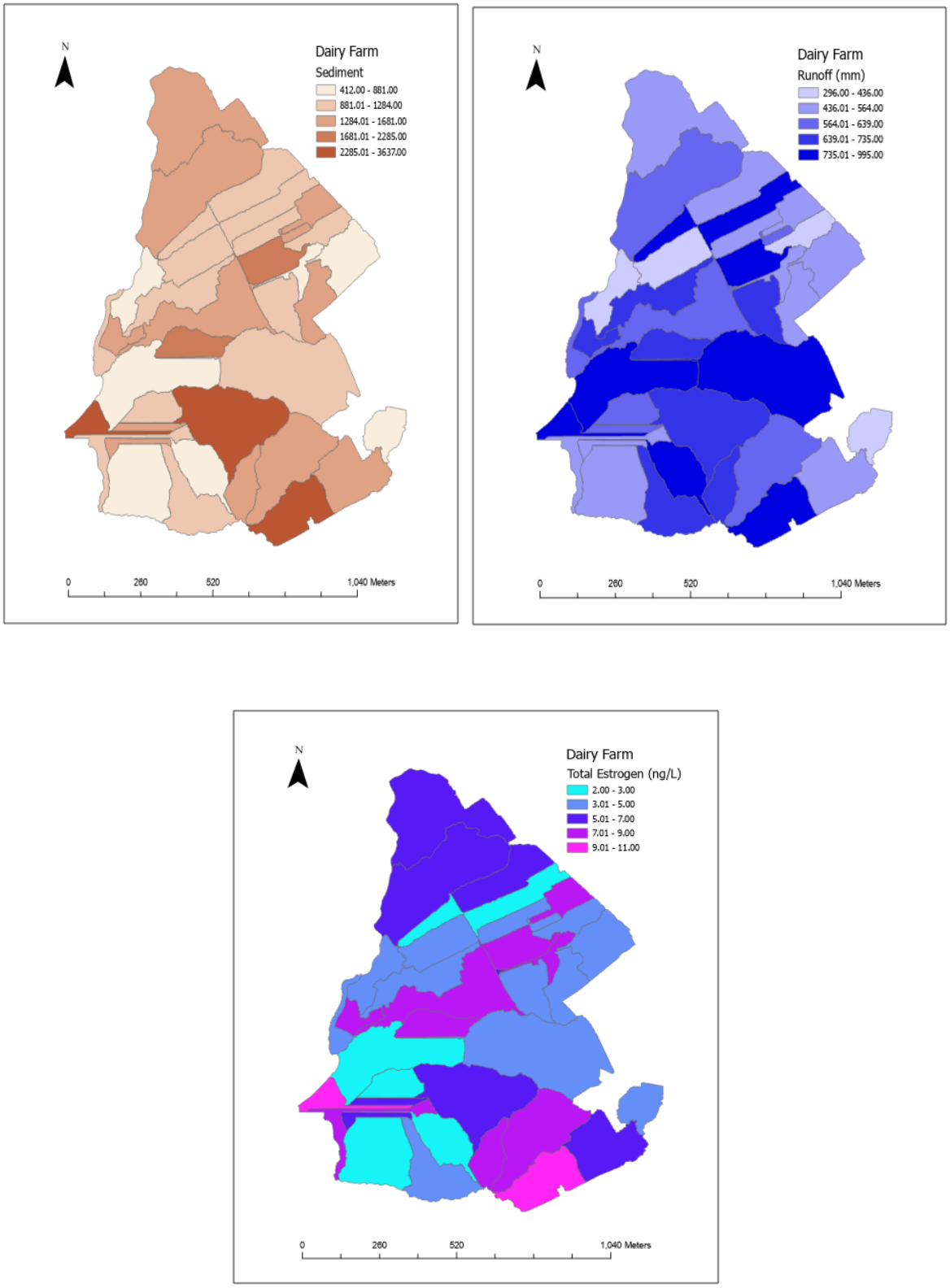

Figure 7-22: Spatial distribution of sediment loss (kg/ha (top left)), runoff (mm) (top right), and total estrogen concentrations (ng/L) (bottom) after riparian management implementation

The spatial distribution maps (Figure 7.22) illustrate the effectiveness of riparian management in reducing sediment loss, runoff, and estrogen concentrations across the watershed. The results indicate substantial improvements in water quality due to the implementation of riparian buffer strips, which enhance sediment retention, infiltration, and contaminant filtration.

The sediment yield reductions demonstrate that most subbasins now exhibit values below 1,000 kg/ha, compared to previous levels exceeding 3,900 kg/ha in some regions. The establishment of vegetative buffer strips contributed to soil stabilization and erosion control, effectively reducing sediment transport to surface waters.

Runoff volumes have also decreased, with most subbasins now experiencing values below 800 mm, whereas previous peak values exceeded 1,500 mm. The enhanced infiltration capacity of riparian zones has reduced overland flow, minimizing direct runoff contributions to nearby streams.

The estrogen concentration reductions across the watershed further highlight the effectiveness of riparian buffers. Previously reaching 19.1 ng/L in critical areas, estrogen levels have now dropped below 7 ng/L in most subbasins. This decline is attributed to vegetation-enhanced filtration, adsorption, and microbial degradation, which play a crucial role in limiting estrogen transport through runoff and sediment movement.

7.9 Conclusion and Management Recommendations

This chapter has comprehensively analyzed the effectiveness of various best management practices (BMPs) in mitigating runoff, sediment loss, and estrogen transport within a dairy farm watershed using the ArcSWAT model. The assessment focused on grazing management, effluent management, wetland implementation, and riparian buffer strips, each addressing specific hydrological and contaminant transport processes. Table 7.2 summarises BMP reductions

7.9.1 Comparative Effectiveness of Management Practices

7.9.1.1 Sediment Reduction

- Wetlands demonstrated the highest sediment retention capacity, achieving 50-90% reductions in sediment yield, effectively trapping particulates before they reached water bodies.

- Riparian buffer zones were also highly effective, reducing sediment transport by 16-80%, with an average of 42%, particularly in high-erosion subbasins, by enhancing deposition and stabilizing streambanks.
- Grazing management contributed an average 17.5% sediment loss reduction, mainly by improving soil cover and reducing trampling-induced erosion.
- Effluent management had a moderate impact, reducing sediment loss by 5-25%, primarily by preventing effluent application during wet months when runoff and erosion risks are highest.

7.9.1.2 Runoff Reduction

- Riparian buffer strips and wetlands provided 10-30% reductions in surface runoff, primarily by increasing infiltration and slowing down overland flow.
- Grazing management reduced runoff by 11.9%, as rotational stocking allowed vegetation recovery and enhanced soil water retention.
- Effluent management contributed to 10-30% reductions in runoff by adjusting application timing and reducing irrigation depth, minimizing direct overland flow contributions.

7.9.1.3 Estrogen Removal

- Wetlands achieved the highest estrogen reductions (30–70%), effectively removing both dissolved and sediment-bound estrogens through microbial degradation, sorption, and sedimentation.
- Riparian buffers closely followed, with 30–70% reductions in soluble estrogens and 50-90% reductions in sediment-bound estrogens, facilitated by increased organic matter adsorption and microbial activity. The total estrogen removal 30-84.5% with an average of 54 from the selected subbasins.
- Effluent management resulted in 5-50% estrogen reduction with an average of 17.5%, achieved by eliminating effluent applications during peak runoff months and allowing natural estrogen degradation in storage ponds before field application.
- Grazing management provided 13.3% estrogen reduction, mainly through reductions in sediment loss and runoff, limiting estrogen transport pathways.

Table 7-2: BMP Efficiency Summary

Best Management Practice (BMP)	Sediment Reduction (%)	Runoff Reduction (%)	Estrogen Reduction (%)
Wetlands	50-90	10-30	30-70
Riparian Buffers	16-80 (Avg: 42)	10-30	30-84.5 (Avg: 54)
Grazing Management	17.5	11.9	13.3
Effluent Management	5-25	10-30	5-50 (Avg: 17.5)

7.10 Best Management Practice Recommendation

Among the evaluated management strategies, wetlands and riparian buffer strips emerged as the most effective comprehensive solutions for improving hydrological and water quality conditions. Their superior performance in sediment trapping, runoff attenuation, and estrogen reduction makes them critical BMPs for mitigating dairy farm-related contamination.

- Wetlands are particularly beneficial due to their multi-contaminant removal capabilities, significantly reducing sediment-bound and dissolved pollutants. Their ability to retain water for 10–15 days enhances biodegradation and settling processes, making them ideal for intercepting high runoff and sediment loads before discharge.
- Riparian buffer zones provide consistent reductions across all contaminants, particularly estrogens and sediment, making them effective at improving stream water quality. Their ability to intercept pollutants before they enter waterways ensures long-term resilience against erosion and contaminant transport.

However, wetlands require designated land areas, making them less feasible for highly constrained farms, whereas riparian buffers can be more easily integrated along streambanks with minimal land use changes. Effluent management and grazing practices, while valuable supporting measures, do not achieve the same level of water quality improvements but remain essential for preventing source contamination.

For optimal watershed-scale management, a combined BMP approach is recommended:

- Prioritize wetlands in high-runoff, high-sediment subbasins to act as primary treatment systems.
- Implement riparian buffers along all stream-connected subbasins to further filter and attenuate contaminants.
- Adopt rotational grazing and limit stocking density to prevent overgrazing-induced soil erosion and runoff.

- Modify effluent application timing to avoid direct estrogen input during peak runoff months.

The integration of these BMPs ensures maximum contaminant reduction, enhanced hydrological resilience, and sustainable agricultural water management, making it the most effective strategy for dairy farm operations.

7.11 Policy-Driven Implementation for Sustainable BMP Adoption

Although estrogens (E1 and E2) are not explicitly mentioned in the New Zealand National Policy Statement for Freshwater Management (NPS-FM) 2024 (Ministry for the Environment, 2024), their transport is closely linked to sediment and nutrient runoff, which are central concerns of the policy. The NPS-FM mandates reductions in sediment and nutrient discharges, protection of wetlands and riparian buffers, and the adoption of best management practices (BMPs) to improve freshwater quality. Since estrogens predominantly bind to sediments and are mobilized through runoff, strategies aimed at mitigating these pollutants, such as riparian buffers, constructed wetlands, and effluent management, are indirectly aligned with NPS-FM objectives. Therefore, integrating estrogen mitigation within dairy farm management supports the policy's broader goals of reducing contaminant transport, enhancing water quality, and protecting aquatic ecosystems. To ensure the long-term effectiveness of BMPs, policy-driven approaches should enforce compliance with water quality standards, establish buffer strip and wetland retention requirements in high-risk subbasins within dairy farms, and promote the inclusion of natural treatment areas in farm drainage systems. Additionally, financial incentives, compliance support, and adaptive management strategies should be incorporated into policy frameworks to facilitate BMP adoption by farmers.

Chapter 8
Conclusions and Recommendations

8.1 Conclusions from the Unsaturated Zone Model (MATLAB Simulation)

- Under typical steady infiltration (representative of moderate rainfall or irrigation), estrogen movement is largely confined to the upper soil layers.
- Both E1 and E2 exhibit a sharp decline in concentration with depth and time. Model simulations show that estrogen plumes penetrate only a limited depth before attenuation concentrations drop by an order of magnitude within the first few tens of centimeters of soil.
- By the end of a 90-day continuous infiltration scenario, estrogen levels were nearly negligible beyond ~1–1.5 m depth in the profile. This indicates that, in homogeneous soil without macro flow channels, vertical transport is diffusion-limited and strongly attenuated by sorption and biodegradation, greatly reducing the risk of these contaminants reaching groundwater in significant amounts.
- The presence of mobile colloidal particles (tiny clay or organic particles) in the infiltrating water provided vehicles to which estrogen molecules could attach.
- However, even with colloids, the total mass of estrogen reaching deep layers remained relatively low. Colloid facilitation hastened the arrival of detectable amounts, but most estrogen still did not escape the soil profile due to continuing sorption and decay.
- 17β-estradiol might pose a marginally higher leaching risk than estrone, though both are substantially attenuated. This difference in mobility aligns with some experimental observations and suggests that models need to treat E1 and E2 as separate species with distinct transport parameters rather than lumping “total estrogen”.
- From the soil model perspective, surface water contamination via runoff is likely a more immediate concern than deep leaching for dairy farm estrogens, except in vulnerable points where rapid flow paths exist.

8.2 Conclusions from the Catchment-Scale Model (ArcSWAT Simulation)

- The spatially distributed model outputs highlighted specific subbasins as critical source areas for estrogen contamination. Not all parts of the farm contribute equally to estrogen export; rather, there is a pronounced heterogeneity, with certain sub-catchments generating disproportionately high loads of hormones and sediments. In particular,

model results pointed to eight subbasins (numbered 12, 14, 19, 26, 28, 30, 33, and 38) as the most significant hotspots.

- The identification of these specific zones is a crucial outcome, as it directs attention to where on the landscape estrogen mitigation efforts would be most needed and most effective.
- The catchment modelling reinforced an important understanding: surface runoff is the dominant mechanism for estrogen transport to streams, with sediment-bound transport acting in tandem with dissolved transport.
- In the high-risk subbasins, rainfall and overland flow wash estrogens off the land surface, either in solution (dissolved in water) or adsorbed to eroded soil particles. These contaminated flows then aggregate in stream channels (such as the Maungatea Stream on the western boundary of the farm).

8.3 Effectiveness of Best Management Practices (BMPs)

- **Constructed Wetlands**

Model outputs showed wetlands could retain between 50% and 90% of incoming sediment, cutting the sediment that reaches streams. This, in turn, reduces sediment-bound estrogen transport. Additionally, the wetland environment (waterlogged soils, abundant microbial activity, and vegetation) facilitated the removal of 30-70% of estrogens.

- **Riparian Buffer Strips**

The ArcSWAT simulations indicated that buffers typically reduced sediment transport by 16-80% across various subbasins (with an average reduction of ~42% in the most erosion-prone areas). Correspondingly, estrogen concentrations in runoff were reduced by roughly 30-70% in areas protected by buffers. The buffer strips also contributed to slowing down runoff flow (leading to ~10-30% runoff volume reduction locally),

- **Grazing Management**

The model scenario for improved grazing management resulted in an average ~17–18% reduction in sediment loss from pasture lands. The model also noted a modest reduction in total runoff volumes (~10-12% less runoff) under improved grazing, because healthier pasture cover enhances infiltration capacity and soil structure.

- **Effluent Application Management**

The ArcSWAT simulation for effluent best practices assumed that manure is applied only during drier conditions and at agronomic rates. Under this scenario, sediment loss was lowered by roughly 5-25% in areas affected by effluent irrigation. Runoff volumes in this scenario also dropped by approximately 10-30% in those subbasins, since irrigation inputs were better synchronized with soil moisture capacity (preventing oversaturation and immediate runoff). Integrated BMP Impact

Each BMP scenario was run independently to isolate its effects; however, the findings suggest that a combined approach would yield the greatest benefit. For instance, using riparian buffers in tandem with grazing controls can address both chronic and acute sources of sediment and estrogen. Meanwhile, constructed wetlands placed downstream of buffered and well-managed fields serve as a final barrier, polishing the water before it exits the farm. Recommendations

8.4 Policy Recommendations Based on Conclusions

The research outcomes have implications beyond the individual farm, informing how policies and regulations could be shaped to address estrogen pollution from agriculture on a broader scale. Policymakers and regulatory agencies are advised to consider the following:

- Environmental regulators should adopt spatially targeted strategies when designing water quality improvement programs.
- Given the demonstrated efficacy of riparian buffers, policies could mandate a minimum buffer strip along waterways in dairy farm areas. Governments might implement regulations requiring, say, a 5m native grass buffer on all dairy farms by a certain date.
- Revise and strengthen guidelines for dairy effluent management to explicitly consider hormone pollution. Currently, effluent guidelines often focus on nutrients; incorporating estrogen content as a factor would be prudent.
- Agencies and councils should consider developing water quality criteria or guidelines for estrogenic compounds in surface waters. While not yet common, establishing threshold concentrations for E1 and E2 that should not be exceeded in streams (to protect aquatic species) would drive action in catchments that are sources of these hormones. Education and Outreach

8.5 Future Modelling Improvements Recommendations

Incorporate Enhanced Degradation and Transformation Processes

Future versions of the catchment model should incorporate a more explicit representation of microbial degradation and hormonal transformations. In reality, E2 can convert to E1 in soils and water, and both can degrade into less active metabolites. The current ArcSWAT modelling used a simplified approach (reductions via BMP proxies and understanding of attenuation) due to software limitations.

Coupled Surface-Subsurface Modelling

The two modelling approaches in this study were kept separate for clarity, but future work could couple unsaturated zone and catchment models for a more holistic simulation. This could involve feeding the output of a field-scale leaching model (like the MATLAB model's percolation estimates) into the baseflow or shallow groundwater component of a watershed model. Such coupling would help examine scenarios where a fraction of estrogen does leach past the root zone and potentially enters shallow groundwater that later discharges to streams (via baseflow).

Field Validation and Calibration

A high priority for future research is to collect field data for model validation. This thesis assumed literature-based parameters for the catchment and soil model in the absence of field measurements. To build on this, field campaigns should be conducted to sample estrogen concentrations in soil profiles (at various depths) and in runoff at the edges of fields and within streams across different subbasins. By comparing such measurements with model predictions, we can calibrate model parameters (e.g., sorption coefficients, degradation rates, runoff partitioning of hormones) to better reflect site-specific conditions. Field validation will increase confidence in the model's accuracy and can reveal any processes the model may be missing.

Expansion of Model to Other Compounds and Scales

The modelling approaches here could be extended to other estrogenic compounds (such as progesterone, or synthetic hormones) or other farms and catchments to test their generality.

Scenario Analysis: Climate and Land Use Change

Incorporating scenario analysis for future conditions would be a valuable extension. Climate change projections suggest changes in rainfall patterns (potentially more intense storms), which could exacerbate runoff and preferential flow, thus affecting estrogen transport.

Model Interface and Usability

To encourage wider use, the complex models could be packaged into more user-friendly tools or guidelines. A simplified Excel-based calculator or GIS toolkit that farmers or consultants can use to estimate estrogen runoff risk from a given paddock (based on soil type, manure rate, and forecasted rain) would translate this research into a practical resource.

In conclusion, the research presented in this thesis has advanced our understanding of estrogen transport in agricultural landscapes through modelling at different scales.

References

A. Leonard, R., G. Knisel, W., & A. Still, D. (1987). GLEAMS: Groundwater Loading Effects of Agricultural Management Systems. Transactions of the ASAE, 30(5), 1403–1418. https://doi.org/10.13031/2013.30578

Adeel, M., Song, X., Wang, Y., Francis, D., & Yang, Y. (2017). Environmental impact of estrogens on human, animal and plant life: A critical review. Environment International, 99, 107–119. https://doi.org/10.1016/j.envint.2016.12.010

Ahaneku, I. E. (2014). Effect of land application of dairy effluent on soil physical and chemical properties. Research Journal of Pharmaceutical, Biological and Chemical Sciences, 5(3), 1669–1674.

Ahmed, M. B., Zhou, J. L., Ngo, H. H., Guo, W., & Chen, M. (2016). Progress in the preparation and application of modified biochar for improved contaminant removal from water and wastewater. Bioresource Technology, 214, 836–851. https://doi.org/10.1016/j.biortech.2016.05.057

Aislabie, J., McLeod, M., Ryburn, J., McGill, A., & Thornburrow, D. (2011). Soil type influences the leaching of microbial indicators under natural rainfall following application of dairy shed effluent. Soil Research, 49(3), 270–279.

Andaluri, G., Suri, R., & Kumar, K. (2011). Occurrence of Estrogen Hormones in Biosolids, Animal Manure and Mushroom Compost. Environmental Monitoring and Assessment, 184(2), 1197–1205. https://doi.org/10.1007/s10661-011-2032-8

Andersen, H., Siegrist, H., Halling-Sørensen, B., & Ternes, T. A. (2003). Fate of Estrogens in a Municipal Sewage Treatment Plant. Environmental Science & Technology, 37(18), 4021–4026. https://doi.org/10.1021/es026192a

Arable Research, F. (XXXX). Using dairy effluent to grow crops. Foundation for Arable Research.https://assets.far.org.nz/blog/files/fc15cdd7-50e1-510c-9e15-bf3cb74a83b6.pdf

Aris, A. Z., Shamsuddin, A. S., & Praveena, S. M. (2014). Occurrence of 17α-ethynylestradiol (EE2) in the environment and effect on exposed biota: A review. Environment International, 69, 104–119. https://doi.org/10.1016/j.envint.2014.04.011

Arnold, J. G., Srinivasan, R., Muttiah, R. S., & Williams, J. R. (1998). Large area hydrologic modelling and assessment part I: model development 1. JAWRA Journal of the American Water Resources Association, 34(1), 73–89.

Arnon, S., Dahan, O., Elhanany, S., Cohen, K., Pankratov, I., Gross, A., Ronen, Z., Baram, S., & Shore, L. S. (2008). Transport of Testosterone and Estrogen From Dairy-Farm Waste Lagoons to Groundwater. Environmental Science & Technology, 42(15), 5521–5526. https://doi.org/10.1021/es800784m

Arora, K., Mickelson, S. K., & Baker, J. L. (2003). Effectiveness of vegetated buffer strips in reducing pesticide transport in simulated runoff. Transactions of the ASAE, 46(3), 635.

Babaei, A. A., Lima, E. C., Takdastan, A., Alavi, N., Goudarzi, G., Vosoughi, M., Hassani, G., & Shirmardi, M. (2016). Removal of tetracycline antibiotic from contaminated water media by multi-walled carbon nanotubes: Operational variables, kinetics, and equilibrium studies. Water Science and Technology, 74(5), 1202–1216. https://doi.org/10.2166/wst.2016.301

Badgery, W. B., Millar, G. D., Broadfoot, K., Michalk, D. L., Cranney, P., Mitchell, D., & Ven, R. (2017). Increased production and cover in a variable native pasture following intensive grazing management. Animal Production Science, 57, 1812. https://doi.org/10.1071/AN15861

Bai, X., Casey, F. X. M., Hakk, H., DeSutter, T. M., Oduor, P. G., & Khan, E. (2015). Sorption and degradation of 17β-estradiol-17-sulfate in sterilized soil–water systems. Chemosphere, 119, 1322–1328. https://doi.org/10.1016/j.chemosphere.2014.02.016

Baldigo, B. P., George, S. D., Phillips, P. J., Hemming, J. D., Denslow, N. D., & Kroll, K. J. (2015). Potential estrogenic effects of wastewaters on gene expression in Pimephales promelas and fish assemblages in streams of southeastern New York. Environmental Toxicology and Chemistry, 34(12), 2803–2815. https://doi.org/10.1002/etc.3120

Barel-Cohen, K., Shore, L. S., Shemesh, M., Wenzel, A., Mueller, J., & Kronfeld-Schor, N. (2006). Monitoring of natural and synthetic hormones in a polluted river. Journal of Environmental Management, 78(1), 16–23. https://doi.org/10.1016/j.jenvman.2005.04.006

Barkle, G. F., Stenger, R., Singleton, P. L., & Painter, D. J. (2000). Effect of regular irrigation with dairy farm effluent on soil organic matter and soil microbial biomass. Australian Journal of Soil Research, 38(6), 1087–1097. https://doi.org/10.1071/SR99127

Baronti, C., Curini, R., D'Ascenzo, G., Di Corcia, A., Gentili, A., & Samperi, R. (2000). Monitoring Natural and Synthetic Estrogens at Activated Sludge Sewage Treatment Plants and in a Receiving River Water. Environmental Science & Technology, 34(24), 5059–5066. https://doi.org/10.1021/es001359q

Barry, D., & Sposito, G. (1989). Analytical solution of a convection-dispersion model with time-dependent transport coefficients. Water Resources Research, 25(12), 2407–2416.

Bartelt–Hunt, S. L., Snow, D. D., Kranz, W. L., Mader, T. L., Shapiro, C. A., Donk, S. J. v., Shelton, D. P., Tarkalson, D. D., & Zhang, T. C. (2012). Effect of Growth Promotants on the Occurrence of Endogenous and Synthetic Steroid Hormones on Feedlot Soils and in Runoff From Beef Cattle Feeding Operations. Environmental Science & Technology, 46(3), 1352–1360. https://doi.org/10.1021/es202680q

Belliss, S., Pairman, D., Dymond, J. R., Amies, A., Zoerner, J., Shepherd, J. J., Drewry, J. J., & North, H. (2019). Identification of high-risk agricultural activities: National mapping of the location, scale, and extent of winter forage cropping and intensive grazing on hill country land. Manaaki Whenua Landcare Research.

Benavidez, R., Jackson, B., Maxwell, D., & Norton, K. (2018). A review of the (Revised) Universal Soil Loss Equation ((R)USLE): With a view to increasing its global applicability and improving soil loss estimates. Hydrology and Earth System Sciences, 22, 6059–6086. https://doi.org/10.5194/hess-22-6059-2018

Berinde, V. (2004). Picard iteration converges faster than Mann iteration for a class of quasi-contractive operators. Fixed Point Theory and Applications, 2004(2), 716359. https://doi.org/10.1155/S1687182004311058

Betteridge, K., Mackay, A. D., Shepherd, T. G., Barker, D. J., Budding, P. J., Devantier, B. P., & Costall, D. A. (1999). Effect of cattle and sheep treading on surface configuration of a sedimentary hill soil. Soil Research, 37, 743. https://doi.org/10.1071/SR97014

Bilal, M., & Iqbal, H. M. N. (2019). Persistence and impact of steroidal estrogens on the environment and their laccase-assisted removal. Science of The Total Environment, 690, 447–459. https://doi.org/10.1016/j.scitotenv.2019.07.025

Bircher, P., Liniger, H. P., & Prasuhn, V. (2019). Comparing different multiple flow algorithms to calculate RUSLE factors of slope length. https://doi.org/10.1016/j.geomorph.2019.106850

Bircher, S., Card, M. L., Zhai, G., Chin, Y.-P., & Schnoor, J. L. (2015). Sorption, uptake, and biotransformation of 17β-estradiol, 17α-ethinylestradiol, zeranol, and trenbolone acetate by hybrid poplar. Environmental Toxicology and Chemistry, 34(12), 2906–2913. https://doi.org/10.1002/etc.3166

Biswas, S., Kranz, W. L., Shapiro, C. A., Snow, D. D., Bartelt-Hunt, S. L., Mamo, M., Tarkalson, D. D., Zhang, T. C., Shelton, D. P., van Donk, S. J., & Mader, T. L. (2017). Effect of rainfall timing and tillage on the transport of steroid hormones in runoff from manure

amended row crop fields. Journal of Hazardous Materials, 324, 436–447. https://doi.org/10.1016/j.jhazmat.2016.11.009

Bolan, N. S., Laurenson, S., Luo, J., & Sukias, J. (2009). Integrated treatment of farm effluents in New Zealand's dairy operations. Bioresource Technology, 100(22), 5490–5497. https://doi.org/10.1016/j.biortech.2009.03.004

Bonin, J. L., & Simpson, M. J. (2007). Sorption of Steroid Estrogens to Soil and Soil Constituents in Single- and Multi-sorbate Systems. Environmental Toxicology and Chemistry, 26(12), 2604–2610. https://doi.org/10.1897/07-118.1

Borrelli, P., Robinson, D. A., Fleischer, L. R., Lugato, E., Ballabio, C., Alewell, C., Meusburger, K., Modugno, S., Schütt, B., & Ferro, V. (2017). An assessment of the global impact of 21st century land use change on soil erosion. Nature Communications, 8(1), 1–13.

Bosznay, M. (1989). Generalization of SCS curve number method. Journal of Irrigation and Drainage Engineering, 115(1), 139–144.

Boughton, W. (1989). A review of the USDA SCS curve number method. Soil Research, 27(3), 511–523.

Bradley, P. M., Barber, L. B., Chapelle, F. H., Gray, J. L., Kolpin, D. W., & McMahon, P. B. (2009). Biodegradation of 17b-estradiol, estrone and testosterone in stream sediments. Environmental Science and Technology, 43(6), 1902–1910. https://doi.org/10.1021/es802797j

Burkitt, L. L., Winters, J. L., & Horne, D. J. (2017). Sediment and nutrient losses under winter cropping on two Manawatu hill country soils. Journal of New Zealand Grasslands, 79, 4.

Cameron, K. C., & Di, H. J. (2019). A new method to treat farm dairy effluent to produce clarified water for recycling and to reduce environmental risks from the land application of effluent. Journal of Soils and Sediments, 19(5), 2290–2302. https://doi.org/10.1007/s11368-018-02227-w

Card, M. L., Schnoor, J. L., & Chin, Y.-P. (2012). Uptake of Natural and Synthetic Estrogens by Maize Seedlings. Journal of Agricultural and Food Chemistry, 60(34), 8264–8271. https://doi.org/10.1021/jf3014074

Casey, F., Šimůnek, J., Lee, J., Larsen, G. L., & Hakk, H. (2005). Sorption, Mobility, and Transformation of Estrogenic Hormones in Natural Soil. Journal of Environmental Quality, 34(4), 1372–1379. https://doi.org/10.2134/jeq2004.0290

Casey, F. X. M., Larsen, G. L., Hakk, H., & Šimůnek, J. (2003). Fate and Transport of 17β-Estradiol in Soil−Water Systems. Environmental Science & Technology, 37(11), 2400–2409. https://doi.org/10.1021/es026153z

Casey, F. X. M., Simunek, J., Lee, J., Larsen, G. L., & Hakk, H. (2005). Sorption, mobility, and transformation of estrogenic hormones in natural soil. Journal of Environmental Quality, 34(4), 1372–1379. https://doi.org/10.2134/jeq2004.0290

Caupos, E., Mazellier, P., & Croue, J.-P. (2011). Photodegradation of estrone enhanced by dissolved organic matter under simulated sunlight. Water Research, 45(11), 3341–3350. https://doi.org/10.1016/j.watres.2011.03.047

Celia, M. A., Ahuja, L. R., & Pinder, G. F. (1987). Orthogonal collocation and alternating-direction procedures for unsaturated flow problems. Advances in Water Resources, 10(4), 178–187. https://doi.org/10.1016/0309-1708(87)90027-3

Chambers, K. B., Casey, F. X., Hakk, H., DeSutter, T. M., & Shappell, N. W. (2014). Potential bioactivity and association of 17b-estradiol with the dissolved and colloidal fractions of manure and soil. Science of the Total Environment, 494, 58–64. https://doi.org/10.1016/j.scitotenv.2014.06.121

Chiang, L., Chaubey, I., W. Gitau, M., & G. Arnold, J. (2010). Differentiating Impacts of Land Use Changes from Pasture Management in a CEAP Watershed Using the SWAT Model. Transactions of the ASABE, 53(5), 1569–1584. https://doi.org/10.13031/2013.34901

Choi, K. J., Kim, S. G., Kim, C. W., & Kim, S. H. (2005). Effects of activated carbon types and service life on removal of endocrine disrupting chemicals: Amitrol, nonylphenol, and bisphenol-A. Chemosphere, 58(11), 1535–1545. https://doi.org/10.1016/j.chemosphere.2004.11.080

Chow, V. T. (1965). Handbook of applied hydrology.

Chowdhury, R. R., Charpentier, P., & Ray, M. B. (2010). Photodegradation of Estrone in Solar Irradiation. Industrial & Engineering Chemistry Research, 49(15), 6923–6930. https://doi.org/10.1021/ie901796x

CHUN, S., LEE, J., GEYER, R., WHITE, D. C., & RAJ RAMAN, D. (2005). Effect of Agricultural Antibiotics on the Persistence and Transformation of 17β-Estradiol in a Sequatchie Loam. Journal of Environmental Science and Health, Part B, 40(5), 741–751. https://doi.org/10.1080/03601230500189691

Cichota, R., & Snow, V. O. (2009). Estimating nutrient loss to waterways—An overview of models of relevance to New Zealand pastoral farms. New Zealand Journal of Agricultural Research, 52(3), 239–260. https://doi.org/10.1080/00288230909510509

Clayden, B., & Webb, T. H. (1994). Criteria for defining the soilform: The fourth category of the New Zealand soil classification. Landcare Research Science Series). Landcare Research.

Climo, W. J., & Richardson, M. A. (1984). Factors affecting the susceptibility of three soils in the Manawatu to stock treading. New Zealand Journal of Agricultural Research, 27, 247–253. https://doi.org/10.1080/00288233.1984.10430426

Colborn, T., Saal, F. S., & Soto, A. M. (1994). Developmental effects of endocrine-disrupting chemicals in wildlife and humans. Environmental Impact Assessment Review, 14(5), 469–489. https://doi.org/10.1016/0195-9255(94)90014-0

Coles, C. A. (2007). Estimating retardation from the Freundlich isotherm for modelling contaminant transport. Engr. Mun. Ca, 6. https://www.engr.mun.ca/~ccoles/Publications/ICWEM-023.pdf

Colucci, M. S., Bork, H., & Topp, E. (2001). Persistence of Estrogenic Hormones in Agricultural Soils: I. 17β-Estradiol and Estrone. Journal of Environmental Quality, 30(6), 2070–2076. https://doi.org/10.2134/jeq2001.2070

Cook, F. J., Kelliher, F. M., & McMahon, S. D. (1994). Changes in Infiltration and Drainage during Wastewater Irrigation of a Highly Permeable Soil. 23(3), 476–482. https://doi.org/10.2134/jeq1994.00472425002300030010x

Council, T. R. (XXXX). Irrigation optimisation part 2: Production response – grazing management. Taranaki Regional Council. https://www.trc.govt.nz/assets/Documents/Environment/Freshwater/irrigation-optim-part2.pdf

Craggs, R. J., Sukias, J. P., Tanner, C. T., & Davies-Colley, R. J. (2004). Advanced pond system for dairy-farm effluent treatment. New Zealand Journal of Agricultural Research, 47(4), 449–460. https://doi.org/10.1080/00288233.2004.9513613

Dairy NZ. (2015). Feeding cows in spring.

DairyNZ. (2011). Guide to good irrigation: Part 1: Good irrigation practices on-farm.

DairyNZ. (2012). Passive systems for effluent solids separation.

DairyNZ. (2015). A farmer's guide to managing farm dairy effluent: A good practice guide for land application systems.

DairyNZ. (2016). New Zealand Dairy Staistics 2015-2016. DairyNZ Limited.

DairyNZ.(2020a).Feed management tools [WWW.Document. https://www.dairynz.co.nz/feed/feed-management-tools/

DairyNZ. (2020b). Pocket guide to determine soil risk for farm dairy effluent application. DairyNZ.https://www.dairynz.co.nz/media/0vphodby/pocket-guide-to-determine-soil-risk-for-farm-dairy-effluent-application-2020.pdf

DairyNZ. (2020c). Pocket guide to determine soil risk for farm dairy effluent application. DairyNZ.

DairyNZ. (2024). New Zealand Dairy Statistics 2023-24. DairyNZ Limited.

DairyNZ Irrigation scheduling. DairyNZ. https://www.dairynz.co.nz/environment/irrigation/scheduling/

D'Alessio, M., Vasudevan, D., Lichwa, J., Mohanty, S. K., & Ray, C. (2014). Fate and transport of selected estrogen compounds in Hawaii soils: Effect of soil type and macropores. Journal of Contaminant Hydrology, 166, 1–10. https://doi.org/10.1016/j.jconhyd.2014.07.006

Das, B. S., Lee, L., Rao, P. S. C., & Hultgren, R. P. (2004). Sorption and Degradation of Steroid Hormones in Soils During Transport: Column Studies and Model Evaluation. Environmental Science & Technology, 38(5), 1460–1470. https://doi.org/10.1021/es034898e

De Moura, C. A., & Kubrusly, C. S. (Eds.). (2013). The Courant–Friedrichs–Lewy (CFL) Condition: 80 Years After Its Discovery. Birkhäuser Boston. https://doi.org/10.1007/978-0-8176-8394-8

Delage, P., & Lefebvre, G. (1984). Study of the structure of a sensitive Champlain clay and of its evolution during consolidation. Canadian Geotechnical Journal, 21, 21–35. https://doi.org/10.1139/t84-003

Deng, Y., & Zhao, R. (2015). Advanced Oxidation Processes (AOPs) in Wastewater Treatment. Current Pollution Reports, 1(3), 167–176. https://doi.org/10.1007/s40726-015-0015-z

Desmet, P. J., & Govers, G. (1996). A GIS procedure for automatically calculating the USLE LS factor on topographically complex landscape units. Journal of Soil and Water Conservation, 51(5), 427–433.

Diamanti-Kandarakis, E., Bourguignon, J.-P., Giudice, L. C., Hauser, R., Prins, G. S., Soto, A. M., Zoeller, R. T., & Gore, A. C. (2009). Endocrine-disrupting chemicals: An Endocrine Society scientific statement. Endocrine Reviews, 30(4), 293–342. https://doi.org/10.1210/er.2009-0002

DJ Houlbrooke, RM Monaghan, & M McLeod. (2010). Matching farmdairy effluent storage requirementsand management practicesto soil and landscape features.

Doetterl, S., Oost, K., & Six, J. (2012). Towards constraining the magnitude of global agricultural sediment and soil organic carbon fluxes. Earth Surface Processes and Landforms, 37, 642–655. https://doi.org/10.1002/esp.3198

Donovan, M. (2022). Modelling soil loss from surface erosion at high-resolution to better understand sources and drivers across land uses and catchments; a national-scale assessment of Aotearoa, New Zealand. Environmental Modelling & Software, 147, 105228. https://doi.org/10.1016/j.envsoft.2021.105228

Donovan, M., & Monaghan, R. (2021). Impacts of grazing on ground cover, soil physical properties and soil loss via surface erosion: A novel geospatial modelling approach. Journal of Environmental Management, 287, 112206.

Dosskey, M. G., Vidon, P., Gurwick, N. P., Allan, C. J., Duval, T. P., & Lowrance, R. (2010). The Role of Riparian Vegetation in Protecting and Improving Chemical Water Quality in Streams. JAWRA Journal of the American Water Resources Association, 46(2), 261–277. https://doi.org/10.1111/j.1752-1688.2010.00419.x

Drewry, J. J. (2006). Natural recovery of soil physical properties from treading damage of pastoral soils in New Zealand and Australia: A review. Agriculture, Ecosystems & Environment, 114, 159–169. https://doi.org/10.1016/j.agee.2005.11.028

Drewry, J. J., Cameron, K. C., & Buchan, G. D. (2008). Pasture yield and soil physical property responses to soil compaction from treading and grazing—A review. Soil Research, 46, 237. https://doi.org/10.1071/SR07125

Drost, F., Renwick, J., Bhaskaran, B., Oliver, H., & McGregor, J. (2006). Simulation of New Zealand's Climate Using a High-resolution Nested Regional Climate Model. International Journal of Climatology. https://doi.org/10.1002/joc.1461

Drost, F., Renwick, J., Bhaskaran, B., Oliver, H., & Williams, M. (2007). A simulation of New Zealand's climate during the Last Glacial Maximum. Quaternary Science Reviews, 26(17–18), 2508–2525. https://doi.org/10.1016/j.quascirev.2007.06.005

Dutta, S., Inamdar, S., Tso, J., Aga, D. S., & Sims, J. T. (2010). Free and conjugated estrogen exports in surface-runoff from poultry litter-amended soil. Journal of Environmental Quality, 39(5), 1688–1698. https://doi.org/10.2134/jeq2009.0339

Dutta, S., Inamdar, S., Tso, J., Aga, D. S., & Sims, J. T. (2012). Dissolved Organic Carbon and Estrogen Transport in Surface Runoff From Agricultural Land Receiving Poultry Litter1. Jawra Journal of the American Water Resources Association, 48(3), 558–569. https://doi.org/10.1111/j.1752-1688.2011.00634.x

Dymond, J. R., Betts, H. D., & Schierlitz, C. S. (2010). An erosion model for evaluating regional land-use scenarios. Environmental Modelling & Software, 25, 289–298. https://doi.org/10.1016/j.envsoft.2009.09.011

Dymond, J. R., Herzig, A., Basher, L., Betts, H. D., Marden, M., Phillips, C. J., Ausseil, A.-G. E., Palmer, D. J., Clark, M., & Roygard, J. (2016). Development of a New Zealand SedNet model for assessment of catchment-wide soil-conservation works. Geomorphology, 257, 85–93. https://doi.org/10.1016/j.geomorph.2015.12.022

Elliot, A. H., Alexander, R. B., Schwarz, G. E., Shankar, U., Sukias, J. P. S., & McBride, G. B. (2005). Estimation of nutrient sources and transport for New Zealand using the hybrid mechanistic-statistical model SPARROW. Journal of Hydrology New Zealand, 44(1), 1–27.

Environment, M., & NZ, S. (2019). In Environment Aotearoa 2019 (New Zealand's Environmental Reporting Series No. ME 1416. Ministry for the Environment & Stats NZ.

Ermawati, R., Morimura, S., Tang, Y., Liu, K., & Kida, K. (2007). Degradation and behavior of natural steroid hormones in cow manure waste during biological treatments and ozone oxidation. Journal of Bioscience and Bioengineering, 103(1), 27–31. https://doi.org/10.1263/jbb.103.27

Fan, Z., Casey, F., Hakk, H., & Larsen, G. L. (2008a). Modelling Coupled Degradation, Sorption, and Transport of 17β-estradiol in Undisturbed Soil. Water Resources Research, 44(8). https://doi.org/10.1029/2007wr006407

Fan, Z., Casey, F., Hakk, H., & Larsen, G. L. (2008b). Modelling Coupled Degradation, Sorption, and Transport of 17β-estradiol in Undisturbed Soil. Water Resources Research, 44(8). https://doi.org/10.1029/2007wr006407

Fan, Z., Casey, F. X., Hakk, H., & Larsen, G. L. (2007a). Persistence and fate of 17b-estradiol and testosterone in agricultural soils. Chemosphere, 67(5), 886–895. https://doi.org/10.1016/j.chemosphere.2006.11.040

Fan, Z., Casey, F. X. M., Hakk, H., & Larsen, G. L. (2007b). Persistence and fate of 17β-estradiol and testosterone in agricultural soils. Chemosphere, 67(5), 886–895. https://doi.org/10.1016/j.chemosphere.2006.11.040

Farthing, M. W., & Ogden, F. L. (2017). Numerical Solution of Richards' Equation: A Review of Advances and Challenges. Soil Science Society of America Journal, 81(6), 1257–1269. https://doi.org/10.2136/sssaj2017.02.0058

Faycal Bouraoui, & Theo A. Dillaha. (1996). ANSWERS-2000: Runoff and Sediment Transport Model. 122(6), 493–502. https://doi.org/doi:10.1061/(ASCE)0733-9372(1996)122:6(493)

Fenner-Crisp, P. A., Maciorowski, A. F., & Timm, G. E. (2000). The endocrine disruptor screening program developed by the US Environmental Protection Agency. Ecotoxicology, 9, 85–91.

Finlayson, J. D., Betteridge, K., Mackay, A., Thorrold, B., Singleton, P., & Costall, D. A. (2002). A simulation model of the effects of cattle treading on pasture production on North Island, New Zealand, hill land. New Zealand Journal of Agricultural Research, 45, 255–272. https://doi.org/10.1080/00288233.2002.9513516

Foote, K. J., Joy, M. K., & Death, R. G. (2015). New Zealand Dairy Farming: Milking Our Environment for All Its Worth. Environmental Management, 56(3), 709–720. https://doi.org/10.1007/s00267-015-0517-x

Gadd, J. B., Northcott, G. L., & Tremblay, L. A. (2010). Passive Secondary Biological Treatment Systems Reduce Estrogens in Dairy Shed Effluent. Environmental Science & Technology, 44(19), 7601–7606. https://doi.org/10.1021/es1008054

Gadd, J. B., Tremblay, L. A., & Northcott, G. L. (2010). Steroid estrogens, conjugated estrogens and estrogenic activity in farm dairy shed effluents. Environmental Pollution, 158(3), 730–736. https://doi.org/10.1016/j.envpol.2009.10.015

Gadd, J., Tremblay, L. A., & Northcott, G. L. (2010). Steroid Estrogens, Conjugated Estrogens and Estrogenic Activity in Farm Dairy Shed Effluents. Environmental Pollution, 158(3), 730–736. https://doi.org/10.1016/j.envpol.2009.10.015

Gall, H. E., Sassman, S. A., Lee, L. S., & Jafvert, C. T. (2011). Hormone Discharges from a Midwest Tile-Drained Agroecosystem Receiving Animal Wastes. Environmental Science & Technology, 45(20), 8755–8764. https://doi.org/10.1021/es2011435

Gineys, N., Giroud, B., Gineys, M., & Vulliet, E. (2012). Retention of Selected Steroids on a Silt-Loam Soil. Journal of Environmental Science and Health Part A, 47(13), 2133–2140. https://doi.org/10.1080/10934529.2012.696021

Goeppert, N., Dror, I., & Berkowitz, B. (2016). Spatial and Temporal Distribution of Free and Conjugated Estrogens During Soil Column Transport. Clean - Soil Air Water, 45(2). https://doi.org/10.1002/clen.201600048

Goeury, K., Munoz, G., Vo Duy, S., Prévost, M., & Sauvé, S. (2022). Occurrence and seasonal distribution of steroid hormones and bisphenol A in surface waters and suspended

sediments of Quebec, Canada. Environmental Advances, 8, 100199. https://doi.org/10.1016/j.envadv.2022.100199

Gomes, F. B. R., Fernandes, P. A. A., Bottrel, S. E. C., Brandt, E. M. F., & Pereira, R. de O. (2022). Fate, occurrence, and removal of estrogens in livestock wastewaters. Water Science and Technology: A Journal of the International Association on Water Pollution Research, 86(4), 814–833. https://doi.org/10.2166/wst.2022.238

Gradwell, M. W. (1960). Changes in pore-space of a pasture topsoil under animal treading. New Zealand Journal of Agricultural Research, 3, 663–674.

Green, W. H., & Ampt, G. A. (1911). Studies on Soil Phyics. The Journal of Agricultural Science, 4(1), 1–24. https://doi.org/10.1017/S0021859600001441

Greenwood, K. L., & McKenzie, B. M. (2001). Grazing effects on soil physical properties and the consequences for pastures: A review. Australian Journal of Experimental Agriculture, 41, 1231. https://doi.org/10.1071/EA00102

Guillette, L. J., & Gunderson, M. P. (2001). Alterations in development of reproductive and endocrine systems of wildlife populations exposed to endocrine-disrupting contaminants. Reproduction (Cambridge, England), 122(6), 857–864. https://doi.org/10.1530/rep.0.1220857

Hakk, H., Sikora, L., & Casey, F. X. M. (2018). Fate of estrone in laboratory-scale constructed wetlands. Ecological Engineering, 111, 60–68. https://doi.org/10.1016/j.ecoleng.2017.11.005

Hancock, G., Ovenden, M., Sharma, K., Rowlands, W., Gibson, A., & Wells, T. (2020). Soil erosion–The impact of grazing and regrowth trees. Geoderma, 361, 114102.

Hanselman, T. A., Graetz, D. A., & Wilkie, A. C. (2003). Manure-Borne Estrogens as Potential Environmental Contaminants: A Review. Environmental Science & Technology, 37(24), 5471–5478. https://doi.org/10.1021/es034410+

Hansen, M., Krogh, K. A., Halling-Sørensen, B., & Björklund, E. (2011). Determination of Ten Steroid Hormones in Animal Waste Manure and Agricultural Soil Using Inverse and Integrated Clean-Up Pressurized Liquid Extraction and Gas Chromatography-Tandem Mass Spectrometry. Analytical Methods, 3(5), 1087. https://doi.org/10.1039/c1ay00007a

Harvey, B. E. (2019). Development of coupled processes numerical models of tracer, colloid and radionuclide transport in field migration experiments [PhD Thesis, University of Birmingham]. https://etheses.bham.ac.uk/id/eprint/9128/

Hawke, R. M., & Summers, S. A. (2003). Land application of farm dairy effluent: Results from a case study, Wairarapa, New Zealand. New Zealand Journal of Agricultural Research, 46(4), 339–346. https://doi.org/10.1080/00288233.2003.9513562

Hawke, R. M., & Summers, S. A. (2006). Effects of land application of farm dairy effluent on soil properties: A literature review. New Zealand Journal of Agricultural Research, 49(3), 307–320. https://doi.org/10.1080/00288233.2006.9513721

Heber Green, W., & Ampt, G. A. (1911). Studies on Soil Phyics. The Journal of Agricultural Science, 4(1), 1–24. Cambridge Core. https://doi.org/10.1017/S0021859600001441

Heindel, J. J., Newbold, R., & Schug, T. T. (2015). Endocrine disruptors and obesity. Nature Reviews Endocrinology, 11(11), 653–661. https://doi.org/10.1038/nrendo.2015.163

Hewitt, A. E. (1993). New Zealand soil classification.

Hewitt, A. E., & Shepherd, T. G. (1997). Structural vulnerability of New Zealand soils. Soil Research, 35, 461. https://doi.org/10.1071/S96074

Hickey, C. W., Quinn, J. M., & Davies-Colley, R. J. (1989). Effluent characteristics of dairy shed oxidation ponds and their potential impacts on rivers. New Zealand Journal of Marine and Freshwater Research, 23(4), 569–584. https://doi.org/10.1080/00288330.1989.9516393

Hildebrand, C., Londry, K. L., & Farenhorst, A. (2006). Sorption and Desorption of Three Endocrine Disrupters in Soils. Journal of Environmental Science and Health Part B, 41(6), 907–921. https://doi.org/10.1080/03601230600806020

Hirschman, D., Collins, K., & Schueler, T. (2008). Technical memorandum: The runoff reduction method. Center for Watershed Protection, 8390.

Hoffman, T. C., Zitomer, D. H., & McNamara, P. J. (2016). Pyrolysis of wastewater biosolids significantly reduces estrogenicity. Journal of Hazardous Materials, 317, 579–584. https://doi.org/10.1016/j.jhazmat.2016.05.088

Houlbrooke, D. J., Drewry, J. J., Monaghan, R. M., Paton, R. J., Smith, L. C., & Littlejohn, R. P. (2009). Grazing strategies to protect soil physical properties and maximise pasture yield on a Southland dairy farm. New Zealand Journal of Agricultural Research, 52, 323–336. https://doi.org/10.1080/00288230909510517

Houlbrooke, D. J., Horne, D. J., Hedley, M. J., Hanly, J. A., & Snow, V. O. (2004). A review of literature on the land treatment of farm-dairy effluent in New Zealand and its impact on water quality. New Zealand Journal of Agricultural Research, 47(4), 499–511. https://doi.org/10.1080/00288233.2004.9513617

Houlbrooke, D. J., Longhurst, R. D., & Laurenson, S. (2011). Characterising dairy manures and slurries. Envirolink Tools Project. https://www.envirolink.govt.nz/assets/Envirolink/R5-4-Characterising-Dairy-Manures-and-Slurries.pdf

Houlbrooke, D. J., Paton, R. J., Littlejohn, R. P., & Morton, J. D. (2011). Land-use intensification in New Zealand: Effects on soil properties and pasture production. Journal of Agricultural Science, 149, 337–349. https://doi.org/10.1017/S0021859610000821

Hu, W., Tabley, F., Beare, M., Tregurtha, C., Gillespie, R., Qiu, W., & Gosden, P. (2018). Short-term dynamics of soil physical properties as affected by compaction and tillage in a silt loam soil. Vadose Zone Journal, 17, 180115. https://doi.org/10.2136/vzj2018.06.0115

Huang, Y., Li, W., Qin, L., Xie, X., Gao, B., Sun, J., & Li, A. (2019). Distribution of endocrine-disrupting chemicals in colloidal and soluble phases in municipal secondary effluents and their removal by different advanced treatment processes. Chemosphere, 219, 730–739. https://doi.org/10.1016/j.chemosphere.2018.11.201

ITPS, F. and. (2015). Status of the world's soil resources (SWSR)—Main report. Food and Agriculture Organization of the United Nations and Intergovernmental Technical Panel on Soils, 650.

Jamal Abu-Ashour, Douglas M. Joy, Hung Lee, Hugh R. Whiteley, & Samuel Zelin. (1994). Transport of microorganisms through soil. Water, Air, and Soil Pollution, 75(1–2), 141–158.

Jenkins, M. B., Endale, D. M., Schomberg, H. H., & Sharpe, R. R. (2006). Fecal bacteria and sex hormones in soil and runoff from cropped watersheds amended with poultry litter. Science of the Total Environment, 358(1), 164–177. https://doi.org/10.1016/j.scitotenv.2005.04.015

Jenkins, M. B., Truman, C. C., Siragusa, G., Line, E., Bailey, J. S., Frye, J., & Sharpe, R. R. (2008). Rainfall and tillage effects on transport of fecal bacteria and sex hormones 17b-estradiol and testosterone from broiler litter applications to a Georgia Piedmont Ultisol. Science of the Total Environment, 403(1), 154–163. https://doi.org/10.1016/j.scitotenv.2008.05.014

Johnson, A. C., Belfroid, A., & Di Corcia, A. (2000). Estimating steroid oestrogen inputs into activated sludge treatment works and observations on their removal from the effluent. Science of The Total Environment, 256(2), 163–173. https://doi.org/10.1016/S0048-9697(00)00481-2

Johnson, A. C., Williams, R. J., & Matthiessen, P. (2006). The potential steroid hormone contribution of farm animals to freshwaters, the United Kingdom as a case study. Science of The Total Environment, 362(1), 166–178. https://doi.org/10.1016/j.scitotenv.2005.06.014

Joseph, L., Heo, J., Park, Y.-G., Flora, J. R. V., & Yoon, Y. (2011). Adsorption of bisphenol A and 17α-ethinyl estradiol on single walled carbon nanotubes from seawater and brackish water. Desalination, 281, 68–74. https://doi.org/10.1016/j.desal.2011.07.044

Kale, R. V., & Sahoo, B. (2011). Green-Ampt Infiltration Models for Varied Field Conditions: A Revisit. Water Resources Management, 25(14), 3505–3536. https://doi.org/10.1007/s11269-011-9868-0

Kaluarachchi, J. J., & Morshed, J. (1995). Critical assessment of the operator-splitting technique in solving the advection-dispersion-reaction equation: 1. First-order reaction. Advances in Water Resources, 18(2), 89–100.

Katou, H., Miyaji, K., & Kubota, T. (1987). Susceptibility of undisturbed soils to compression as evaluated from the changes in the soil water characteristic curves. Soil Science and Plant Nutrition, 33, 539–554. https://doi.org/10.1080/00380768.1987.10557603

Khanal, S. K., Xie, B., Thompson, M. L., Sung, S., Ong, S. K., & Leeuwen, J. v. (2006). Fate, Transport, and Biodegradation of Natural Estrogens in the Environment and Engineered Systems. Environmental Science & Technology, 40(21), 6537–6546. https://doi.org/10.1021/es0607739

Kim, S. D., Cho, J., Kim, I. S., Vanderford, B. J., & Snyder, S. A. (2007). Occurrence and removal of pharmaceuticals and endocrine disruptors in South Korean surface, drinking, and waste waters. Water Research, 41(5), 1013–1021. https://doi.org/10.1016/j.watres.2006.06.034

Klik, A., Haas, K., & Dvorackova, A. (2015). Spatial and temporal distribution of rainfall erosivity in New Zealand. Soil Research, 53, 815. https://doi.org/10.1071/SR14363

Klinar, D. (2016). Universal model of slow pyrolysis technology producing biochar and heat from standard biomass needed for the techno-economic assessment. Bioresource Technology, 206, 112–120. https://doi.org/10.1016/j.biortech.2016.01.053

Koh, Y. K. K., Chiu, T. Y., Boobis, A., Cartmell, E., Scrimshaw, M. D., & Lester, J. N. (2008). TREATMENT AND REMOVAL STRATEGIES FOR ESTROGENS FROM WASTEWATER. Environmental Technology, 29(3), 245–267. https://doi.org/10.1080/09593330802099122

Kopperi, M., Parshintsev, J., Ruiz-Jimenez, J., & Riekkola, M.-L. (2016). Nontargeted Evaluation of the Fate of Steroids During Wastewater Treatment by Comprehensive Two-Dimensional Gas Chromatography–time-of-Flight Mass Spectrometry. Environmental Science and Pollution Research, 23(17), 17008–17017. https://doi.org/10.1007/s11356-016-6800-4

KREISS, H.-O., & SCHERER, G. (1974). Finite Element and Finite Difference Methods for Hyperbolic Partial Differential Equations. In C. de Boor (Ed.), Mathematical Aspects of Finite Elements in Partial Differential Equations (pp. 195–212). Academic Press. https://doi.org/10.1016/B978-0-12-208350-1.50012-1

Kumar, S., Udawatta, R. P., Anderson, S. H., & Mudgal, A. (2010). APEX model simulation of runoff and sediment losses for grazed pasture watersheds with agroforestry buffers. Agroforestry Systems, 83(1). https://doi.org/10.1007/s10457-010-9350-7

Kuok, K. K., Mah, D. Y., & Chiu, P. (2013). Evaluation of C and P factors in universal soil loss equation on trapping sediment: Case study of Santubong River. Journal of Water Resource and Protection, 2013.

Laegdsmand, M., Andersen, H., Jacobsen, O. H., & Halling-Sørensen, B. (2009). Transport and fate of estrogenic hormones in slurry-treated soil monoliths. Journal of Environmental Quality, 38(3), 955–964. https://doi.org/10.2134/jeq2007.0569

Lambert, M. G., Devantler, B. P., Nes, P., & Penny, P. E. (1985). Losses of nitrogen, phosphorus, and sediment in runoff from hill country under different fertiliser and grazing management regimes. New Zealand Journal of Agricultural Research, 28, 371–379. https://doi.org/10.1080/00288233.1985.10430441

Ledgard S F, Williams P H, Broom F D, Thorrold B S, Wheeler D M, & Willis V J. (1999). OVERSEER™—A nutrient budgeting model for pastoral farming, wheat, potatoes, apples and kiwifruit. In Best soil management practices for production (pp. 143–152).

Lee, L. S., Strock, T. J., Sarmah, A. K., & Rao, P. S. C. (2003). Sorption and Dissipation of Testosterone, Estrogens, and Their Primary Transformation Products in Soils and Sediment. Environmental Science & Technology, 37(18), 4098–4105. https://doi.org/10.1021/es020998t

Lee, L., Strock, T. J., Sarmah, A. K., & Rao, P. S. C. (2003). Sorption and Dissipation of Testosterone, Estrogens, and Their Primary Transformation Products in Soils and Sediment. Environmental Science & Technology, 37(18), 4098–4105. https://doi.org/10.1021/es020998t

LeVeque, R. J. (1998). Finite difference methods for differential equations. Draft Version for Use in AMath, 585(6), 112.

Liu, S., Ying, G., Zhang, R., Zhou, L., Lai, H., & Chen, Z. F. (2012). Fate and Occurrence of Steroids in Swine and Dairy Cattle Farms With Different Farming Scales and Wastes Disposal Systems. Environmental Pollution, 170, 190–201. https://doi.org/10.1016/j.envpol.2012.07.016

Liu, Z., Kanjo, Y., & Mizutani, S. (2009). Removal mechanisms for endocrine disrupting compounds (EDCs) in wastewater treatment—Physical means, biodegradation, and chemical advanced oxidation: A review. Science of The Total Environment, 407(2), 731–748. https://doi.org/10.1016/j.scitotenv.2008.08.039

Loch, R. J., Robotham, B. G., Zeller, L., Masterman, N., Orange, D. N., Bridge, B. J., Sheridan, G., & Bourke, J. J. (2001). A multi-purpose rainfall simulator for field infiltration and erosion studies. Soil Research, 39(3), 599–610. https://doi.org/10.1071/sr00039

Lucas, S. D., & Jones, D. L. (2009). Urine enhances the leaching and persistence of estrogens in soils. Soil Biology and Biochemistry, 41(2), 236–242. https://doi.org/10.1016/j.soilbio.2008.10.022

Maciver, A. (2023, September 5). Dairy's contribution to NZ. NZ Dairy Exporter. https://dairyexporter.co.nz/dairys-contribution-to-nz/

Maeng, S. K. (2023). Multiple Objective Treatment Aspects of Bank Filtration. https://doi.org/10.1201/9781003419846

Mahjoub, O., Escande, A., Rosain, D., Casellas, C., Gómez, E., & Fenet, H. (2011). Estrogen-Like and Dioxin-Like Organic Contaminants in Reclaimed Wastewater: Transfer to Irrigated Soil and Groundwater. Water Science & Technology, 63(8), 1657–1662. https://doi.org/10.2166/wst.2011.322

Marfurt, K. J. (1984). Accuracy of finite-difference and finite-element modelling of the scalar and elastic wave equations. GEOPHYSICS, 49(5), 533–549. https://doi.org/10.1190/1.1441689

Mastersizer | Laser Diffraction Particle Size Analyzers | Malvern Panalytical. (n.d.). @dkshgroup. Retrieved February 27, 2025, from //www.dksh.com/global-en/products/ins/malvernpanalytical-mastersizer-range

Mathew, K. R. (2021). A Field-Scale Study of Controlled Tile Drainage and a Pond-Wetland to Attenuate Nutrients from Agricultural Overland Runoff and Subsurface Drainage on a Farmer-Operated Seed Farm in Saint-Isidore, ON [PhD Thesis, Université

d'Ottawa/University of Ottawa]. https://ruor.uottawa.ca/items/0039f27d-23a2-4c22-8861-723496fc6554

Matsuoka, S., Kikuchi, M., Kimura, S., Kurokawa, Y., & Kawai, S. (2005). Determination of Estrogenic Substances in the Water of Muko River Using <I>in Vitro</I> Assays, and the Degradation of Natural Estrogens by Aquatic Bacteria. Journal of Health Science, 51(2), 178–184. https://doi.org/10.1248/jhs.51.178

Mayer, P. M., Reynolds, S. K., McCutchen, M. D., & Canfield, T. J. (2007). Meta-analysis of nitrogen removal in riparian buffers. Journal of Environmental Quality, 36(4), 1172–1180. https://doi.org/10.2134/jeq2006.0462

Mbagwu, J. S. C. (1989). Effects of organic amendments on some physical properties of a tropical ultisol. Biological Wastes, 28(1), 1–13. https://doi.org/10.1016/0269-7483(89)90044-X

McDowell, R. W., Drewry, J. J., Muirhead, R. W., & Paton, R. J. (2003). Cattle treading and phosphorus and sediment loss in overland flow from grazed cropland. Soil Research, 41, 1521. https://doi.org/10.1071/SR03042

McDowell, R. W., van der Weerden, T. J., & Campbell, J. (2011). Nutrient losses associated with irrigation, intensification and management of land use: A study of large scale irrigation in North Otago, New Zealand. Agricultural Water Management, 98(5), 877–885. https://doi.org/10.1016/j.agwat.2010.12.014

McDowell, R., & Wilcock, R. (2008). Water quality and the effects of different pastoral animals. New Zealand Veterinary Journal, 56, 289–296. https://doi.org/10.1080/00480169.2008.36849

McLeod, M., Aislabie, J., McGill, A., Rhodes, P., Hunter, D. W. F., & Thornburrow, D. (2019). Mapping the potential risk of Escherichia coli leaching through soils of the Waikato River catchment, New Zealand. Soil Research, 57(2), 132–148.

Mean, P. E., & Efficiencies, B. P. R. (2006). Pennsylvania stormwater best management practices manual. Harrisburg: Pennsylvania Department of Environmental Protection. https://www …. https://www.dep.state.pa.us/dep/subject/advcoun/stormwater/Manual_DraftJan05/Appendix-A-jan-rev.pdf

Mein, R. G., & Larson, C. L. (1973). Modelling infiltration during a steady rain. Water Resources Research, 9(2), 384–394. https://doi.org/10.1029/WR009i002p00384

Michael Dunbier, Hamish Brown, Doug Edmeades, Reece Hill, & Alister Metherell. (2013). A peer review of OVERSEER® in relation to modelling nutrient flows in arable crops. The Foundation for Arable Research.

Mina, O., Gall, H. E., Saporito, L. S., & Kleinman, P. J. A. (2016). Estrogen Transport in Surface Runoff From Agricultural Fields Treated With Two Application Methods of Dairy Manure. Journal of Environmental Quality, 45(6), 2007–2015. https://doi.org/10.2134/jeq2016.05.0173

Minea, G., Mititelu-Ionuș, O., Gyasi-Agyei, Y., Ciobotaru, N., & Rodrigo-Comino, J. (2022). Impacts of Grazing by Small Ruminants on Hillslope Hydrological Processes: A Review of European Current Understanding. Water Resources Research, 58(3), e2021WR030716. https://doi.org/10.1029/2021WR030716

Ministry for Primary Industries. (2024, February 19). Information on dairy farming systems: Determining feed eaten by New Zealand dairy cows 1990-2020 through combining data sets. Ministry for Primary Industries. https://www.mpi.govt.nz/dmsdocument/61051-Information-on-dairy-farming-systems-Determining-Feed-Eaten-by-New-Zealand-Dairy-Cows-1990-2020-through-Combining-Data-Sets

Ministry for the Environment. (2024). New Zealand Government. https://environment.govt.nz/publications/national-policy-statement-for-freshwater-management-2020-amended-october-2024/

Mitasova, H., Hofierka, J., Zlocha, M., & Iverson, L. R. (1996). Modelling topographic potential for erosion and deposition using GIS. International Journal of Geographical Information Systems, 10(5), 629–641.

Monaghan, R., Cecile A. M. de Klein, & Muirhead, R. W. (2008). Prioritisation of Farm Scale Remediation Efforts for Reducing Losses of Nutrients and Faecal Indicator Organisms to Waterways: A Case Study of New Zealand Dairy Farming. Journal of Environmental Management, 87(4), 609–622. https://doi.org/10.1016/j.jenvman.2006.07.017

Monaghan, R. M., Laurenson, S., Dalley, D. E., & Orchiston, T. S. (2017). Grazing strategies for reducing contaminant losses to water from forage crop fields grazed by cattle during winter. New Zealand Journal of Agricultural Research, 60, 333–348. https://doi.org/10.1080/00288233.2017.1345763

Monaghan, R. M., & Smith, L. C. (2004). Minimising surface water pollution resulting from farm-dairy effluent application to mole-pipe drained soils. II. The contribution of preferential flow of effluent to whole-farm pollutant losses in subsurface drainage from

a West Otago dairy farm. New Zealand Journal of Agricultural Research, 47(4), 417–428. https://doi.org/10.1080/00288233.2004.9513610

MPI. (2024). Farm dairy requirements. https://www.mpi.govt.nz/agriculture/dairy-farming/farm-dairy-requirements/

Nearing, M. A., Jetten, V., Baffaut, C., Cerdan, O., Couturier, A., Hernandez, M., Le Bissonnais, Y., Nichols, M. H., Nunes, J. P., Renschler, C. S., Souchère, V., & Oost, K. (2005). Modelling response of soil erosion and runoff to changes in precipitation and cover. CATENA, 61, 131–154. https://doi.org/10.1016/j.catena.2005.03.007

Neitsch, S., Arnold, J., Kinry, J. R., & Williams, J. R. (2011). Soil and water assessment tool theoretical documentation version 2009 (No. 406; Report, p. 647).

Newsome, P., Wilde, R. H., & Willoughby, E. J. (2008). Land Resource Information System Spatial Data Layers (Data Dictionary. Landcare Research.

Nghiem, L. D., Manis, A., Soldenhoff, K., & Schäfer, A. I. (2004). Estrogenic hormone removal from wastewater using NF/RO membranes. Journal of Membrane Science, 242(1), 37–45. https://doi.org/10.1016/j.memsci.2003.12.034

NIWA. (2012). National and regional climate maps | NIWA. https://niwa.co.nz/climate-and-weather/national-and-regional-climate-maps

Pagsuyoin, S. A., Lung, W. S., & Colosi, L. M. (2012). Predicting EDC concentrations in a river mixing zone. Chemosphere, 87(10), 1111–1118. https://doi.org/10.1016/j.chemosphere.2012.02.004

Panagos, P., Borrelli, P., & Meusburger, K. (2015). A new European slope length and steepness factor (LS-Factor) for modelling soil erosion by water. Geosciences, 5, 117–126. https://doi.org/10.3390/geosciences5020117

Parker, W. J. (1998). Standardisation between livestock classes: The use and misuse of the stock unit system. Proceedings of the New Zealand Grassland Association, 243–248.

Peskin, C. S., & Schlick, T. (1989). Molecular dynamics by the Backward-Euler method. Communications on Pure and Applied Mathematics, 42(7), 1001–1031. https://doi.org/10.1002/cpa.3160420706

Peterson, E. W., Wicks, C. M., & Kelley, C. A. (2005). Persistence of 17 β-Estradiol in Water and Sediment-Pore Water from Cave Streams in Central Missouri. Environmental and Engineering Geoscience, 11(3), 221–228. https://doi.org/10.2113/11.3.221

Plenty Regional Council, B. (XXXX). A guide to managing farm dairy effluent. Bay of Plenty Regional Council.

Prater, J. (2012). The impacts of colloidal material on the fate and transport of 17 beta-estradiol in three Iowa soils. https://api.semanticscholar.org/CorpusID:128801952

Prater, J. R., Horton, R., & Thompson, M. L. (2015). Reduction of estrone to 17 β-estradiol in the presence of swine manure colloids. Chemosphere, 119, 642–645. https://doi.org/10.1016/j.chemosphere.2014.07.072

Prater, J. R., Horton, R., & Thompson, M. L. (2016). Impacts of Environmental Colloids on the Transport of 17 B-Estradiol in Intact Soil Cores. Soil and Sediment Contamination an International Journal, 25(2), 164–180. https://doi.org/10.1080/15320383.2016.1112360

Prince, H. D., Cullen, N. J., Gibson, P. B., Conway, J. P., & Kingston, D. G. (2021). A Climatology of Atmospheric Rivers in New Zealand. Journal of Climate. https://doi.org/10.1175/jcli-d-20-0664.1

Proffitt, A., Jarvis, R., & Bendotti, S. (1995). The impact of sheep trampling and stocking rate on the physical properties of a red duplex soil with two initially different structures. Australian Journal of Agricultural Research, 46, 733. https://doi.org/10.1071/AR9950733

Qi, Y., & Zhang, T. C. (2016). Transport of manure-borne testosterone in soils affected by artificial rainfall events. Water Research, 93, 265–275. https://doi.org/10.1016/j.watres.2016.01.052

Radu, F., Pop, I. S., & Knabner, P. (2004). Order of Convergence Estimates for an Euler Implicit, Mixed Finite Element Discretisation of Richards' Equation. SIAM Journal on Numerical Analysis, 42(4), 1452–1478. https://doi.org/10.1137/S0036142902405229

Ratha, D., Babbar, R., Hariprasad, K. S., Ojha, C. S. P., Baranwal, M., Rout, P. R., & Parihar, A. (2023). Mathematical Transport System of Microconstituents. In Microconstituents in the Environment (pp. 107–131). John Wiley & Sons, Ltd. https://doi.org/10.1002/9781119825289.ch5

Rawls, W. J., Brakensiek, D. L., & Miller, N. (1983). Green-ampt Infiltration Parameters from Soils Data. Journal of Hydraulic Engineering, 109(1), 62–70. https://doi.org/10.1061/(ASCE)0733-9429(1983)109:1(62)

Reddy, S., & Brownawell, B. J. (2005). Analysis of Estrogens in Sediment From a Sewage-impacted Urban Estuary Using High-performance Liquid Chromatography/Time-of-flight Mass Spectrometry. Environmental Toxicology and Chemistry, 24(5), 1041–1047. https://doi.org/10.1897/04-167r.1

Renard, K. G. (1997). Predicting soil erosion by water: A guide to conservation planning with the Revised Universal Soil Loss Equation (RUSLE). US Department of Agriculture, Agricultural Research Service. https://books.google.com/books?hl=en&lr=&id=cQEUAAAAYAAJ&oi=fnd&pg=PR7&dq=Renard,+K.+G.,+1997.+Predicting+soil+erosion+by+water:+a+guide+to+conservation+planning+with+the+Revised+Universal+Soil+Loss+Equation+(RUSLE).+United+States+Government+Printing.&ots=HDKdqb5yOc&sig=fSm8Nx1iFtgpliZFm4RhjBzc42s

Resource Management, N. Z. A. (XXXX). Irrigation & effluent knowledge hub. NZARM. https://nzarm.org.nz/resources/knowledge-hub/irrigation-and-effluent

Richards, L. A. (1931). CAPILLARY CONDUCTION OF LIQUIDS THROUGH POROUS MEDIUMS. Physics., 1(5), 318–333. https://doi.org/10.1063/1.1745010

Risk, J. T., Old, A. B., Peyroux, G. R., Brown, M., Yoswara, H., Wheeler, D. M., Lucci, G. M., & McDowell, R. W. (2015). MitAgator^{TM}-in action solutions for managing nitrogen, phosphorus, sediment and e. Coli loss.

Robinson, J. A., Ma, Q., Staveley, J. P., Smolenski, W. J., & Ericson, J. (2017). Degradation and transformation of 17α-estradiol in water–sediment systems under controlled aerobic and anaerobic conditions. Environmental Toxicology and Chemistry, 36(3), 621–629. https://doi.org/10.1002/etc.3383

Rouleau, W. T., & Osterle, J. F. (1955). The Application of Finite Difference Methods to Boundary-Layer Type Flows. Journal of the Aeronautical Sciences, 22(4), 249–254. https://doi.org/10.2514/8.3320

S. Bircher. (2011). Phytoremediation of Natural and Synthetic Steroid Growth Promoters Used in Livestock Production by Riparian Buffer Zone Plants. M.Sc. Thesis, University of Iowa, U.S.A.

Sanders, K. R., Beasley, J. S., Bush, E. W., & Conger, S. L. (2019). Fertilizer Source and Irrigation Depth Affect Nutrient Leaching During Coleus Container Production. Journal of Environmental Horticulture, 37(4), 113–119. https://doi.org/10.24266/0738-2898-37.4.113

Sangsupan, H. A., Radcliffe, D. E., Hartel, P. G., Jenkins, M. B., Vencill, W. K., & Cabrera, M. L. (2006). Sorption and transport of 17beta-estradiol and testosterone in undisturbed soil columns. Journal of Environmental Quality, 35(6), 2261–2272. https://doi.org/10.2134/jeq2005.0401

Sanjari, G., Yu, B., Ghadiri, H., Ciesiolka, C. A. A., & Rose, C. W. (2009). Effects of time-controlled grazing on runoff and sediment loss. Soil Research, 47(8), 796–808. https://doi.org/10.1071/SR09032

Sansom, J., & Renwick, J. (2007). Climate Change Scenarios for New Zealand Rainfall. Journal of Applied Meteorology and Climatology. https://doi.org/10.1175/jam2491.1

Sarmah, A. K., Close, M. E., Pang, L., Lee, R., & Green, S. R. (2005). Field study of pesticide leaching in a Himatangi sand (Manawatu) and a Kiripaka bouldery clay loam (Northland). 2. Simulation using LEACHM, HYDRUS-1D, GLEAMS, and SPASMO models. Soil Research, 43(4), 471–489.

Sarmah, A. K., & Northcott, G. L. (2008). Laboratory degradation studies of four endocrine disruptors in two environmental media. Environmental Toxicology and Chemistry, 27(4), 819–827. https://doi.org/10.1897/07-231.1

Sarmah, A. K., Northcott, G. L., Leusch, F. D. L., & Tremblay, L. A. (2006). A survey of endocrine disrupting chemicals (EDCs) in municipal sewage and animal waste effluents in the Waikato region of New Zealand. Science of The Total Environment, 355(1), 135–144. https://doi.org/10.1016/j.scitotenv.2005.02.027

Sarmah, A. K., Northcott, G. L., & Scherr, F. F. (2008). Retention of estrogenic steroid hormones by selected New Zealand soils. Environment International, 34(6), 749–755. https://doi.org/10.1016/j.envint.2007.12.017

Sarmah, A. K., Srinivasan, P., Smernik, R. J., Manley-Harris, M., Antal, M. J., Downie, A., & Zwieten, L. van. (2010). Retention capacity of biochar-amended New Zealand dairy farm soil for an estrogenic steroid hormone and its primary metabolite. Soil Research, 48(7), 648–658. https://doi.org/10.1071/SR10013

Scherr, F. F., Sarmah, A. K., Di, H. J., & Cameron, K. C. (2009). Sorption of estrone and estrone-3-sulfate from CaCl2 solution and artificial urine in pastoral soils of New Zealand. Environmental Toxicology and Chemistry, 28(12), 2564–2571. https://doi.org/10.1897/08-534.1

Schoenborn, A., Kunz, P., & Koster, M. (2015). Estrogenic Activity in Drainage Water: A Field Study on a Swiss Cattle Pasture. Environmental Sciences Europe, 27(1). https://doi.org/10.1186/s12302-015-0047-4

Schug, T. T., Abagyan, R., Blumberg, B., Collins, T. J., Crews, D., DeFur, P. L., Dickerson, S. M., Edwards, T. M., Gore, A. C., Guillette, L. J., Hayes, T., Heindel, J. J., Moores, A., Patisaul, H. B., Tal, T. L., Thayer, K. A., Vandenberg, L. N., Warner, J., Watson, C. S., … Myers, J. P. (2013). Designing Endocrine Disruption Out of the Next Generation

of Chemicals. Green Chemistry : An International Journal and Green Chemistry Resource : GC, 15(1), 181–198. https://doi.org/10.1039/C2GC35055F

Schwarte, K. A., Russell, J. R., Kovar, J. L., Morrical, D. G., Ensley, S. M., Yoon, K.-J., Cornick, N. A., & Cho, Y. I. (2011). Grazing management effects on sediment, phosphorus, and pathogen loading of streams in cool-season grass pastures. Journal of Environmental Quality, 40(4), 1303–1313. https://doi.org/10.2134/jeq2010.0524

Selby, M. J. (1993). Hillslope Materials and Processes (2nd ed.). Oxford University Press.

Shargil, D., Gerstl, Z., Fine, P., Nitsan, I., & Kurtzman, D. (2015). Impact of Biosolids and Wastewater Effluent Application to Agricultural Land on Steroidal Hormone Content in Lettuce Plants. The Science of the Total Environment, 505, 357–366. https://doi.org/10.1016/j.scitotenv.2014.09.100

Shaver, E. (2020). Waikato stormwater runoff modelling guideline [(Technical Report 2020/06).]. https://waikatoregion.govt.nz/assets/WRC/TR20-06.pdf

Shore, L. S., & Shemesh, M. (2003). Naturally produced steroid hormones and their release into the environment.

Shrestha, S. L., Casey, F., Hakk, H., Smith, D. J., & Padmanabhan, G. (2012). Fate and Transformation of an Estrogen Conjugate and Its Metabolites in Agricultural Soils. Environmental Science & Technology, 46(20), 11047–11053. https://doi.org/10.1021/es3021765

Silburn, D. M., Carroll, C., Ciesiolka, C. A. A., Voil, R. C., & Burger, P. (2011). Hillslope runoff and erosion on duplex soils in grazing lands in semi-arid central Queensland: I. Influences of cover, slope, and soil. Soil Research, 49, 105. https://doi.org/10.1071/SR09068

Šimůnek, J., Brunetti, G., Jacques, D., van Genuchten, M. Th., & Šejna, M. (2024). Developments and applications of the HYDRUS computer software packages since 2016. Vadose Zone Journal, 23(4), e20310. https://doi.org/10.1002/vzj2.20310

Simunek, J., & van Genuchten, M. T. (1999). Using the HYDRUS-1D and HYDRUS-2D codes for estimating unsaturated soil hydraulic and solute transport parameters. Characterization and Measurement of the Hydraulic Properties of Unsaturated Porous Media, 1, 523–1.

Šimůnek, J., van Genuchten, M. Th., & Šejna, M. (2016). Recent Developments and Applications of the HYDRUS Computer Software Packages. Vadose Zone Journal, 15(7), vzj2016.04.0033. https://doi.org/10.2136/vzj2016.04.0033

Sinkkonen, S., & Paasivirta, J. (2000). Degradation half-life times of PCDDs, PCDFs and PCBs for environmental fate modelling. Chemosphere, 40(9), 943–949. https://doi.org/10.1016/S0045-6535(99)00337-9

Sirabahenda, Z., St-Hilaire, A., Courtenay, S. C., & van den Heuvel, M. R. (2020). Assessment of the effective width of riparian buffer strips to reduce suspended sediment in an agricultural landscape using ANFIS and SWAT models. CATENA, 195, 104762. https://doi.org/10.1016/j.catena.2020.104762

S-Map Online | Manaaki Whenua—Landcare Research. (2025). https://smap.landcareresearch.co.nz/

Smetanová, A., Nunes, J. P., Symeonakis, E., Brevik, E., Schindelwolf, M., & Ciampalini, R. (2020). GUEST EDITORIAL—SPECIAL ISSUE: Mapping and modelling soil erosion to address societal challenges in a changing world. Land Degradation & Development, 31(17), 2519–2524.

Sophia A, C., & Lima, E. C. (2018). Removal of emerging contaminants from the environment by adsorption. Ecotoxicology and Environmental Safety, 150, 1–17. https://doi.org/10.1016/j.ecoenv.2017.12.026

Sparling, G. P., Schipper, L. A., & Russell, J. M. (2001). Changes in soil properties after application of dairy factory effluent to New Zealand volcanic ash and pumice soils. Soil Research, 39(3), 505–518.

Steiner, L. D., Bidwell, V. J., Di, H. J., Cameron, K. C., & Northcott, G. L. (2010a). Transport and Modelling of Estrogenic Hormones in a Dairy Farm Effluent through Undisturbed Soil Lysimeters. Environmental Science & Technology, 44(7), 2341–2347. https://doi.org/10.1021/es9031216

Steiner, L. D., Bidwell, V. J., Di, H. J., Cameron, K. C., & Northcott, G. L. (2010b). Transport and Modelling of Estrogenic Hormones in a Dairy Farm Effluent Through Undisturbed Soil Lysimeters. Environmental Science & Technology, 44(7), 2341–2347. https://doi.org/10.1021/es9031216

Stumpe, B., & Marschner, B. (2010a). Dissolved Organic Carbon From Sewage Sludge and Manure Can Affect Estrogen Sorption and Mineralization in Soils. Environmental Pollution, 158(1), 148–154. https://doi.org/10.1016/j.envpol.2009.07.027

Stumpe, B., & Marschner, B. (2010b). Organic Waste Effects on the Behavior of 17β-estradiol, Estrone, and 17α-ethinylestradiol in Agricultural Soils in Long- and Short-Term Setups. Journal of Environmental Quality, 39(3), 907–916. https://doi.org/10.2134/jeq2009.0225

Sukias, J. P. S., Craggs, R. J., Tanner, C. C., Davies-Colley, R. J., & Nagels, J. W. (2003). Combined photosynthesis and mechanical aeration for nitrification in dairy waste stabilisation ponds. Water Science and Technology, 48(2), 137–144. https://doi.org/10.2166/wst.2003.0105

Sukias, J. P., & Tanner, C. C. (2023a). A constructed wetland receiving dairy farm run-off: Effectiveness during high flow events compared with baseflow. Diverse Solutions for Efficient Land, Water and Nutrient Use.(Eds. CL Christiansen, DJ Horne and R. Singh). Http://Flrc. Massey. Ac. Nz/Publications. Html. Occasional Report, 35. https://flrc.massey.ac.nz/workshops/23/Manuscripts/Sukias.pdf

Svenson, A., Allard, A.-S., & Ek, M. (2003). Removal of estrogenicity in Swedish municipal sewage treatment plants. Water Research, 37(18), 4433–4443. https://doi.org/10.1016/S0043-1354(03)00395-6

Tait, A., Henderson, R., Turner, R., & Zheng, X. (2006). Thin plate smoothing spline interpolation of daily rainfall for New Zealand using a climatological rainfall surface. International Journal of Climatology, 26, 2097–2115. https://doi.org/10.1002/joc.1350

Tait, A., & Turner, R. (2005). Generating multiyear gridded daily rainfall over New Zealand. Journal of Applied Meteorology, 44(9), 1315–1323. https://doi.org/10.1175/JAM2279.1

Tanner, C. C., Depree, C., Sukias, J. P. S., Wright-Stow, A. E., Burger, D. F., & Goeller, B. (2022). Constructed Wetland Practitioner Guide: Design and Performance Estimates. DairyNZ Hamilton, New Zealand. https://www.researchgate.net/profile/Brandon-Goeller/publication/371038269_Constructed_Wetland_Practitioners_Guide_Design_and_Performance_Estimates/links/646fcc6159d5ad5f9c74ed33/Constructed-Wetland-Practitioners-Guide-Design-and-Performance-Estimates.pdf

Tanner, C. C., Nguyen, M. L., & Sukias, J. P. S. (2005). Nutrient removal by a constructed wetland treating subsurface drainage from grazed dairy pasture. Agriculture, Ecosystems & Environment, 105(1), 145–162. https://doi.org/10.1016/j.agee.2004.05.008

Te Ara Encyclopedia of New Zealand. (n.d.). Dairy farming New Zealand. In Te Ara Encyclopedia of New Zealand. https://teara.govt.nz/en/dairy-farming

Ternes, T. A., Meisenheimer, M., McDowell, D., Sacher, F., Brauch, H.-J., Haist-Gulde, B., Preuss, G., Wilme, U., & Zulei-Seibert, N. (2002). Removal of Pharmaceuticals during Drinking Water Treatment. Environmental Science & Technology, 36(17), 3855–3863. https://doi.org/10.1021/es015757k

Teshager, A. D., Gassman, P. W., Secchi, S., Schoof, J. T., & Misgna, G. (2016). Modelling Agricultural Watersheds with the Soil and Water Assessment Tool (SWAT): Calibration and Validation with a Novel Procedure for Spatially Explicit HRUs. Environmental Management, 57(4), 894–911. https://doi.org/10.1007/s00267-015-0636-4

Thorpe, K. L., Cummings, R. I., Hutchinson, T. H., Scholze, M., Brighty, G., Sumpter, J. P., & Tyler, C. R. (2003). Relative potencies and combination effects of steroidal estrogens in fish. Environmental Science and Technology, 37(6), 1142–1149. https://doi.org/10.1021/es0201348

Tomer, M. D., Dosskey, M. G., Burkart, M. R., James, D. E., Helmers, M. J., & Eisenhauer, D. E. (2005). Placement of riparian forest buffers to improve water quality. In: Brooks, K.N. and Ffolliot, P.F. (Eds) Moving Agroforestry into the Mainstream. Proc. 9th N. Am. Agroforest. Conf. Rochester, MN. 12-15 June 2005. https://research.fs.usda.gov/treesearch/21369

Tong, X., Li, Y., Zhang, F., Chen, X., Zhao, Y., Hu, B., & Zhang, X. (2019). Adsorption of 17β-estradiol onto humic-mineral complexes and effects of temperature, pH, and bisphenol A on the adsorption process. Environmental Pollution, 254, 112924. https://doi.org/10.1016/j.envpol.2019.07.092

Tousignant, E., Fankhauser, O., & Hurd, S. (1999). Guidance manual for the design, construction and operations of constructed wetlands for rural applications in Ontario. https://atrium.lib.uoguelph.ca/bitstream/10214/15203/1/FDMR_wetlands_manual.pdf

Tremblay, L. A., Gadd, J. B., & Northcott, G. L. (2018). Steroid estrogens and estrogenic activity are ubiquitous in dairy farm watersheds regardless of effluent management practices. Agriculture, Ecosystems & Environment, 253, 48–54. https://doi.org/10.1016/j.agee.2017.10.012

Tremblay, L. A., & Northcott, G. L. (2003). Analysis of Waikato river water samples for selected endocrine disrupting chemicals and hormonal activity [Technical Report,]. Manaaki Whenua - Landcare Research.

Tzatchkov, V. G., Aldama, A. A., & Arreguin, F. I. (2002). Advection-Dispersion-Reaction Modelling in Water Distribution Networks. Journal of Water Resources Planning and Management, 128(5), 334–342. https://doi.org/10.1061/(ASCE)0733-9496(2002)128:5(334)

Unc, A., & Goss, M. J. (2004). Transport of bacteria from manure and protection of water resources. Applied Soil Ecology, 25(1), 1–18. https://doi.org/10.1016/j.apsoil.2003.08.007

United States Department of Agriculture, Soil Conservation Service. (1954). Author.

Urase, T., Kagawa, C., & Kikuta, T. (2005). Factors affecting removal of pharmaceutical substances and estrogens in membrane separation bioreactors. Desalination, 178(1), 107–113. https://doi.org/10.1016/j.desal.2004.11.031

U.S.Department Agriculture, U. S. D. A., & Natural Resource Conservation, N. R. C. (2009). Hydrology National Engineering Handbook. Chapter 7, Hydrologic Soil Groups. http://directives.sc.egov.usda.gov/OpenNonWebContent.aspx?content=22526.wba

Uwizeyimana, D., Mureithi, S. M., Mvuyekure, S. M., Karuku, G., & Kironchi, G. (2019). Modelling surface runoff using the soil conservation service-curve number method in a drought prone agro-ecological zone in Rwanda. International Soil and Water Conservation Research, 7(1), 9–17. https://doi.org/10.1016/j.iswcr.2018.12.001

Vajda, A. M., Lasky, J. R., & Denny, J. S. (2011). Endocrine-disrupting effects of wastewater effluent on freshwater fish: A study of the chemical nature of hormones. Environmental Science and Technology, 45(1), 64–70. https://doi.org/10.1021/es101854p

Van Horn, H. H., Wilkie, A. C., Powers, W. J., & Nordstedt, R. A. (1994). Components of Dairy Manure Management Systems[1]. Journal of Dairy Science, 77(7), 2008–2030. https://doi.org/10.3168/jds.S0022-0302(94)77147-2

Vandenberg, L. N., Colborn, T., & Hayes, T. B. (2012). Hormones and endocrine-disrupting chemicals: Low-dose effects and mechanisms of action. Endocrine Reviews, 33(3), 234–271. https://doi.org/10.1210/er.2011-1050

Vereecken, H., Weynants, M., Javaux, M., Pachepsky, Y., Schaap, M. G., & van Genuchten, M. Th. (2010). Using Pedotransfer Functions to Estimate the van Genuchten–Mualem Soil Hydraulic Properties: A Review. Vadose Zone Journal, 9(4), 795–820. https://doi.org/10.2136/vzj2010.0045

W. Hamilton, D., Fathepure, B., D. Fulhage, C., Clarkson, W., & Lalman, J. (2006). TREATMENT LAGOONS FOR ANIMAL AGRICULTURE. Journal of Agricultural Safety and Health. https://doi.org/10.13031/2013.20266

W McDowell, R., M Lucci, G., Peyroux, G., Yoswara, H., Cox, N., Brown, M., Wheeler, D., Watkins, N., Smith, C., Monaghan, R., Muirhead, R., Catto, W., & Risk, J. (2014). MitAgatorTM: a Farm Scale Tool to Estimate and Mitigate the Loss of Contaminants from Land to Water. 1–7. https://doi.org/10.13031/wtcw.2014-024

Wang, Y., Zhong, L., Song, X., Adeel, M., & Yang, Y. (2022). Natural colloids facilitated transport of steroidal estrogens in saturated porous media: Mechanism and processes. Environmental Pollution, 315, 120315. https://doi.org/10.1016/j.envpol.2022.120315

Webb, T. H., & Wilson, A. D. (1995). A Manual of Land Characteristics for Evaluation of Rural Land (Landcare Research Science Series. Manaaki Whenua Press.

Wei, H., Yan-xia, L., Ming, Y., & Wei, L. (2011). Presence and Determination of Manure-borne Estrogens from Dairy and Beef Cattle Feeding Operations in Northeast China. Bulletin of Environmental Contamination and Toxicology, 86(5), 465–469. https://doi.org/10.1007/s00128-011-0247-6

Weinan, E., & Liu, J.-G. (1996). Vorticity boundary condition and related issues for finite difference schemes. Journal of Computational Physics, 124(2), 368–382.

Wheeler, D., Ledgard, S., Monaghan, R., McDowell, R., & De Klein, C. (2009). OVERSEER nutrient budget model—What it is, what it does (pp. 231–236).

Whisler, F. D., & Bouwer, H. (1970). Comparison of methods for calculating vertical drainage and infiltration for soils. Journal of Hydrology, 10(1), 1–19. https://doi.org/10.1016/0022-1694(70)90051-X

Williams J.R, W. (1975). Sediment-Yield Prediction with Universal Equation Using Runoff Energy Factor. In: Present and Prospective Technology for Predicting Sediment Yield and Sources. US Department of Agriculture, Agriculture Research Service, Washington DC, 244–252.

Wilson, N., Slaney, D., Baker, M. G., Hales, S., & Britton, E. (2011). Climate Change and Infectious Diseases in New Zealand: A Brief Review and Tentative Research Agenda. Reviews on Environmental Health. https://doi.org/10.1515/reveh.2011.013

Wischmeier, W. H. (1978). Predicting rainfall erosion losses:a guide to conservation planning (W. H. Wischmeier, D. D. Smith, S. United, Science, A. Education, U. Purdue, & S. Agricultural Experiment, Trans.). 58 p. : ill., maps 26 cm.---USDA.

Wratt, D., Tait, A., Griffiths, G. A., Espie, P., Jessen, M. R., Keys, J. E., Ladd, M., Lew, D., Lowther, W. L., Mitchell, N. C., Morton, J. D., Reid, J., Reid, S., Richardson, A. C., Sansom, J., & Shankar, U. (2006). Climate for Crops: Integrating Climate Data With Information About Soils and Crop Requirements to Reduce Risks in Agricultural Decision-making. Meteorological Applications. https://doi.org/10.1017/s1350482706002416

Writer, J. H., Dodson, S. I., & Tsai, S. (2011). Estrogen attenuation in lakes and streams in the United States. Environmental Toxicology and Chemistry, 30(2), 289–298. https://doi.org/10.1002/etc.503

Xuan, R., Blassengale, A. A., & Wang, Q. (2008). Degradation of Estrogenic Hormones in a Silt Loam Soil. Journal of Agricultural and Food Chemistry, 56(19), 9152–9158. https://doi.org/10.1021/jf8016942

Yamamoto, H., Liljestrand, H. M., Shimizu, Y., & Morita, M. (2003). Effects of Physical−Chemical Characteristics on the Sorption of Selected Endocrine Disruptors by Dissolved Organic Matter Surrogates. Environmental Science & Technology, 37(12), 2646–2657. https://doi.org/10.1021/es026405w

Yang, Y.-Y., Gray, J. L., Furlong, E. T., Davis, J. G., ReVello, R. C., & Borch, T. (2012). Steroid Hormone Runoff from Agricultural Test Plots Applied with Municipal Biosolids. Environmental Science & Technology, 46(5), 2746–2754. https://doi.org/10.1021/es203896t

Ying, G.-G., Kookana, R. S., & Ru, Y.-J. (2002). Occurrence and fate of hormone steroids in the environment. Environment International, 28(6), 545–551. https://doi.org/10.1016/S0160-4120(02)00075-2

Yost, E. E., Meyer, M. T., Dietze, J. E., Williams, C. M., Worley-Davis, L., Lee, B., & Kullman, S. W. (2014). Transport of Steroid Hormones, Phytoestrogens, and Estrogenic Activity Across a Swine Lagoon/Sprayfield System. Environmental Science & Technology, 48(19), 11600–11609. https://doi.org/10.1021/es5025806

You, Q., & Zhang, T. C. (2016). Transport of Manure-Borne Testosterone in Soils Affected by Artificial Rainfall Events. Water Research, 93, 265–275. https://doi.org/10.1016/j.watres.2016.01.052

Yu, C.-P., Deeb, R. A., & Chu, K.-H. (2013). Microbial degradation of steroidal estrogens. Chemosphere, 91(9), 1225–1235. https://doi.org/10.1016/j.chemosphere.2013.01.112

Yu, W., Du, B., Fan, G., Yang, S., Yang, L., & Zhang, M. (2020). Spatio-temporal distribution and transformation of 17α- and 17β-estradiol in sterilized soil: A column experiment. Journal of Hazardous Materials, 389, 122092. https://doi.org/10.1016/j.jhazmat.2020.122092

Yu, Z., Xiao, B., Huang, W., & Peng, P. (2004). Sorption of steroid estrogens to soils and sediments. Environmental Toxicology and Chemistry, 23(3), 531–539. https://doi.org/10.1897/03-192

Zhang, C., Li, S., Jamieson, R. C., & Meng, F.-R. (2017). Segment-based assessment of riparian buffers on stream water quality improvement by applying an integrated model. Ecological Modelling, 345(C), 1–9.

Zhang, H., Wei, J., Yang, Q., Baartman, J. E. M., Gai, L., Yang, X., Li, S., Yu, J., Ritsema, C. J., & Geissen, V. (2017). An improved method for calculating slope length (λ) and the LS parameters of the Revised Universal Soil Loss Equation for large watersheds. Geoderma, 308, 36–45. https://doi.org/10.1016/j.geoderma.2017.08.006

Zhang, Y., Sangster, J. L., Gauza, L., & Bartelt-Hunt, S. L. (2016). Impact of sediment particle size on biotransformation of 17β-estradiol and 17β-trenbolone. The Science of the Total Environment, 572, 207–215. https://doi.org/10.1016/j.scitotenv.2016.08.004

Zhao, X., Grimes, K. L., Colosi, L. M., & Lung, W.-S. (2019). Attenuation, transport, and management of estrogens: A review. Chemosphere, 230, 462–478. https://doi.org/10.1016/j.chemosphere.2019.05.086

Zhao, X., & Lung, W.-S. (2017). Modelling the fate and transport of 17β-estradiol in the South River watershed in Virginia. Chemosphere, 186, 780–789. https://doi.org/10.1016/j.chemosphere.2017.08.058

Zheng, W., Li, X., Yates, S. R., & Bradford, S. A. (2012). Anaerobic Transformation Kinetics and Mechanism of Steroid Estrogenic Hormones in Dairy Lagoon Water. Environmental Science & Technology, 46(10), 5471–5478. https://doi.org/10.1021/es301551h

Appendices A

Some Additional plots from the Soil Model to better understand the infiltration, water and estrogens profiles.

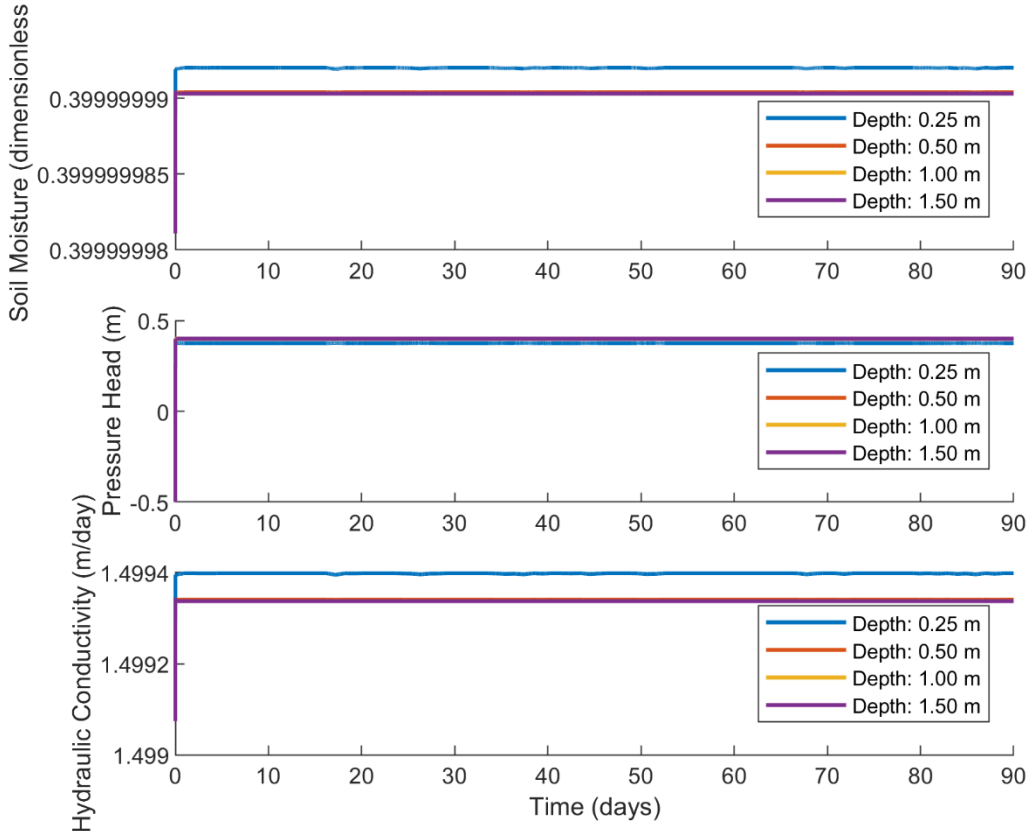

Figure A-1: Temporal profiles of soil moisture (dimensionless), pressure head (m), and hydraulic conductivity (m/day) at selected depths (0.25 m, 0.5 m, 1.0 m, and 1.5 m) over 90 days from model 1.

Figure A-1 compares soil moisture, pressure head, and hydraulic conductivity at different depths: 0.25 m, 0.5 m, 1.0 m, and 1.5 m. The top layer (0.25 m) shows slightly higher moisture and hydraulic conductivity compared to the deeper layers. This reflects the immediate effect of infiltration near the surface. In contrast, deeper layers show minimal change, with moisture and hydraulic conductivity remaining stable and the pressure head staying negative, indicating unsaturated conditions.

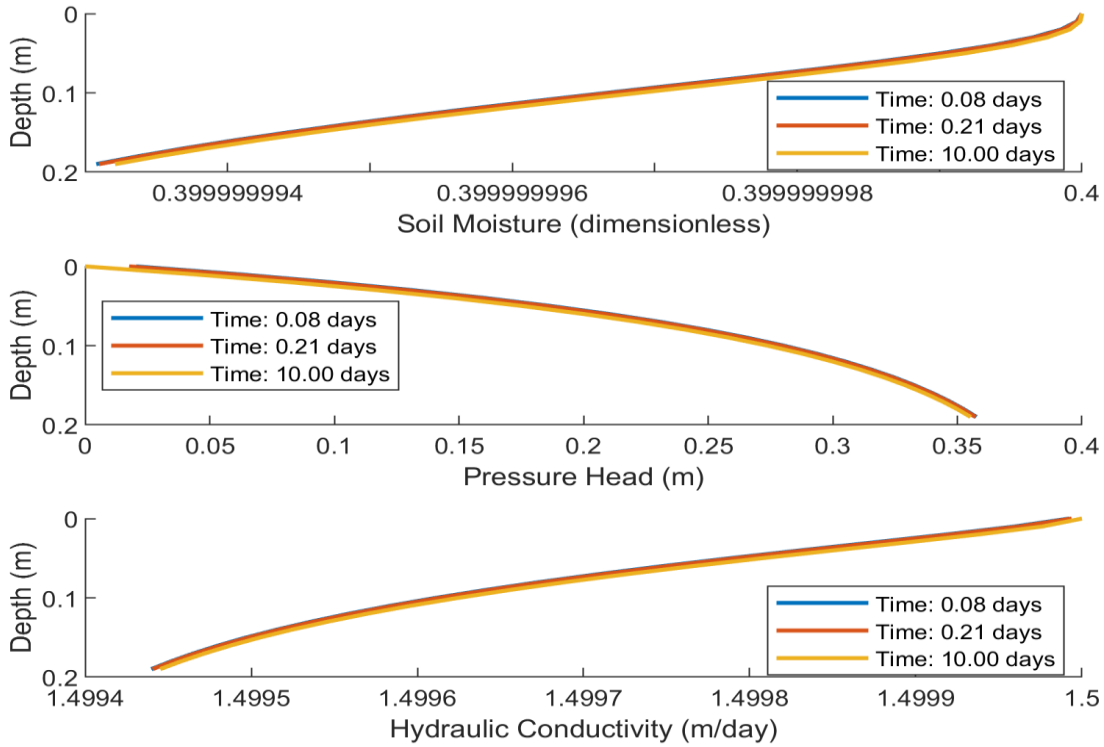

Figure A-2: Profiles of soil moisture (dimensionless), pressure head (m), and hydraulic conductivity (m/day) with depth in the top 20 cm at three selected times (0.08 days, 0.21 days, and 10 days) from model 1.

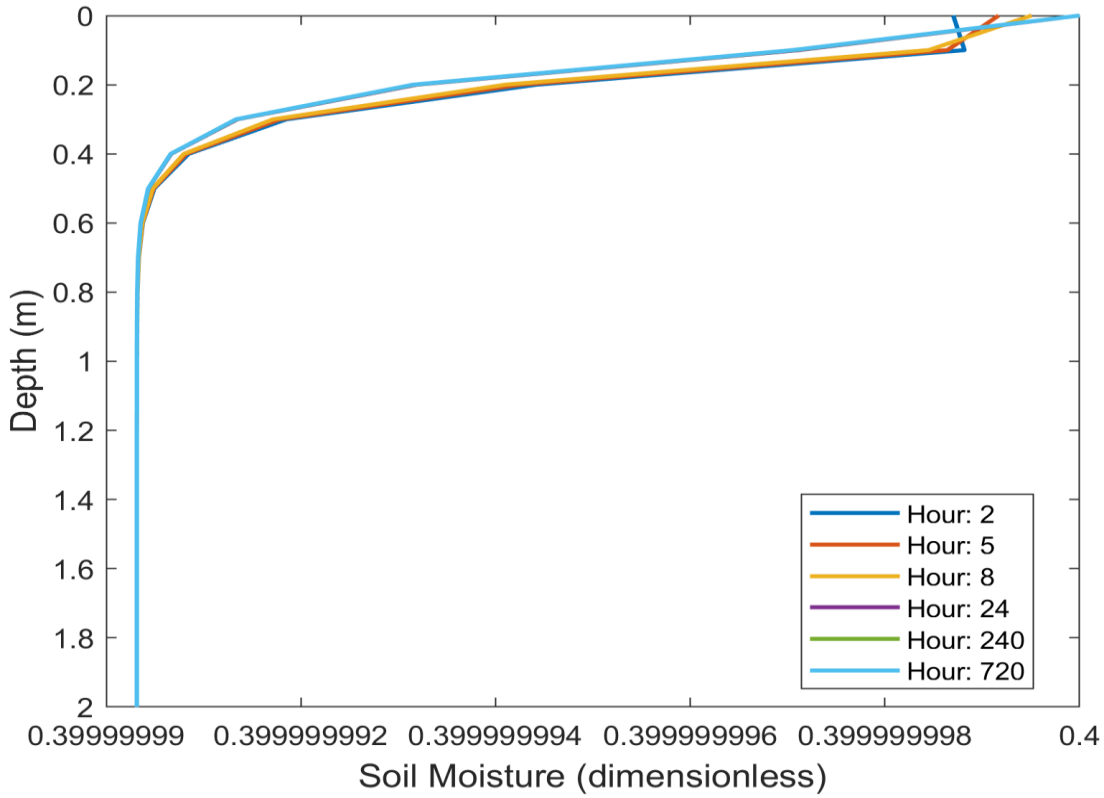

Figure A-3 Variation of soil moisture vs depth at various time intervals from model 2.

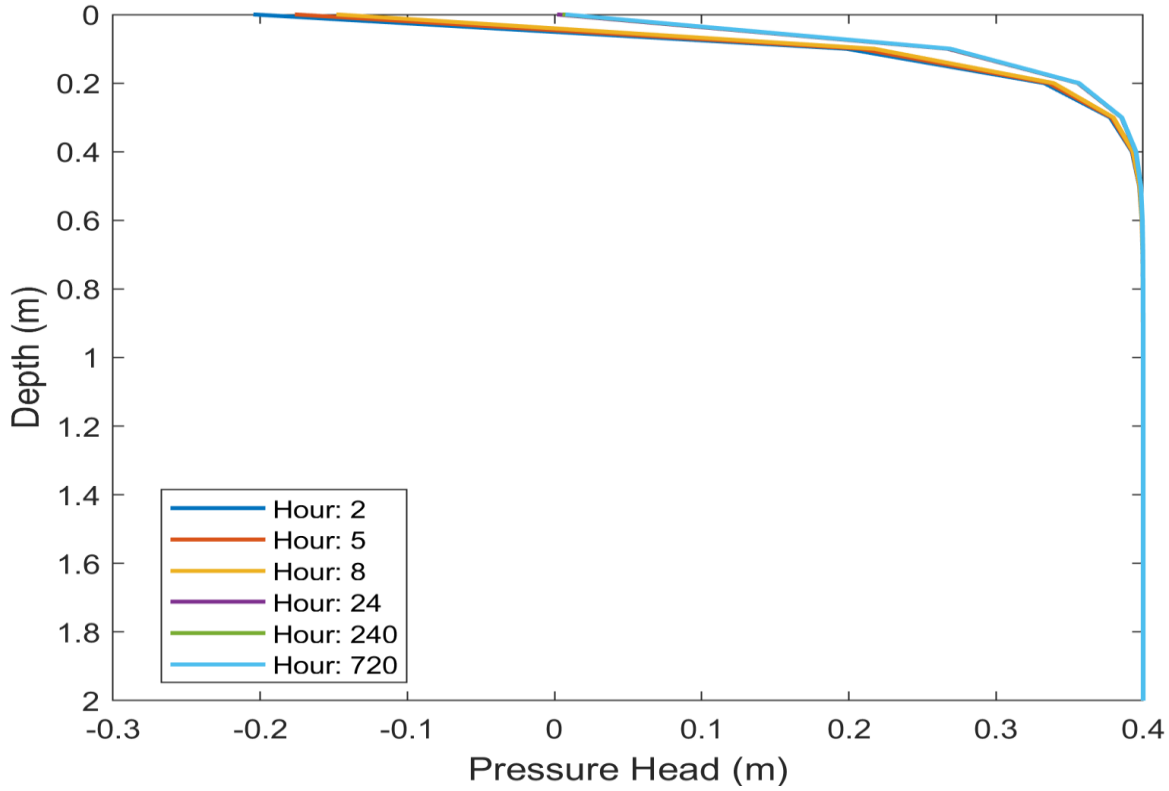

Figure A-4: Variation of pressure head vs depth at various time intervals from model 2.

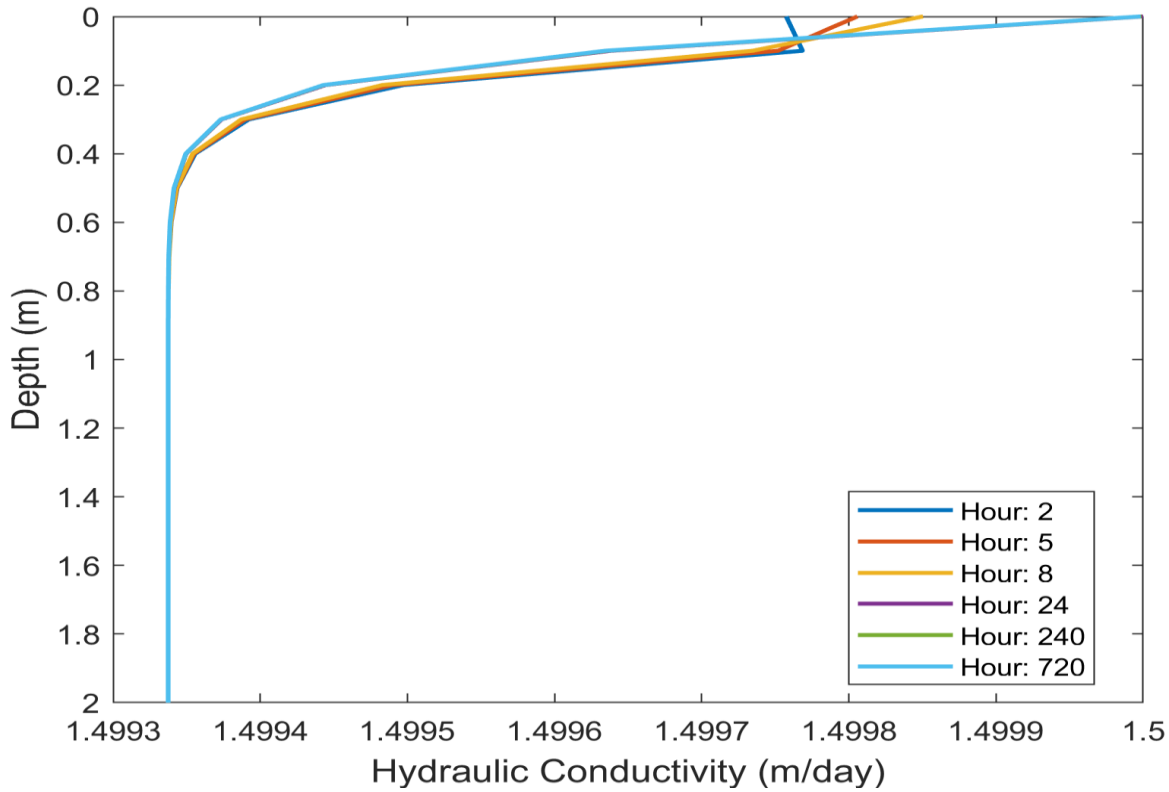

A-5: Hydraulic conductivity along the soil depth for various time intervals from mdeol 2.

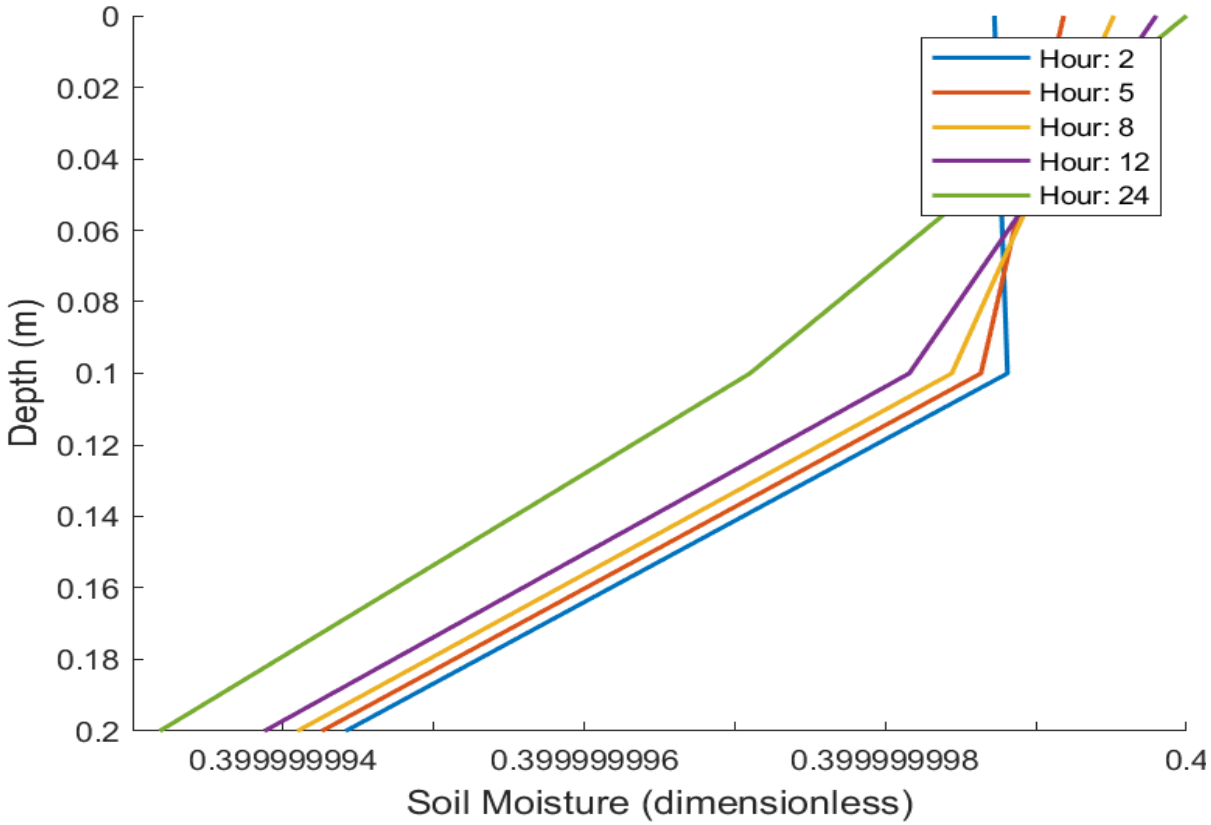

Figure A-6: Soil moisture vs depth for 20 cm top layer from model 2.

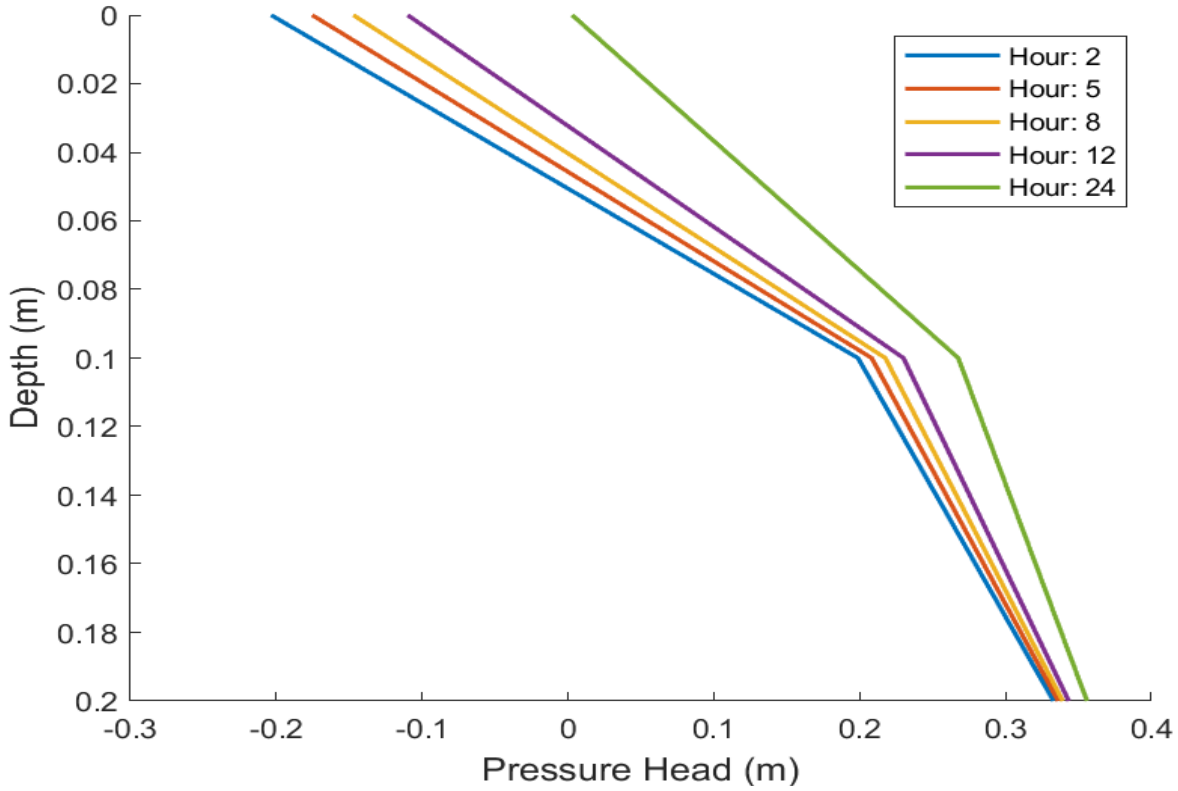

Figure A-7: Pressure head vs depth for the top layer (20cm) from mdeol 2.

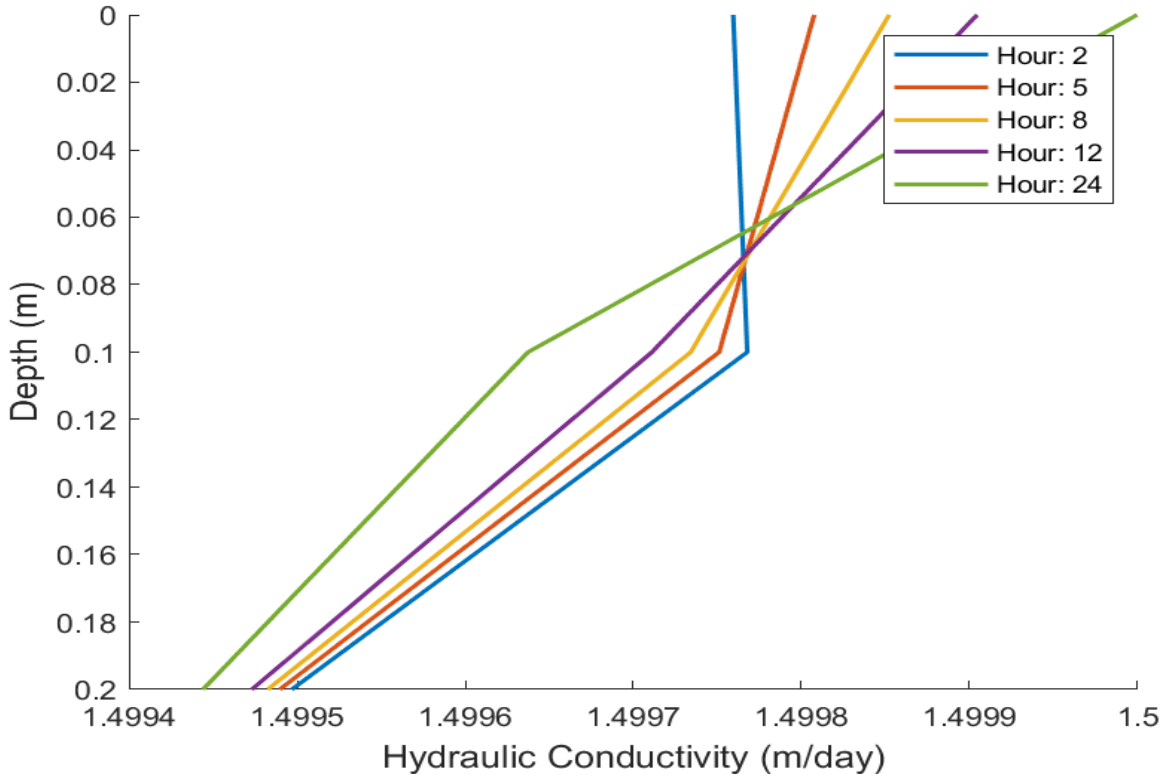

Figure A-8: Hydraulic conductivity vs depth for top layer 20 cm from model 2.

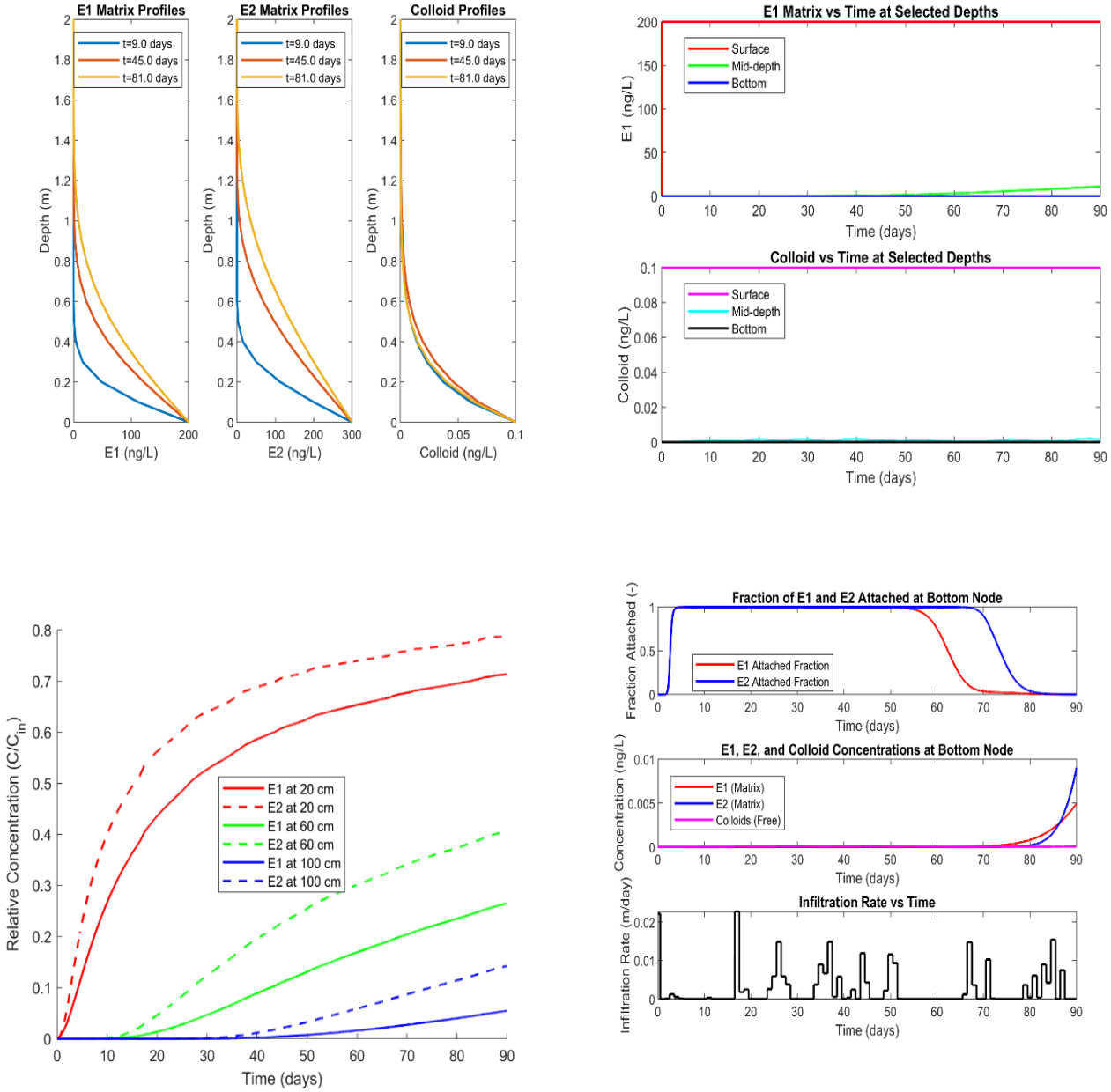

Figure A-9: Left top depth profiles of estrone (E1), estradiol (E2), and free colloids at 9, 45, and 81 days.Right top Time-series of E1 (top panel) and free colloids (bottom panel) at three depths: surface, mid-depth, and bottom.Left bottom Modeled E1 and E2 concentrations normalized to their inlet concentrations (C/C_in) at 20, 60, and 100 cm depth.Right bottom (Top) The fraction of E1 (red) and E2 (blue) that is sorbed or attached at the bottom node transitions from near 100% attached initially to near 0% after about 70–80 days, reflecting the shift from strongly bound to primarily dissolved as infiltration continues. (Middle) The time-series of total E1, E2, and free colloids at the bottom node remains very low until around day 60, then rapidly rises. (Bottom) The infiltration rate ($m\ d^{-1}$) used in the simulation shows intermittent pulses that drive the observed breakthrough.

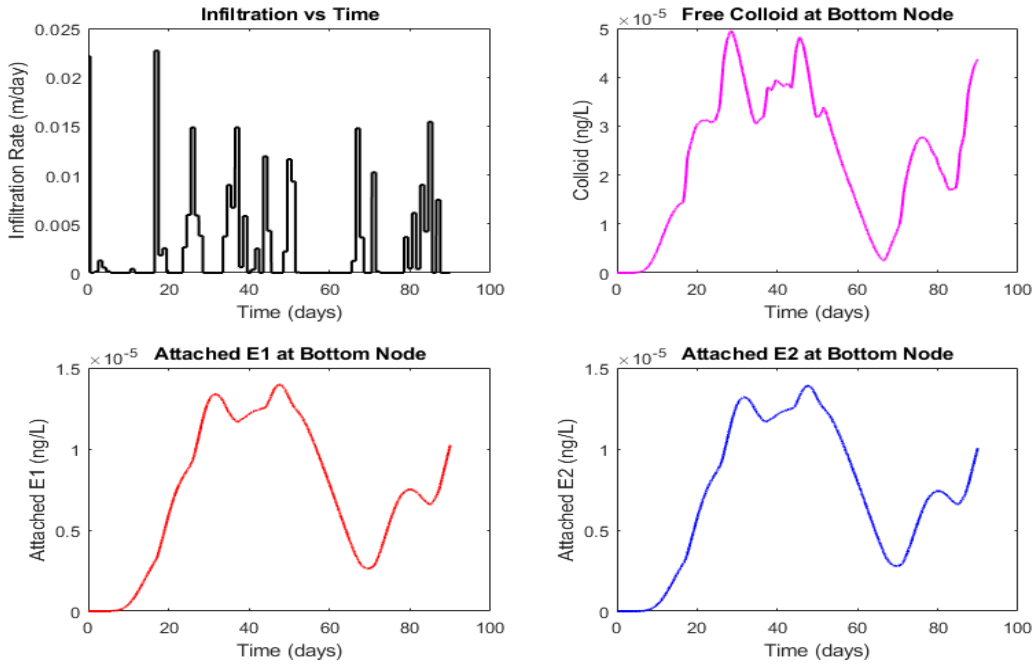

Figure A-10: The infiltration rate (top left) shows episodic pulses. Correspondingly, free colloid concentrations at the bottom (top right) peak soon after infiltration spikes. Attached E1 (bottom left) and attached E2 (bottom right) both fluctuate in phase with colloid pulses, consistent with colloid-facilitated transport to the bottom node.

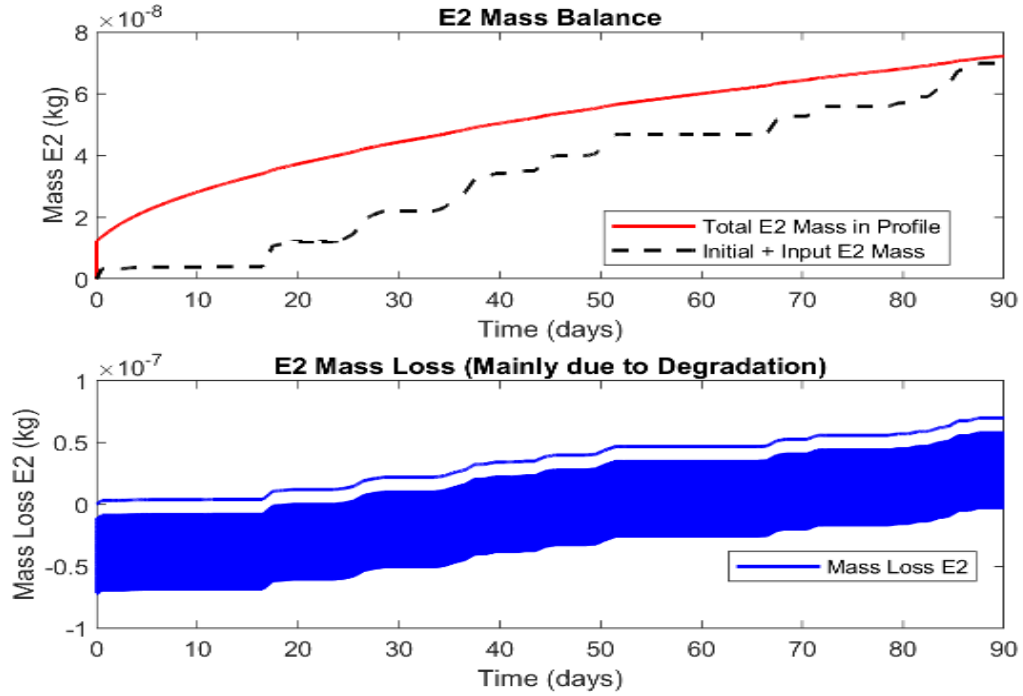

Figure A-11: The red line tracks total E2 mass remaining in the soil profile; the dashed black line is the cumulative initial plus input E2 mass. The difference between them increases over time as E2 is degraded or lost. (Bottom) The net E2 mass loss, mostly via biodegradation, steadily grows throughout the 90 days, reaching about 0.5–0.6 × 10^{-7} kg by the end

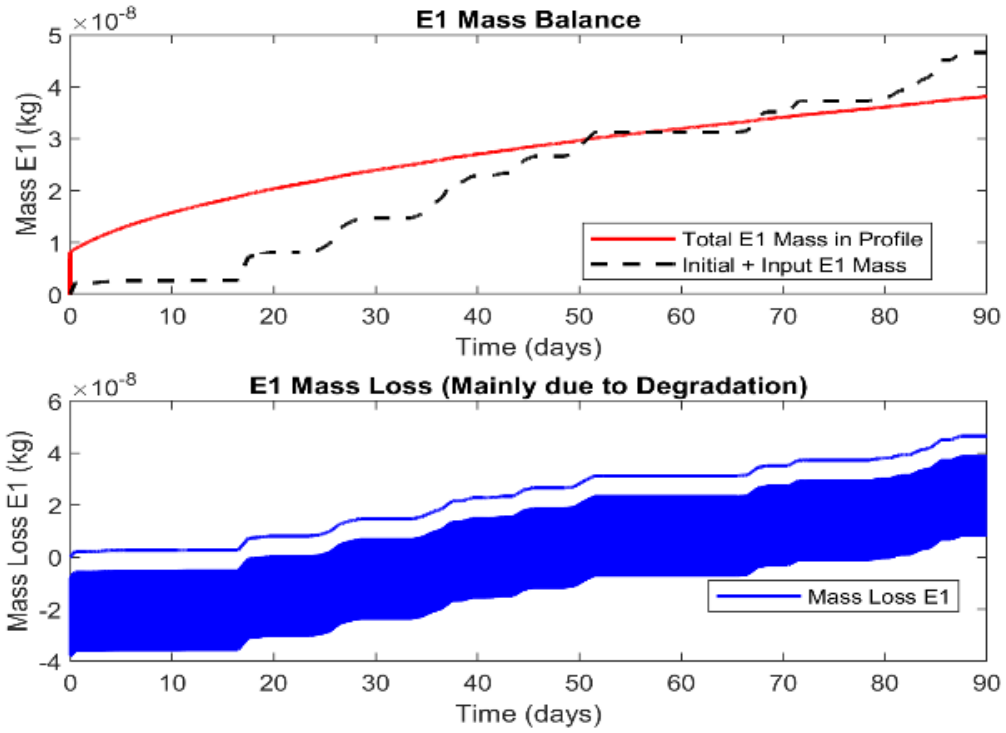

Figure A-12: Left bottom (Top) Similar to E2, the total E1 mass in the soil (red) rises initially and lags the cumulative input (dashed black) due to sorption and partial degradation. (Bottom) Cumulative E1 mass loss from degradation shows a steady increase, exceeding 2×10^{-8} kg by around day 90, highlighting E1's ongoing breakdown in the soil matrix.

Numerical stability

The oscillations in both the pressure head and soil moisture content graphs(Figures A-13 and A-14) suggest that the numerical solution was unstable. This could be due to the time step size (dt) being too large or the initial conditions being too extreme. Reducing the time step size and boundary conditions might help to numerical stability.

We changed the time step from 0.2 days to 0.05 days to improve numerical stability and also added a small variation to the top boundary condition to prevent abrupt changes.

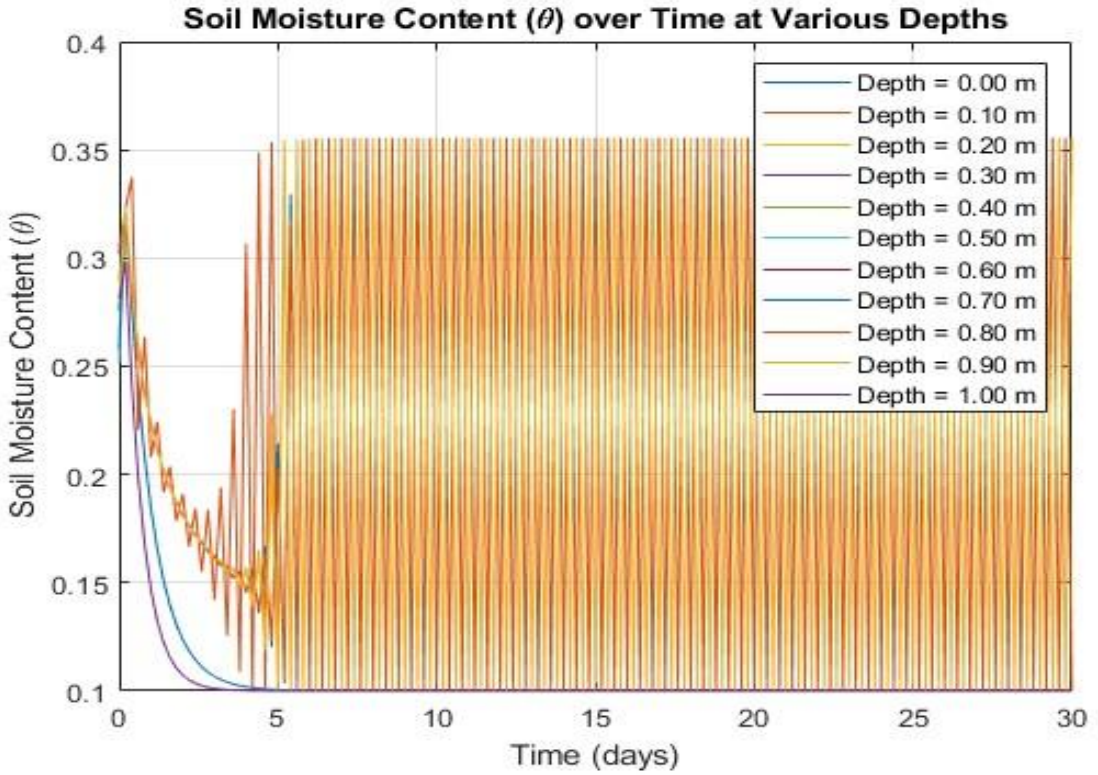

Figure A-13: The soil moisture content (θ) over time at various depths upto 1 m

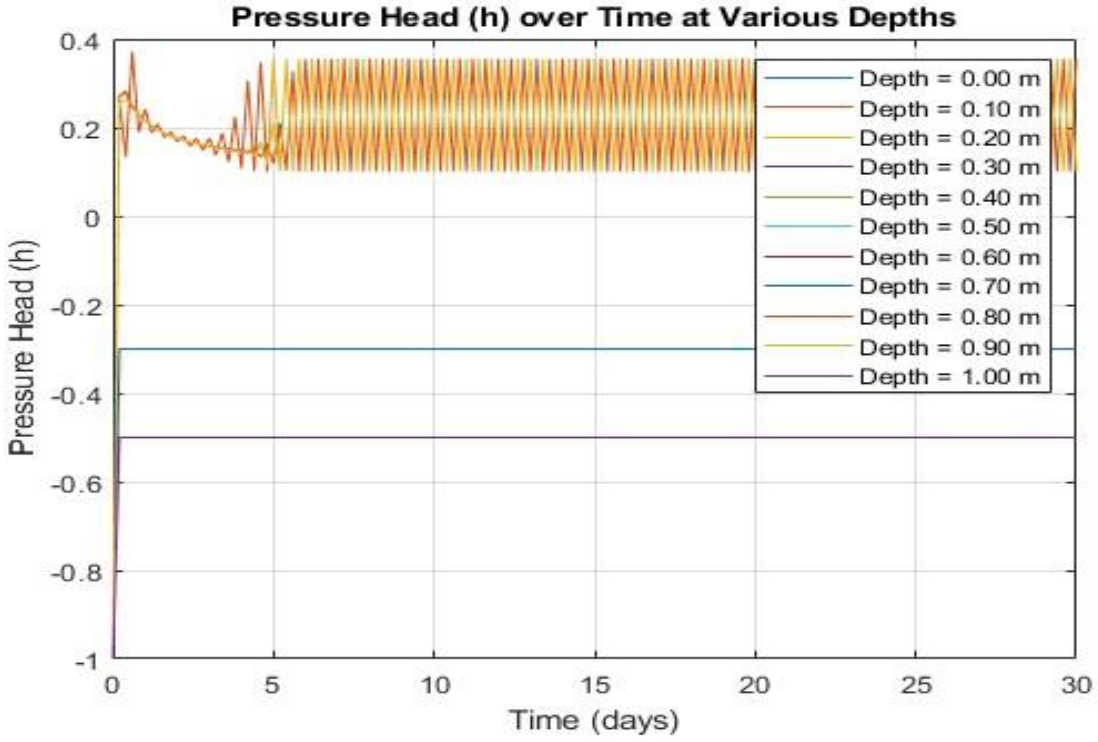

Figure A-14: Pressure Head (h) over time at various depths upto 1 m

Table A1: Soil Physical Properties

Property	Symbol	Typical Range	Comments	References
Texture Classification	–	e.g. Silt Loam, Clay Loam	We classified soil texture using the USDA/NZ system and verified these classifications via S-map and lab measurements.	USDA, S-map; (McLeod et al., 2019)
Bulk Density	ρ	1.1 – 1.4 g/cm³	We used local field measurements (and S-map data where possible) to confirm this range, which influences infiltration, retention, and compaction.	(Barkle et al., 2000; Hawke & Summers, 2006c)
Saturated Hydraulic Conductivity	Ks	0.5 – 2.0 m/day	Our measured Ks data align well with published values; we also consulted S-map to refine layer-specific Ks.	S-map data; McLeod et al. (2019), (Cook et al., 1994)
Field Capacity (NZ standard)	FC	~0.25 – 0.35 m³/m³	In New Zealand conditions, −10 kPa was used instead of −33 kPa; we took S-map values as a reference and adjusted if needed for site specifics.	S-map; DairyNZ guidelines
Wilting Point	WP	~0.10 – 0.15 m³/m³	We derived WP from S-map . This helps define the lower limit of plant-available water.	S-map (Neitsch et al., 2011)
Available Water Content	AWC	-	In practice, we used S-map's stone-corrected water content for both field capacity and wilting point to compute AWC.	S-map
Organic Carbon (%)	OC	3 – 10% (typical for Waikato soils)	We emphasized OC because higher OC typically increases estrogen sorption. We used local soil test results to confirm these ranges.	(Hanselman et al., 2003; Sarmah et al., 2006a)
pH	–	5.0 – 6.0	We considered local soil test reports showing slightly acidic pH, which can affect estrogen degradation kinetics. Also did lab testing.	(*S-Map Online | Manaaki Whenua - Landcare Research*, 2025)

Table A2: Parameters for Green-Ampt Infiltration Module

Parameter	Symbol	Typical Range	Unit	Comments	References
Initial Water Content	θi	~0.20 – 0.30	m³/m³	We used a typical pre-irrigation moisture content observed on-site. Different studies confirmed this range	Griffiths (1991); Pollacco et al. (2017)
Saturated Water Content	θs	~0.35 – 0.45	m³/m³	This range reflects a silt loam's total pore space. We validated it against field cores in the top 0.5 m.	(Cook et al., 1994)
Suction Head at Wetting Front	ψ	0.10 – 0.20	m	Based on soil texture. We cross-checked our infiltration data to refine the final ψ for our model.	(Green & Ampt, 1911; Kale & Sahoo, 2011)
Saturated Hydraulic Conductivity	Ks	0.01 – 0.03	m/day	We used a moderate infiltration rate, consistent with topsoil measurements. Lower horizons may have smaller Ks	(DairyNZ, 2020c)
Time Step Size	Δt	0.001 – 0.01	days	We found smaller Δt essential for stable infiltration calculations, especially under intense rainfall.	(Farthing & Ogden, 2017)

Maximum Infiltration Depth	–	e.g. 0.50	m	We capped infiltration depth (topsoil layer) to match observed root zone influence. This can be adjusted if deeper infiltration is relevant.	Model assumption (user-defined)

Table A3: Water Flow (Richards Equation) Parameters

Parameter	Symbol	Typical Range	Unit	Comments	References
Residual Water Content	θr	0.01 – 0.05	m^3/m^3	We derived these from van Genuchten fitting on local soil moisture curves. The slightly lower end helps capture our well-drained Waikato topsoil.	(Farthing & Ogden, 2017; Simunek & van Genuchten, 1999)
Saturated Water Content	θs	0.35 – 0.45	m^3/m^3	Matches the infiltration module for consistency, though subsoil layers can have different θs.	(Simunek & van Genuchten, 1999)
van Genuchten α	α	0.005 – 0.01	1/cm	We calibrated α by comparing model predictions of soil moisture profiles to measured data.	van Genuchten, 1999)
van Genuchten n	n	1.2 – 3.0	–	Soils closer to 3.0 show sharper retention curves, which we observed in certain layers with more pronounced macropore structures.	van Genuchten, 1999)
Pore Tortuosity (λ or τ)	λ	0.4 – 0.7	–	We used typical Mualem-based exponents. Sensitivity analyses showed moderate effect on K(θ).	Neitsch et al. (2011);
Spatial Increment	dz	0.01 – 0.05	m	Fine vertical discretisation helps capture steep gradients near the surface, though it increases computation time.	Farthing & Ogden (2017)
Time Step	Δt	0.001 – 0.01	days	We used smaller steps during heavy rainfall to stabilize the solution.	Farthing & Ogden (2017)

Table A4: Estrogen Transport (Advection-Dispersion) Parameters

Parameter	Symbol	Typical Range	Unit	Comments	References
Dispersivity	λ	0.02 – 0.10	m	The chosen range captures moderate spreading in the unsaturated zone.	(Das et al., 2004; Steiner et al., 2010a)
Bulk Density	ρ	1.1 – 1.3	g/cm^3	Consistent with silt loam fields in our site, verified via intact core sampling.	Barkle et al. (2000); Sarmah et al. (2006)
Freundlich Sorption Coeff. (E1/E2)	Kf	0.5 – 1.0	L/kg	Reflects moderate sorption for estrone and estradiol in soils with ~5–10% OC. We note E2 typically sorbs more strongly but also degrades faster.	(Adeel et al., 2017; Aris et al., 2014)
Degradation Rate	kd	0.001 – 0.01	day^{-1}	These values correspond to ~2–20 days half-life, consistent with field/lab data from Waikato soils.	(Bradley et al., 2009; Sarmah et al., 2006a)
Dispersion Coefficient	D	1×10^{-4} – 1×10^{-3}	m^2/day	We add both molecular diffusion and pore-scale dispersion. Column studies guided the upper bound.	Das et al. (2004); Steiner et al. (2010)

For colloidal facilitated transport we used these studies as a reference (Chambers et al., 2014; Harvey, 2019; J. Prater, 2012b; J. R. Prater et al., 2015; Steiner et al., 2010a; Wang et al., 2022).

Supplementary Tables for ArcSWAT Estrogen Simulation and for Best Management Practices

The input values are based on the literature. Tables D1 to Table D6 represented the inputs for the base scenario for the hotspots of estrogen concentration. Table D7 to Table D9 provided information for best management practices input.

The following studies we used to manipulate the parameters for the model which cover irrigation management, manure and fertilizer properties, grazing impacts, estrogen sorption/transport, half-lives, as well as riparian/buffer zone and wetland BMPs.

For Irrigation, Manure, and Effluent Management (Bolan et al., 2009; Dairy NZ, 2015; DairyNZ, 2011, 2012; J. B. Gadd, Tremblay, et al., 2010).

For Grazing Intensity, Manure Deposition, and Soil Physical Impacts (Andaluri et al., 2011; Badgery et al., 2017; Belliss et al., 2019; Betteridge et al., 1999; Climo & Richardson, 1984; Drewry, 2006; Greenwood & McKenzie, 2001b).

For Estrogen Sorption, Half-Life, and Transport Parameters (Adeel et al., 2017; Aris et al., 2014; Bradley et al., 2009; J. B. Gadd, Northcott, et al., 2010; Sarmah et al., 2006a, 2008a, 2010; Steiner et al., 2010b; Tremblay et al., 2018a). For Riparian Buffers and Vegetative Filter Strips (Arora et al., 2003; Dosskey et al., 2010; Kuok et al., 2013; Mayer et al., 2007; S. Bircher, 2011; Sirabahenda et al., 2020; Tomer et al., 2005; C. Zhang et al., 2017). For Wetlands as a Best Management Practice (BMP) (Arnold et al., 1998; Hakk et al., 2018; Mathew, 2021; J. P. Sukias & Tanner, 2023a; Tanner et al., 2005, 2022; Tousignant et al., 1999).

Table A5: Irrigation Parameters for ArcSWAT

Parameter	Description	Value	Unit
IRR_AMT	Amount of irrigation water applied	1010	mm/application
IRR_SALT	Salt concentration in irrigation water (effluent)	150	mg/L
IRR_EFM	Nutrient mass applied with effluent irrigation (includes nitrogen and phosphorus)	10	kg/application
IRR_SQ	Irrigation efficiency factor	0.9	Fraction
IRR_SC	Sprinkler coefficient to adjust irrigation efficiency	0.8	Fraction
IRR_NO	Number of irrigation events	12	Count (Monthly)
Start Date	Start of irrigation operations	August	Month
End Date	End of irrigation operations	July	Month
Irrigation Source	Effluent pond used as irrigation source	Effluent Pond	-

Table A6:Fertilizer Properties and Application

Field	Description	Value	Unit
FERTNM	Name of the fertilizer	Beef Fresh Manure	-
FMINP	Mineral Phosphorus	0.01	kg P/kg manure
FMINS	Mineral Nitrogen	0.2	kg N/kg manure
FORGP	Organic Phosphorus	0.02	kg P/kg manure
FORGN	Organic Nitrogen	0.4	kg N/kg manure
BACTPDB	Bacteria Concentration	250	CFU/g manure
MANURE_KG	Application Rate	15	kg/application
Schedule	Fertilizer application schedule	Monthly	
Application Method	Application method for fertilizer	Surface Spread	

Table A7: Grazing Management Parameters

Parameter	Value	Unit	Description
MANURE_ID	Dairy-Fresh Manure	-	Specifies the type of manure applied to the grazing area.
GRZ_DAYS	365	Days	Number of grazing days in a year.
BIO_EAT	0.70	Fraction	Biomass removed by livestock grazing.
BIO_TRMP	0.60	Fraction	Biomass trampled by livestock during grazing.
MANURE_KG	5000	kg/ha/year	Amount of manure deposited by grazing animals.
Schedule by Date	Yes	-	Grazing operations scheduled by specific dates rather than heat units.
Year of Rotation	1	-	Indicates annual rotation for grazing management.
Month	Throughout the year	-	Grazing operations applied continuously throughout the year.

Table A8: Dairy Farm Grazing Details

Parameter	Value	Unit	Description
Farm Size	110	ha	Total area of the dairy farm under study.
Number of Dairy Cows	180	head	Total livestock population grazing on the farm.
Grazing Density	1.64	head/ha	Stock density, representing livestock per hectare.
Grazing Intensity (i)	0.013	RSU/m²	A measure of grazing intensity based on livestock weight and grazing area.
Normalized Hoof Pressure	25	kPa	Pressure exerted by cattle hooves during grazing, influencing soil structure.
Duration of Grazing	0.5	Unitless (0-1)	Fraction of the year cattle are actively grazing.
Manure Application	5000	kg/ha/year	Amount of fresh manure applied or deposited during grazing activities.

Table A9: Pesticide Equivalents for Estrogens (E1 and E2)

Parameter	Estrone (E1)	Estradiol (E2)	Unit	Description
Pesticide Name	Estrone	Estradiol	-	estrogen modelled as a pesticide equivalent.
SKOC	80	400	mg/kg/(mg/L)	Sorption coefficient normalized to organic carbon (E2 has a higher tendency to bind to sediments).
WOF	0.45	0.3	Fraction	Wash-off fraction indicating the portion of the pesticide removed by surface runoff.
HLIFE_F	10	6	Days	Half-life in the field; E2 degrades faster than E1.
HLIFE_S	24	12	Days	Half-life in sediment; E2 degrades faster than E1 in sediment as well.
AP_EF	0.75	0.6	Fraction	Application efficiency; represents how much of the compound remains active after application.
WSOL	13	13	mg/L	Water solubility; both compounds are moderately water-soluble.

Table A10: Estrogens load

Summary of Estrogen Loads		
Source	Load (kg/month)	Notes
Manure Application	40.216	Based on 1200 g/m²/year
Grazing Contribution	1.458	Direct excretion during grazing
Runoff Contribution	7.501	18% mobilization of total estrogen loads
Stream Deposition (E2 only)	0.026	Assumes 10% grazing time near streams also used same for E1

Table A11: Grazing Parameters

Parameter	Before Management Change	After Management Change	Expected Effect
Grazing Days (GRZ_DAYS)	365 days (year-round grazing)	330 days (35 days reduction)	Allows pasture recovery, reduces soil compaction
Biomass Consumption (BIO_EAT)	0.7 (70% biomass consumption)	0.56 (56% reduction)	Increases ground cover, improves soil structure (20% reduction)
Biomass Trampling (BIO_TRMP)	0.6 (60% trampling effect)	0.48 (48% reduction)	Decreases soil disturbance, enhances infiltration (20% reduction)

Table A12: Effluent management

ter	Description	Current Value (Before)	Modified Value (After)	Unit	Comments
IRR_AMT	Amount of irrigation water applied	10	8	mm/application	20% reduction to prevent runoff in wet soils.
IRR_SALT	Salt concentration in irrigation water (effluent)	150	120	mg/L	Reduced by 20%, assuming effluent treatment.
IRR_EFM	Nutrient mass applied with effluent irrigation (N, P)	10	7.5	kg/application	25% reduction, better nutrient retention.
IRR_SQ	Irrigation efficiency factor	0.9	0.95	Fraction	Improved irrigation control, reducing excess losses.
IRR_SC	Sprinkler coefficient to adjust irrigation efficiency	0.8	0.85	Fraction	Adjusted for better water distribution.

IRR_NO	Number of irrigation events	12 (Year-round)	8 (Excluding June–August)	Count	No irrigation in winter months to prevent runoff.
Start Date	Start of irrigation operations	January	September	Month	Avoids wet winter period (June–August).
End Date	End of irrigation operations	December	May	Month	Stops before winter rainfall increases.
Irrigation Source	Effluent pond used as irrigation source	Effluent Pond	Same	-	No change (the effluent pond remains the source).

Table A13: Adjustments for Riparian Buffers

Parameter	Description	Default Value	Modified Value (With Buffers)	Justification
CN2 (Curve Number)	Controls runoff generation	72–85 (pasture)	65–78 (buffered areas)	Reduced to reflect higher infiltration in vegetated buffers
USLE_P (Support Practice Factor)	Represents erosion control effectiveness	1.0 (no conservation)	0.3 – 0.6 (buffer strips)	Decreased to simulate erosion control by vegetation
USLE_C (Crop Management Factor)	Affects soil erosion rate	0.007–0.15 (pasture)	0.001 – 0.01 (riparian vegetation)	Reduced for grass and tree buffers to represent higher soil protection
SLSUBBSN (Slope Length Factor)	Influences overland flow sediment transport	Varies (based on topography)	Reduced by 20–40%	Shorter slope lengths in buffers slow sediment movement
CH_EROD (Channel Erodibility Factor)	Represents streambank erosion potential	0.3 – 0.5	0.1 – 0.2	Lowered to reflect stabilization from riparian roots
CH_COV (Channel Cover Factor)	Vegetative cover along streams	0.0 – 0.3	0.5 – 0.7	Increased to account for streamside vegetation reducing erosion
SPCON (Sediment Reentrainment Coefficient)	Controls sediment deposition vs. transport	0.0001 – 0.01	Reduced by 25–50%	Less sediment is reentrained due to buffer sediment trapping
SPEXP (Sediment Transport Exponent)	Determines sediment transport intensity	1.0 – 1.5	Reduced by 20–40%	Buffers slow down flow velocity, reducing erosion

OV_N (Manning's Roughness Coefficient for Overland Flow)	Resistance to surface runoff	0.13 – 0.35 (pasture)	0.4 – 0.7 (dense riparian zones)	Higher values represent increased resistance due to vegetation
LAT_TTIME (Lateral Flow Travel Time, days)	Water residence time in buffer zones	2–5	Increased by 20–50%	Buffers increase infiltration and delay runoff arrival
SED_FILTER (Sediment Filtering Efficiency, %)	Fraction of sediment removed	Default: 0%	50–80%	Set to reflect buffer effectiveness in trapping sedimen

Table A14: Wetlands Implementation

Parameter	Description	Value/Range	Unit
WET_FR	Fraction of subbasin draining into wetland	0.01 - 0.05	Fraction
WET_NSA	Surface area at normal water level	300 - 3000	m^2
WET_MXSA	Surface area at max storage	1.2 - 1.5 × WET_NSA	m^2
Storage Volumes & Retention Time			
WET_NVOL	Normal water volume	1500 - 5000	m^3
WET_MXVOL	Maximum storage volume	1.5 × WET_NVOL	m^3
Hydraulic Residence Time	Time water remains in wetland	15-Oct	Days
WET_K	Wetland bottom hydraulic conductivity	0.1 - 1.0	mm/hr
Sediment & Nutrient Trapping Efficiencies			
Sediment Retention Efficiency	Percentage of sediment trapped	50 - 90	%
Nitrogen Retention Efficiency	Percentage of nitrogen removed	20 - 50	%
Phosphorus Retention Efficiency	Percentage of phosphorus removed	25 - 50	%
Estrogen Removal Efficiency	Percentage of estrogen removed	30 - 70	%

Nutrient Settling Rates			
NSETLW1, NSETLW2	Nitrogen settling rate	15 - 40	m/year
PSETLW1, PSETLW2	Phosphorus settling rate	10-20	m/year
WET_SED, WET_NSED	Initial wetland sediment concentration	50 - 100	mg/L
Vegetation Composition recommended			
Dominant Macrophytes	Key wetland plants for contaminant removal	*Carex secta, Schoenoplectus tabernaemontani, Typha orientalis*	-
Riparian Buffer Species	Edge vegetation for additional filtration	*Harakeke, Toetoe, Manuka, Ti kouka*	-

Table A15: Estimated parameters for Green Amp model by (Rawls et al., 1983)

Texture class	**Effective porosity**	**Capillary suction at wetted front (cm)**	**Hydraulic conductivity(cm/h)**
Sand	0.417 (0.354–0.480)*	4.95 (0.97–25.36)**	11.78
Loam sand	0.401 (0.329–0.473)	6.13 (1.35–27.94)	2.99
Sandy loam	0.412 (0.283–0.541)	11.01 (2.67–45.47)	1.09
Loam	0.434 (0.334–0.534)	8.89 (1.33–59.38)	0.34
Sandy clay loam	0.330 (0.235–0.425)	21.85 (4.42–108.0)	0.15
Clay loam	0.309 (0.279–0.501)	20.88 (4.79–91.10)	0.10
Clay	0.385 (0.269–0.501)	31.63 (6.39–156.5)	0.03

1. *Numbers in parentheses: one standard deviation around the average
2. **Antilog of the log mean and standard deviation